On novel functions of cholinesterases: implications for the development of two model organisms (*Gallus gallus* and *Danio rerio*) and for human recombinant mutant enzymes

Dissertation zur Erlangung des akademischen Grades "Doctor *Rerum Naturalium*" am Fachbereich Biologie der Technischen Universität Darmstadt

Dissertation vorgelegt von

Karla Viviani Allebrandt

aus Darmstadt/Deutschland

geb. in Planalto/Brasilien

Darmstadt 2005

D17

Dekan: Prof. Dr. Gerhard Thiel

Berichterstatter: Prof. Dr. Paul G. Layer

Mitberichterstatter: Prof. Dr. Werner Himstedt

Tag der Einreichung: 22.09.2005

Tag der mündlichen Prüfung: 04.11.2005

For a better feedback of the results of the investigations conducted, this work is reported in three chapters, accordingly to the research approach used. A previous overview on cholinesterases and their novel functions can be found in "Literature review", chapter 1. Chapters 2, 3, and 4 comprise my studies addressing novel functions of cholinesterases during development of chick pineal and zebrafish, and in human recombinant enzymes. An introduction to each new model organism or approach applied for research, with the respective description of the methodology used, is at the beginning of each of these three chapters. The results of each study are followed by a discussion and a summary of the research achievements. The general findings are summarized at the end of this work, and in "Concluding remarks" new perspectives of research are discussed.

Chapter 3 - A malformation of zebrafish (*Danio rerio*) embryogenesis is generated by serotonin administration, and is related to acetylcholinesterase expression

Chapter 4 – Aryl acylamidase activity from *in vitro* expressed human BChE wild-type and active site mutant enzymes

AAA   aryl acylamidase
AChE   acetylcholinesterase
ACHE   acetylcholinesterase gene
Asn   asparagine
Asp   aspartic acid
ATC   acetylthiocholine iodide
BChE   butyrylcholinesterase
BCHE   butyrylcholinesterase gene
BCIP   5-Brom-4-chlor-3-indolylphosphat
BrdU   5-bromo-2'-deoxyuridine
BSA   bovine serum albumin
BTC   butyrylthiocholine
cDNA   complementary DNA
ChEs   cholinesterases
C-terminus   COOH-terminus of the protein
D   aspartic acid
DAB   3,3'-diaminobenzidine
DAPI   4,6-diamidin-2'-phenylindoldihydrochlorid
dATP   deoxyadenosine triphosphated
dH$_2$O.   distilled H$_2$O
df   degree of freedom
DIG   digoxigenin
DMEM   Dulbecco's modified eagle medium
DMF   dimethylformamid
DNA   deoxyribonucleic acid
dNTPs   deoxynucleotide triphosphates
E   glutamic acid
E11   embryonic day 11
E. coli   *Escherichia coli*
EDTA   ethylenedinitrilo-tetraacetic acid
e.g.   exempli gratia
et al.   *et alteres*
FCS   fetal calf serum
FITC   fluorescein isothiocyanate
Gln   glutamine
Glu   glutamic acid
Gsc   goosecoide
5-HT   5-Hydroxytryptamine or serotonin
hpf   hours post fertilization
Kb   kilo base pair
kDa   kilo Dalton
KO   knock-out
LMW   low molecular weight
Mm   milimolar
M   molar
min   minutes
mRNA   messenger RNA
myo-D   myogenic differentiation marker
MW   molecular weight
NBT   4-Nitro Blue Tetrazolium Chloride
Ngn-1   neurogenin-1
N-terminal   NH$_2$-terminus of a protein

ONACA	o-nitroacetanilide
ONPRA	N-2-nitrophenylpropanamide
OD	optical density
p	probability
PCNA	proliferation cellular nuclear antigen
PBS	phosphate buffered saline
PCR	polymerase chain reaction
PRCs	photoreceptor cells
PFA	paraformaldehyde
pH	potentia hydrogenii
Q	glutamine
RNA	ribonucleic acid
rpm	rotations per minute
RT	room temperature
S	serine
S-phase	DNA synthesis phase
[S]	substrate concentration
SDS	sodium dodecyl sulfate
Ser	serine
S-phase	DNA synthesis (replication)
TAE	tris-acetic acid-EDTA buffer
TBE	tris-borate-EDTA
TdTe	terminal deoxynucleotidyl-transferasemediated
TE	tris-EDTA-buffer
Tris	tris-hydroxymethyl-aminomethane
TUNEL	terminal deoxynucleotidyltransferasemediated dUTP nick end labeling assay
U	enzymatic unit
UV	ultraviolet
3'	3 prime
5'	5 prime
X_2	chi-square

CHAPTER 1

1 Literature review

1.1   Overview

At the beginning of the last century, pharmacological investigations of the cholinergic nervous system brought to light the existence of cholinesterases (Dale, 1914; Loewi and Navratil, 1926; Stedman *et al.*, 1932). On the early 1940s, the presence of two cholinesterases, with slightly different substrate affinities (Mendel and Rudey, 1943), was verified on human blood. The serum enzyme, butyrylcholinesterase (BChE; E.C. 3.1.1.8), hydrolyzed preferentially butyrylcholine (BuCh) and propionylcholine (PCh), while the red blood cells enzyme, acetylcholinesterase (AChE; E.C. 3.1.1.7), displayed high affinity for acetylcholine. The following years of research were concentrated on understanding the properties, physiological function, pharmacology, localization and development of these enzymes.

1.1.1 The cholinesterase (ChEs) family and homologous proteins

Higher eukaryotes have many distinct esterases. The cholinesterases belong to the lipase/esterase family, beyond other phylogenetically related groups of enzymes (carboxylesterases, lipases and hormone-sensitive lipases) sharing a similar structure of a central beta-sheet surrounded by alpha-helices.

Among these proteins, molecules implicated in cell-cell interactions by promoting cell adhesion present 42 to 50% of sequence similarities with AChE from *Torpedo* (Schumacher *et al.*, 1986), mouse (Rachinsky *et al.*, 1990), human (Soreq *et al.*, 1990) and AChE and BChE from Drosophila (Oslo *et al.*, 1990; Barthalay *et al.*, 1990; De La Escalara *et al.*, 1990; Darboux *et al.*, 1996); see dendrogram (Fig. 1.1). In despite of the high homology of sequence with AChE, these proteins do not have the catalytic serine and therefore, do not display cholinergic activity. Some of these proteins are known to be transiently expressed during development, like gliotactin and neurotactin in *Drosophila* (Soreq *et al.*, 1990; Auld *et al.*, 1995). Neuroligins are also suggested to play an indirect role on cell-cell interaction and synaptic organization (Ichtchenko *et al.*, 1995).
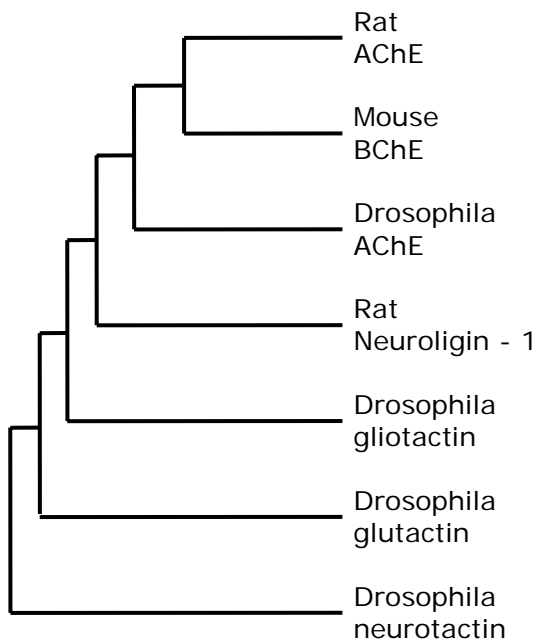
Fig. 1.1: The serine esterase domain proteins. A dendrogram illustrates the relationship between proteins involved in cell-cell interactions to cholinesterases from representative species (Brimijoin and Koenigsberger, 1999).

1.1.2 The cholinesterases

BChE is the closest serine proteases structural relative to AChE. Human BChE and *Torpedo* AChE are 54% identical (Chatonnet and Lockridge, 1989). AChE and BChE are distinguished by their distinct substrate specificity and inhibitor sensitivity, determined by their functional sites (Massoulié and Bon, 1982; Chatonnet and Lockridge, 1989). AChE is selectively inhibited by BW 284c51, while BChE is specifically inhibited by iso-OMPA (Austin and Berry, 1953). Nevertheless, both are inhibited by 10^{-5} M physostigmine and organophosphate compounds used as insecticides and neurotoxins. Moreover, they can also be distinguished by their affinity to monoclonal antibodies (La Motta and Woronick, 1971; Brimijoin *et al.*, 1983).

In humans, each BChE subunit comprises 574 amino acids and weights 85.5 kDa (monomer). The mature catalytic subunit of AChE consists of a major common domain of about 535 residues. Each subunit of AChE is composed by 614 amino acids and weights 67.9 kDa. Both AChE and BChE molecules are comprised by a central beta-sheet surrounded by alpha-helices (Fig. 1.2).
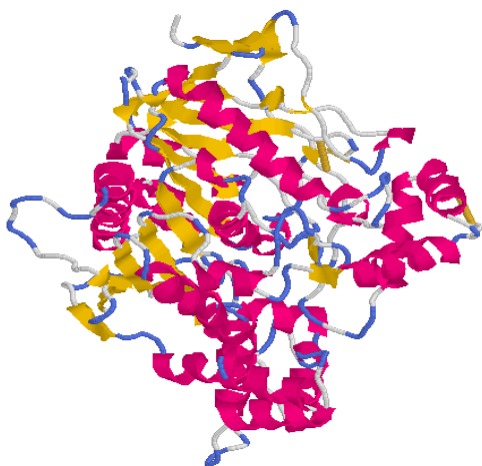
Fig. 1.2: Secondary structure of BChE. Neighboring amino acids twist in relation to each other to form a variety of three-dimensional structures including sheets and helices.

1.1.2.1   Cholinesterases function

Henry Dale established acetylcholine's role as a chemical transmitter of nerve impulses on the early 30s. AChE (EC 3.1.1.7) rapidly terminates the nerve impulse by hydrolyzing acetylcholine (ACh) in cholinergic synapse, thereby limiting the action of the neurotransmitter (Quinn, 1987). Therefore, AChE is essential to maintain continuous synaptic transmission.

Although BChE (EC 3.1.1.8) is 3 fold less efficient than AChE on hydrolyzing acetylcholine, it can also hydrolyze many other esters, like proprionylthiocoline, butyrylcholine and benzoylcholine. It was initially suggested to work as a detoxifying agent, by hydrolyzing succinylcholine, a pre-surgery short-acting myorelaxant (Davies and Kalow, 1963). The interest in BChE grew as some patients experienced prolonged apnea after treatment with succinylcholine, caused by a genetic variation of the BChE (Whittaker and Britten, 1980). However, the exact physiological function of BChE is not known. It is generally viewed as a back up for the homologous AChE and, as a scavenger for anticholinesterases compounds (Schwarz *et al.*, 1995; Fontoura-da-Silava and Chautard-Freire-Maia, 1996).

1.1.3 Cholinesterases catalytic mechanisms and kinetics

Catalysis by ChEs occurs by a mechanism similar to that of the serine proteases, via an acyl-enzyme intermediate. First the substrate is broken into

choline and acetate (Fig. 1.3). Choline can remain temporarily trapped in the muscular end plate or can be immediately taken up again by the high affinity choline uptake system on the pre-synaptic membrane. In a second step, a deacetylation reaction takes place to re-establish the functionality of the enzyme (Fig. 1.3).

The cholinesterases are among the most efficient enzymes known. The AChE hydrolysis rate is similar to the natural rate of diffusion for acetylcholine, displaying a turnover number of ~10000 molecules per second, and thus operating close to the diffusion-controlled limit (Quinn, 1987).
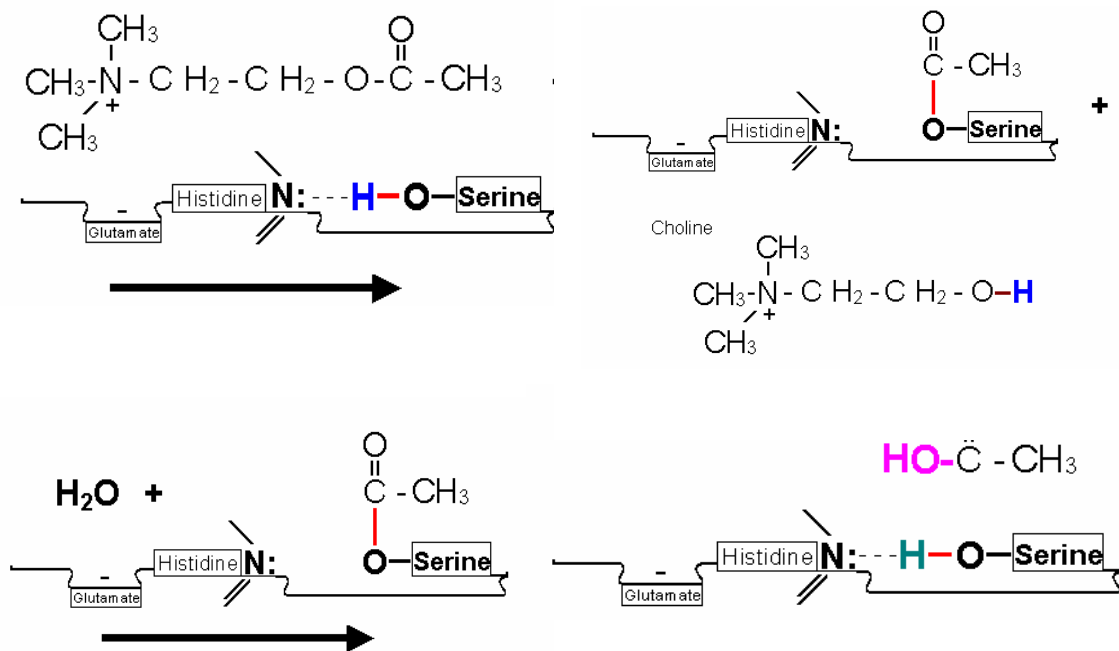
Fig. 1.3: General cholinesterases catalysis schema: the substrate, in this case acetylcholine, binds to the esteratic site, where it is broken by nucleophilic attack by a serine, followed by general-base catalysis assisted by a histidine, generating acetate and choline (Quinn, 1987). Acetate remains covalently bonded to serine residues within the esteratic subsite, forming a temporary acetylated form of AChE. A molecule of water then reacts with this intermediate, liberating the acetate group and restoring the active form of the enzyme.

1.1.4 Cholinesterases structure and functional sites

Several approaches were undertaken to unravel the functional sites of AChE and BChE since the last decade. The structure of the *Torpedo californica* (Pacific Electric Ray) AChE (*Tc*AChE), allowed the idealization of a computational model for the human BChE (hBChE) crystal structure, which was just recently determined (Nicolet *et al.*, 2003). Based on the amino-acid sequence, x-ray crystal structure, site-directed-mutagenesis and ligant binding studies, it was possible to elucidate functional sites on AChE and BChE.

*Tc*AChE active site catalytic Ser-His-Glu triad is found at the bottom of a 20 Å deep gorge lined mostly with aromatic residues (Sussman *et al.*, 1991). The catalytic triad is the same for both cholineterases and the overall structure of the hBChE is very similar to *Tc*AChE (Fig. 1.4). The difference lies on the residues lining the gorge, 14 aromatic residues on AChE and 8 on BChE (Harel *et al.*, 1992). As a result, bulkier molecules can be accommodated in the catalytic gorge of BChE.

Studies of the pH and charge dependence of catalytic hydrolysis of substrates and of the binding of reversible inhibitors suggested that the active site of ChEs contains two major subsites, the "esteratic" and the "anionic" (Wilson and Bergmann, 1950). These subunits correspond, respectively, to the catalytic machinery and the choline-binding pocket (Froede and Wilson, 1970). The AChE peripheral anionic site (PAS), which localization was established in 1980 (Berman *et al.*, 1980), lays 20 Å from the rim of the active center gorge (Fig. 1.4). Functionally, the primary binding of compounds to the peripheral site slows down the traffic of substrate and product at the acylation site (Szegletes *et al.*, 1999; De Ferrari *et al.*, 2001). Moreover, it has been speculated that the PAS is involved in the phenomenon of substrate inhibition and activation through binding of a second substrate molecule.

A similar peripheral site is known to be present on BChE, although, its response to ligand binding differs significantly from that of AChE (Nachon *et al.*, 1998; Masson *et al.*, 1997). Based on structure function relationship and reverse genetics, it was concluded that the aromatic residues lying in the PAS from *Tc*AChE are essential for AChE functioning and substrates selectivity (Radic *et al.*, 1993; Barak *et al.*, 1994). This was considered when looking for a PAS in

BChE, which was previously thought to do not have a secondary site (Harel *et al.*, 1992). However, in BChE the aromatic residues not take part in the PAS, and the negatively charged residue Asp70 plays a central role on it (Masson *et al.*, 1996). This residue is strategically placed near the top of the active-site gorge (Fig. 1.4), also on AChE (Barak *et al.*, 1995), although the Trp-277 is the crucial component for the functioning of the AChE PAS (Masson *et al.*, 1997). Therefore, the features of the PAS are similar for both enzymes, except those that rely on aromatic amino acids.
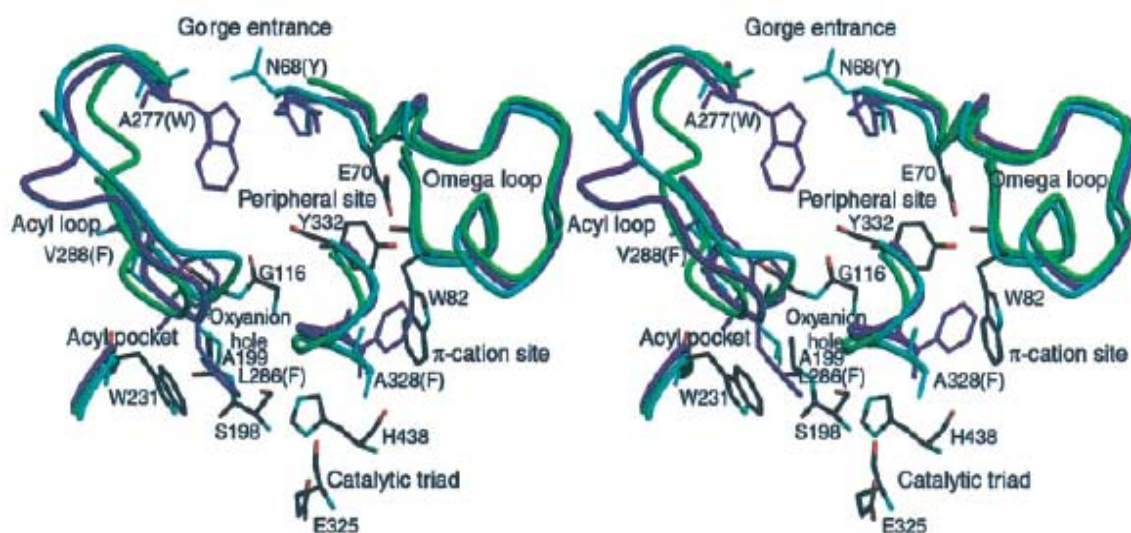
Fig. 1.4: Stereo view of cholinesterases. Superposition of native hBChE (cyan), TcAChE (pink), and Drosophila AChE (green) around the active site gorge (Nicolet et al., 2003).

1.1.5 A non-cholinolytic activity on cholinesterases

A second activity, besides the esterase activity, sitting on the ChEs molecule has been proposed to exist. AChE was found to hydrolyze o-nitroacetanilide (Fujimoto, 1976), an artificial substrate, which is hydrolyzed by the activity of aryl acylamidase (Hoagland and Graf, 1971). The aryl acylamidase is an ancient enzyme (AAA; EC 3.5.1.13), found in bacteria (Engelhardt *et al.*, 1971; Hsiung *et al.*, 1975) and plants (Still and Kuzirian, 1967), which cleaves acyl-amide bonds, catalyzing the de-acetylation of aryl acylamides. This activity is known since 1909, discovered by Minkowki in rabbit and kidney extracts, using phenactin and acetanilide as substrates.

In basal ganglia, electric eel and, erythrocyte membrane, both AChE and AAA have been co-purified by affinity chromatography. They displayed identical behavior on gel electrophoresis and in response to the inhibitors eserine, neostignine and BW 284C51 (George and Balasubramanian, 1980; Majumdar *et al.*, 1982; Majumdar and Balasubramanian, 1982; Checler *et al.*, 1994). The association of AAA with AChE and BChE has been reported mostly in mammals (Fujimoto, 1976; Oommen and Balasubramanian, 1977; Tsujita *et al.*, 1983; Jayanthi *et al.*, 1992; Balasubramanian and Bhanumathy, 1993), however, it also occurs in chicken (Weitnauer *et al.*, 1998). The distinction between the AAA activities non-associated to the AAA-ChEs associated, was possible due to their differential sensitivity towards compounds like serotonin and tryptamine, which just affect the latter activity (Fujimoto, 1974, 1976; Oommen and Balasubramanian, 1977; Oommen and Balasubramanian, 1979; George and Balasubramanian, 1981). AAA ChEs associated is inhibited towards the classical cholinesterases inhibitors BW and ISO-OMPA and towards the ChEs substrate acetylcholine (Oommen and Balasubramanian, 1977; Checler *et al.*, 1994; Weitnauer *et al.*, 1998). However, these biochemical evidences of an aryl acylamidase associated to cholinesterases were not enough to convince all the scientific community working on cholinesterases about the existence and functionality of this second activity on cholinesterases. Nevertheless, chemical mutagenesis was conducted to find evidence of a co-relation structure/catalytic efficiency of AAA in comparison to the esterase activity (Majumdar and Balasubramanian, 1984; Boopathy and Balasubramanian, 1985). However, the puzzling results produced with this kind of approach could not clarify which

amino acids are essential for the functionality of AAA. In resume, a catalytic site for this activity on cholinesterases is not known, in despite of the attempts to indicate the amino acids comprising its active site (Majumbar and Balasubramanian, 1984; Boopathy and Balasubramanian, 1985).

Furthermore, the natural substrate for AAA is also not known, increasing the uncertainty of a real physiological function for it. It has been suggested to contribute to the degradation of substance P (Balasubramanian and Bhanumathy, 1993), which is involved in transmission of pain signals to the brain. Besides, AAA was shown to be highly sensitive to inhibitors used for the treatment of Alzheimer's disease (Darvesh *et al.*, 2003) and to contribute to the maturation of amyloid plaques (Costagli *et al.*, 1998), suggesting it could be correlated to the clinic condition of this disease (Darvesh *et al.*, 2003).

Developmental studies, using chicken as model organism, have indicated temporal variation of the AAA activity and of its sensitivity to inhibitors in relation to the esterase activity (Boopathy and Layer, 2004).

The sensitivity of this activity towards serotonin (Fujimoto 1974, 1976; Oommen and Balasubramanian, 1977) is a particular property of the AAA activity associated to ChEs that deserves more attention. Nevertheless, the publications on the subject are limited and more investigations are required to describe a functional relevance for this activity and to corroborate its association with cholinesterases.

1.1.6 Cholinesterases genetic background

1.1.6.1   Evolutionary aspects

Despite of the high homology of the sequence (Prody *et al.*, 1987; McTiernan *et al.*, 1987; Soreq and Prody, 1989), BChE and AChE are encoded by different genes, located on different chromosomes (Soreq *et al.*, 1987; Arpagaus *et al.*, 1990; Gaughan *et al.*, 1991). The human *BCHE* locus is located on the long arm of the chromosome 3, band 26, while *ACHE* is on the long arm of the chromosome 7, on the band 22 (Getman *et al.*, 1992). They possibly were originated by a gene duplication, which occurred in different phylogenetic lineages (McClellan *et al.*, 1998). AChE is primarily found in nematodes (*Caenorhabditis elegans*), being encoded by four ACHE genes (Grauso *et al.*,

1998), and two genes in *Amphioxus* (McClellan *et al.*, 1998). Insects possess a single ChE gene coding for an enzyme with specificity intermediate between those of AChE and BChE (Massoulié *et al.*, 1993a; Taylor and Radic, 1994). In vertebrates there is a single gene encoding ACHE, whose structure differs slightly with taxonomic group (Massoulié *et al.*, 1993b). BChE is not present in invertebrates, its first appearance occurs before the split of cartilaginous fish, in *Torpedo*. However, it is not present in zebrafish, suggesting it had been lost, emerging later in birds (McClellan *et al.*, 1998).

1.1.6.2 *Cholinesterases diversity*

The human BCHE gene is known to be very polymorph (Arpagaus *et al.*, 1990), circa 40 variants have been described (McGuire *et al.*, 1989; Gnatt *et al.*, 1990; Muratani *et al.*, 1991; Bartels *et al.*, 1992; Jensen *et al.*, 1992; Hada *et al.*, 1992; Hidaka *et al.*, 1992; Nogueira *et al.*, 1992; Greenberg *et al.*, 1995; Maekawa *et al.*, 1995; 1997; Primo-Parmo *et al.*, 1996, Sudo *et al.*, 1997). The existence of *BCHE* variants with very low esterase activity, 25 with less than 10% of activity, suggests a non-cholinergic mechanism could be maintaining some of these variants as polymorphisms in some populations. For instance, in European populations, the frequency of individuals with substantially decreased enzyme activity does not exceed 1:2000. However, among Eskimos of Alaska, 1-2% of individuals produce a variant of the BCHE enzyme without esterase activity, due to a silent polymorphism, and 25% are usual/silent heterozygotes and exhibit 70% of the activity as compared to normal usual homozygotes (Whittaker and Britten, 1989). The existence of silent homozygotes is a strong indication of the involvement of BChE in non-cholinergic processes.

The plasma BChE is present in three main globular forms, monomer, dimer and tetramer, according to the number of subunits (Muensch, 1976; Masson, 1979). Other subunits of BChE can be detected by electrophoresis, which are suggested to be aggregates from the main globular forms of AChE and BChE (Tsim *et al.*, 1997) or complexes of some forms of BChE with lipoproteins or lipid molecules (Kutty, 1980). Although, the significance of the molecular polymorphism of BChE is not clear, association studies indicate a correlation of variants with reduced cholinergic activity to increased susceptibility to intoxication by organophosphorus compounds (Fontoura-da-Silva and Chautard-Freire-Maia, 1996).

Acetylcholinesterase is a highly structural polymorphic enzyme, existing as soluble, membrane bund and basal lamina-associated forms (Massoulié *et al.*, 1998; Feng *et al.*, 1999; Gennari *et al.*, 1987). Through alternative splicing (Fig. 1.5), the mammalian AChE gene produces three types of coding regions, generating proteins that possess the same catalytic domain associated with distinct C-terminal peptides, which dictate where the enzyme will be located (Massoulié, 2002). AChE subunits of type R ('read through') produce soluble monomers, and of type H ('hydrophobic') glycophosphatidylinositol-anchored dimmers (Silman and Futerman, 1987), but also secreted molecules. Subunits of type T ('tailed') exist for both AChE and BChE. They represent the enzyme forms expressed in brain and muscle. These subunits generate a variety of quaternary structures, including homomeric oligomers (G1 - monomers, G2 – dimmers and G4 - tetramers), as well as hetero-oligomeric assemblies with anchoring proteins, ColQ and PRiMA.

The C-terminal region of BChE is not subject to alternative splicing, presenting high homology to the vertebrate T-spliced AChE (AChET). The association of AChET or BChE subunits with ColQ produces collagen-tailed molecules, which are inserted in the extracelular matrix, e.g. in the basal lamina of neuromuscular junctions (Feng *et al.*, 1999; Hall, 1973). Their association with PRIMA is required to anchor it to the basal lamina of cells and organize into tetramers, which constitute the predominant form of cholinesterases in the mammalian brain (Gennari *et al.*, 1987; Inestrosa *et al.*, 1987; Perrier *et al.*, 2002). The alternatively spliced exons are not common to all invertebrates (Fig. 1.5). In insects only H cDNAs are present (Massoulié *et al.*, 1998). In nematodes it is not the same for all four AChE genes they present. In vertebrates the absence of the H exon can be frequent (Simon and Massoulié, 1997; Simon *et al.*, 1998).

The assembly of the cholinesterases molecular forms is supposed to take place in the trans-Golgi apparatus (Massoulié *et al.*, 1993b). Rotundo (1989) reported AChE is packaged in coated vesicles and transported to the plasma membrane, where the vesicles fuse and result in either secretion of AChE or insertion to the membrane.
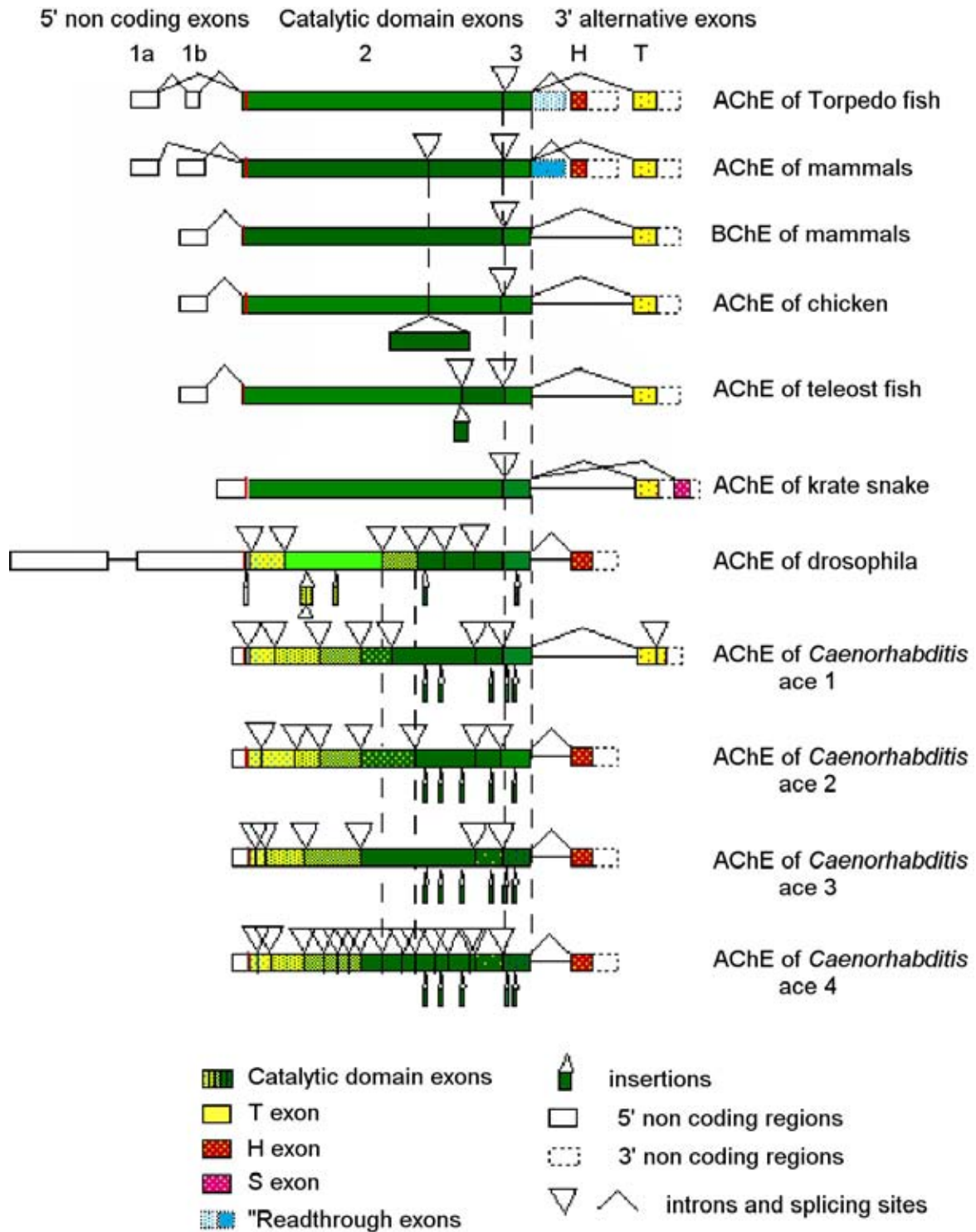
Fig. 1.5: Alternative splicing at the 3' end of the coding sequence of AChE transcripts generating peptides with different C-terminal regions (Cousin et al., 1997): exon 4 is either read through to give the R subunit, or alternatively spliced to exon 5 (H subunit) or exon 6 (T subunit).
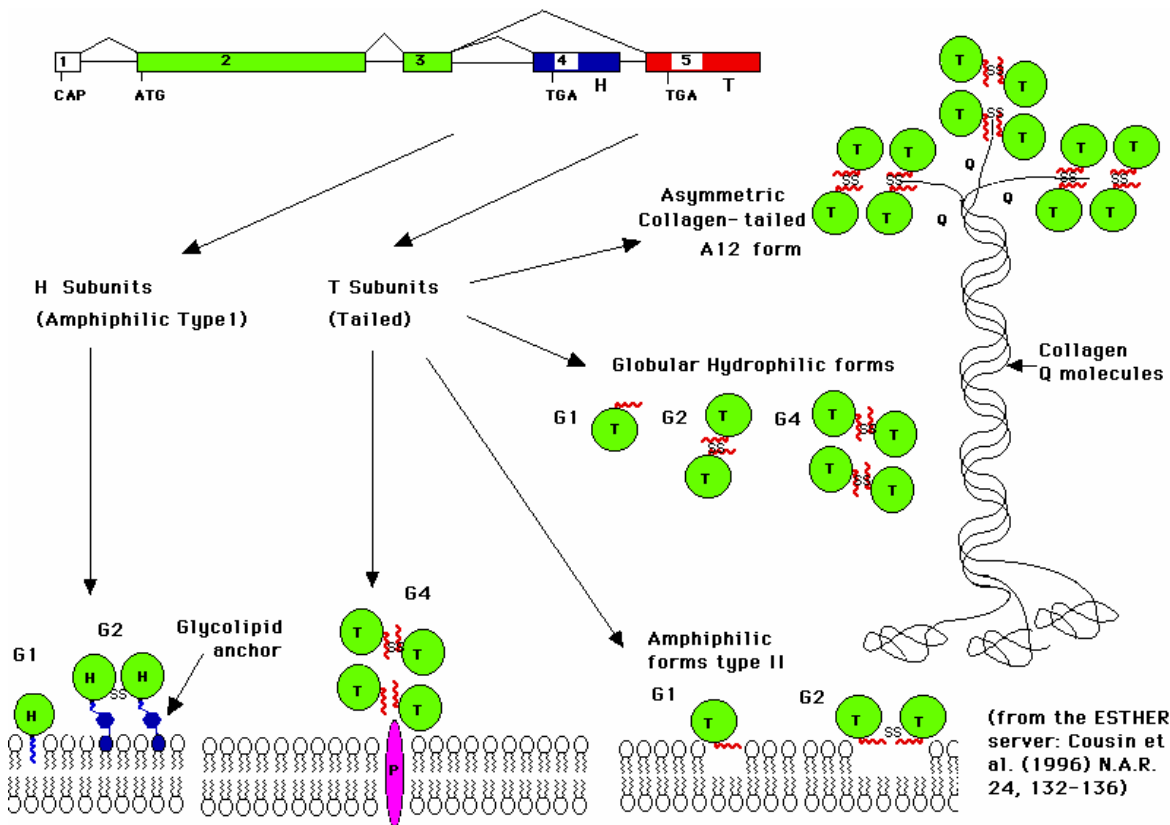
Fig. 1.6: AChE subunits. The AChEH subunits undergo a post-translational modification, the C-terminal region of the H peptide is replaced by GPI (shown in blue), and the resulting dimmers are anchored in the cell membranes. The AChET subunit develops an amphiphilic alpha helix (red), which is exposed in amphiphilic forms type II (monomers, dimmers and tetramers). AChET subunits form tetramers linked to PRIMA (pink) or ColQ (Collagen Q), generating membrane-bound and collagen tailed hetero-oligomers.

1.1.7 Cholinesterases expression and localization on tissues

Consistent with the classical role of AChE, it predominates in neuromuscular junctions and is also intensely expressed in the human central nervous system, where cholinergic synapses are found. On the other hand, AChE also occurs in non-neural and embryonic tissues like red blood cells, megakaryocytes, and migrating neural crest cells (Lev-Lehman *et al.*, 1997; Smith *et al.*, 1979). BChE appears in a limited group of neurons, as it occurs primarily in non-neural or non-synaptic sites like adipose tissue, liver, intestine, lung, plasma, and neuroglia (Silver, 1974; Graybiel and Ragsdale, 1982). The Weizmann Institute of Science has a website reporting cholinesterases expression on human tissues based on DNA array experiments (Fig. 1.7).

(A)

(B)
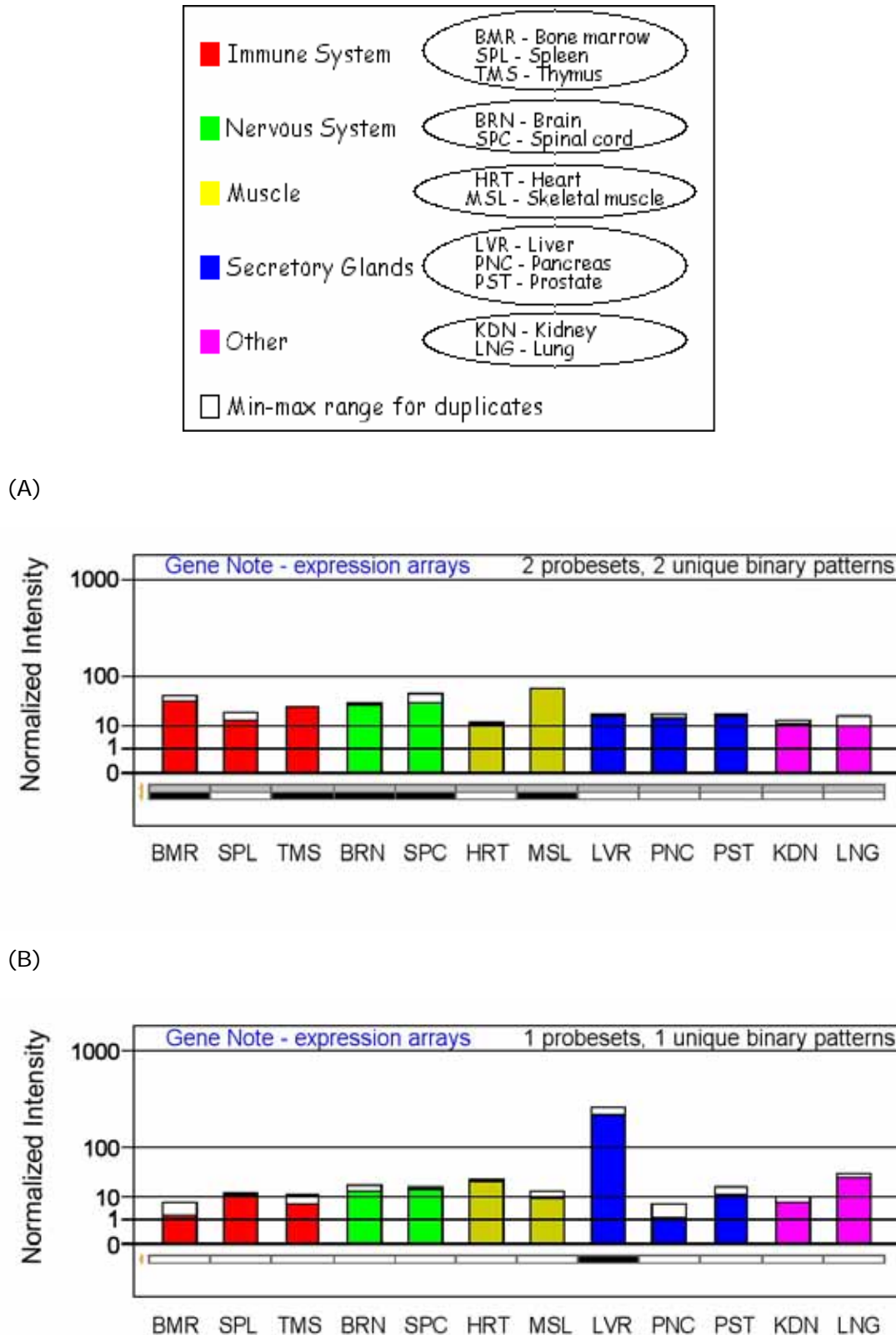
Fig. 1.7: Cholinesterases expression. AChE (A) and BChE (B) expression in cholinergic (nervous system and muscles) and non-cholinergic tissues (immuno system, secretory glands and others) according to the Weizmann Institute of Science DNA array experiments (Gene Cards web site; http://au-kbc.org/beta/bioproj2/genecard.html).

Whereas the human BChE is synthesized in liver and white matter of the brain (Prody *et al.*, 1987; McTiernan *et al.,* 1987), acetylcholinesterase is released from the *substatia nigra* into the cerebrospinal fluid (Jones *et al.*, 1994). AChE and BChE can be found as soluble forms or can be attached to cellular or basement membranes (Henderson and Greenfield, 1984; Massoulié, 2002). In vertebrates, AChE and BChE asymmetric forms are present just in peripheral nervous system and muscles. Membrane bound tetramers from both enzymes, are present in mammalian brain and AChE monomers in erythrocytes (Massoulié, 1982).

1.2   Novel functions of cholinesterases

Novel functions of cholinesterases, which do not involve termination of the nervous impulse, have been speculated. These non-classical events involving ChEs, between several others, are suggested to be: promotion of cell differentiation (Layer and Willbold, 1990; Lapidot-Lifson *et al.*, 1992), cell migration (Drews, 1975; Layer and Kaulich, 1991), cell proliferation (Layer, 1987), tumor growth (Patinkin *et al.*, 1990; Soreq *et al.*, 1992; 1994b) and, cell apoptosis (Robitzki *et al.*, 2000; Zhang *et al.*, 2002; Jin *et al.*, 2004; Park *et al.*, 2004).

1.2.1 Cholinesterases disfunction in pathological states

The possible involvement of BChE in neurological diseases, like Alzheimer`s disease (AD), has been postulated by association studies on human populations (Raygani *et al.*, 2004; Cook at al., 2005). It has been known for several years that BChE activity is increased in AD brain (Perry *et al.*, 1978). As well, the inhibition of AChE was shown to improve long-term memory processes (Davis *et al.*, 1978).

The progressive disfunction of cholinergic neurotransmission in the brain is a factor for the development of cognitive and behavioral problems in Alzheimer`s patients (Whitehouse *et al.*, 1981; Coyle *et al.*, 1983). In consequence, drugs to treat AD (rivastigmine, huperzine A, donepezil and eptastigmine) act mainly on the cholinergic neurotransmission system.

Neuronal death related to the deposition of the B-amyloid protein on the brain plaques and tangles is suggested to be the major cause of AD. The increase in

AChE and BChE expression around amyloid plaques and tangles supports the involvement of these enzymes on AD (Geula and Mesulam, 1989; Gomez-Ramos *et al.*, 1994; Rees and Brimijoin, 2003). It is suggested that a physical interaction between AChE and beta amyloid could take place (Alvarez *et al.*, 1995; 1998). However, the mechanism by which cholinesterases would be interfering with AD progress is not completely understood.

The involvement of BChE with other multifactorial diseases is also speculated. BChE is reported to be associated with lipoproteins like LDL and HDL (Lawrence and Melnick, 1961; Ryhänen *et al.*, 1982), and therefore, its activity is increases in conditions associated with abnormal lipid metabolism such as hyperlipidemia (Chu *et al.*, 1978). The relation of BChE polymorphism to body weight and Body Mass Index has been also shown in population's genetics studies (Simpson 1966; Souza *et al.*, 2005).

1.2.2 Cholinesterases and developmental events

AChE has been shown to be very early expressed during development of several organisms. It is known since the 1970s, from the work of developmental biologists like Whittaker. They verified AChE expression in two-cell stage of bllastomers of tunicates. The relevance of such an early onset of AChE is therefore, not related to termination of nervous impulse and supports a developmental function for it.

Investigating closely the expression of ChEs during development, it was verified a growth-related shift in molecular forms generated by alternative 3´-mRNA splicing. The monomeric BChE and dimeric AChE forms, mainly intracellular, are predominant during brain development (Drews, 1975; Layer and Sporns, 1987; Layer and Willbold, 1994). In the adult brain, there are mainly tetramers of both enzymes anchored to neurons.

1.2.2.1   Non-catalytic functions of cholinesterases

BChE and AChE expression have been shown to be correlated, respectively, to cell proliferation and cell differentiation processes. In early chick neuroepithelium, BChE was found to be highly expressed in mitotic and post-mitotic migrating cells, being replaced by AChE when the differentiation process takes place (Layer and Sporns, 1987). In parallel, a switch from BChE to AChE,

observed in *in vitro* culture of chicken embryonic cells, was described occurring when neuroblasts cease dividing and the development of the axonal processes takes place (Layer, 1983). Reinsuring these findings, antisense 5`- BChE transfected spheroids, originated from chicken retina cells, displayed inhibition of the BChE translation, declining the proliferation process (Robitzki *et al.*, 1997).

Axonal outgrowth and synaptic connection formation have been associated with transient AChE expression, during human brain (Kostovic *et al.*, 1983) and chicken neural crest cells (Layer and Alber, 1990) development. It has been demonstrated that neutrite outgrown is affected by peripheral site anticholinesterases compounds (Layer *et al.*, 1993) and enhanced in neuronal cell lines over expressing AChE (Koenigsberger *et al.*, 1997). In agreement with these findings, specific AChE antibodies interfere with the extension of neural processes after binding to external cell surfaces in culture (Koenigsberger *et al.*, 1997). The physiological process leading to these events is not clear. However, Small (1995) has demonstrated that the neutrite outgrowth is equally stimulated in substrata containing irreversible inactivated AChE or active AChE, indicating a non-enzymatic contribution of AChE for the axonal outgrowth.

1.2.2.2 *Non-cholinolytic function of cholinesterases*

Another developmental relevance of ChEs is related to their associated aryl acylamidase activity. Boopathy and Layer (2004) verified transient AAA activity associated to cholinesterases during distinct embryonic periods. This activity was dependent of the cholinesterase associated: AAA on AChE increasing constantly in relation to AChE and AAA on BChE, initially high (until E10), becoming negligible towards hatching.

1.2.2.3 *Development without cholinesterases*

In *Drosophila*, a temperature dependent mutation may be induced during pupation, leading to absence of the wild-type type AChE and causing improper assembly of the visual system (Hall *et al.*, 1980).

In zebrafish (*Danio rerio*), a naturally occurring mutant lacking AChE activity displayed impaired motility at the 48 h larvae stage, caused by muscle fiber formation defects (Behra *et al.*, 2002).

On AChE *knockout* mice (Xie *et al.*, 1999), the brain tissue was normally structured and cholinergic pathways were fully developed (Minic *et al.*, 2003). This normality was suggested to be due to the widely distributed BChE activity in the KO mice (Li *et al.*, 2000). However, in a close inspection of the retina, a strong effect caused by the absence of AChE was revealed by the degeneration of photoreceptors during development of the KO mice (Bytyqi at al., 2004), clearly indicating the relevance of AChE on organization and function of the mammalian retina.

1.3   The aim of this work

Four premises support the involvement of ChEs in physiological processes unrelated to cholinergic neurotransmission: 1) their non-specificity to cholinergic innervated tissues; 2) their homologous structure to cell adhesion molecules; 3) their early onset during development of several organisms and, 4) their non-cholinolytic aryl acylamidase activity.

This study is an attempt to unravel roles of cholinesterases in a broad spectrum of possibilities. ChEs expression and function is investigated during the development of two-model organisms, zebrafish and chicken, with focus on non-cholinolytic and non-catalytic events.

By reverse genetics, BChE structure and function relationship are studied. *In vitro* expressed human recombinant enzymes are investigated to learn about the cholinesterases associated aryl acylamidase activity.

CHAPTER 2

2   Spatio-temporal expression of ChEs during chick pineal gland embryogenesis and their relation to developmental events

2.1   Overview

The pineal organ is characterized as a primitive "third" eye structure in fishes, amphibians, and reptiles (Meakin, 1973). In avians, the pineal organ still presents directly photosensitive response. However, in mammals, the influence of light in the pineal gland metabolism is mostly indirect.

Cholinesterases expression has been shown to be implicated with proliferation and differentiation events occurring in retinal cells (Robitzki *et al.*, 1997). The close relationship of the pineal organ to the eye makes it an interesting tissue for the study of cholinesterases functionality in developmental processes.

In addition, the pineal gland metabolism is controlling physiological processes following a circadian rhythm. Therefore, it is also implicated in pathological states showing disturbances of this rhythmicity. Cholinergic activity is also altered during physiological disfunction of circadian activities associated to pathological states, like the Alzheimer`s disease, or metabolical alterations in aging or seasonal adaptation (Mishima *et al.*, 1999; Small, 1996; Avidan, 2005; Wu and Swaab, 2005), suggesting these events are correlated.

AChE is known to be expressed in the post-hatching pineal of several species, although, the pineal gland does not receive significant cholinergic input. The relevance of ChEs for the pineal gland metabolism is not clear, and their expression during embryonic development has not been characterized until now.

2.1.1 The pineal gland

Herophilos (circa 325-280 B.C.) described the pineal organ as being a tap between the third to the fourth brain ventricle, which was found to be a gland by Galen, in the 16th century. The first anatomical studies on pineal gland date from the beginning of the last century (Hill, 1900; Cameron, 1903), and the detailed morphological descriptions from more than 50 years later (Spirof, 1958; Oksche *et al.*, 1965, Campbell and Gibson, 1970; Calvo and Boya, 1978).

The avian pineal gland represents a transitional type between a photosensory organ of lower vertebrates and the endocrine gland of mammals, responding to photosensory and hormonal stimuli (Deguchi, 1981; Takahashi *et al.*, 1989). In

fish and amphibians, the circadian rhythm is directly regulated by light, because their pineal gland is located on the surface of the brain (Axelrod *et al.*, 1965; Cahill, 1996). In reptile and birds the pineal responds to photosensory and hormonal stimulus. In mammals, due to the pineal location in deep midbrain, its response to light is limited to signs arriving from the retina (Marieb, 2001).

The pineal organ is responsible for the control of physiological functions that follow a circadian rhythm, like sleep-wake cycles. The link between photoperiod to metabolic and endocrinal changes is established by melatonin (Yu *et al.*, 1993). In the pineal gland, serotonin is metabolized to melatonin, in the absence of light, by the enzymes 5-HT N-acetyl transferase and 5-hydroxyindole-O-methyltransferase, and secreted to the hypothalamus in a rhythmic manner (Quay, 1974; Aloyo and Walker, 1987).

In mammals, this circadian rhythm is generated by the suprachiasmatic nucleus and regulated by the stimulus of light perceived by the retina (Zimmerman and Menaker, 1979; Binkley, 1983). For sight to be possible, binding of a form of vitamin A (retinaldehyde) to rhodopsin, a photopigment of the retina, is required. When struck by light, the retinaldehyde-rhodopsin complex undergoes physical changes that induce a series of chemical reactions. These reactions ultimately generate an electrical signal that travels via retinohypothalamic tract to the suprachiasmatic nucleus (SCN), localized in the hypothalamus. From the SCN, nerve impulses travel via the sympathetic nervous system to the pineal gland (Fig. 2.1).

In chicken, the circadian rhythm is regulated by a multiple oscillator system that consists of endogenous clocks in the retina, in the pineal gland and in the hypothalamus (Cassone and Menaker, 1984; Gwinner and Brandstatter, 2001; Underwood *et al.*, 2001). Direct light stimuli can down-regulate melatonin synthesis on pineal, because an intrinsic oscillator is found within the chicken pinealocytes (Takahashi *et al.*, 1980; Nakahara *et al.*, 1997). Another endogenous oscillator is located in the hypothalamus, and is functionally equivalent to the SCN of mammals (Underwood *et al.*, 2001). In addition, a peripheral synthesis of melatonin happens in the retina, also following a clock-dependent rhythm (Hamm and Menaker, 1980; Bernard *et al.*, 1997; Iuvone *et al.*, 2002). Light stimulus perceived by the retina, also induces a response

affecting melatonin metabolism in the pineal gland of avian, in a similar way it does for mammals (Fig. 2.1).
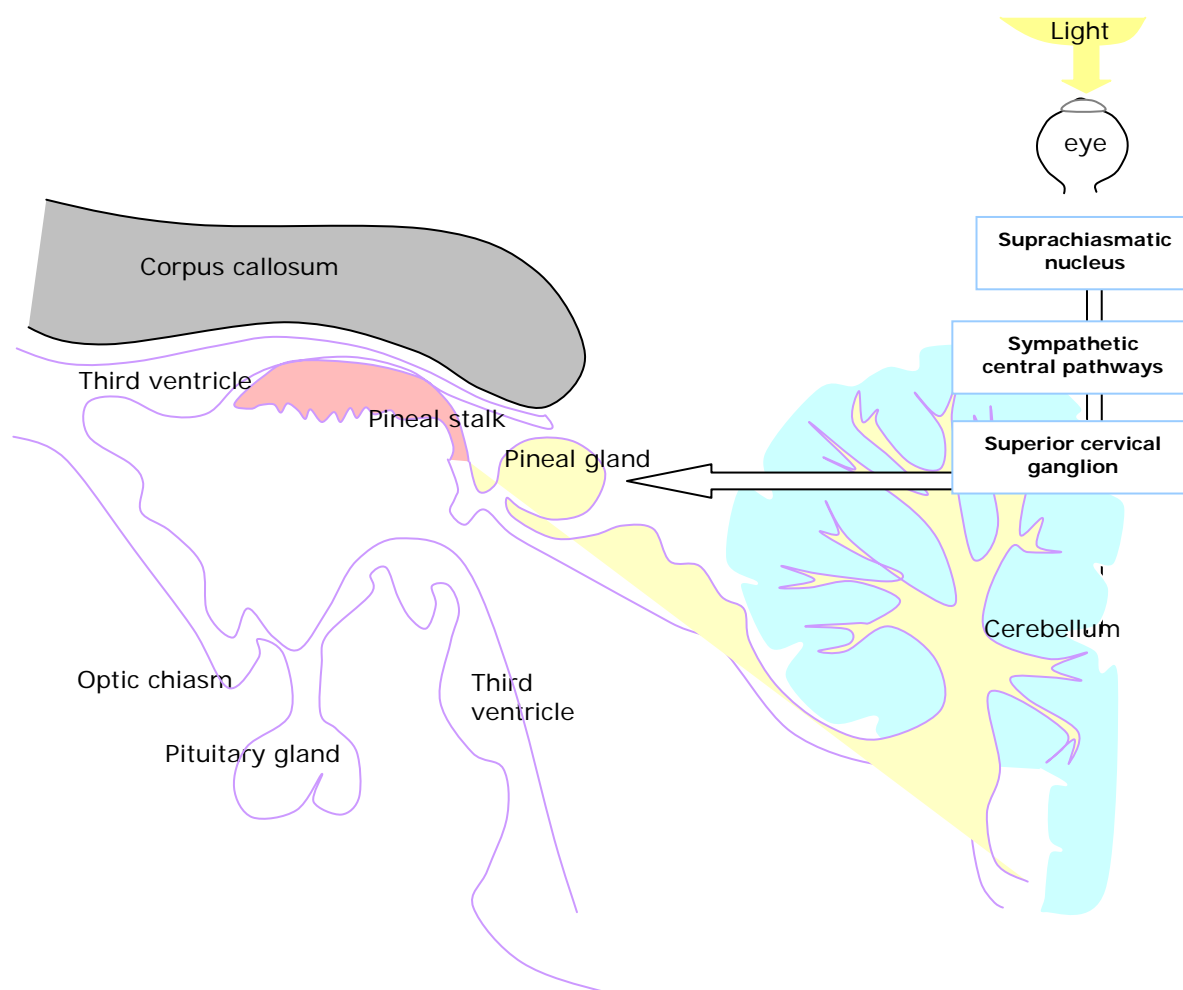
Fig. 2.1: General schema of the pineal gland anatomical location in the brain of avian and mammals. The pineal is localized between the two hemispheres of the diencephalon, attached to the third ventricle. In mammals, ganglion cells in the retina, via the retino-hypothalamic tract, have direct connection to the SCN, the oscillator which regulated the pineal gland (schema on the right side corresponds to mammals). In avians, oscillators are found within the retina, pineal and SCN-like structure, differing from mammals.

The pineal photoreceptors in birds differ from the regular mammalian pineal photoreceptors, having specific associated photopigments distributed on several types of photoreceptors (Okano *et al.*, 2000). Pinopsin, a blue-sensitive photoreceptive molecule, is the predominant photoreceptive pigment found in chicken photoreceptors (Okano *et al.*, 1994), which presents very few rhodopsin and iodopsin positive cells (Korf, 1994). Melanopsin, a novel opsin involved in entrainment of circadian rhythms, has been recently described as a photopigment also occurring in chicken pineal (Chaurasia *et al.*, 2005).

Partial extracranial pineal organs of submammalians are cone-dominated photoreceptors sensitive to different wavelengths of light. Intracranial pineal organs predominantly contain rod-like photoreceptor cells, which are sensitive to very low levels of illumination.

Photo regulation of pineal function in adult mammals is entirely mediated by retinal photoreceptors (Blackshaw and Snyder, 1999). However, phototransduction elements are present in the pinealocytes during embryogenesis and early neonatal life in rat, suggesting that the pineal is directly photosensitive during these periods. Neonatal rats, which had their eyes removed, demonstrated light-induced regulation of the pineal gland serotonin levels (Zweig *et al.*, 1966). In rat, the pineal is underneath a thin neonatal skull and receives more incidence of light than the retina, as the eyes of the newborn rats remain closed for three weeks. Besides, crucial neurons for phototransduction in the retina do not develop until the second to the third week of life (Cepko, 1996). However, in primates the pineal gland does not detect light and retinal photoreceptors do not produce melatonin (Klein, 2004).
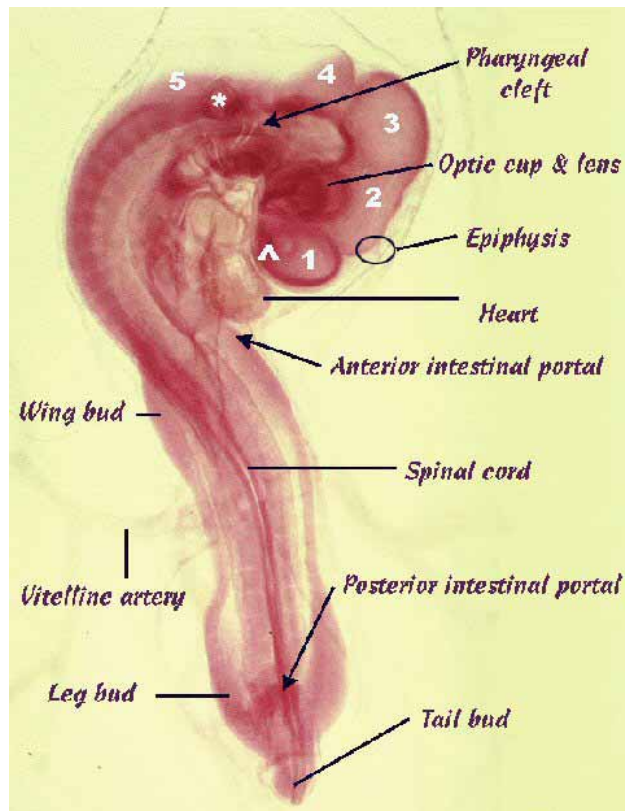
Fig. 2.2: Lateral view of a 72 h chick embryo. By this embryonic stage, the chick pineal is already outlined on the roof of the diencephalon (circle). 1 = Telencephalon; 2 = Diencephalon; 3 = Mesencephalon; 4 = Metencephalon; 5 = Myelencephalon; * = Otic capsule; ^ = Olfactory pit.

2.1.1.1   Chicken pineal gland structure and development

A detailed description of the chick pineal embryogenesis was published by Calvo and Boya (1978). The chick pineal appears outlined on the roof of the third ventricle of the diencephalon by embryonic day 3 (E3), and becomes attached to the same by a small stalk during development (Fig. 2.1; Fig. 2.2). The evagination of the roof of the third ventricle forms the pineal recess (R); which has ample communication with it. By E5, mammilliform projections appear on the pineal outline, in the opposite site of the lumen of the recess (Fig. 2.3, a). By E7, these mammilliform projections develop into vesicles by the appearance of a central lumen (Fig. 2.3, a-b). Mesenchyme forms the connective tissue stroma of the gland; it starts to envelop vesicles by this stage. By E8 until E10, the pineal organ is under intensive proliferation, showing an increase in the number and size of vesicles. By E11 and 12, remarkable pineal growth is observed, achieving a volume which will slightly increase until the end of the embryogenesis.

The mechanism of vesicle formation is based in mammilliform projections of proliferating cells, which migrate through interruptions of the basal lamina of the outline of the recess and follicles (Fujieda *et al.*, 1997). Cells outside the basal lamina or inside the pineal lumen present the highest differentiation activity in relation to the rest of the epithelium, as found during development of the rat pineal with the marker synaptophysin (Fujieda *at al.*, 1997). A rosette cell arrangement is characteristic of these migrating mammilliform projections, cells which will fill the future central cell lumen of vesicles (Fig. 2.3, b).

The vesicles become follicles by the reorganization of their cells into two layers and, by the thickening of their walls. This transformation happens by E11, when columnar cells with ovoid nucleus become radially orientated in relation to the lumen, forming a distinct layer surrounded by smaller cells with spherical nuclei, which are adjacent to the basal lamina (Fig. 2.3, d). By E11, basal lamina surrounds the recess and the follicles. From the lumen to the basal lamina, the first layer of cells comprises the follicular region. The next distinct layer of cells, pursuing a rounded shaped nucleus, comprises the parafollicular zone (Fig. 2.3), according to Boya and Zamorano (1975). Vesicles are classified as primary, secondary and tertiary. The primary vesicles are the ones initially formed on the walls of the pineal recess, and the secondary are originated from the walls of

these primary vesicles (Fig. 2.3, a-c). Tertiary vesicles are originated from cells of the parafollicular region of structured follicles and recess (Fig. 2.3, d). Therefore, before E11, the vesicles belong to the primary and secondary order. By E11, the communication of the recess with the ventricular lumen becomes narrow and is strangulated from E12 onwards.

By E13 onwards, the parenchyma grows progressively and the pineal organ develops a compact aspect, which is characteristic of the post-hatching life (Fig. 2.4, C). By E14 onwards, the parafollicular zone expands, which contributes for the densification of the pineal, and the recess extends caudally into the pineal stalk. From E15 onwards, cell differentiation is the main developmental event occurring until the end of the embryogenesis. From E19 until hatching, no morphological variation is observed.

The chick pineal gland presents sympathetic noradrenergic innervation, therefore, reduced cholinergic input (Sato *et al.*, 1988). The number of neurons (pineal ganglion cells) varies markedly with within avian species (Sato and Wake, 1981), but so far, only AChE-positive neurons have been identified.

The pineal gland structure resembles the retina of the eyes, containing neurosensory ciliary photoreceptor cells, sensory nerve cells, and supporting elements. Both pineal and the eyes are derived from the diencephalon roof, however, from different regions of the neural plate. Briefly, pineal development initiates as the diencephalic roof protrudes to make contact with the epidermis (Fig. 2.4, A), secondary projections of the primary evagination form follicles and, after an intensive proliferative period, cell differentiation takes place (Fig. 2.4, B-C). The eye development also begins by an evagination of the diencephalon, forming the optic vesicle (Fig. 2.4, a). This evagination is followed, however, by an invagination of the distal part of the primary vesicle (Fig. 2.4, b). The optic vesicle also induces the formation of the lens from the ectoderm (Fig. 2.4, c). During pineal organ embryogenesis no invagination happens, therefore, differing from the eye formation.

During closure of the neural tube, the eye field is located on the most antero ventral part of the neural tube, while the pineal is placed on the dorsal diencephalon (Fig. 2.5).
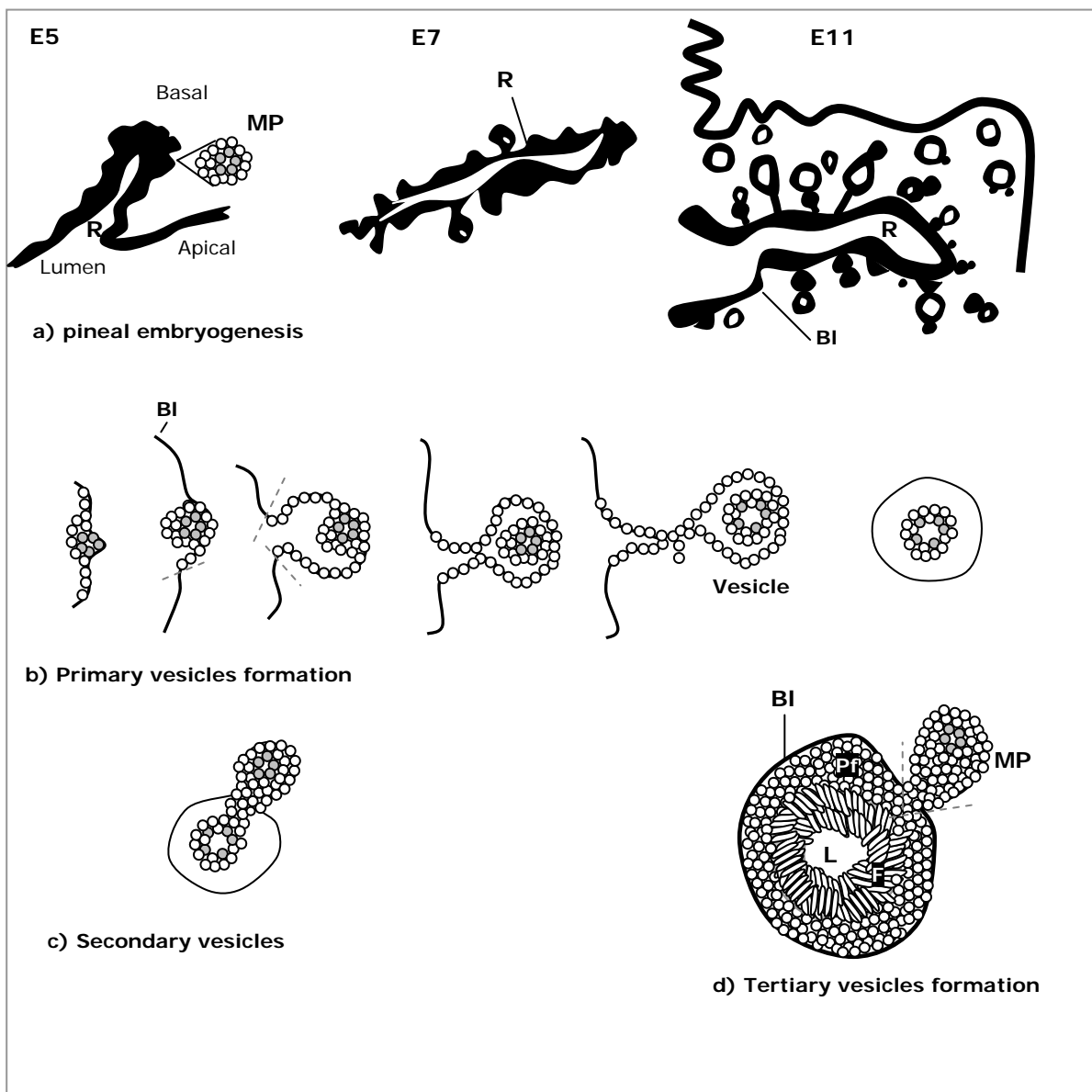
Fig. 2.3: Embryogenesis of the chick pineal gland. a) E5, E7 and E11 are periods of intensive vesicles formation. Mammilliform projections, initiated by a rosette of cells (grey), give rise to new vesicles: b) primary vesicles, derived from the recess; c) secondary vesicles, developed on the walls of the primary vesicles; d) Tertiary vesicles, originated from the cells of the parafollicular zone of structured follicles. Bl = basal lamina; (--) basal lamina interruptions; F = follicular region; L = lumen; MP = mammilliform projections; R = recess.
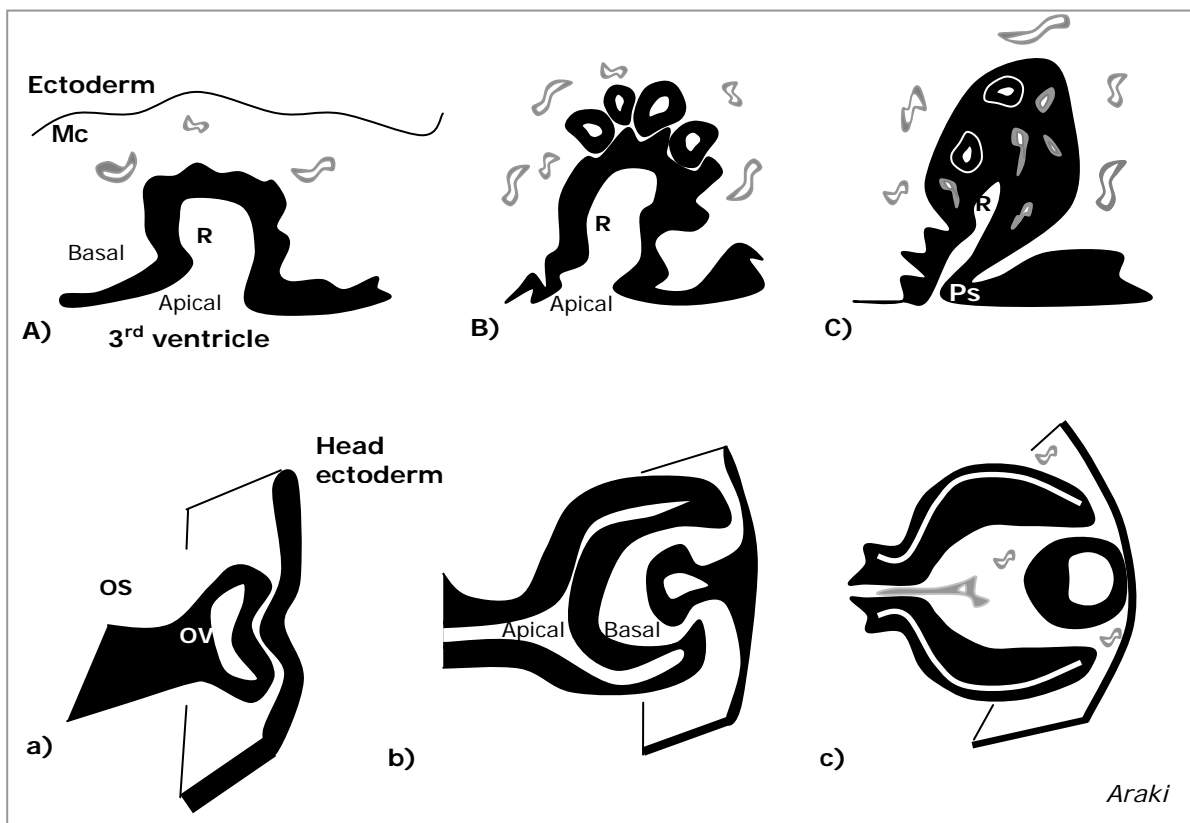
Fig. 2.4: Pineal and eye development. A) Evagination of the diencephalon. B) Follicles formation. C) Pineal towards the end of the embryogenesis, mainly cell differentiation happening. a-b) Evagination of the diencephalon, and invagination of the optic vesicle of the eye. c) Lens formation. Mc = mesenchymal cells; OS = optic stalk; OV = optic vesicle; Ps = pineal stalk; R = recess.
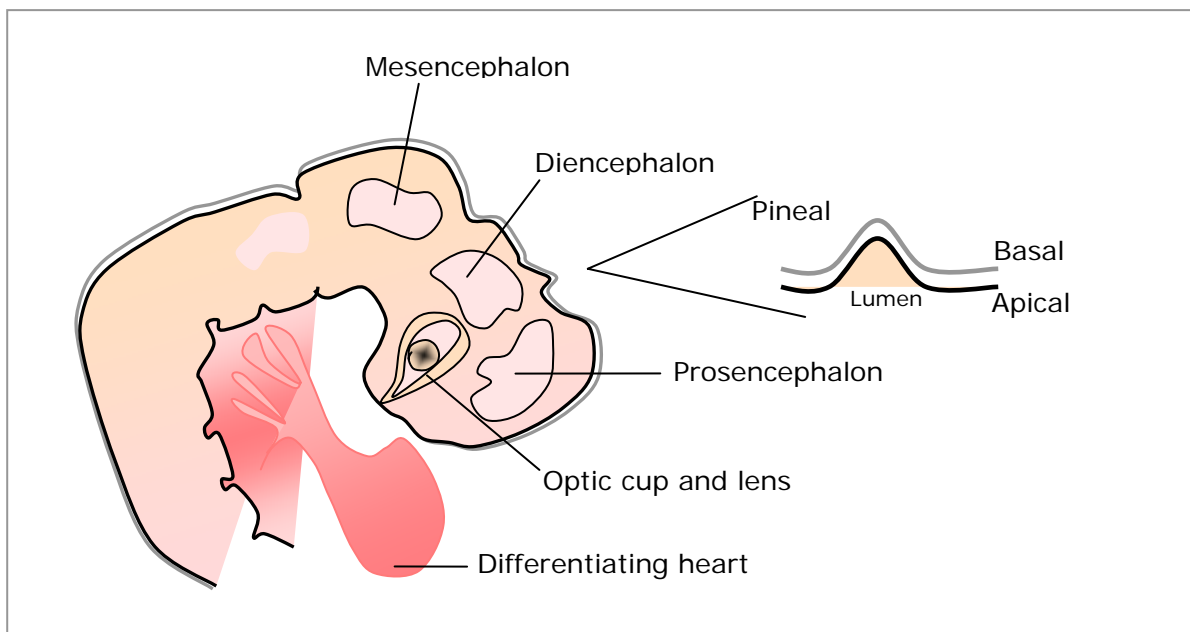
Fig. 2.5: Schema of a side view of a 60 h chick embryo. Brain segments, location of the eye, and pineal gland.

2.1.2 Approach and aims

The pineal gland has a great relevance on sustaining physiological processes following a circadian rhythm. It is known that acetylcholinesterase is expressed in the mature pineal gland of several organisms, although, the link of pineal gland metabolic processes to this enzyme is not clear. Development can provide one of the answers for the relevance of AChE expression in pineal gland. However, AChE expression has not been, until now, characterized during pineal embryogenesis. Therefore, to test this hypothesis, I conducted a close investigation of cholinesterases activity during chick pineal embryogenesis in relation to developmental events.

Cell proliferation, cell differentiation and cell apoptosis are correlated events, which are essential for development. The spatio-temporal distribution of BChE and AChE-positive cells was compared to the above-mentioned events during chick pineal embryogenesis, using markers for cell proliferation, differentiation, and apoptosis.

AChE and BChE histochemistry and BChE immunohistochemistry were conducted on pineal organs from several embryonic stages. Proliferative states of the chick pineal were investigated using two markers: PCNA and BrdU, for G1-S and S phases of the cell cycle, respectively. The combined information given by these proliferation markers was compared to the BChE histochemistry in parallel pineal sections.

Immunolabeling with an anti-vimentin antibody was conducted to detect potential glia cells in the chick pineal. Photoreceptors differentiation was followed by immunohistochemistry of a photopigment molecule (pinopsin), and compared to AChE histochemistry in parallel pineal sections. Apoptosis was followed by TUNEL assay and compared to AChE activity revealed by histochemistry.

2.2   Methodology

Histological studies were performed on chick pineal gland (*Gallus gallus*). Chicken was chosen as model organism for this work because of the easy accessibility to embryos. Chick embryos need a relative short period (21 days) to complete embryogenesis and, fertilized eggs can be conveniently incubated to develop until the desired period for experimentation.

The fertilized eggs were obtained from a local supplier and incubated in a humid incubator at 38°C. Chicks' embryonic stages were determined according to the Hamburger and Hamilton (Hamburger and Hamilton, 1951) criteria. Pineal from the embryonic stages E7 until E20 were investigated. After decapitation, pineals were removed and fixed in 4% paraformaldehyde (PFA) for 2-4 hours at room temperature, depending on the embryonic day of the pineal, washed in PBS 3 x for 15 min, and kept in 30% sucrose solution at 4°C. PFA preserves most of the structures detectable at the confocal microscope level and sucrose increases the osmolarity of the tissue, avoiding dehydration at low cryostat temperatures.

2.2.1 Tissue sectioning in microtome

Pineals, stored in 30% sucrose, were placed in a frozen platform with Tissue Tek medium at −28°C. Sagittal sections of frozen tissue were cut with thickness of 8, 12 and 18 µm, according to purpose, in an Ultracut S microtome. Sections were mounted either in superfrost or 0.5% gelatin coated slides.

2.2.2 Histochemistry for AChE and BChE activities

Histochemistry was performed on 18 µM thick sections. Frozen slides were placed in 0.1 M Tris-maleic buffer for 10 min, before staining.

2.2.2.1   Preparation of Karnovsky-Roots staining solution

According to the Karnovsky and Roots (1964) method, for the staining solution, 37 mg of ATC (for AChE staining) or 50 mg of BTC (for BChE staining) were added to 32.5 ml of 0.1 M Tris-maleic buffer, pH 6.0. For a final volume of 50 ml, 2.5 ml of 0.1 M sodium citrate ($C_6H_5Na_3O_7$ x $2H_2O$), plus 5 ml of 30 mM cupper sulphate ($CuSo_4$), were added, respectively, drop wise to the initial solution under stirring. Distilled H_2O was added (4.5 ml for the AChE staining and 4.75 ml for the BChE staining) before the inhibitors, 10 mM Iso-OMPA (500

µl for AChE staining) or 10 mM BW284C51 (250 µl for BChE staining). To finalize, 5 ml of 5 mM $K_3Fe(CN)_6$ were added drop wise under stirring. Slides were incubated for 3 h at 37°C under dark. To finalize the reaction, slides were washed 2x for 10 min with distillate H_2O. For negative controls, neither of the substrates nor inhibitors were used.

2.2.3 Direct and indirect methods used for immuno- and histochemical labeling

a) Indirect labeling with Avidin-biotin-peroxidase complex (ABC) method was performed as a non-fluorescent labeling for PCNA and pinopsin immunohistochemistry.

b) Indirect labeling with binding of a primary antibody to the epitope of interest, followed by a fluorescein isothiocyanate conjugate (FITC) or $Cy^{TM}3$ labeled secondary antibody, was used for the BrdU, vimentin and BChE stainings.

c) Direct labeling was performed with fluorescent nucleotides (d-UTP) that were incorporated into the DNA, or with a fluorescent dye (DAPI), for apoptosis and cell nucleus staining, respectively.

2.2.4 Cell nucleus staining with DAPI

DAPI (4´, 6-Diamidin-2-phenylidol-dihydrochlorid) was used for cell nucleus staining in combination with Karnovsky-Roots staining or immunostainings. DAPI was used at the concentration of 0.1 µg/ml in PBS (200 µl/slide, 3 min incubation followed by 10 min in PBS) as the last step of double stainings. DAPI is a fluorescent dye which emits blue fluorescence when bound to A-T (adenine-thymine) base pars of the double strand DNA.

2.2.5 Immunochemical stainings

All antibodies were characterized either by the company suppliers or by the scientists who developed them (Table 2.1). The specificity of the immunoreactivity was tested omitting the primary antibody from the protocols. In all cases, it resulted in absence of specific immunostaining.

Antigen Target	Antibody	Host	Dilution	Supplier/ Collaborat.
Primary Antibodies				
BChE mAb/7D11	monoclonal	mouse	1:500	Tsim *et al.*, 1988.
BrdU	monoclonal	mouse	1:10	Roche
PCNA (Clone PC10)	monoclonal	mouse	1:2500	DAKO
Pinopsin	monoclonal	mouse	1:250-1:500	Okano *et al.*, 1997.
Vimentin	monoclonal	mouse	1:100	Boehringer
Secondary Antibodies				
Cy^{TM}3	IgG (H+L)	rabbit	1:100	DIANOVA
Anti-mouse Ig-fluorescein	IgG (H+L)	sheep	1:10	Roche
Anti-mouse IgG (biotinylated)	IgG (H+L)	horse	1:200	Vector Lab

Table 2.1: Antibodies used for Immunohistochemistry.

2.2.5.1   *Pinopsin labeling protocol*

To follow photoreceptors differentiation, an antibody for the N-terminal region of chicken pinopsin was used. Frozen sections, 12 μm thick, were treated with 3% H_2O_2 in methanol for removal of intrinsic peroxidase activity and washed 3 x 5 min with PBS. Slides were blocked for 1 h at room temperature with PBS containing 0.02% Triton and 1.5% normal horse serum. 4-8 μg/ml of anti-pinopsin antibody (P1) IgG, raised in mice, were used for immunohistochemistry. After incubation with the primary antibody (overnight at 4°C), slides were washed in PBST 0.02% and incubated with the secondary antibody, biotinylated anti-mouse IgG (H+L), 1:200 in blocking solution, for 30 minutes at room temperature. The Vectastain Elite ABC anti-mouse IgG kit contained the secondary antibody and the avidin peroxidase conjugate and biotinylated horseradish peroxidase H reagents, which were used according to manufactures instructions. Avidin is an egg-white derived glycoprotein with a high affinity for biotin. Thus, it binds the biotinylated secondary antibody (Fig. 2.6). The peroxidase activity was revealed with the VIP substrate kit, which produces an intense purple precipitate. The reaction was terminated by washing the slides in water for 10 min. For the negative control, anti-pinopsin was replaced by mouse-IGg.

2.2.5.2   *Immunostaining for cell proliferation with PCNA*

Monoclonal mouse anti-proliferating cell nuclear antigen (PCNA) was used to detect proliferating pineal cells. PCNA is a 36 kDa multifunctional protein originally defined as cyclin because it was found expressed at high levels in cycling cells during the last 5% of the G1-phase and the first 35% of the S-phase of the cell cycle. PCNA is therefore, expressed only in proliferating cells and is absent in resting cells (Hall, 1990).

Procedure: After removal of intrinsic peroxidase activity (like for the pinopsin staining), 8 µM thick slides were blocked for 1 h at room temperature with PBS containing 0.03% Triton and 20% normal horse serum. After blocking, slides were incubated with PCNA antibody (1:2500) in 1.5% normal horse serum PBST 0.03%, overnight at 4°C. Secondary antibody, biotinylated anti-mouse IgG, was diluted 1:200 in 1.5% normal horse serum PBST 0.03% and incubated for 30 minutes at room temperature. An avidin peroxidase conjugate system was used to amplify the positive immunoreaction (Fig. 2.6). The peroxidase activity was revealed with the VIP substrate kit, producing an intense purple precipitate.
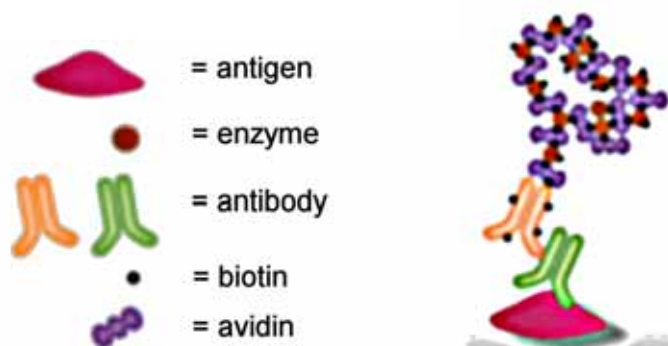
Fig. 2.6: Indirect labeling with avidin-biotin-peroxidase complex. A biotinylated secondary antibody binds to the primary antibody for the specific antigen. The avidin peroxidase conjugate binds to the biotin. Its activity is revealed by a peroxidase substrate.

2.2.5.3   *Immunostaining for cell proliferation with the BrdU antibody*

BrdU (5-Bromo-2´-deoxy-uridine) is a thymidine analog, which can be incorporated into DNA during the synthesis (S) phase. BrdU labeled DNA was detected using a monoclonal antibody against BrdU and fluorescein isothiocyanate conjugate (FITC) anti mouse IgG second antibody (Fig. 2.7).

Procedure: Chicken embryos received an *in vivo* BrdU treatment. The amount of BrdU used was related to the weight of the developing embryo, based on

Romanoff (1939). For each g weight, circa 15 µl BrdU were injected in the allantois of the embryos, which were placed for 2.5 h in an egg incubator at 38°C, under dark. After incubation, the pineal glands were removed, washed 3 times with PBS and fixed in PFA 4% for 2-3 h at room temperature. After fixation, pineals were incubated for 1 to 7 days at 4°C in PBS solution with 30% sucrose. Frozen sections, 12 µM thick, were incubated with a solution of 50 mM glycine in 70% ethanol for 20 min at -20 °C. Before immunostaining slides were incubated with blocking solution (10% horse serum in PBS) for 30 min at RT. The staining procedure was basically conducted according to the "5-Bromo-2´-deoxy-uridine Labeling and Detection Kit" manufactures instruction. Slides were incubated for 30 min with 100 µl of primary antibody at 37°C. After incubation with primary antibody, slides were washed in PBS, 3 x for 5 min, and incubated with the secondary antibody for 30 min at 37°C. Slides were washed 3 x for 5 min with PBS and results were captured by confocal scanning microscopy. Negative staining controls were performed without the first antibody.
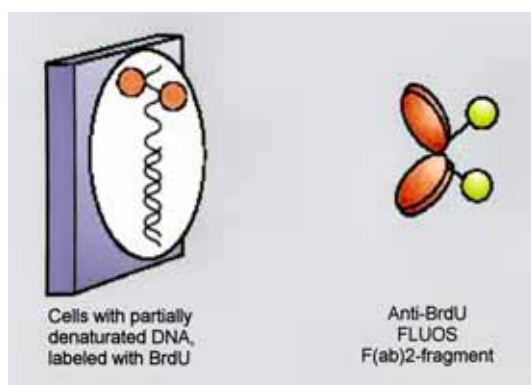
Fig. 2.7: BrdU labeling principle. The antibody conjugate (anti-BrdU-fluorescein) binds to BrdU-labeled DNA.

2.2.5.4   *Vimentin and BChE immunohistochemistry*

Frozen sections, 12 µm thick, were blocked for 10 min at room temperature with PBS containing 1% bovine serum albumin (BSA) and 0.1% Triton. 200 µl of the anti-vimentin antibody or of the mAb antibody for BChE, diluted (1:100) in blocking solution, were added to each slide. Slides were incubated at RT for 45 min for vimentin and 2 h for the BChE immunostaining. 200 µl of the secondary antibody Cy^{TM}3, diluted 1:100 in blocking solution, were added to the slides after two washing steps (PBS 3 x for 10 min). Slides were incubated at RT for 60 min, washed in PBS and stained with DAPI as previously described.

2.2.6 Apoptotic cells labeling

The enzyme terminal deoxynucleotidyl transferase (TdT) is able to label blunt ends of double-stranded DNA breaks independent of a template. The end-labeling TUNEL assay (TdT-mediated XdUTP end labeling) is based on this principle. The use of fluorescein-dUTP to label the DNA strand breaks allows the detection of the incorporated nucleotides directly with a fluorescence microscope.

To allow exogenous enzymes to enter the cell, the plasma membrane was permeabilized prior to the enzymatic reaction. To avoid loss of LMW DNA from the permeabilized cells, cells were re-fixed with 4% formaldehyde, for 5 min, before permeabilization. This fixation cross links LMW DNA to other cellular constituents and avoids its extraction during the permeabilization step. To enhance permeanilization of the slides, they were placed in a jar containing 200 ml of 0.1 M citrate buffer, pH 6.0, and heated in a microwave oven; 350 W (high) microwave irradiation for 4 min. For rapid cooling, 80 ml of distillated water was added, and slides were then transferred into PBS (20°–25°C). Slides were blocked for 30 min at room temperature (RT) with a blocking solution containing 0.1 M Tris-HCl pH 7.5, 3% BSA, and 20% normal horse serum. The slides were rinsed twice with PBS at RT and excess fluid was drain off.

Procedure: after fixation and permeabilization, 50 µl of TUNEL reaction mixture, containing TdT and fluorescein-dUTP, were applied to the sections and slides were incubated for 60 min at 37°C in a humidified atmosphere. During this incubation step, TdT catalyzes the attachment of fluorescein-dUTP to free 3′OH ends in the DNA (Fig. 2.8). At the end, slides were rinsed three times in PBS (5 min for each wash) and evaluated under a laser scanning confocal microscope (Leica). For staining controls, the enzyme TdT was omitted from the protocol.
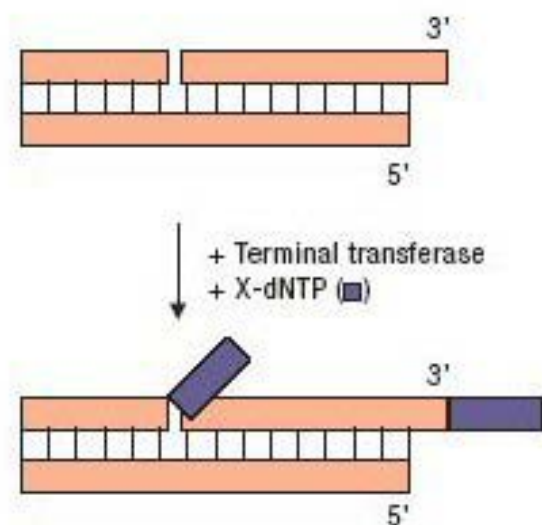
Fig. 2.8: Schematic illustration of the TUNEL DNA end labeling method. The enzyme "terminal deoxynucleotidyl transferase" (TdT) catalyzes the attachment of fluorescein-dUTP to free 3'OH ends in the DNA.

2.2.7 Mounting

Following the staining procedure, sections were left for 40 min over a 37°C hot plate until they got dried or were air-dried overnight at RT. Sections used for conventional light or fluorescence microscopy were mounted with Kaisers-glycerin-gelatin medium and coverslips were applied. For the confocal microscopy, slides were mounted with glycerin or Vectorschield mounting medium (Vector).

2.2.8 Microscopy of labeled sections

A Zeiss-Axiophot microscope and a laser Leica TCS confocal microscope were used for capturing the labeling results. The Zeiss-Axiophot microscope was equipped with epifluorescence and Nomarsky-optics. Images were captured with a digital video camera INTAS.

The Leica was equipped with argon-crypton-laser and the TCS software (http://www.llt.de/TCSNT1.html) was used for capturing images of the confocal microscopy.

2.2.8.1 Conventional and confocal microscopy

In a conventional microscope, light passes through the sample and images from out-of-focus-planes overlap with the focal plane, thus the image sharpness is compromised. Therefore, sharp focus can be achieved with thin specimens only.

Cell density of the chick pineal tissue makes it more difficult to obtain a good resolution with fluorescence labeling than for the cultured cell specimen. General contrast is reduced and weak signal is buried. With the confocal system, most of the out-of-focus-plane signal is restricted by pinholes, resulting in a cleaner background. Detected background could be further reduced in relation to the specific signal.
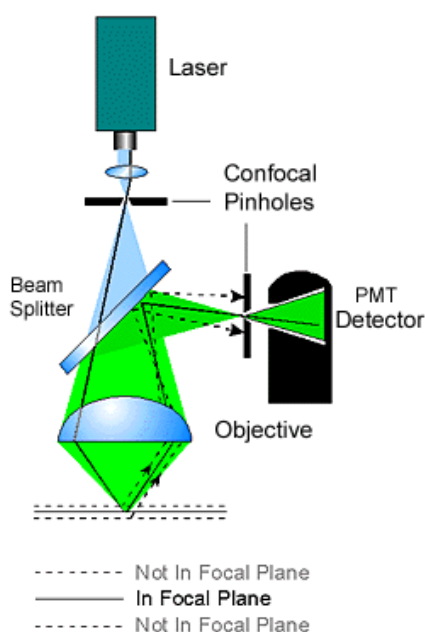
Fig. 2.9: Confocal laser microscopy system.

2.2.9 Image processing

Images were processed using the Jasc Paint Shop Pro 8 program. The modifications were restricted to brightness and contrast to enhance clarity. The only pictures that had the original color altered were those concerning cell nucleus staining (DAPI) to provide a better contrast between cell nucleus shapes.

2.3   Results

The pinealocytes are arranged in follicles surrounding narrow or wide spaces. Sympathetic nerve fibers, denser at the distal portion, penetrate on the walls of the pineal follicles accompanied by blood vessels (Sato and Wake, 1983). Pineal cells, connective tissue, nerve fibers and erythrocytes can be distinguished by "Kernechtrot-Kombinations" staining on a pineal section (Fig. 2.10).

On the structured pineal follicles, two distinct cell zones can be identified. The follicular area (F), surrounding the central luminal space (L), and the parafollicular zone (PF), from where new vesicular walls are originated (Fig. 2.10; A). The structure containing these follicles is called pineal vesicle, and the pineal stalk is located in the most distal part of it. The posterior commissure (PC) can be seen caudally associated to the pineal anlage.
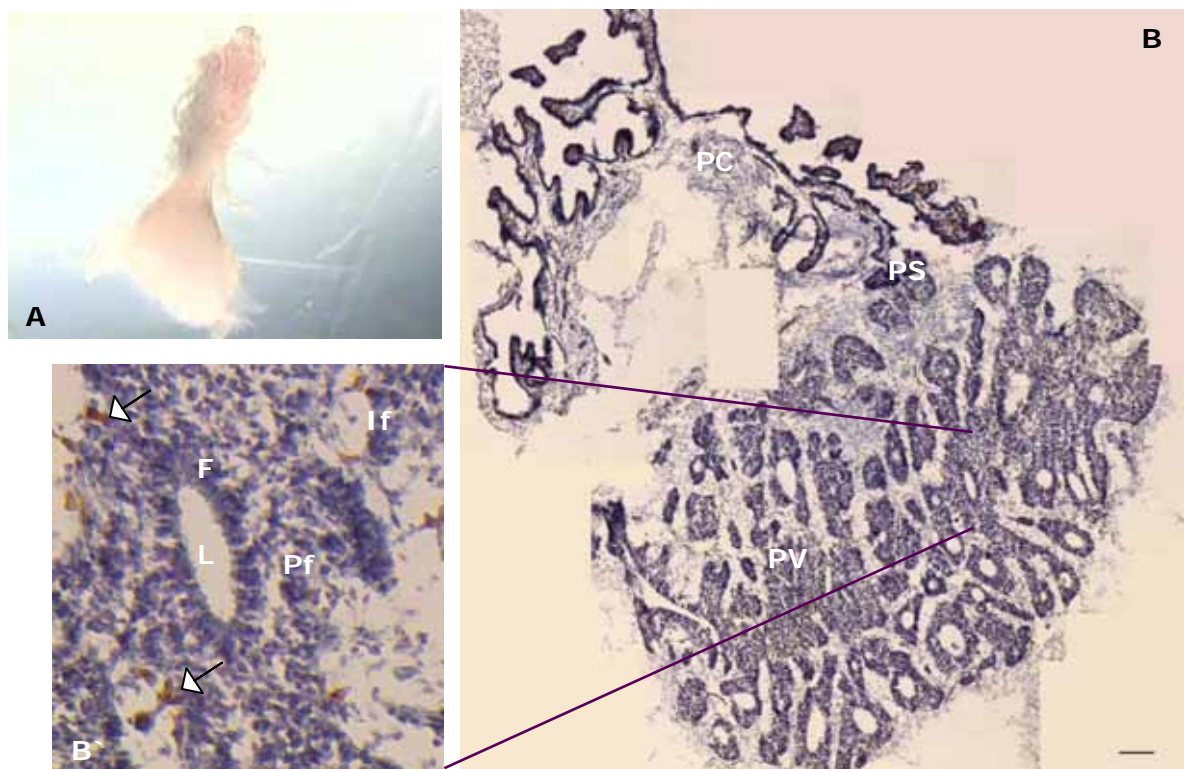
Fig. 2.10: The chick pineal gland structure. (A) Pineal gland of an E18 chick embryo and (B) respective pineal section stained with "Kernechtrot", showing the pineal cells (violet) and connective tissue (blue). (B`) Amplified follicle from image B, arrows indicate erythrocytes and nerve fibers (orange). PC = posterior commissure; PS = pineal stalk; PV = pineal vesicle; F = follicular zone; PF = parafollicular zone; If = interfollicular area. Bar: 100 µm.

2.3.1 Characterization of the AChE and BChE expression patterns during embryonic development of the chicken pineal gland

The distribution of AChE-positive cells has been characterized for the post-hatching chick pineal gland (Sato and Wake, 1984). Here, we characterize AChE and BChE expressions during chick pineal embryogenesis, according to the histochemical method of Karnovsky-Roots (Karnovsky and Roots, 1964).

This methodology is based on AChE and BChE substrate affinities and inhibitors specificity. For the AChE histochemistry, acetylthiocholine (ATC) was used as substrate with the respective BChE inhibitor (IsoOMPA). For BChE staining, the substrate butyrylthiocoline (BTC) was applied, with the respective AChE inhibitor (BW284C51). Once cleaved by these enzymes, the substrates ATC and BTC are split in thiocholine, in both cases, and acetate or butyrate, respectively. Thiocholine reduces ferricyanate to ferrocyanide, which binds to copper ferrrocyanate forming a brown complex. The brownish precipitate will mark the sites of AChE and BChE activity, according to the substrate and inhibitor used during this procedure. A typical result of this procedure can be seen below (Fig. 2.11) in follicles of an 18 days old embryonic chick pineal.
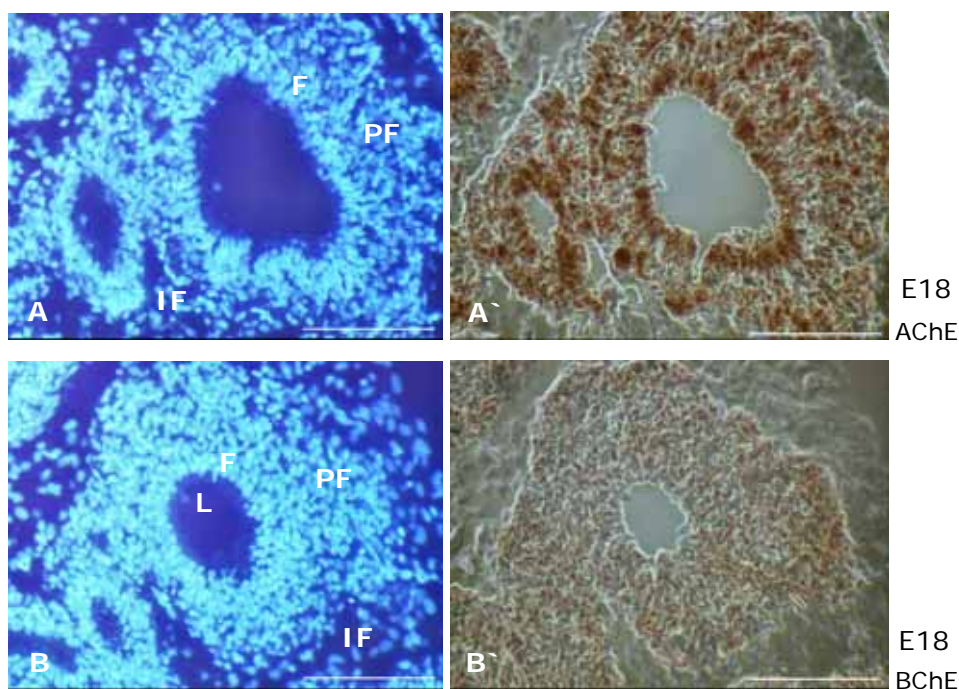
Fig. 2.11: Histochemistry for AChE and BChE, in parallel sections of the chick pineal, with respective DAPI staining (left). (A´) E18, AChE is strongly expressed in cells surrounding the luminal space and parafollicular zone. (B´) No pronounced BChE activity can be seen in the follicle by the same embryonic stage. F = follicular zone; PF = parafollicular zone; IF = interfollicular area. Bar: 100 µm.

Histochemistry for AChE and BChE, revealed a characteristic pattern of expression during chick pineal embryogenesis. Until E11, AChE activity is restricted to a few vesicular cells, while BChE displays a diffuse and intense activity distributed among the pineal vesicles (Fig. 2.12, A-F).

With a close inspection, it is possible to see that AChE fills the future luminal space of vesicular walls, and surrounds the luminal space of vesicles by E9 and E10 (Fig. 2.16, A, C, C`). By E11, with the re-organization of cells into two distinct layers (follicular and parafollicular zone), AChE activity is mostly present between follicular and parafollicular areas of follicles (Fig. 2.17, E). In contrast, BChE activity is intense until E11, particularly in the area surrounding luminal spaces (Fig. 2.16, B, D, D`; Fig. 2.17, F).

AChE and BChE activities are nearly equivalent by E12, as BChE activity starts to decrease and AChE expression to increase by this stage (Fig. 2.13, G-H; Fig. 2.17, G-H`). AChE-positive cells start to organize themselves around the luminal spaces, and also on the borders of the parafollicular zone by this stage (Fig. 2.17, G`). In parallel, vesicles proliferating from the pineal recess and follicular walls display BChE activity (Fig. 2.13, H; Fig. 2.17, H-H`).

From E13 onwards, the increase on AChE-positive cells becomes more evident, specially surrounding the luminal space of the recess (Fig. 2.18, I). The AChE activity by this stage is more pronounced than the BChE activity, which presents a visible decrease in relation to earlier periods (Fig. 2.13, I-J; Fig. 2.18, I-J). This shift on BChE to AChE expression will be addressed later in this chapter.

By E13, the pineal assumes the characteristic shape seen at older stages of development. From this stage until hatching, the pineal volume will not increase in the same proportion as before (Calvo and Boya, 1978); rather differentiation occurs. By E14, AChE activity increases in the parafollicular region and surrounding the luminal space of recess and follicles (Fig. 2.13, K; Fig. 2.18, K). BChE activity has decreased in overall, but remains intense in proliferating vesicular walls (Fig. 2.13, L; Fig. 2.18, L). These expression patterns for AChE and BChE remain basically the same until E17, with intensification of the AChE activity and decrease of BChE activity (Fig. 2.14, M-P). BChE activity remains present in mammilliform projections, and it is low in the rest of the pineal

epithelium (Fig. 2.18, N). Many large vesicles can be seen by E17 (Fig. 2.14, O-P).

From E18 to the end of development, vesicles start to reduce in number (Fig. 2.14, Q-R) and a reinvasion of connective tissue into the gland takes place, as earlier described by Campbell and Gibson (1970). However, by E18, vesicles formation is still in progress on the recess, accompanied by concentrated BChE expression limited to mammilliform projection and borders of the parafollicular zone of some follicles (Fig. 2.14, R; Fig. 2.19, P). From E18 to E20 some follicles close the luminal space and the pineal acquires a compact aspect (Fig. 2.15, S-V). BChE activity reduces gradually, being absent by E19 onwards (Fig. 2.15; Fig. 2.19, P, R, T). AChE, however, becomes even more intense by the end of the pineal embryogenesis (Fig. 2.19, O, Q, and S).

By comparing the histochemical results obtained with pineals younger than 12 embryonic days (Fig. 2.12; Fig. 2.16; Fig. 2.17) with later stages of development (Fig. 2.14; Fig. 2.15; Fig. 2.19), a distinct temporal expression is revealed for BChE and AChE.

To understand which developmental events could implicate this differential expression of ChEs, their expression patterns were investigated in relation to remodeling events during chick pineal gland embryogenesis.

AChE

BChE

A

B

E9

C

D

E10

E

PC

F

E11
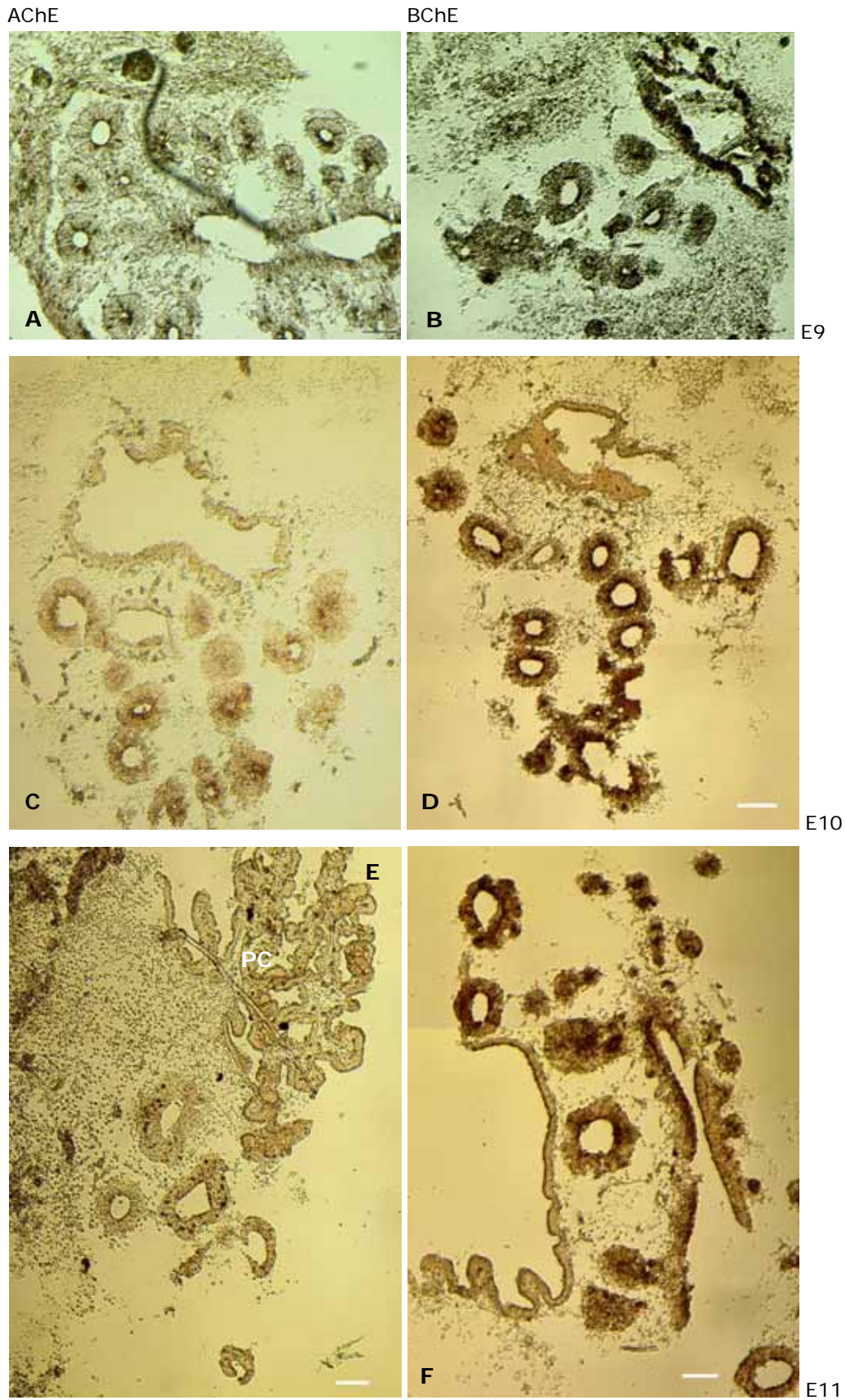
Fig. 2.12: AChE versus BChE histochemistry in parallel sagittal sections of chick pineal organs. By embryonic days 9, 10 and 11, a few AChE-positive cells become detectable (A, C and E, respectively). In contrast, BChE expression is very pronounced on vesicles and pineal recess (B, D and F, respectively). PC = posterior commissure. Nomarsky optics; bar: 100 µm.
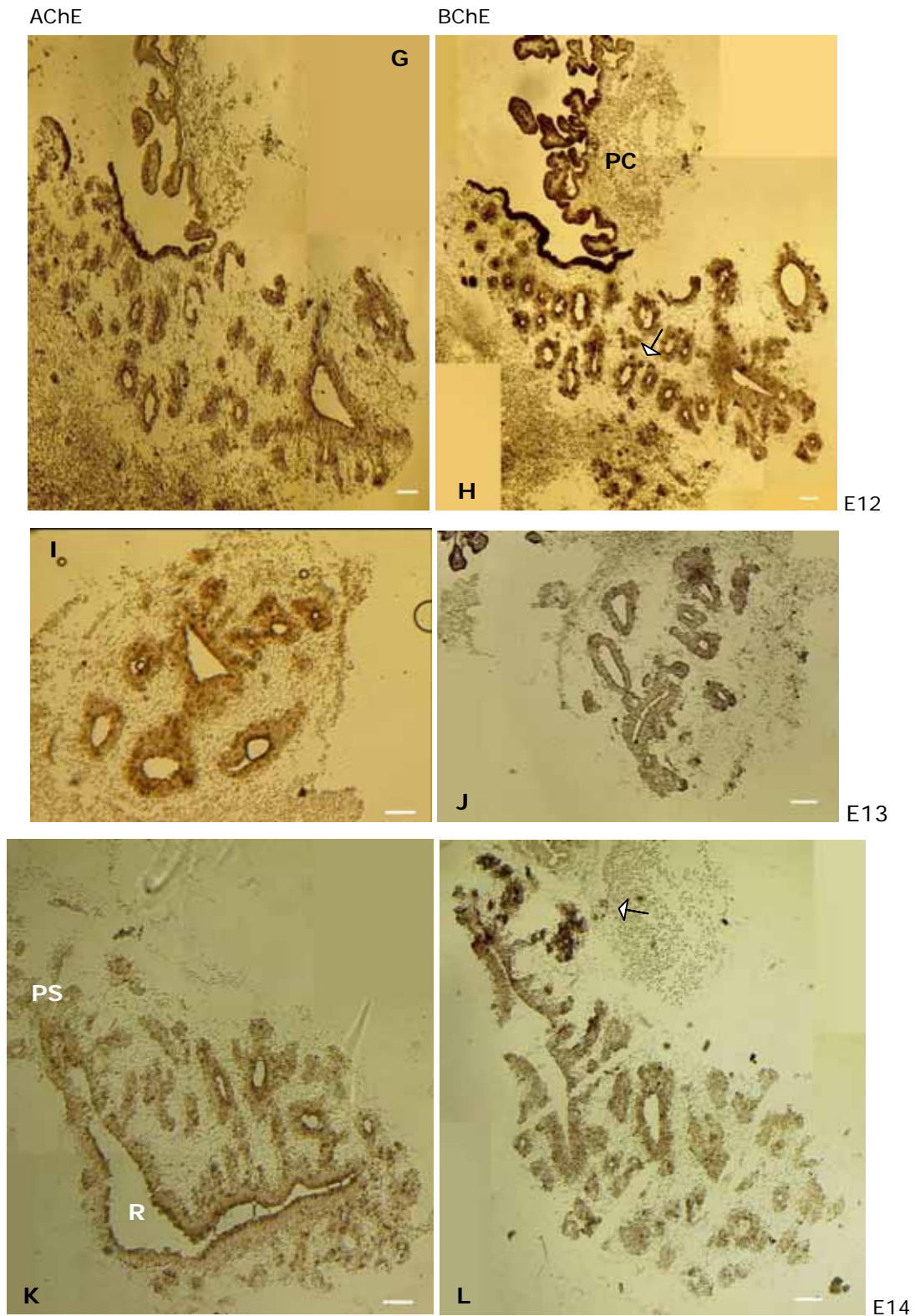
AChE

BChE

Fig. 2.13: AChE versus BChE histochemistry in parallel sagittal sections of chick pineal organs. From embryonic day 12 onwards (E12, G-H; E13, I-J; E14, K-L), BChE expression gradually diminishes and AChE increases drastically towards development of the chick pineal. However, BChE activity still remains prominent in proliferating follicles (arrows), by E12 (H) and E14 (L). PC = posterior commissure. Nomarsky optics; bar: 100 μm.
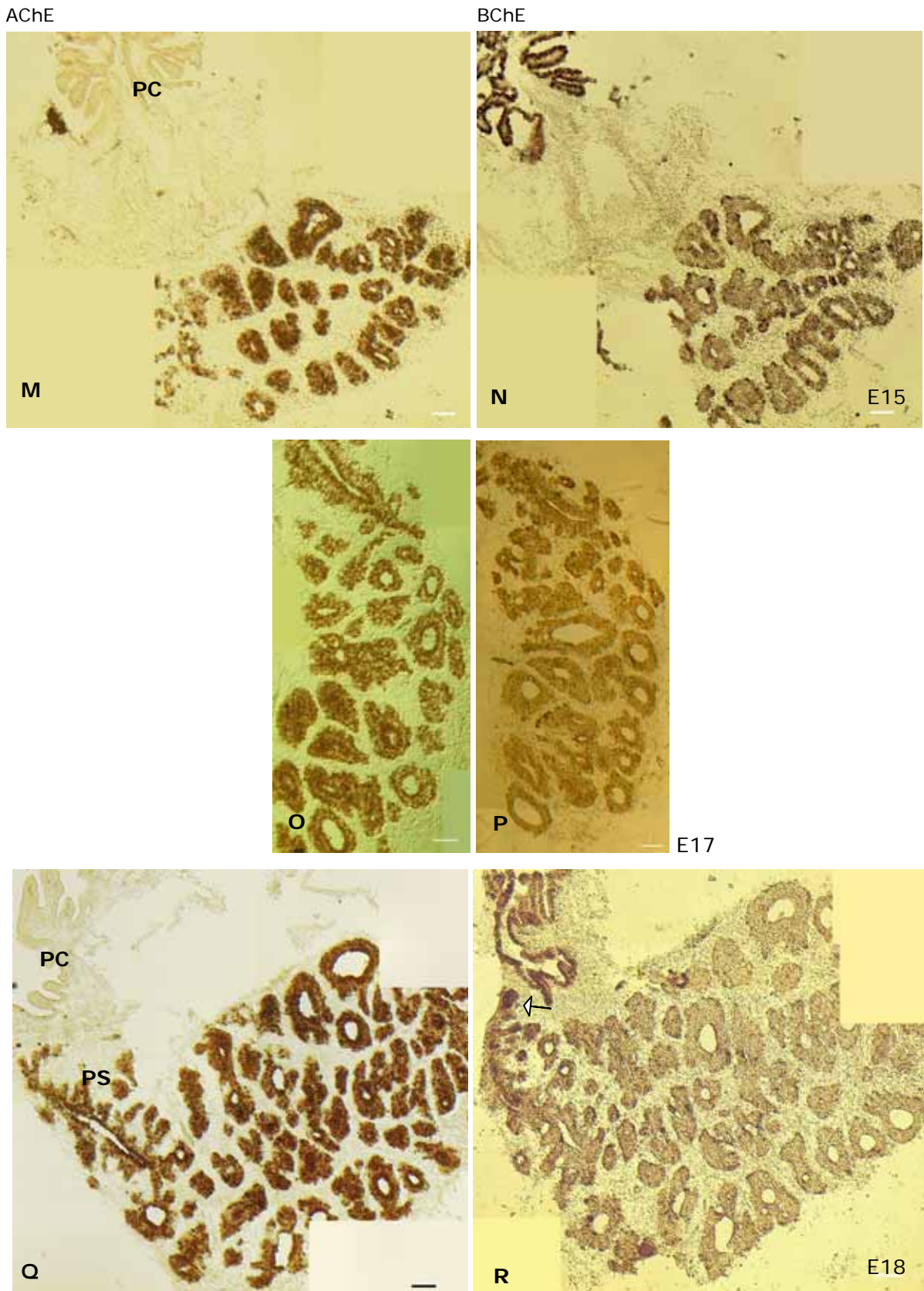
AChE

BChE

Fig. 2.14: AChE versus BChE histochemistry in parallel sagittal sections of chick pineal glands. From E15 (M, N) to the end of the embryonic development of the chick pineal, the shift on cholinesterases expression becomes clearer. BChE activity continues to decrease from E15 until E18 (N, P, R). From E15 to E18 (M, O, Q, S) an intensive activity of AChE can be seen on the follicles and on the pineal recess (PS). A progressive regression of the number of vesicles starts at this stage. PC = posterior commissure. Nomarsky optics; bar: 100 µm.

AChE

BChE

S

T

E19

U

V

E20
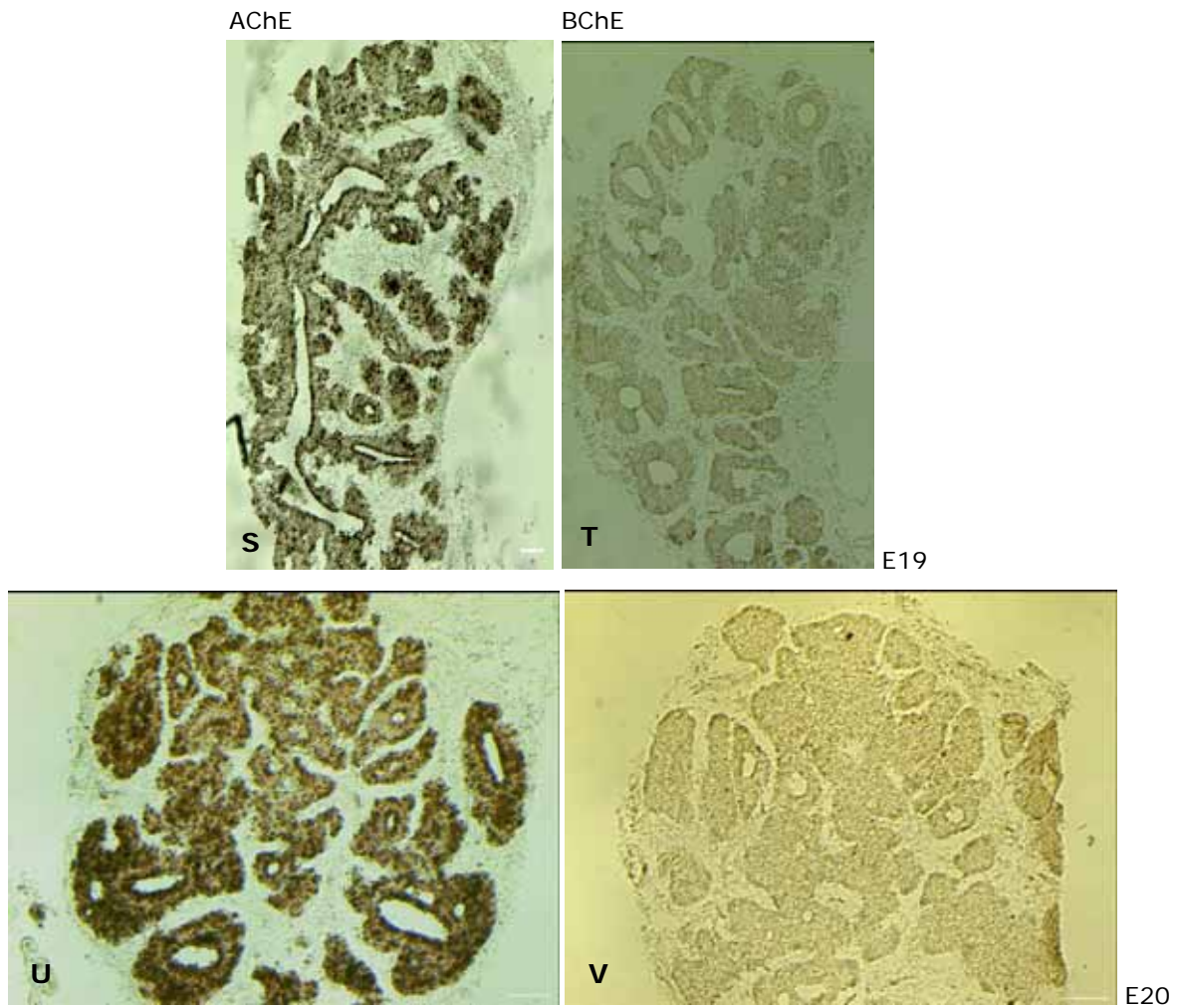
Fig. 2.15: AChE versus BChE histochemistry in parallel sagittal sections of chick pineal glands. Basically no BChE activity is found by E19 and E20 (T, V), while a very intensive activity of AChE is revealed (U); showing an inverse pattern in relation to early embryonic stages. Nomarsky pictures; bar: 100 µm.
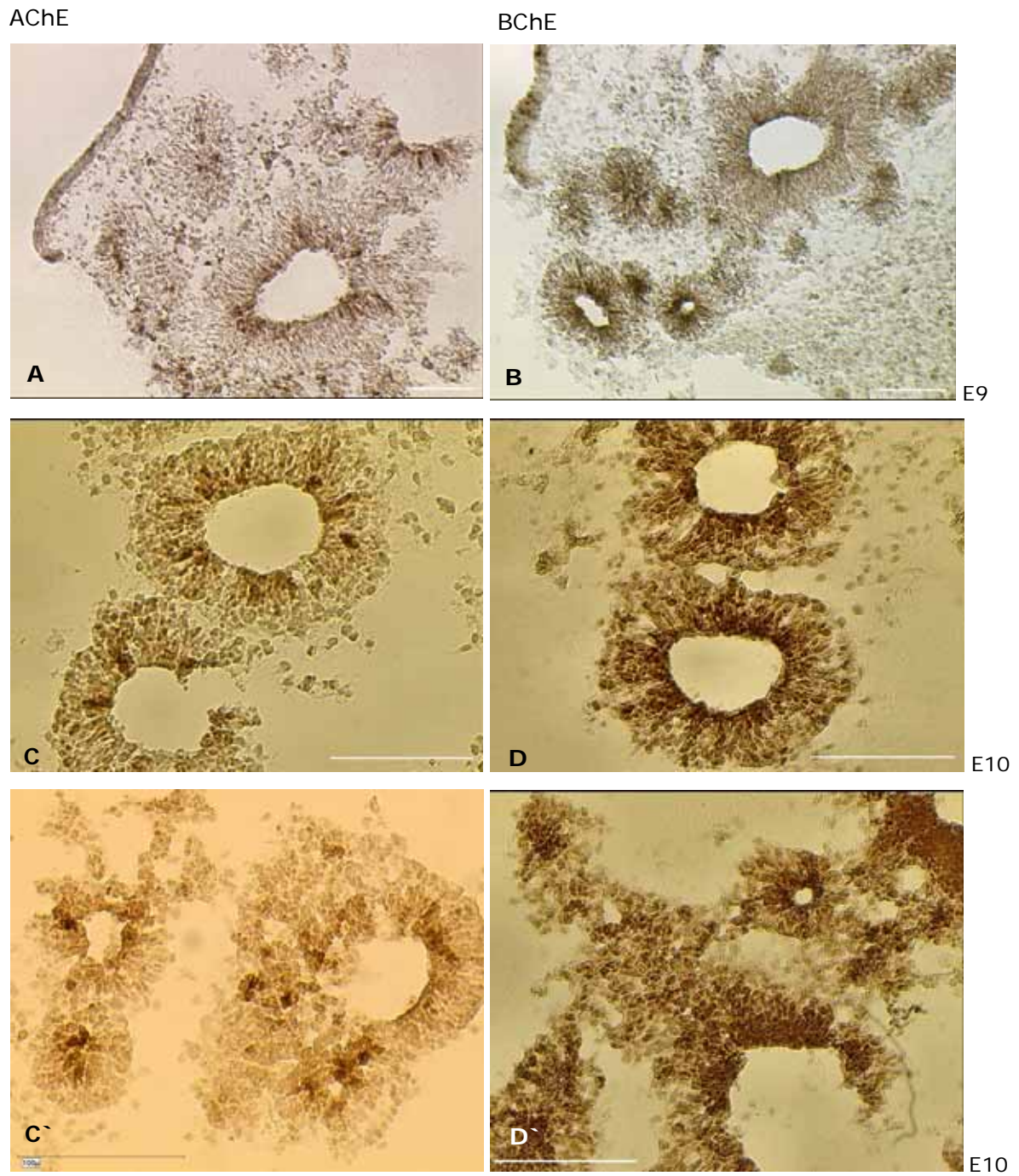
AChE

BChE

Fig. 2.16: AChE (left) and BChE (right) histochemstry in sagittal sections of the chick pineal organ. By E9 and E10, a few AChE-positive cells surround the luminal space of vesicles (A, C and C`). In contrast, BChE expression is strong among vesicles and pineal recess (B, D and D`). Nomarsky pictures; bar: 100 µm.
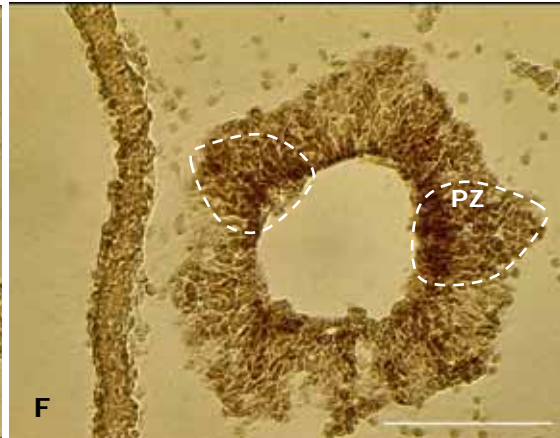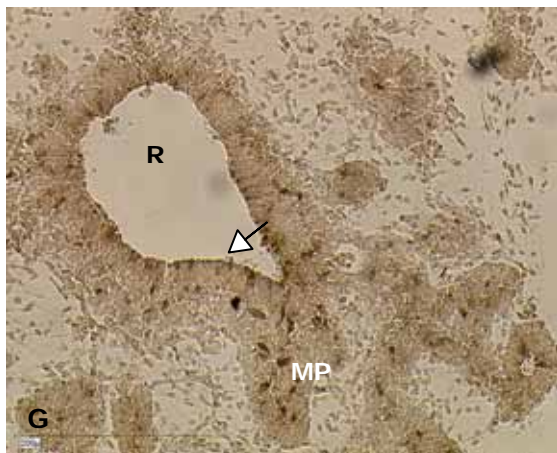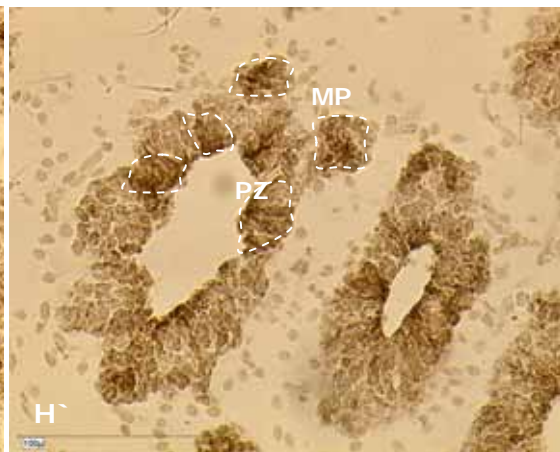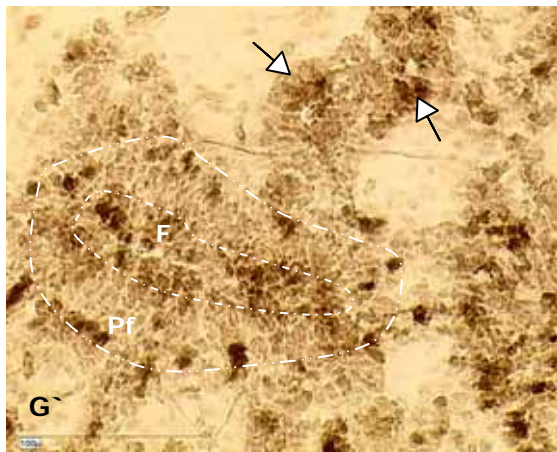
AChE

BChE

Fig. 2.17: AChE (left) versus BChE (right) histochemistry in sagittal sections of chick pineal glands. By E11, follicular (F) and parafollicular (PF) zones of cells can be distinguished. AChE is mainly concentrated in parafollicular cells (E), while BChE activity is strong in the cells surrounding the luminal space of follicles (F). By E12, AChE-positive cells are present in the parafollicular zone and also surround the luminal space (arrows) of the recess and follicles (G-G`). By this stage, BChE activity is mostly concentrated in mammilliform projections (MP) of the recess (H) and on proliferating follicles (H`). PZ = proliferation zone. Nomarsky pictures; bar: 100 µm.
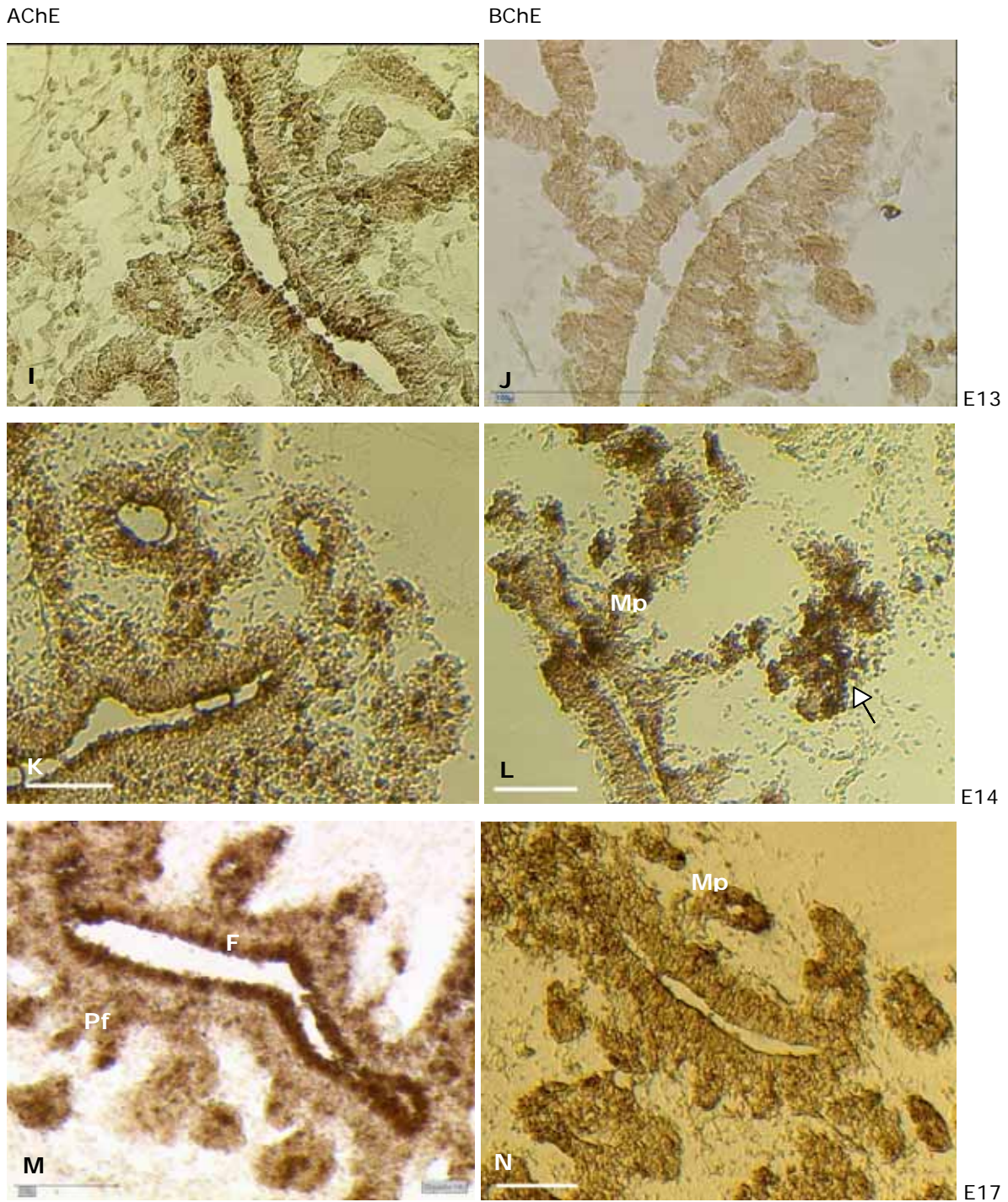
AChE

BChE

Fig. 2.18: AChE (left) versus BChE (right) histochemistry in sagittal sections of chick pineal glands. By E13, AChE-positive cells surround the luminal space of the recess (I), while BChE activity drastically decreases in relation to earlier embryonic stages (J). By E14, AChE activity increases in cells of the parafollicular zone of the recess (K). BChE activity is still intense in newly formed vesicles (arrow). By E17, the number of AChE-positive cells increase, however, showing the same expression pattern as before (M). BChE activity decreases gradually (N). Nomarsky pictures; bar: 100 μm (I-L); 200 μm (M-N).

AChE   BChE
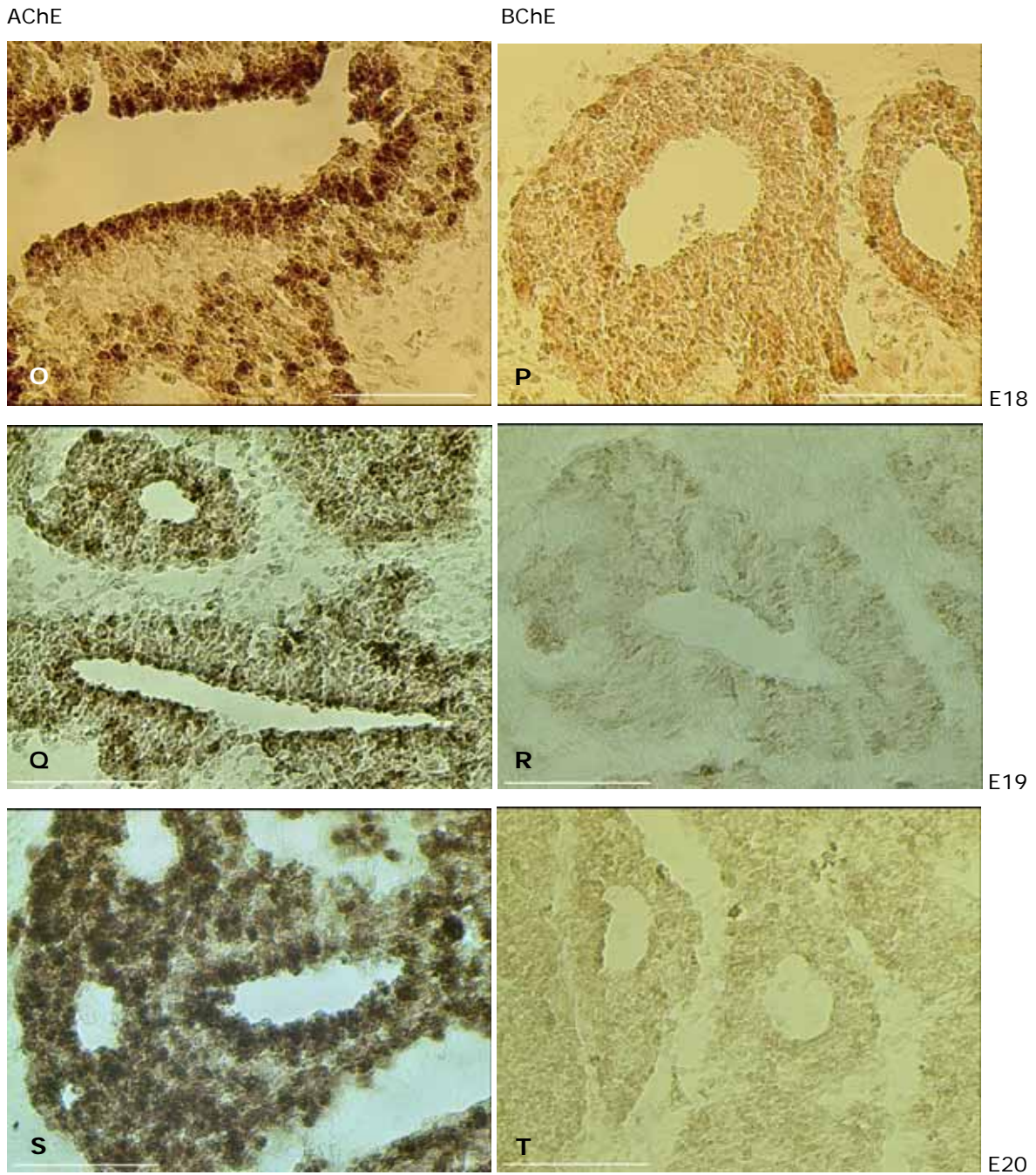
Fig. 2.19: AChE and BChE histochemistry in sagittal sections of chick pineal glands. By E18, (O) an intensive activity of AChE can be seen at the borders of the luminal space and parafollicular zone, which remains strong by E19 (Q) and E20 (S). By E18, BChE activity is decreased (P), and is basically absent by E19 and E20 (R, T); showing an inverse pattern in relation to early embryonic stages. Nomarsky pictures; bar: 100 µm.

2.3.2 Pineal remodeling and distribution of AChE and BChE positive cells

E7 is the initial stage for chick pineal vesicles formation. Vesicular walls, formed by mammilliform projections of the recess, develop a central lumen by this period and are then called vesicles (Fig. 2.20, A). By E8, these vesicles start to spread around the recess and increase in size (Fig. 2.20, B). AChE and BChE distribution on vesicles and recess partially overlaps (Fig. 2.20). AChE cells are adjacent to luminal spaces, and BChE, starting from the same area, has a broader and more diffuse distribution (Fig. 2.20, A-D).

Vesicles are originated as mammilliform projections of cells of the recess, and also as extension of primary vesicles originated by them (Fig. 2.20). BChE activity expands from the recess towards the borders of vesicles in development (Fig. 2.20; Fig. 2.21). From E9 until E11 a gradient of its activity, which is more intense surrounding luminal spaces in relation to the whole vesicular epithelium, can be seen (Fig. 2.15, B, D, D`; Fig. 2.16, F).

By E11, vesicular cells assume a specific distribution in two distinct layers, as part of the development of vesicles into follicles. Columnar cells, arranged perpendicular to the central lumen of the follicle, can be distinguished from spherical cells, forming the parafollicular zone (Fig. 2.22, a). By this stage, the distribution of AChE-positive cells is mainly concentrated between the follicular and the parafollicular zones of follicles, in contrast to its initial distribution in the luminal space (Fig. 2.15; Fig. 2.22, A`;Fig. 2.23). Cells have migrated from the luminal surface towards the follicular borders during follicles remodeling and, therefore, are rarely found in the luminal surface by this stage.

With the development of distinct cell layers, vesicles formation takes place in the parafollicular area of recess and follicles (Fig. 2.24, A). AChE-positive cells migrate to the borders of the parafollicular zone and form rosettes of cells giving rise to mammilliform projections, which develop into vesicles and later into follicles (Fig. 2.22, B; Fig. 2.23; Fig. 2.24, b-B). By E12, AChE-positive cells appear again in the luminal surface, and for the first time they are present in the follicular and parafollicular areas (Fig. 2.17, G`; Fig. 2.23). This pattern of AChE expression is intensified throughout development. AChE activity, positive in the cellular rosettes of the parafollicular area, will be also present on the central lumen of new vesicles originated by them (Fig. 2.23; Fig. 2.24, A-B; Fig.

2.25, A-B). Follicles, which generate tertiary vesicles, will also present rosettes of AChE-positive cells on their parafollicular zone, and these cells will also give rise to the future central lumen of respective vesicles originated from them (Fig. 2.25, B`). Therefore, AChE-positive rosettes of cells, which accompany the mammilliform projections, are the starting and end points for vesicles formation (Fig. 2.24, A-B; Fig. 2.25, A-B).

As follicles grow, consequently, new cells will become AChE-positive, sustaining the number of cells to reinitiate the remodeling events of the transient parafollicular zone (Fig. 2.23). Migration of AChE-positive cells can be observed, either from the follicular area to the parafollicular zone or from the region between them in direction to the luminal surface (Fig. 2.26). Therefore, a mechanism to supply new AChE-positive cells to accompany the remodeling process is suggested. First, AChE-positive cells migrate from the luminal surface towards the parafollicular area to originate new rosettes of cells to guide the remodeling of follicles (Fig. 2.23). Second, new AChE-positive cells appear in the luminal surface as a result of AChE-positive post-mitotic cells migration to this area, also possibly migrating in direction to the parafollicular zone (Fig. 2.27).

After E12, BChE activity decreases progressively, appearing only in mammilliform projections or newly formed follicles (Fig. 2.17, L, N). It is interesting to address that until E11 BChE activity is concentrated in the surrounding area of luminal spaces and recess, and by E12 it starts to be concentrated in regions, of recess and vesicles, that are expanding (Fig. 2.17, H, H`). With the decrease in BChE activity in overall, a parallel increase in AChE activity occurs. Intensive increase in volume of the chicken pineal is known to happen until E12 (Calvo and Boya, 1978). Therefore, the following stages of the chick pineal embryogenesis are marked by cell differentiation.

The shift from BChE to AChE activity suggest a relation to proliferation and differentiation events, respectively (Fig. 2.21), which will be here presented in detail in the following.

AChE   BChE
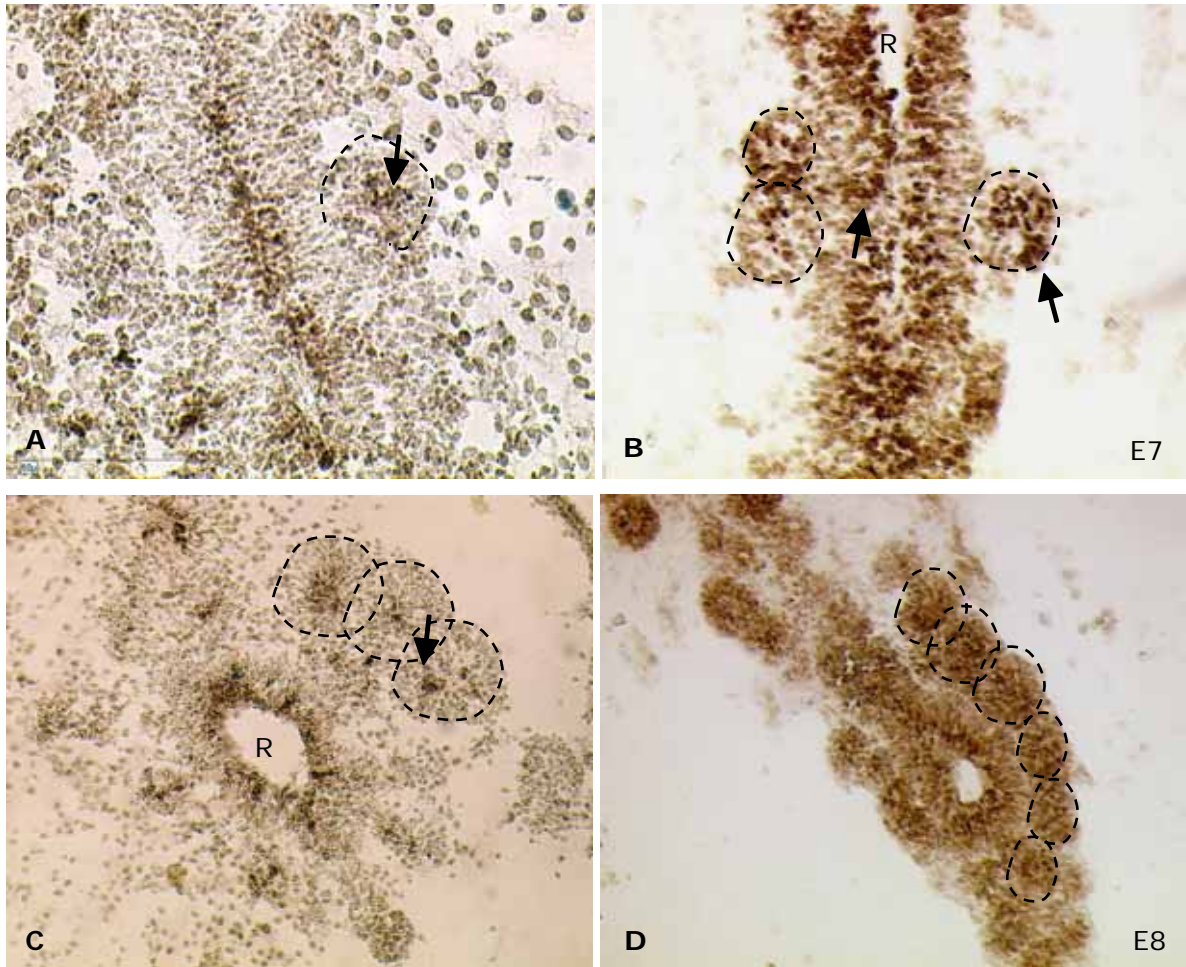
Fig. 2.20: AChE (left) and BChE (right) histochemistry in sagittal sections of chick pineal organs. By E7 (A-B) and E8 (B-D), AChE-positive cells fill the future central lumen of vesicular walls (arrows), whereas BChE displays a diffuse activity over the pineal epithelium, with prominent activity on the borders of vesicles, and lumen of the recess (arrows). R = recess. Bar: 50 µm (A-B); 100 µm (C-D).
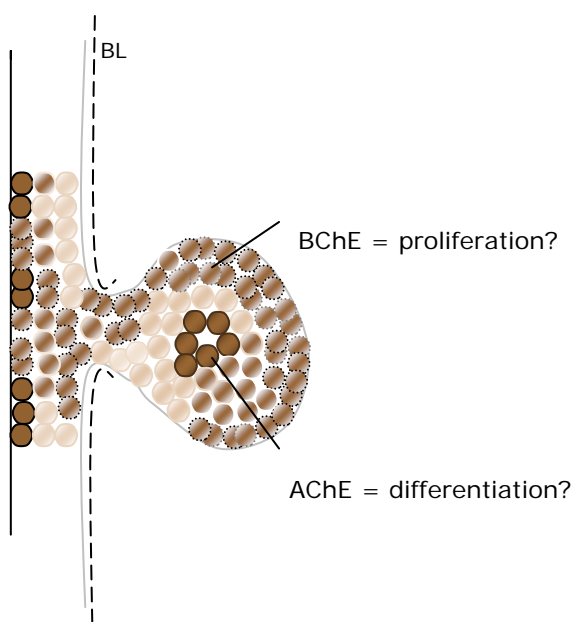
Fig. 2.21: Vesicle formation sheme with AChE and BChE positive cells distribution by E7-E8.

DAPI/AChE
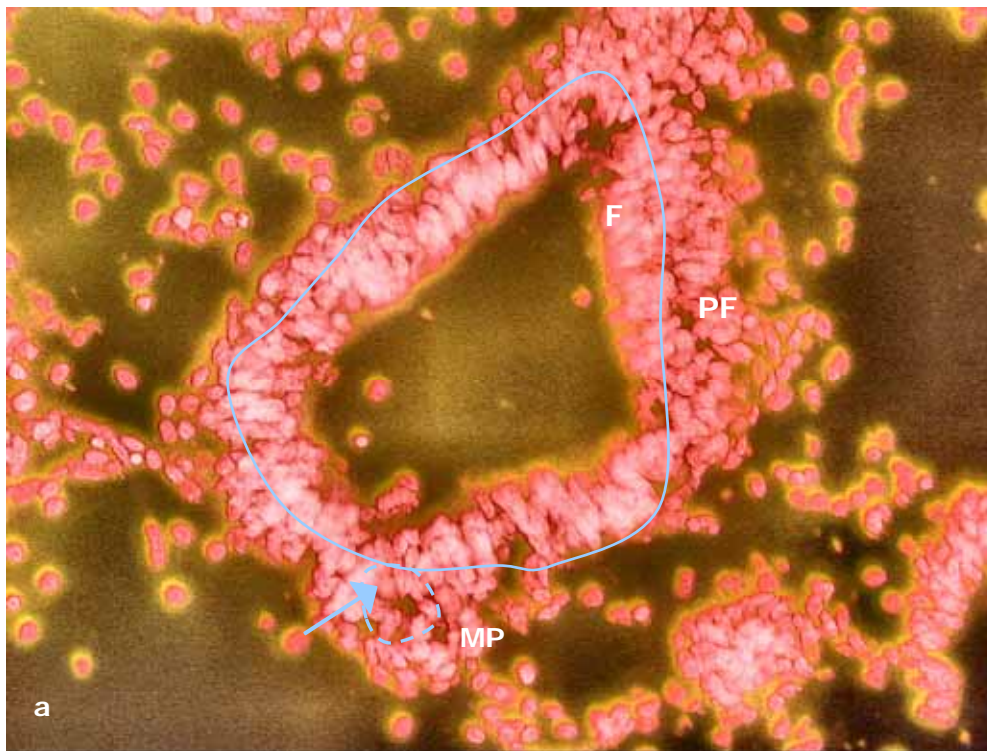
Fig. 2.22: (a-A) Double staining DAPI (above) and AChE histochemistry (below). By E11, the follicles are comprised by columnar cells, surrounding the lumen, and spherical parafollicular cells. AChE-positive cells lie on the parafollicular zone and next to mammilliform projections (arrow). The rosette of AChE-positive cells migrates to form new vesicles. F = follicular zone; MP = mamilliform projection; PF = parafollicular zone. Bar: 50 µm.
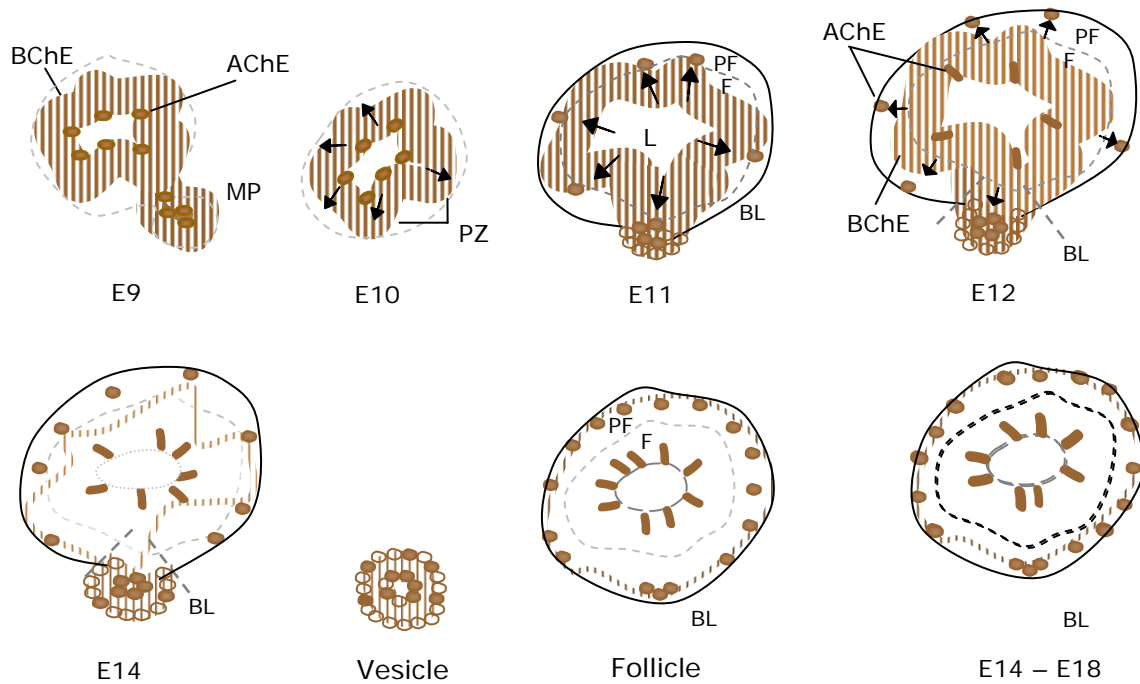
Fig. 2.23: Schema of AChE and BChE expression during pineal tissue remodeling. Until E10, AChE-positive cells occupy the luminal surface of vesicles. By E11 these cells have migrated in direction to the newly established parafollicular zone. BChE activity, which was already abundant in vesicular surface by earlier stages, initially expands in proliferative zones (PZ) and then declines, becoming limited to regions with proliferation activity. By E12, AChE-positive cells migrate to the borders of the parafollicular zone, and new AChE cells reappear in the luminal surface. As vesicles grow and form structured follicles, new cells become AChE-positive and vesicles formation continues until E18.

AChE
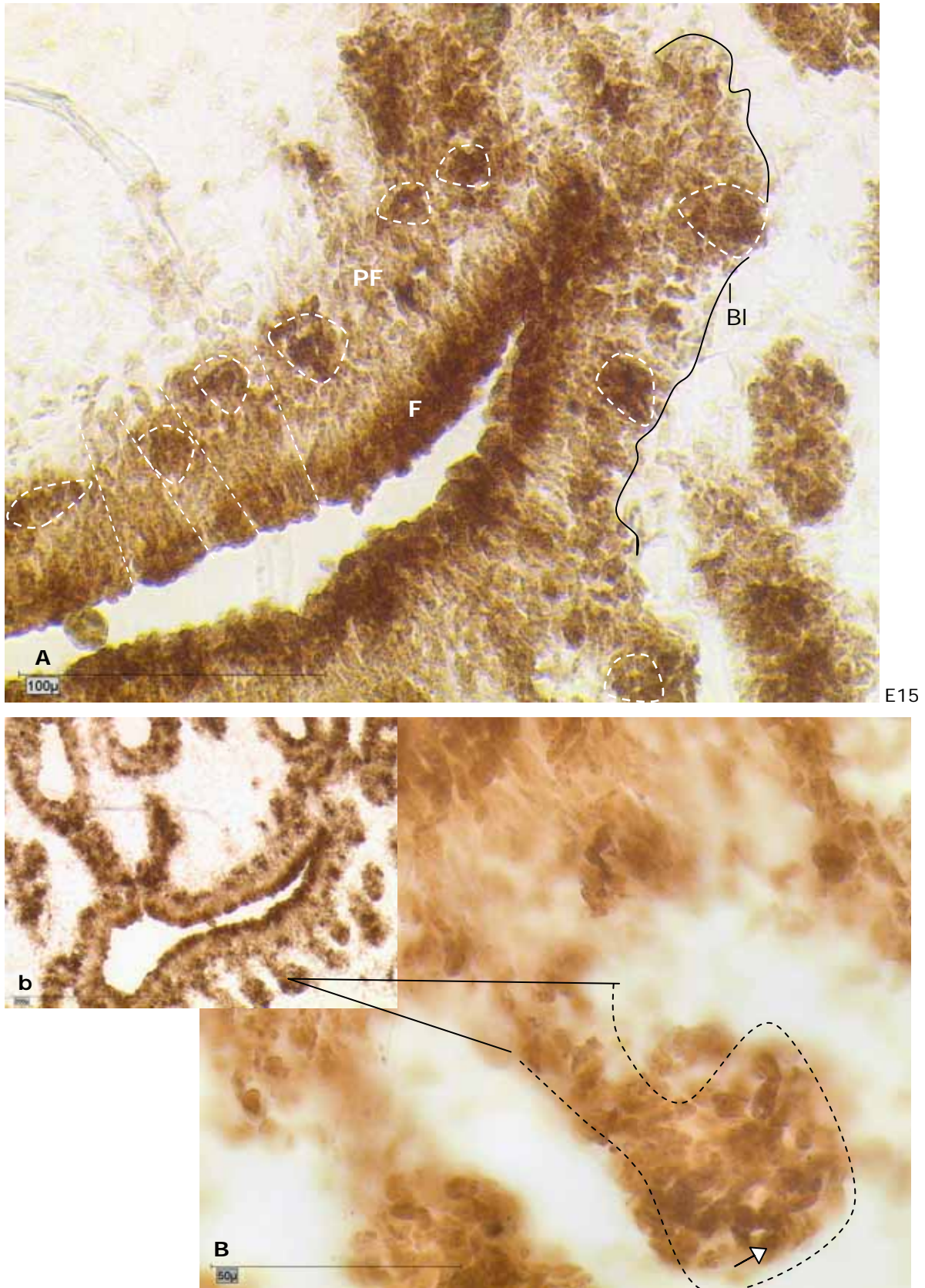
Fig. 2.24: AChE histochemistry in sections of an E15 pineal. A) AChE-positive cells arranged in rosettes on the parafollicular region of the recess (arrows) migrate with surrounding cells to form the mammilliform projections. B) The future lumen of the vesicles will be filled with the AChE-positive rosette (arrow). Bar: 50 µm (B), 100 µm (A), and 200 µm (b).
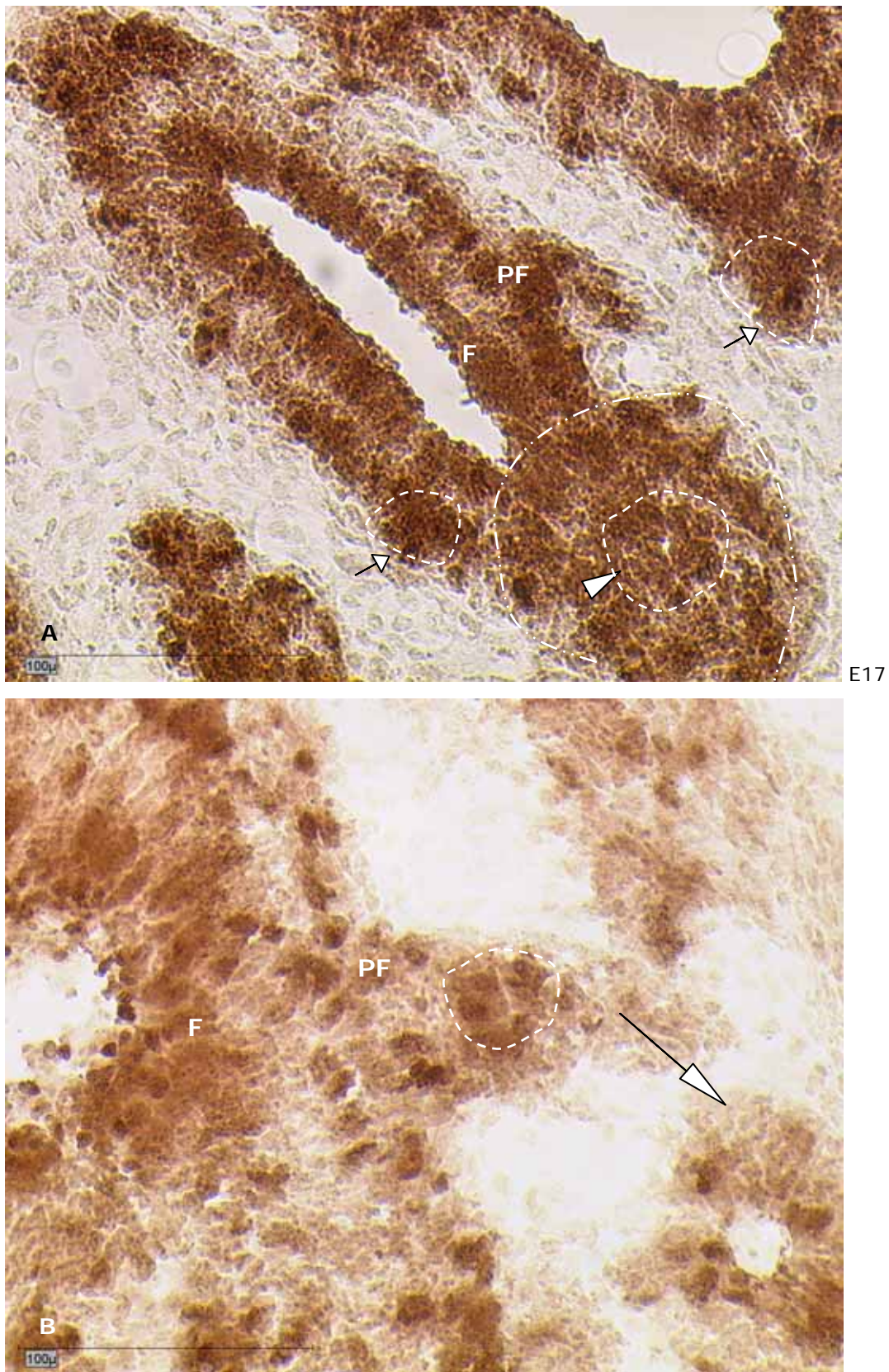
AChE

Fig. 2.25: AChE histochemistry in E17 pineal sections. A) Vesicles in development, originated from the migration of AChE-positive rosettes of cells (arrows). B) The rosette of AChE-positive cells forms the central lumen of vesicles. Bar: 100 μm.
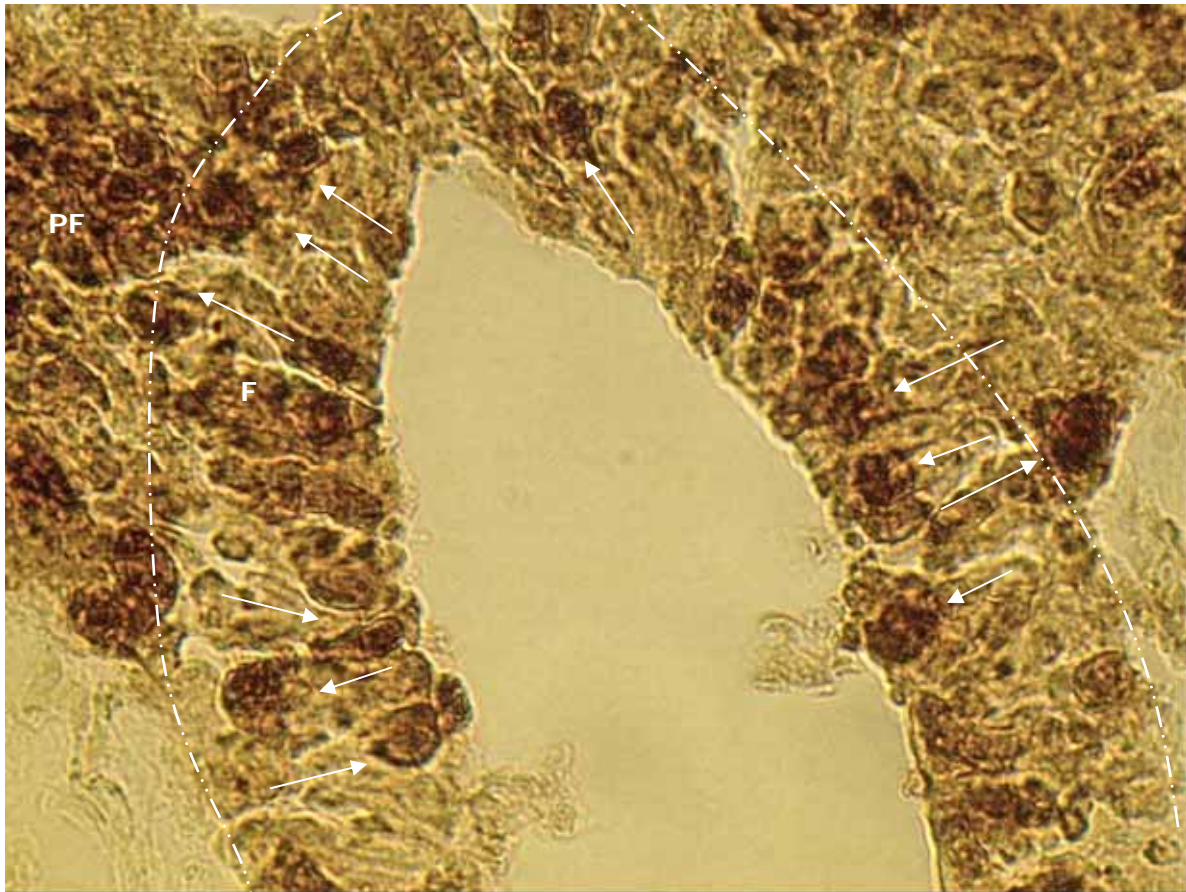
Fig. 2.26: AChE histochemistry of a sagittal section of an E18 chick pineal. AChE-positive cells on the follicular zone migrate in direction to the parafollicular zone and luminal surface. Magnification X100.
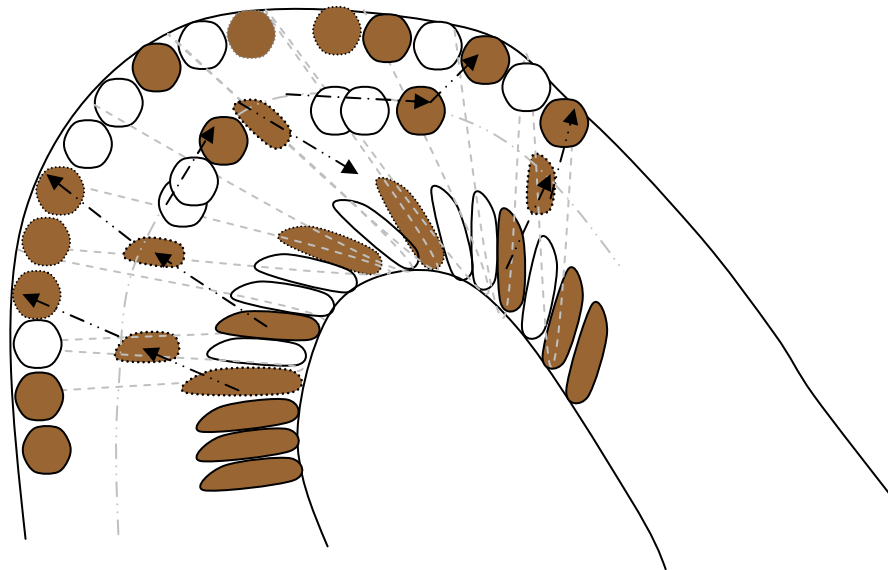
Fig. 2.27: Possible mechanism of cells migration and proliferation. AChE-positive cells migrate from the luminal surface to the parafollicular zone as the follicular area expands to form the parafollicular cells. After proliferative periods, several new cells become AChE-positive and migrate from the follicular region to the luminal surface and parafollicular zone.

2.3.3 Chick pineal cells proliferation

2.3.3.1   Cell proliferation studies with PCNA

The proliferating cell nuclear antigen (PCNA) is expressed during the G1-phase and S-phase (DNA synthesis) of the cell cycle. The cell fate is determined on the interplay between G1 and S phases. When cells undergo proliferation, PCNA expression is needed. The expression of PCNA was investigated during the embryonic development of the chick pineal. Immunohistochemistry for PCNA was compared to BChE histochemistry in parallel sagittal sections of pineal organs from several embryonic stages. By the embryonic days 7 and 8, most of the cells show proliferation activity. By E7 and E8, mammilliform projections appear on cells of the pineal recess to form new vesicles (Fig. 2.28, A-B; Fig. 2.29). These vesicles will expand to form follicles, by E11, with the appearance of a parafollicular area.

Proliferation activity was found on the borders of vesicles, on cells which give rise to the parafollicular zone in later stages of development (Fig. 2.30). A diffuse BChE expression partially overlaps with the proliferative areas, detected by immunostaining against PCNA.

The BChE activity shows a very intensive pattern for high proliferative periods, from E7 to E11 (Fig. 2.28; Fig. 2.29, A`), and decreasing proportionally with the state of proliferation, from E12 onwards (Fig. 2.31). BChE displayed a more pronounced activity than seen for AChE at highly proliferative stages (Fig. 2.28 and, Fig. 2.20 A-B, respectively). Comparing their expression with PCNA by E7, it is possible to see that AChE expression and proliferation occurs in opposite areas (Fig. 2.29). The areas where AChE and BChE activities overlap are, therefore, not mitotic zones. However, BChE is more extensively distributed than AChE until E11, also covering proliferative areas (Fig. 2.29).

The proliferation activity remains intense until E12 (Fig. 2.28, D), with the development of several new follicles, and it is significantly reduced by reaching late embryonic development. By E17, it is mostly limited to the interfollicular cells. However, follicles in development still present PCNA positive cells, showing proliferation activity (Fig. 2.31). By E18, even less PCNA immunoreactivity can be found, and basically no BChE activity (Fig. 2.31).

PCNA   BChE
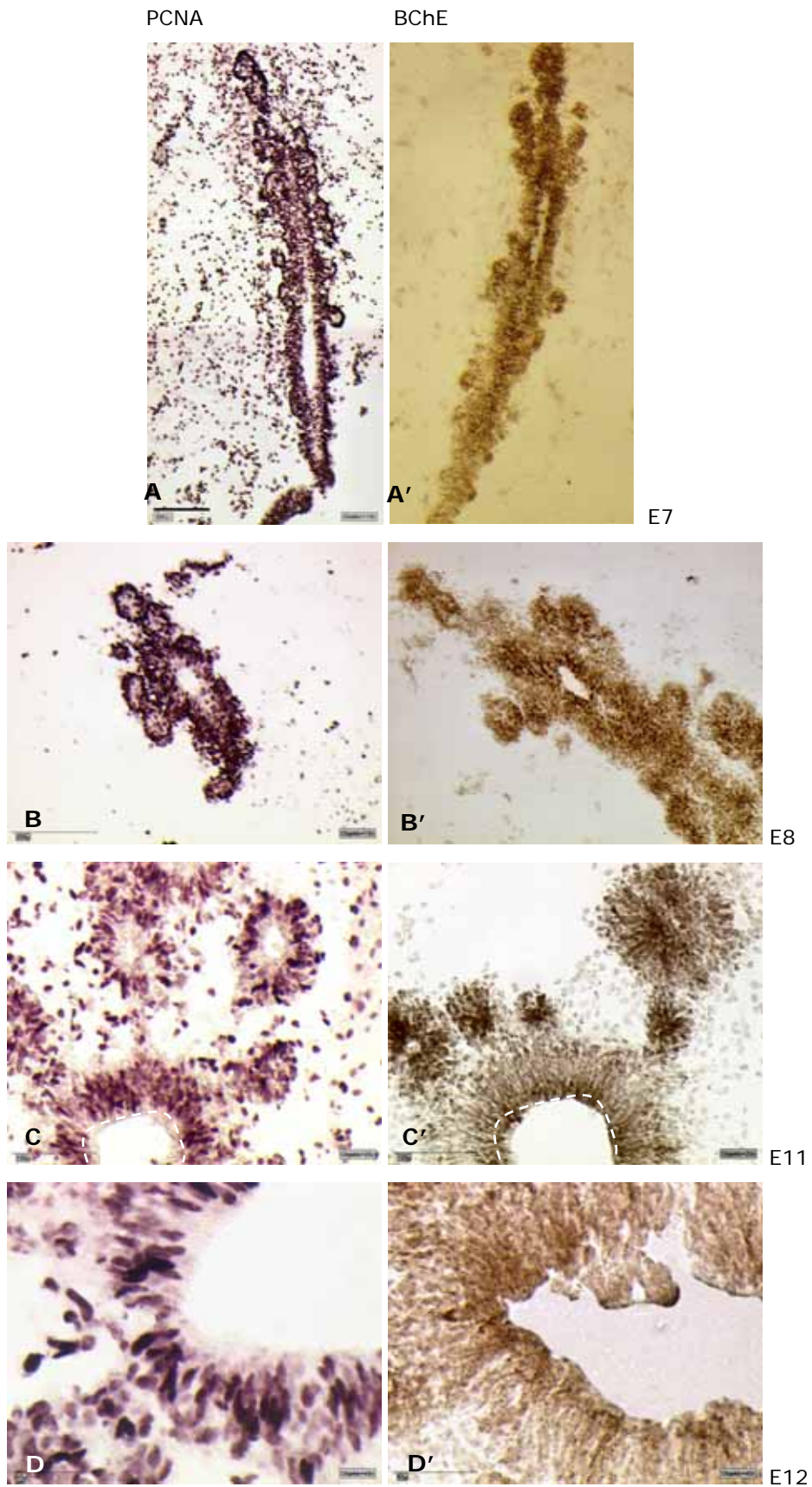
Fig. 2.28: PCNA (left) and BChE histochemistry (right) on sagittal sections of the chick pineal organ. (A-A`) E7, (B-B`) E8, (C-C`) E11 and (D-D`) E12 are intensive proliferative periods and display noticeable strong BChE activity. Bar: 100 μm (C-C`) and 200 μm (A`-B`).

PCNA   BChE   AChE
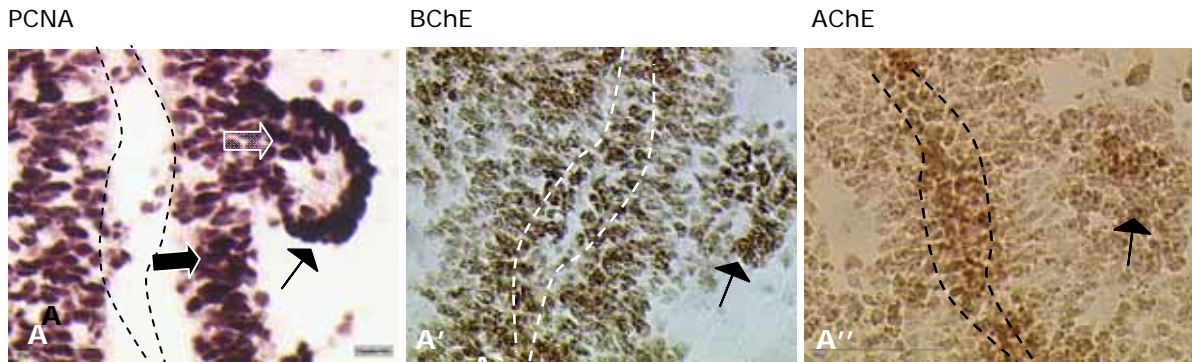
Fig. 2.29: PCNA (left) and BChE histochemistry (right) on sagittal sections of the chick pineal organ. By E7, strong proliferation activity can be seen on the cells of the vesicular borders (arrow) and among cells surrounding the recess. Correspondent BChE activity accompanies proliferation. Areas where AChE and BChE activities overlap (---). Bar: 50 µm.
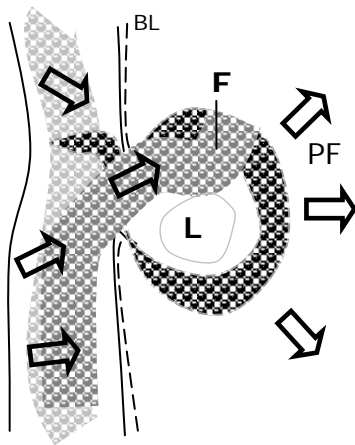
Fig. 2.30: Mechanism of follicular development. Vesicles become follicles by E11, as cells proliferate to form the parafollicular zone. Mitotic cells from the follicular area develop the parafollicular zone.

Control stainings were performed omitting the primary antibody of the protocol.

Controls did not present specific immunoreactivity with secondary antibody.
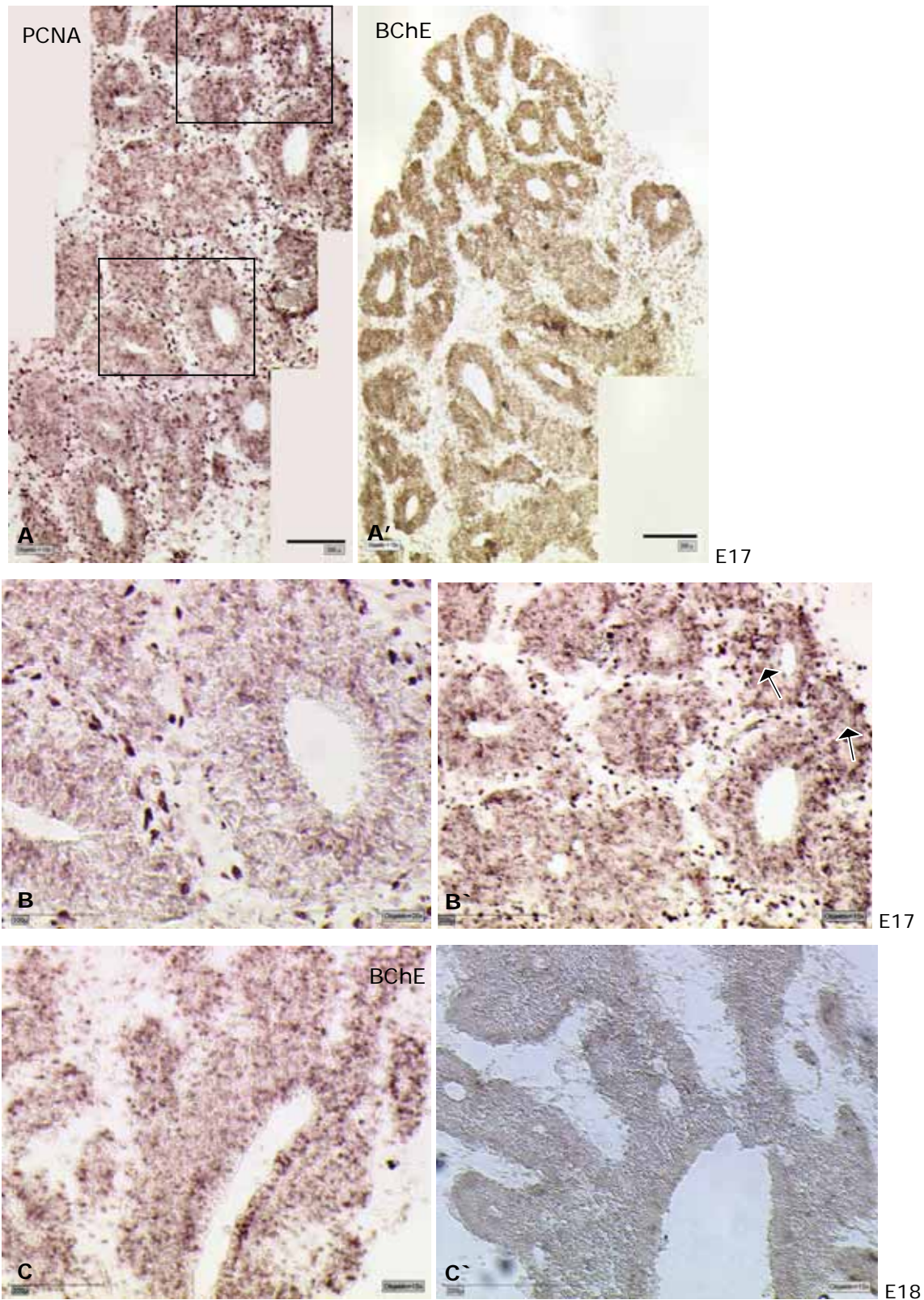
Fig. 2.31: PCNA - immunoreactive cells (left) and BChE histochemistry (right) on sagittal sections of the chick pineal organ. By E17, PCNA positive cells can be seen just on the pineal interfollicular area (A) and on the follicular region of growing vesicles (B-B`, arrows). (A`) BChE activity has decreased in relation to earlier stages of development. By E18, basically no proliferation and no BChE activity can be seen (C-C`). Bar: 100 µm (B) and 200 µm (A, B`-C`).

2.3.3.2   BChE immunohistochemistry

Histochemistry for BChE using the method of Karnovsky-Roots is largely used to detect its activity. However, due to the resulting diffuse brownish tissue staining obtained with this methodology for BChE activity; it is not possible to identify single positive cells, like it is for AChE. To validate the histochemical results, immunostainings were also conducted with a specific antibody against chicken BChE. The immunoreactivity observed with the BChE antibody, confirmed high BChE expression and localization in growing vesicular walls (Fig. 2.32; Fig. 2.33, A`), by E9. As shown earlier by histochemistry, only a few BChE positive cells are present during late development, e.g. by E17 there is almost no immunoreaction for BChE (Fig. 2.33, B`). Therefore, the results obtained with immunolabeling of BChE are compatible with the results observed with histochemistry for BChE activity. However, with immunolabeling it is possible to visualize that the BChE immunoreactivity is restricted to the cytoplasm of the cells, as detected by confocal microscopy (Fig. 2.32, c).
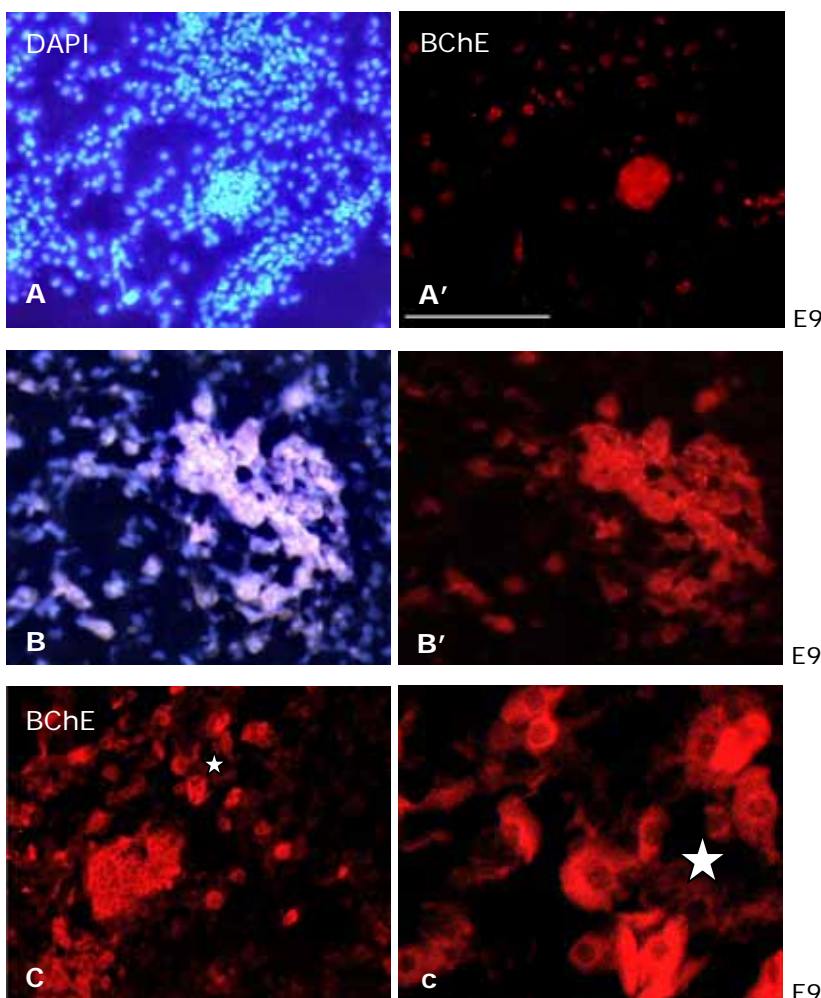
Fig. 2.32: (A-B`) DAPI and BChE Immuno-histochemistry: sagittal sections of an E9 chick pineal. (A-A`) A rosette of cells stained for DAPI and BChE. (B-B`) Double staining DAPI/BChE, and only BChE immuno-reactivity in a new born vesicle. (C) Confocal picture of immunolabeled BChE cells. (c) Amplified cells from image C (star) displaying BChE immuno-reactivity on the cyto-plasm, but not on the nucleus. 20x Magnification Bar: 100 µm.
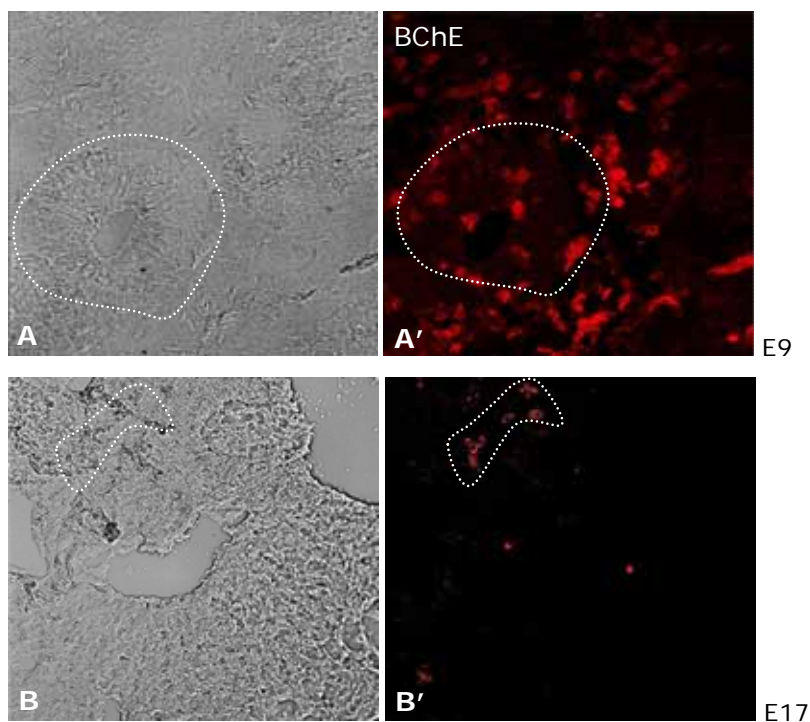
Fig. 2.33: Immunolabeled BChE (right) detected by confocal microscopy. (A-A´) E9, expression of BChE in growing vesicles. (B-B´) E17, immunoreactivity for BChE is mainly restricted to the parafollicular zone. Magnification X20.

The omission of the primary antibody from the protocol resulted in absence of immunolabeling.

2.3.3.3 Cell proliferation studies with BrdU

To corroborate the PCNA studies, BrdU was also used as a proliferation marker, and its expression was compared with the BChE histochemistry in pineal sections.

BrdU (5-Bromo-2´-deoxy-uridine) is a thymidine analogue, which can be incorporated into DNA during the synthesis (S) phase. The proliferation activity of the pineal cells was labeled with BrdU during the exposure time of two and a half hours. A fluorescent conjugate secondary antibody revealed immunoreactivity for BrdU. Controls did not present immunoreactivity.

Also here, high proliferation activity in the follicles can be observed from E9 to E11 (Fig. 2.34). S-phase BrdU positive cells are almost homogeneously distributed throughout the pineal epithelium and intense BChE activity accompanies the proliferative states. By E17, when just a few BrdU positive cells can be identified in the parafollicular area, BChE activity is respectively very low (Fig. 2.34, D-D`).
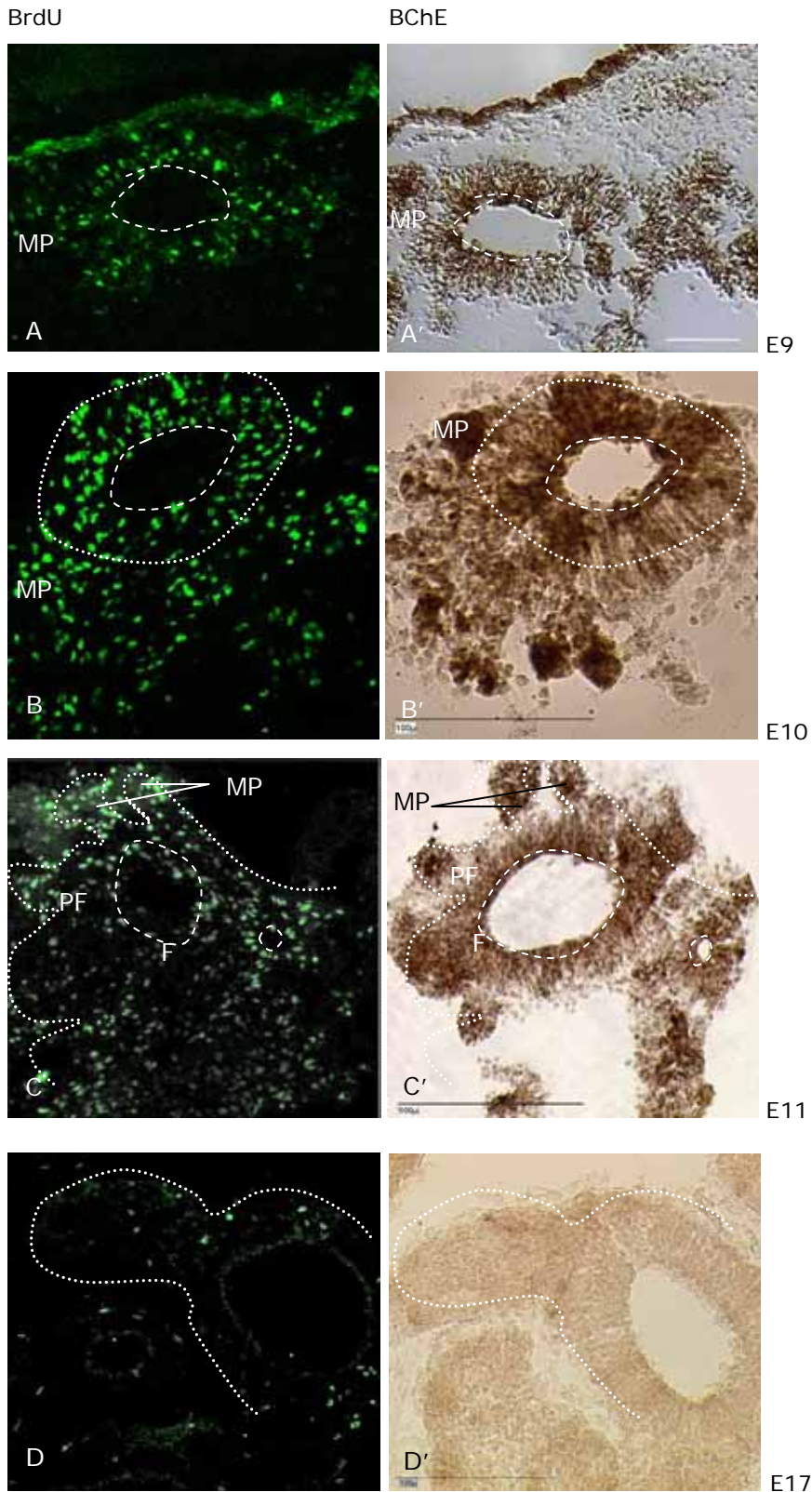
BrdU

BChE

Fig. 2.34: DNA syntheses detected by immunoreactivity of incorporated BrdU versus BChE histo-chemistry of chick pineal sections. (A) By E9, BrdU positive cells surround the luminal space of the follicle. (A') Histochemistry for BChE in a parallel pineal section reveals a correlation of BChE activity to proliferating areas. (B-B') By E10, intense proliferation, in the follicular area, and respective strong BChE activity can be seen. (C) By E11, BrdU positive cells surround the luminal space of an adult follicle, and the future central lumen of MP. (C') Follicular area and mammilliform areas present intense BChE activity. (D) E17, a few BrdU positive cells appear on the para-follicular zone; no pronounced immuno-reactivity is found on the follicular area. (D') Basically no BChE activity is found in correspondent areas by this stage. MP = mammilliform project-tions; PF = para-follicular zone. Bar: 100 µm.

Before E11, the majority of the cells are mitotically active. By E11, the proliferative cells population expand the follicular area, forming the parafollicular zone (Fig. 2.35). Proliferative cells coming from the follicular area invade the parafollicular mammilliform projections, as verified by BrdU incorporation (Fig. 2.35). The follicular epithelium gives rise to the parafollicular zone and, allows the migration of follicular cells in that direction, as it happens with AChE-positive cells.
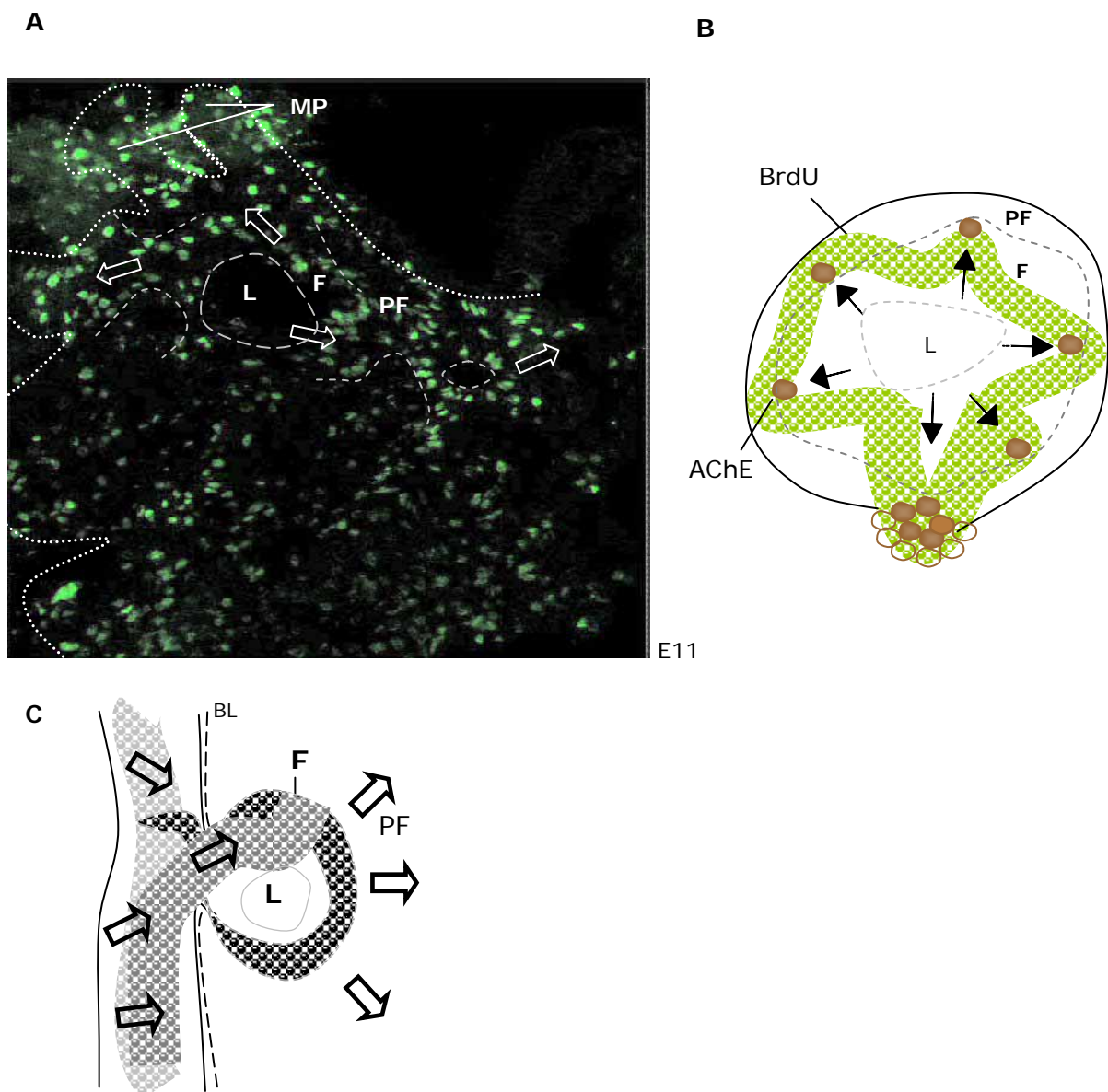
Fig. 2.35: Pineal cells proliferation. (A) Mitotic activity detected by immunoreactivity of incorporated BrdU on a chick pineal slice by E11. (B) Schema of proliferative areas (green) expansion, and AChE (brown) cells migration during the development of the parafollicular zone. (C) Mechanism of follicular expansion. Vesicles become follicles by E11, as cells proliferate to form the parafollicular zone. Mitotic cells from the follicular area develop the parafollicular zone. Magnification X20.

2.3.4 Characterization of the expression of vimentin in the developing chick pineal

The organization of vesicles into two distinct layers transforms them into follicles. The implication of this remodeling for supportive cells was investigated using vimentin as a glia cell marker.

The intermediate filament (IF) protein vimentin belongs to a class of well-characterized cytoskeleton elements. In the pineal glands of rat, mice, cat and dog interstitial cells were shown to be astrocytes by electron microscopy, and by immunolabeling techniques, using antibodies against vimentin, glial fibrillary acidic protein, M1 and C1 antigens (Schachner *et al.*, 1984; Calvo and Boya, 1988; Lopez-Muñoz *et al.*, 1992; Boya and Calvo, 1993). Vimentin positive cells showed morphology characteristic of astrocytes, a glia cell type which provides chemical and physical support for the neurons (Keilhauer *et al.*, 1985).

Immunostainings for vimentin revealed that a glia-like cell type, with astrocyte morphology, is predominant in the chick pineal interfollicular area and also abundant in the parafollicular and follicular zone of structured follicles of the chick pineal organ (Fig. 2.36). However, until the embryonic day 10, these vimentin positive cells are still limited to the interfollicular area, not invading the vesicular walls space (Fig. 2.36, A–A`). By E11, when two cell zones become established (follicular and parafollicular), follicular glia cells differentiate (Fig. 2.36, B–B`). By E17, the follicles are mostly developed and the interfollicular cells are abundant (Fig. 2.36, C-F). Marked vimentin expression on the interfollicular cells was found by this period. In addition, vesicular walls did not display immunoreactivity for vimentin, but newly formed follicles did (Fig. 2.36, G-H). For control stainings, primary antibody was omitted from the protocol, resulting in absence of specific immunoreactivity.

Glia cells are known to be supportive cells for neuronal differentiation. Therefore, the remodeling of follicles and the appearance of glia cells into the follicular can be associated with neuronal differentiation. The differentiation of photoreceptors is the further question to be addressed in this chapter.

Vimentin
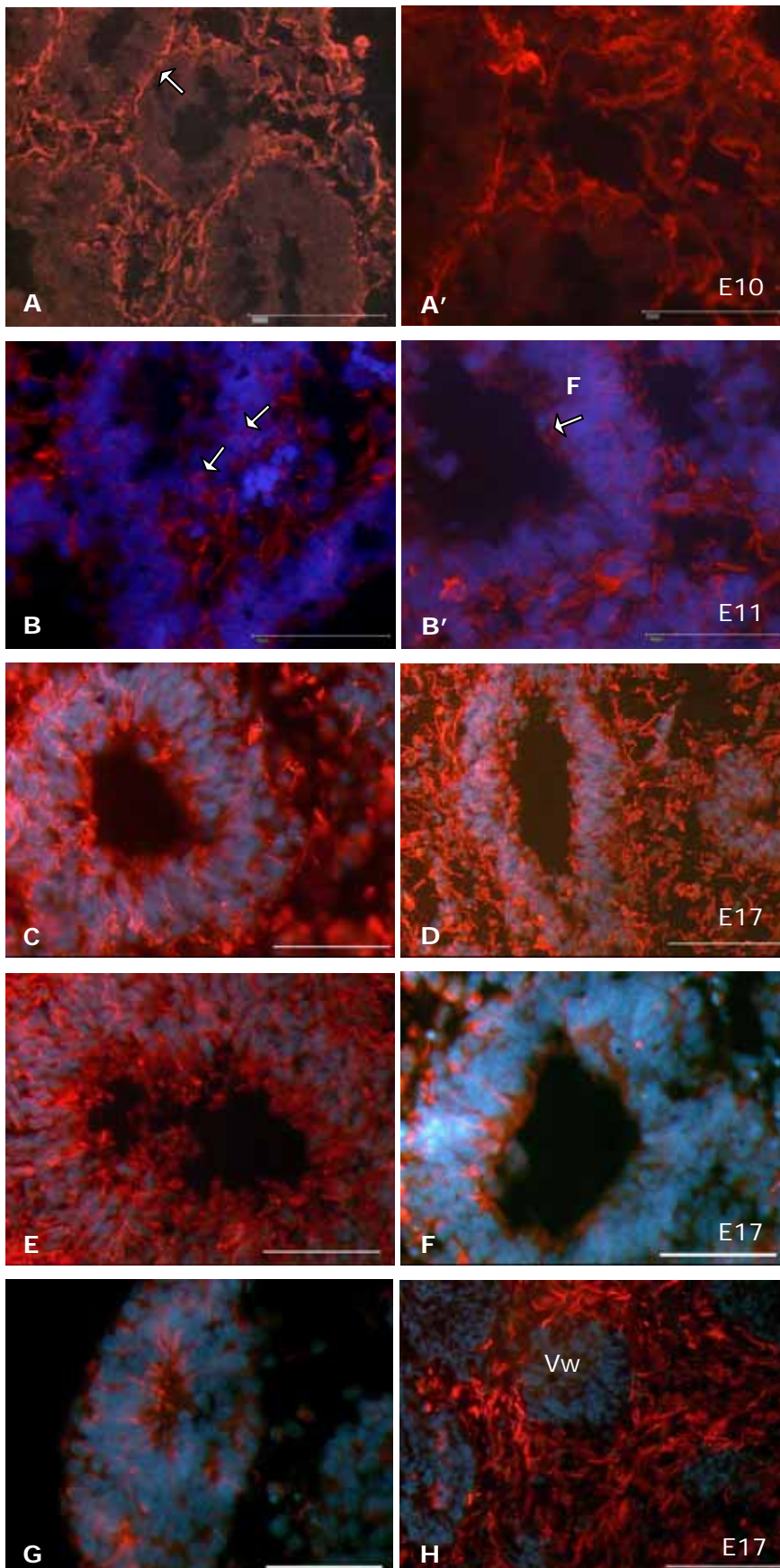
Fig. 2.36: Vimentin immunostaining of sagittal sections of chick pineal organs. By E10 and E11, respectively, pineals present no (A-A´) or just a few (B-B´) vimentin positive cells in comparison to later stages. By E10, vimentin positive cells are restricted to the interfollicular space, being absent in vesicles (A-A`). By E11, the follicular space is invaded by vimentin positive cells (B-B´). By E17, immunostaining for vimentin positive cells is abundant in structured follicles (C-F). Vimentin is also present in the lumen of young follicles (G), but not on vesicular walls (H). Vimentin: red; DAPI: blue; F: follicular area; Vw: vesicular wall. Bar: 100 µm (A, B, C-D, H) and 50 µm (A`, B`, E-G).

2.3.5 Cell differentiation: expression of the pinopsin photopigment in AChE-positive cells of the developing chick pineal organ

Pinopsin is a photoreceptive molecule expressed in most of the photoreceptors of the avian pineal organ (Okano, 1994). In the Japanese quail pinopsin expression is detected earlier than rhodopsin-like and iodopsin-like molecules (Yamao *et al.*, 1999).

The expression onset of photoreceptive pigments during chick pineal embryogenesis has not been characterized until now. To detect when pinopsin positive cells first appear during pineal development, young chick embryos were investigated. In parallel, AChE histochemistry was conducted to verify if any alteration in expression would happen with the differentiation of photoreceptors.

Until the embryonic day 11 (Fig. 2.37, A), pinopsin was not detected in pineal tissue. On the other side, a few AChE-positive cells were detected in the luminal surface from E7 to E10 (Fig. 2.16; Fig. 2.20). AChE expression by E11 was mainly concentrated in the region between follicular and parafollicular zones (Fig. 2.17; Fig. 2.22). By E12, these AChE-positive cells migrate to the borders of the parafollicular zone and new cells on the luminal surface become to express AChE. At the same time, by E12, the first pinopsin positive cells appear in protrusions extending into the luminal space of the pineal recess (Fig. 2.37, B). AChE histochemistry revealed correspondent activity for structures in the luminal surface of the recess (Fig. 2.37, B`).

As earlier demonstrated, AChE-positive cells start to surround the luminal space of structured follicles by E12 (Fig. 2.17, G). After E12 the AChE activity increased significantly (Fig. 2.18; Fig. 2.19), as well as the number of pinopsin positive cells. By E15, cells surrounding the luminal space of follicles present intense AChE activity and several other AChE-positive cells are found in the protrusions of the parafollicular region (Fig. 2.37, C-C`). AChE activity shows a remarkable increase by this embryonic stage, around the luminal space of recess and follicles, accompanying the increase in pinopsin expression (Fig. 2.37, C). By the embryonic day 18, pinopsin positive cells are abundant not just on luminal protrusions, but also on the follicular zone (Fig. 2.38, A). By the end of the chick embryogenesis follicles become denser and the pineal acquires a

compact aspect, as earlier shown (Fig. 2.15, U). Most follicles diminish their luminal space by E20, and the distribution of the pinopsin positive cells is restricted (Fig. 2.39, A). However, the AChE activity remains intensive in the follicular and parafollicular area (Fig. 2.37, E`).
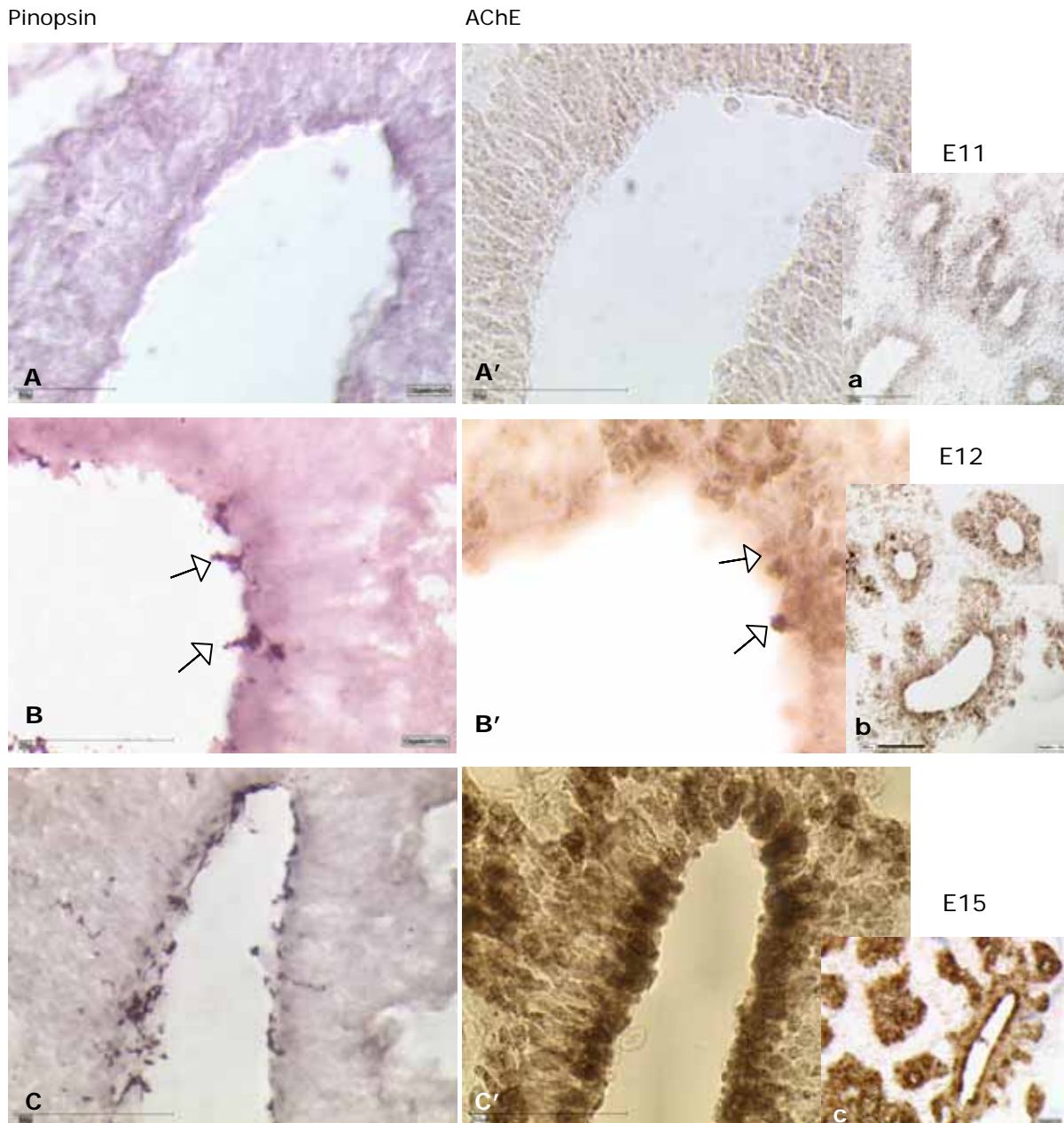
Pinopsin   AChE

Fig. 2.37: Immunohistochemistry for pinopsin (left) and histochemistry for AChE (right) in parallel sagittal sections of chick pineal glands. By E11 there are no pinopsin positive cells and no pronounced AChE activity (A-a). By E12, anti-pinopsin immunoreactivity (arrow) can be seen in the lumen of the pineal recess (B), co-localized to AChE-positive cells (B`- arrow). By E15, pinopsin positive cells surround the entire luminal space of the recess (C), and present AChE activity (C`). This increase in AChE activity on cells surrounding the luminal space accompanies, therefore, the differentiation of photoreceptive cells. (a, b and c) View of the pineal sections with 10X magnification. Bar: 20 µm (B; B`); 50 µm (A-A`; C-C`); 200 µm (a; b; c).

Pinopsin   AChE   E18
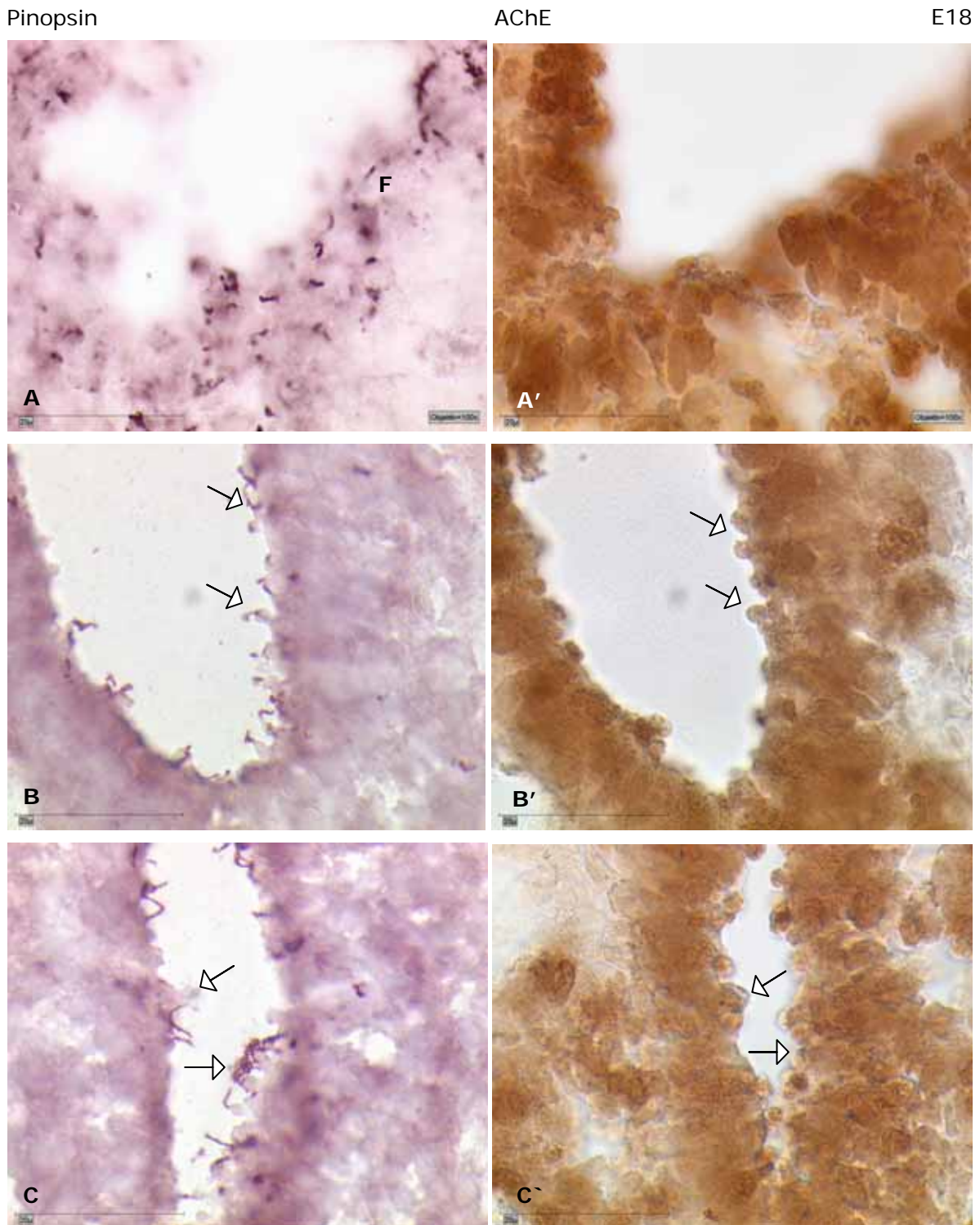
Fig. 2.38: Immunohistochemistry for pinopsin (left) and histochemistry for AChE (right) in parallel sagittal sections of an E18 chick pineal gland. Pinopsin immunoreactivity structures and correspondent AChE-positive cells on the follicular area (A-A`) and luminal surface (B-C` - arrows).

Pinopsin

AChE
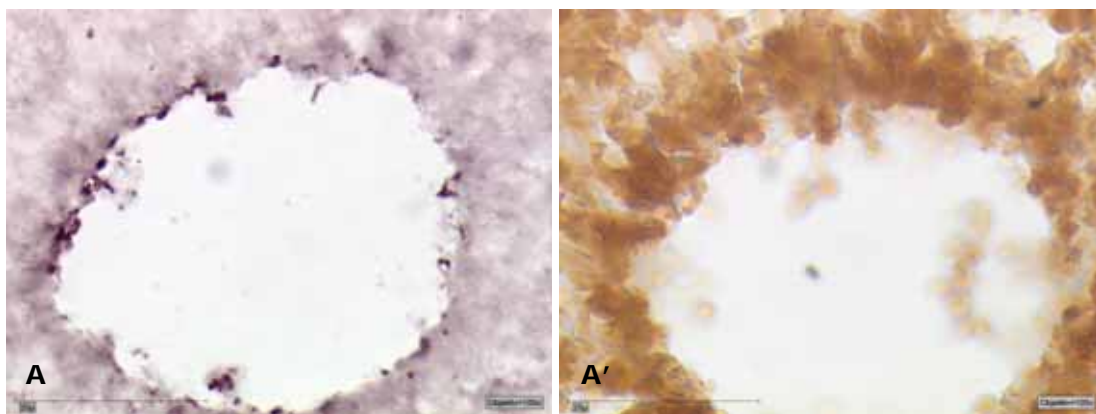
E20

Fig. 2.39: Immunohistochemistry for pinopsin (left) and histochemistry for AChE (right) in parallel sagittal sections of an E20 chick pineal gland. Pinopsin immunoreactivity structures and correspondent AChE-positive cells on the luminal surface of follicles (A-A`). Bar: 20 µm.
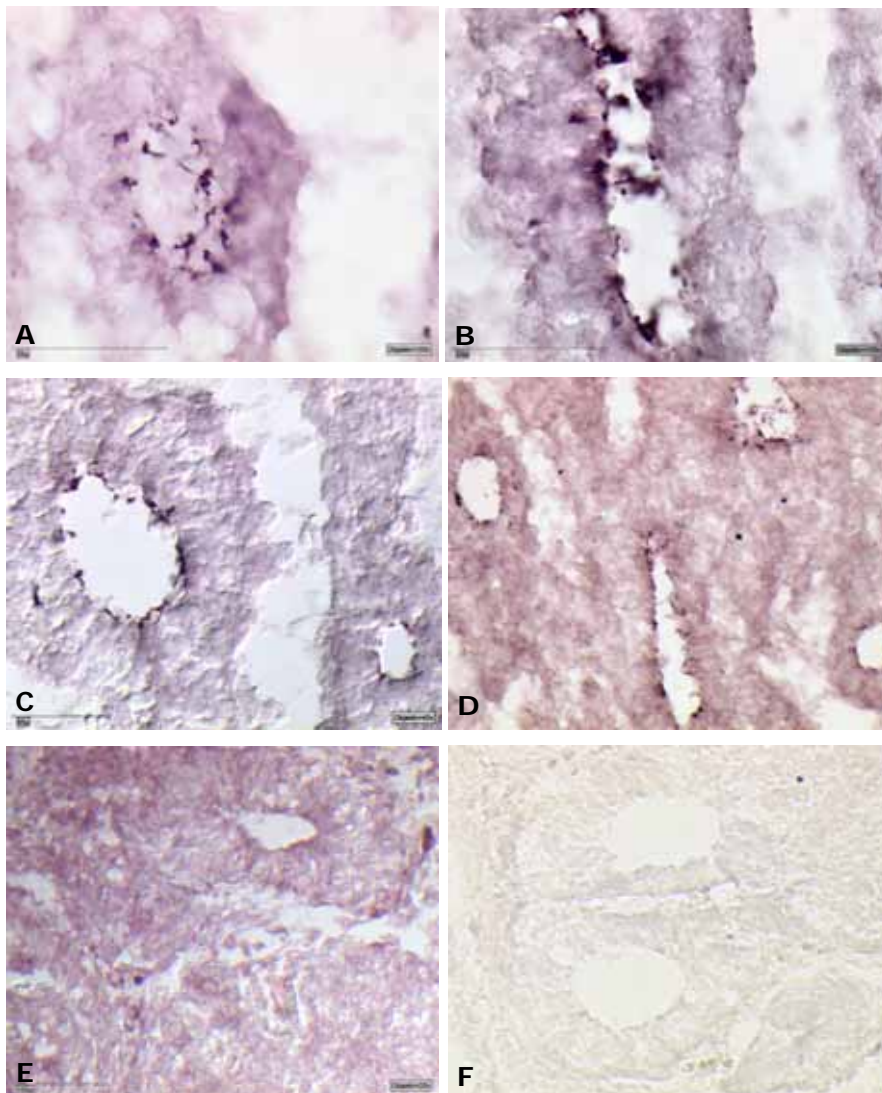
Pinopsin

Fig. 2.40: Pinopsin immunoreactivity on chick pineal gland structures. By E18, the luminal surface of newly formed follicles presents immunoreactivity for pinopsin positive cells (A-C). By E15 onwards, pinopsin positive cells show a homogeneous distribution (D). Negative controls: mouse IgG (used instead of anti-pinopsin antibody) (E), and immuno-staining without the primary antibody (F). Bar: 20 µm (A-B); 50 µm (C); 100 µm (D-F).

At late stages of the pineal embryogenesis, pinopsin positive cells are also present in the luminal projections of newly formed follicles (Fig. 2.40, B-D). Control experiments were conducted following the same protocol for pinopsin staining, except for the omission of the primary antibody or substitution of it by purified mouse IgG. Control stainings resulted in absence of specific immunoreaction (Fig. 2.40, F-G).

Glia cells appear by E11 in follicles, just before the onset of PRCs expressing pinopsin, by E12. This correlation can also be seen later in development. By E17 newly formed follicles present already pinopsin positive cells on the future central lumen region. By E17 vimentin will also be expressed in newly formed follicles (Fig. 2.41), in contrast to earlier stages, when neither vimentin nor pinopsin expression was found.
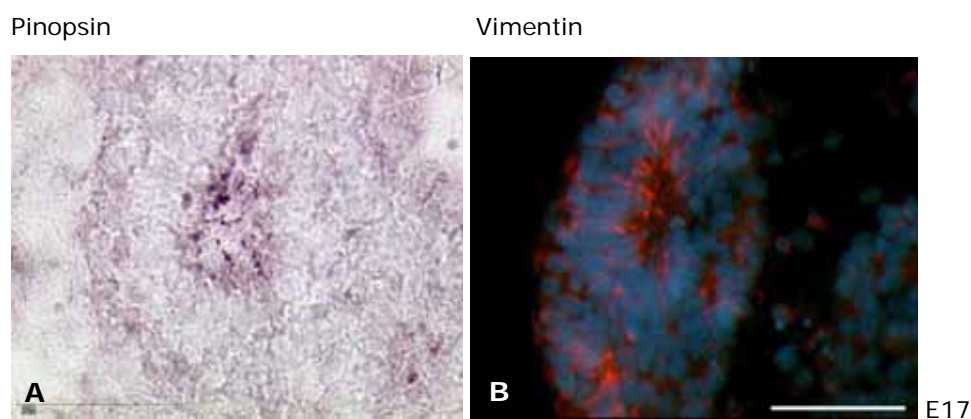
Pinopsin   Vimentin

Fig. 2.41: Pinopsin (left) and vimentin (right) immunostainings. By E17, pinopsin (A) and vimentin (B) positive cells fill the future central lumen of young follicles. Bar: 20 µm (A); 50 µm (B).

2.3.5.1   Pineal photoreceptors morphology

During chick post-hatching life, two types of pinopsin positive pinealocytes were earlier reported. Photoreceptors with ciliary shaped outer-segments, and comma-like elements (without outer segments) were characterized by immunoelectron-miscroscopy (Okano and Fukada, 2001). The cilium-like structures were visualized as string-shaped process, which sometimes presented an enlarged distal portion (pear-shaped). Bulbous-shaped or comma-like elements, presented ultrastructural lamellar complexes, and were detected in the parafollicular region of the follicles.

Several distinct morphologies for pinopsin immunoreactive structures during development of the chick pineal were detected in this study. Pinopsin positive

segments were mainly concentrated in luminal surfaces, presenting elongated string-shaped or pear-shaped projections.

A few pinopsin positive cells first appear by E11, initially only on the pineal recess (Fig. 2.37, B). By E13, several cells containing pinopsin immunoreactive granules surround the luminal space of follicles were detected (Fig. 2.42, A-a). By E15, numerous photoreceptive cells appear in the luminal surface, homogeneously distributed among follicles (Fig. 2.42, B-b). By this stage, it is possible to characterize photoreceptor types according to their morphology under light microscopy. String-shaped or pear-shaped outer segments, and string-shaped segments associated to a bulbous structure, are mainly localized in the luminal surface. Comma-like pinopsin immunoreactive elements were found in the parafollicular area and were much less numerous than string-shaped structures (arrows Fig. 2.42, B).

Comma-like elements and string-shaped structures, immunoreactive to the anti-pinopsin antibody, were earlier described by immunoelectron-microscopic investigations during ontogenesis of the chick pineal (Hirunagi *et al.*, 1997; Okano and Fukada, 2001). However, string-shaped cilia associated to bulbous structures (Fig. 2.42, A-b) have not been found in the mature chick pineal gland. During embryogenesis of quail, similar structure was described being immunoreactive to anti-rhodopsin (Araki *et al.*, 1992).

The string-shaped form associated to a bulbous structure was first visualized by E15 (Fig. 2.42, B-b) and was still present in some follicles by E18 (Fig. 2.43, B-b). By E18, elongated string-shaped pinopsin immunoreactive segments are more frequently visualized (Fig. 2.43) and only a few follicles display the string-shaped form associated to a bulbous structure. By E15, string-shaped elements with an enlarged distal portion can be also found projected to the luminal space of some follicles (Fig. 2.42, C-c). By E18, the same ciliary PRCs are also found in the follicular surface (Fig. 2.43, C-c). By E20, pinopsin positive cells protrude into the luminal space, although, outer segments are not distinguishable (Fig. 2.39, A).

Pinopsin
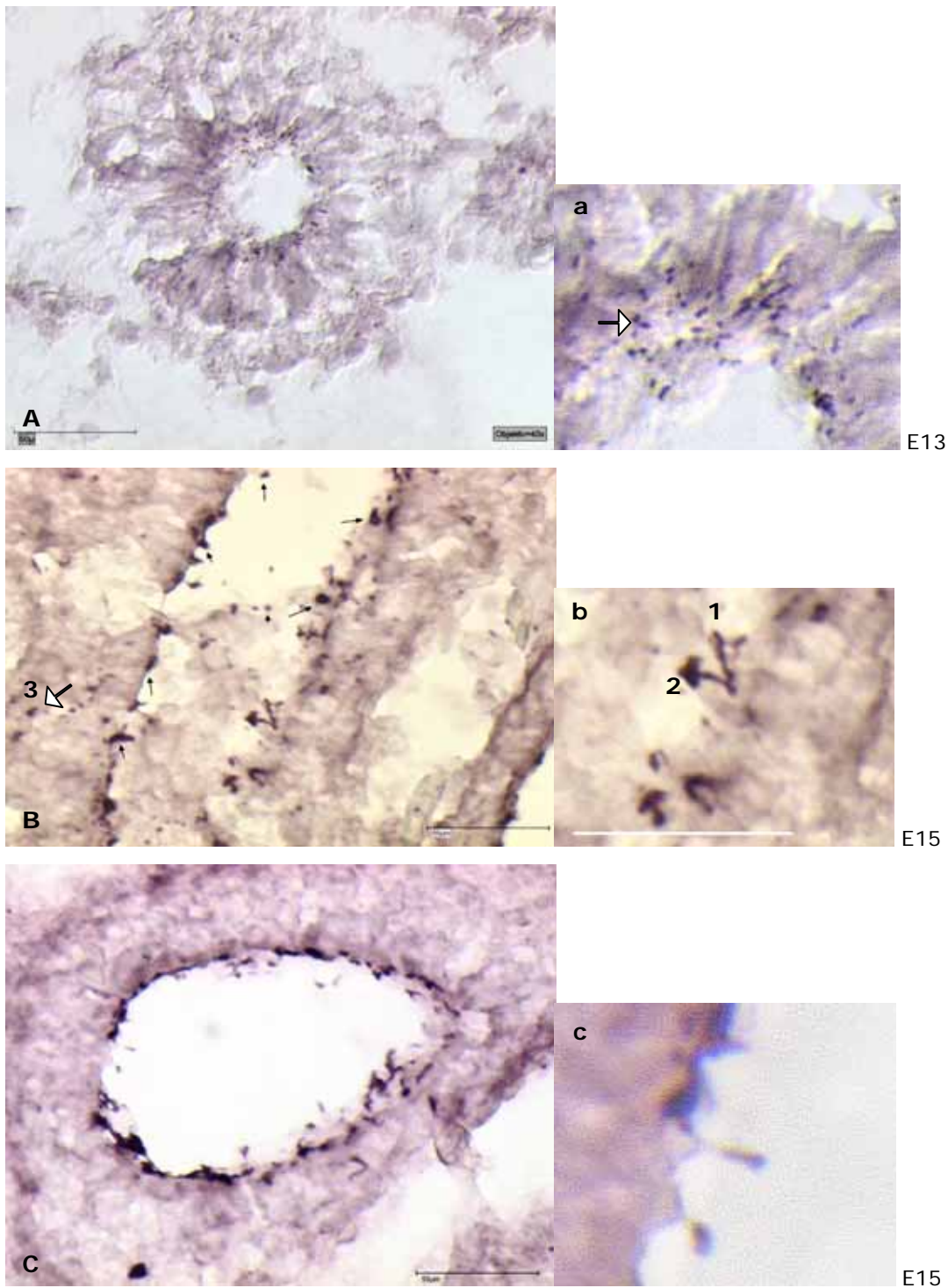
Fig. 2.42: Immunoreactivity for pinopsin in sagittal sections of chick pineal glands. (A-b) By E13, pigment granules surround the luminal space of follicles and pinopsin positive structures are rarely found. (B-c) By E15, pinopsin positive cells are abundant and present three morphologies: string-shaped (1) or string-shaped associated to a bulbous structure (2), and coma-like elements on the parafollicular area (3). Bar: 10 µm (c), 20 µm (C), 25 µm (a), and 50 µm (A and B).

Pinopsin   E18
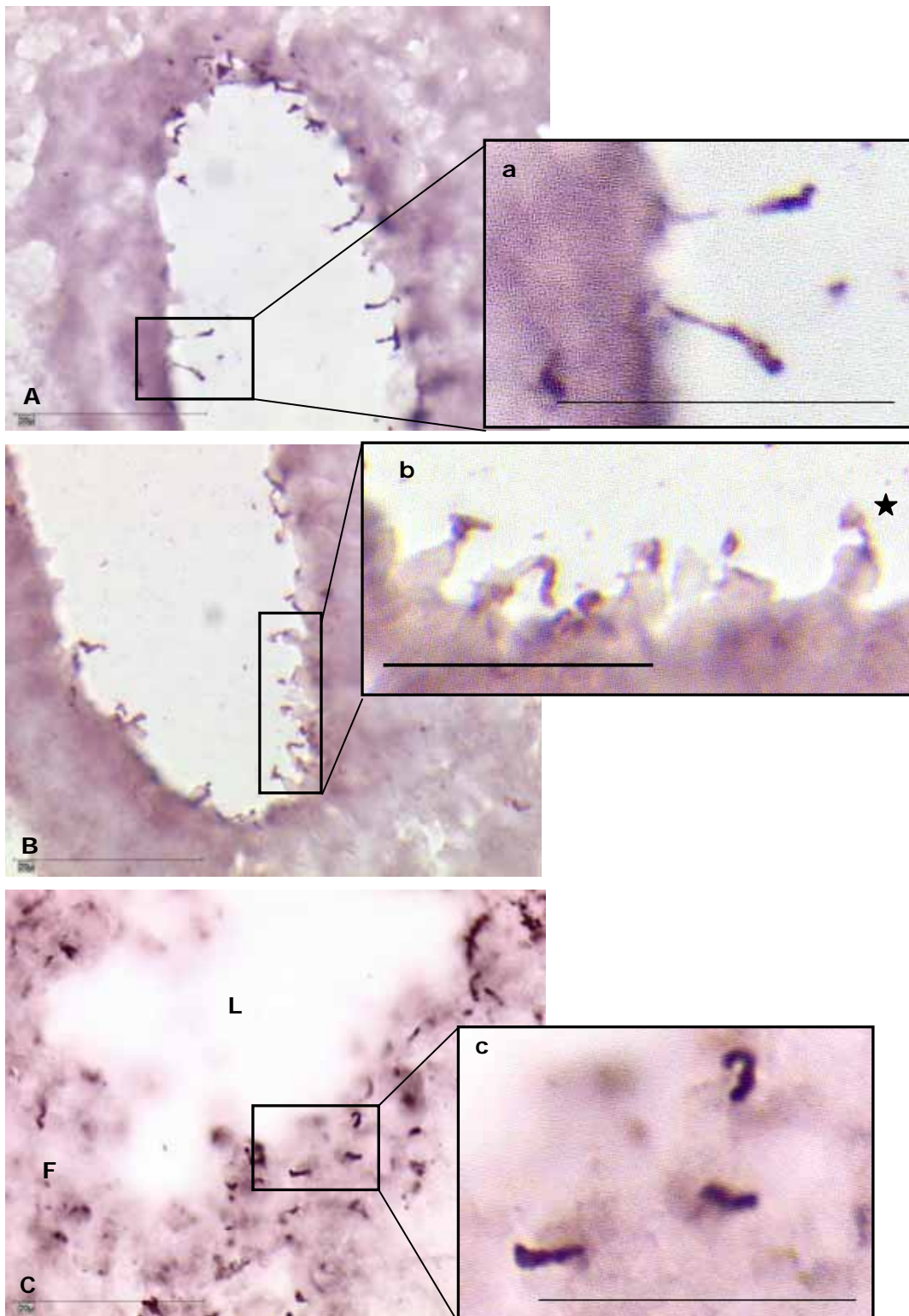
Fig. 2.43: Immunoreactivity for pinopsin in sagittal sections of an E18 chick pineal gland. Pinopsin positive outer segments, string-shaped elongated (A-a) or with an enlarged distal portion (B-c), extend into the luminal space and follicular area of the follicles. (b) String-shaped outer segments associated to bulbous structures were also detected in the luminal surface of some follicles (star). F = follicular area; L = lumen. Bar: 10 μm (a, b, c), 20 μm (A, B, C).

2.3.6 Apoptosis and AChE expression in the developing chick pineal gland

Cell death is an essential process for normal development. When embryonic cells stop dividing, they differentiate, become quiescent, and eventually die. During development of the central nervous system, the original number of neuronal cells is excessive, and part of them undergoes apoptosis during development (Oppenheim, 1991).

Apoptosis was followed by TUNEL assay. Fluorescent-labeled dUTP nucleotides incorporated on DNA strand breaks allowed detection of cells undergoing apoptosis. AChE histochemistry was also conducted for comparison with apoptosis.

Apoptotic cells are shown here to present increased AChE activity (Fig. 2.44). By E19, single cells undergoing apoptosis, and presenting increased AChE activity can be distinguished (Fig. 2.44, arrows). Areas with intensive AChE activity are also shown to be apoptotic (stars).

Earlier stages of development also presented apoptotic activity in correspondent AChE-positive cells (Fig. 2.45; Fig. 2.46).

Apoptosis   AChE

E19
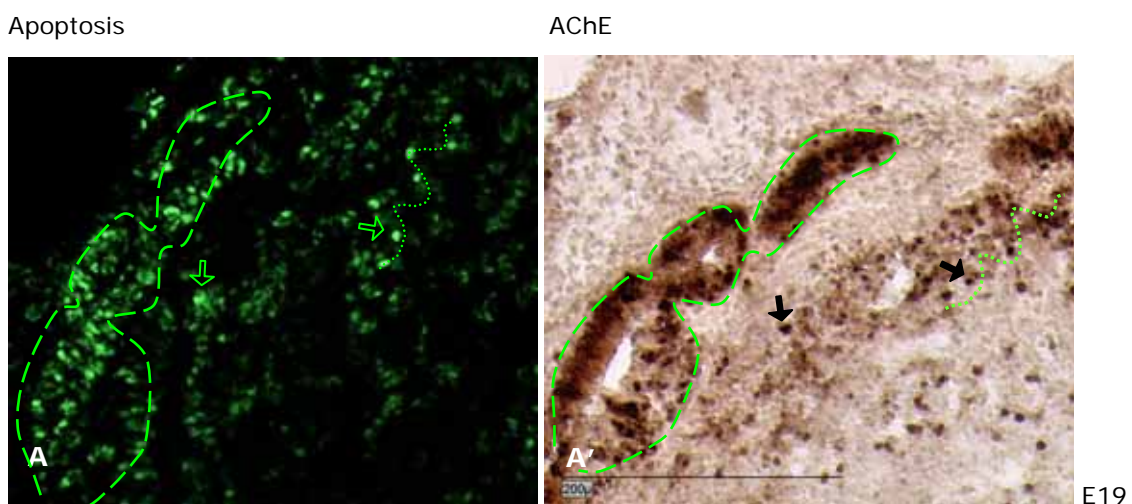
Fig. 2.44: Apoptotic cells (A) are AChE-positive (A´). By E19, apoptotic cells are concentrated in areas with intense AChE activity (stars). Single apoptotic cells, detected by TUNEL assay, can be distinguished by their strong AChE activity in a parallel section histochemically stained (arrows). Bar: 200 μm.

The relation of AChE activity and pinopsin positive cells has been earlier shown in this chapter (Fig. 2.37). However, more AChE than pinopsin positive cells were detected. Here, it is shown that AChE-positive cells, in the luminal space and in the parafollicular region are in great part correspondent to apoptotic cells during development (Fig. 2.44; Fig. 2.45; Fig. 2.46). By E12, a period when AChE activity starts to increase in relation to earlier stages of development, several apoptotic cells are found to be correspondent to AChE-positive cells in the follicles (Fig. 2.45). By E17, a correlation of apoptotic areas and high expression of AChE can be seen (Fig. 2.46, A-A`). By E18, apoptotic cells, surrounding the luminal space, present AChE activity, but not the ones in the interfollicular region (Fig. 2.46, B-B`). By E19, follicles with intense AChE activity also display apoptotic activity in correspondent areas and vice-versa (Fig. 2.46, C-C`).

Control experiments were conducted omitting the enzyme terminal deoxynucleotidyl transferase (TdT), which catalyzes the attachment of fluorescein-dUTP to free 3'OH ends in the DNA breaks, from the protocol. Control stainings resulted in absence of specific fluorescence.
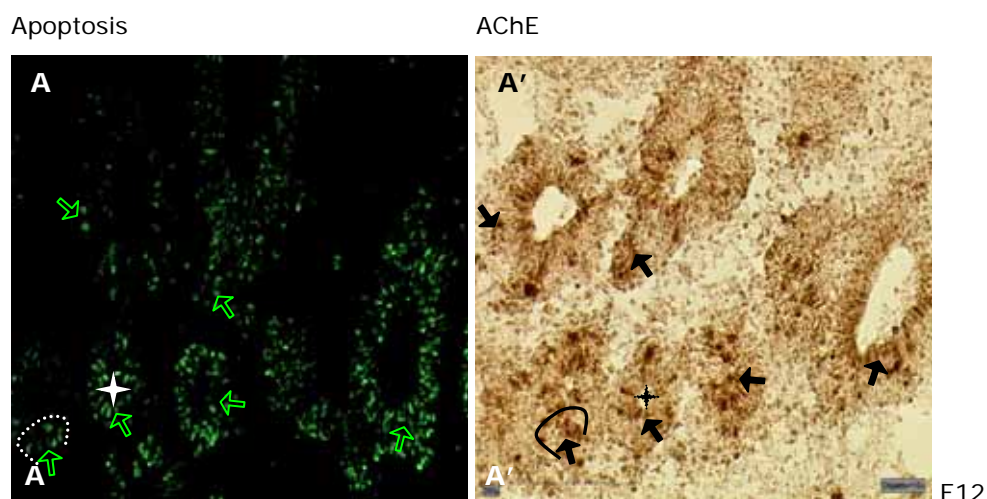
Apoptosis   AChE

Fig. 2.45: Genomic DNA fragmentation by TUNEL assay (A) and AChE histochemistry (A´) in parallel sections of pineal organs. By E12, apoptotic cells (left arrows) are AChE-positive (right arrows). Bar: 200 µm.

Apoptosis   AChE
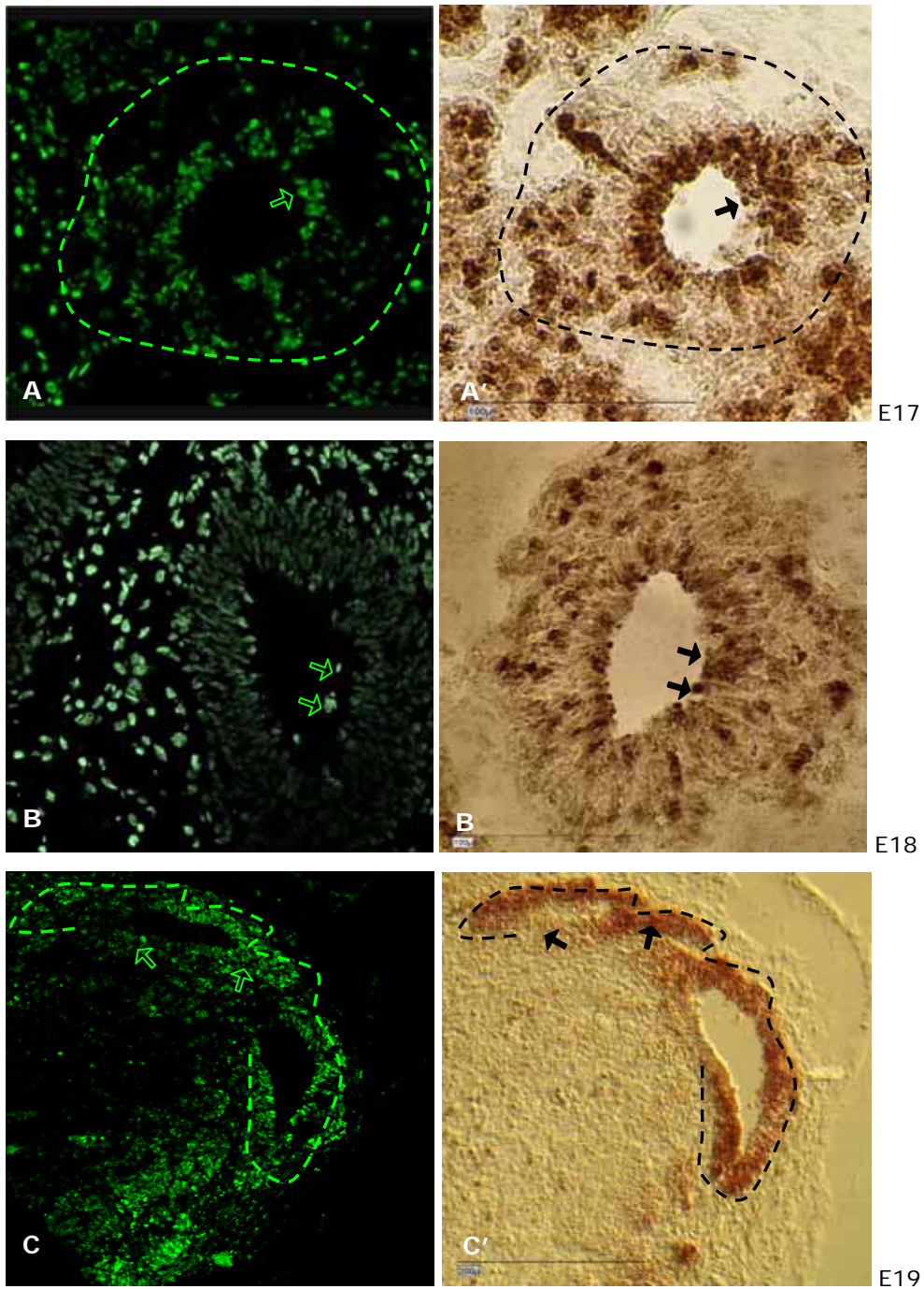
Fig. 2.46: Genomic DNA fragmentation by TUNEL assay (left) and AChE histochemistry (right) in parallel sections of pineal organs. By E17 (A-A`), E18 (B-B`) and E19 (C-C`) apoptotic cells (left arrows) are AChE-positive (right arrows). By E19, areas without apoptotic activity also do not present AChE (C-C`). Bar: 100 µm (A-B`); 200 µm (C-C`).

2.4   Discussion

2.4.1 Remodeling of the chick pineal gland and spatio-temporal implication for cholinesterases expression

AChE accompanies the remodeling of the pineal epithelium during embryogenesis. By E11, with the re-organization of follicular cells into two distinct layers, most AChE-positive cells migrate from the luminal surface to the area between follicular and parafollicular layers (Fig. 2.22; Fig. 2.23). By E12, with the establishment of the parafollicular zone, by the expansion of the follicular area, AChE-positive cells migrate to the borders of the parafollicular zone and become adjacent to the basal lamina. By this stage, cells of the luminal surface reinitiate the expression AChE. This becomes clearer during the prospective stage, with the respective decrease of the BChE activity, a constant increase of AChE-positive cells surrounding the luminal space and the parafollicular area takes place.

AChE activity in whole chick brain homogenates also peaks after E12, displaying predominantly tetramers, as demonstrated in earlier studies (Boopathy and Layer, 2005). Monomers and dimers were shown to be prevalent at younger stages, E7-E11. However, tetramers are much more frequent than the other molecular forms of AChE in brain.

This increase of AChE expression on the parafollicular area accompanies the remodeling of the chick pineal gland.

Mammilliform projections of cells, from the parafollicular region of follicles or recess, migrate through dissolutions of the basal lamina, giving rise to new vesicles. These mammilliform projections are initiated by rosettes of AChE-positive cells, which migrate with surrounding cells until the establishment of a new vesicle, filling its future central lumen. Therefore, the parafollicular zone is transient, as it is constantly rearranged into new follicles. The expansion of the mammilliform projections is followed by a rupture of the basal lamina surrounding the pineal epithelium, as shown during rat pineal development (Calvo and Boya, 1981). It was also demonstrated that cells migrate through these local dissolutions of the basal lamina to form aggregates into the parafollicular area or into the pineal lumen. While cells migrate through the

basal lamina they lose their attachment to it, and the junctions between them, acquiring a round shape (Fujieda *et al.*, 1997). The re-organization of these cells in structured follicles is necessary for their morphological and functional stability, so that cells can differentiate. AChE-positive rosettes of cells guide surrounding cells to migrate through the pineal epithelium and to form the mammilliform projections. As shown here, the borders of these mammilliform projections, surrounding the central rosettes of AChE-positive cells, present proliferation activity and sustain the vesicles growth. With vesicular growth and establishment of organized follicles, remodeling will happen on the newly formed parafollicular area, always ending in new follicular structures that will repeat this process. AChE-positive cells are the beginning and the end point for these remodeling events. The association of AChE with tissue remodeling during development has been also indicated by other authors (Coleman and Taylor, 1996; Layer, 1991; Bigbee *et al.*, 1999).

Beyond its involvement with cell migration, AChE was demonstrated to be in association with PRCs differentiation. Some luminal surface AChE-positive cells suffer differentiation into photoreceptors, and other migrate to the newly formed parafollicular region reinitiating the de novo rearrangement of the parafollicular zone. AChE-positive cells, therefore, have to increase in number during pineal embryogenesis to support developmental events.

Proliferation activity is homogeneously distributed among follicles (Fig. 2.34) until E12. The decrease in proliferation is followed by a decrease in BChE activity, which is completely absent after E19, when vesicle formation ceases. The progressive decrease in BChE activity after E12 is followed by an immediate increase in AChE expression. Cells which were BChE positive, while proliferating, become later AChE-positive and sustain the number of AChE cells for follicular expansion and remodeling. Migration of the AChE-positive cells occurs from the follicular area in direction to parafollicular zone and central lumen (Fig. 2.26; Fig. 2.27). With the formation of the parafollicular area, follicular post mitotic cells become AChE-positive and migrate along development. Cells can either migrate back to the central lumen or occupy the borders of the parafollicular zone. As vesicles become bigger (E17), AChE-positive cells occupy the luminal surface densely, as well as the borders of the parafollicular region. By E18, remaining BChE activity can be seen on the recess in limited regions responsible

for vesicles formation (Fig. 2.13, Q). However, by this period the compactation process of pineal follicles takes place and follicles expansion ceases.

The shift in expression of BChE to AChE reflects the transition from cell proliferation to cell differentiation. Therefore, this suggests BChE expression is implicated in cell proliferation and its absence in cell differentiation. This assumption is supported by other studies on chick development (Layer, 1990; Alber *et al.*, 1994). Furthermore, an antisense 5`- BChE inhibited cell proliferation and accelerated differentiation in transfected retina cells reagregates cultures (Robitzki *et al.*, 1997). A co-regulation of AChE and BChE was also demonstrated by the suppression of BChE, resulting in increased AChE transcription and protein activity (Robitzki *et al.*, 1998).

2.4.1.1   *Remodeling implication for supportive cells*

The remodeling of the pineal gland vesicles into follicles is accompanied by the appearance of supportive cells into follicular tissue by E11 (Fig. 2.22, B; Fig. 2.36, C). Using vimentin as a glia cell marker, glia was shown to be the predominant cell type of the chicken pineal gland, in the interfollicular and follicular area of structured follicles (Fig. 2.36). Glia-like cells are known to occur in the pineal gland of rat, mouse, gerbil and others (Schachner *et al.*, 1984; Redecker, 1998).

Regarding its relevance, glia was originally thought to serve only as connective-tissue cells. Nowadays, more relevant roles for the glial cells have been described. They regulate the initiation of axonal sprouting and outgrowth and support the structural stability of synapses (Hatten 1990; Bechmann and Nitsch, 2000; Pfrieger, 2002). Moreover, vimentin immunoreactive-astrocytes are suggested to serve as a source of cytokines or as a physical conduit for migrating cells (Wang *et al.*, 2004). The appearance of glia cells on follicles, just before the pinopsin photopigment expression onset, is potentially related to their relevance for neuronal cells differentiation. Differentiation of supportive and follicular cells was earlier shown, in electron microscopy studies, to happen before the differentiation of parafollicular cells during chicken pineal embryogenesis (Ohshima and Matsuo, 1988). Therefore, supportive cells are supposed to became more distinct by the differentiation of photoreceptors.

The remodeling events happening on the chick pineal gland by the moment vimentin positive cells appear in the follicular zone are temporally correlated with the differentiation of photoreceptors, and occasionally are contributing for it. It is already known that mechanical stimuli can promote changes in shape, growth, and gene expression of many cell types (Curtis and Seehar, 1978; Ingber *et al.*, 1994). However, chemical stimulus is also essential for migrating cells, eventually supported by glia. Therefore, the correlated temporal events of follicles structure definition, glia cells appearance in follicles, and subsequent onset of photoreceptors differentiation, are interconnected within the pineal remodeling process.

2.4.1.2 *Photoreceptors differentiation and AChE expression during pineal embryogenesis*

The AChE expression pattern is altered during pineal´s remodeling process. AChE has been already reported to be an early marker for differentiation (Miki and Mizoguti, 1982).

By E12, when photoreceptor differentiation becomes prominent, AChE-positive cells, which were between follicular and parafollicular layer by E11, migrate to the borders of the parafollicular layer. Then, they reappear in the luminal space (Fig. 2.17, G`), correlating with the onset of pinopsin positive cells. The distribution of AChE-positive cells increases constantly in intensity and number from E13 onwards, as well the number of pinopsin PRCs. The spatio-temporal distribution of pinopsin positive cells and AChE activity shows that these events are interconnected. Therefore, central lumen AChE-positive cells are involved in cell differentiation.

With these findings, a schema of the relationship of cholinesterases with remodeling and differentiation of the pineal gland can be drawn (Fig. 2.47).
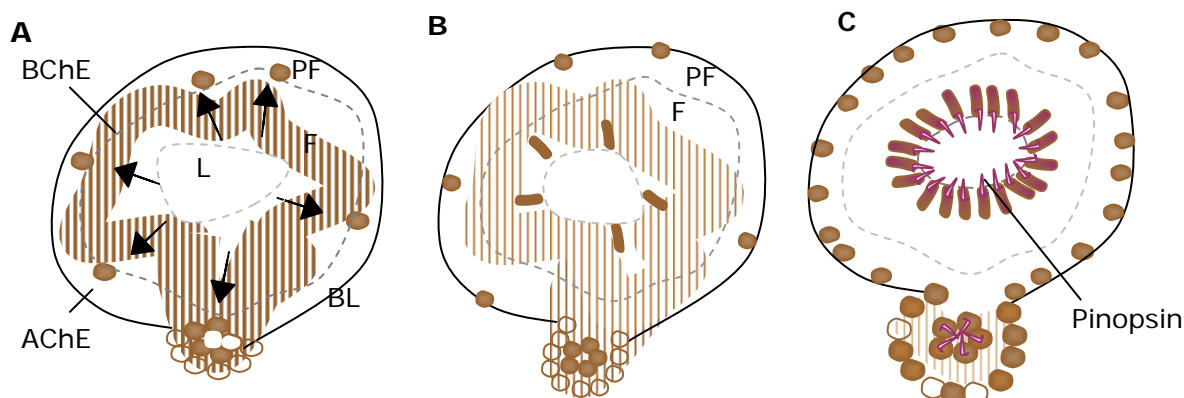
Fig. 2.47: Schema of AChE, BChE and pinopsin expression during pineal embryogenesis. (A) By E11, AChE-positive cells have migrated from the luminal surface in direction to the newly established parafollicular zone. BChE activity, which was abundant in vesicular surface, declines with the proliferative state, becoming limited to regions with proliferation activity. (B) By E12, AChE-positive cells migrate to the borders of the parafollicular zone, and new AChE cells reappear in the luminal surface with the increase of photoreceptive cells. (C) As vesicles grow and form structured follicles, new cells become AChE-positive with respective pinopsin expression on central lumen of newly formed vesicles.

2.4.1.3   *Photoreceptors diversity*

From the three kinds of photoreceptor morphologies detected in this study, at least one is not described in the literature. Whether this morphology is transformed during post-hatching life by the loss of lamellar structures associated to outer segments, or whether it is a unique type of PRC that appears just during embryonic period is not clear. During ontogenesis, the pineal organ of chicken undergoes transformation from a photosensory organ to an endocrine gland. A sensory regression of the chick pineal during the post-hatching period is nevertheless contradictory. Several pineal follicles are invaded by connective tissue towards hatching period implying a compactation of the pineal organ and decrease of photoreceptors number (Sato, 2001). On the other side, Omura (1977) describes one type of photoreceptor in fifteen day old Brown leghorns chicks, which was not found during earlier periods. Bischoff (1969) also observed lamellar whorls associated to cilia outer segments in adult chicks. These, among others, are contradictory studies about the failure of outer segments to mature in the chicken pineal gland. The temporal dependence of the expression of different types of photoreceptors might have a relation with regulatory mechanisms, rather than with the hypothesis that one type of PRC evolved to another during avian ontogenesis.

2.4.1.4   Relation pineal/retina AChE expression

Non-catalytic involvement of AChE in neurogenesis, based on its spatio-temporal expression pattern during development of the chick, has been earlier described in retina (Layer, 1990).

Though structurally similar, retina and pineal differ in relation to AChE activity. In retina, the outer segments of the photoreceptors are facing outwards to the pigment epithelium (PE). AChE-positive cells (amacrine and ganglion cells) are distributed on the ganglion cell layer and on the adjacent inner plexiform layer (Fig. 2.48). In the pineal gland on the other hand, the photoreceptors outer segments are projected into the luminal space and show AChE activity.

Nevertheless, retina spheroids, developed from reaggregates of dissociated cells of the chick retina, form rosettes displaying photoreceptor outer segments projecting into their luminal space (Layer *et al.*, 1997a), resembling the follicles of the pineal organ. These spheroids, therefore, show an inverse cell layer structuration compared to the one found in retina, though originally composed of retina cells (Willbold and Layer, 1992).
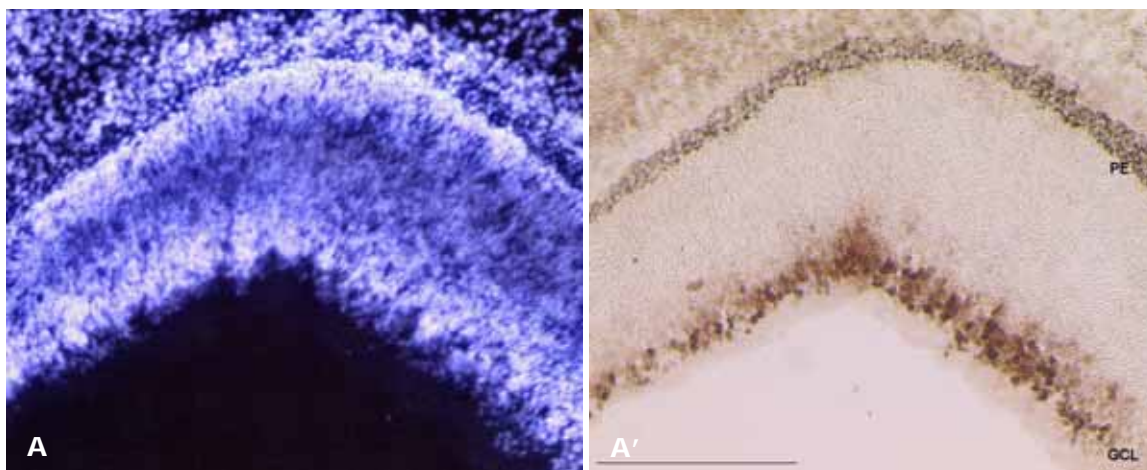
Fig. 2.48: Double staining, DAPI (A) and AChE (A`) histochemistry, of an E6 retina. By this stage it is possible to distinguish the GCL and the PE of the retina. (A`) Cells of the ganglion cell layer present AChE activity. PE = Pigment epithelium; GCL = Ganglion cell layer. Bar: 100 µm.

Pinealocytes have evolved from a common ancestral photoreceptor of both the pinealocytes and retinal photoreceptors (Klein, 2004). Even though PRCs of the retina are not AChE-positive, their differentiation is indicated to be dependent on AChE expression. In AChE knockout mice an impaired inner retina formation was shown, which resulted in the degeneration of photoreceptor cells (Bytyqi *et*

al., 2004). AChE clearly accompanies the embryonic development of photoreceptive cells in chick pineal (Fig. 2.37), indicating that AChE also plays a role on photoreceptor differentiation in this tissue. Therefore, AChE is involved in PRC differentiation in both retina and pineal gland.

AChE is also indicated to be involved in retina photoreceptor functioning. Layer *et al.* (1997b) proposed a regulatory role for AChE on the establishment of excitatory and inhibitory channels ("on-off decisions") in retina. AChE has been also associated with post-natal photoreceptor development, because an increased expression of AChE takes place during this period (Hutchins, 1987). Similarly, the presence of AChE in PRCs of the pineal might imply the involvement of this enzyme with the physiological processes dependent on the PRCs stimulus. Therefore, a link between the presence of AChE on PRCs and metabolism can be hypothesized. How AChE would interfere on melatonin regulation is still not clear, but earlier reports have shown that the AChE activity is altered during circadian rhythm (Quay *et al.*, 1971; Schiebeler, 1974; Mohan, 1974; Wood, 1979; Lewandowski, 1986; Pan, 1991).

2.4.1.5 AChE associated with PRCs during post-hatching life

The association of AChE with PRCs during chick pineal embryogenesis has been investigated for the first time. Similarly, during postnatal periods, AChE expression decreases in parallel to the number of PRCs (Sato and Wake, 1983; 1984).

During post-hatching life, a functional transition of the avian pineal organ from a photoreceptive to an endocrine gland takes place (Sato and Wake, 1983; 1984). The failure of pineal photoreceptive cells in establishing appropriate synaptic connections might trigger the death of other neurons associated to them (Sato *et al.*, 1988), since neurons need to make or to receive synaptic connections to be functional (Clarke and Cowan, 1975). Therefore, PRCs differentiate and die being AChE-positive.

2.4.2 Apoptosis and AChE

Half of the cells originally produced on the central nervous system die during establishment of neuronal connections with the target tissue (Oppenheim, 1991). It is hypothesized that the excessive population of neurons has to

compete for a limited amount of neurotrophic factors, and just the neurons that connect to a target tissue will access neurotrophic factors and survive. Therefore, apoptosis in development is a natural process, which ensures that neurons make the appropriate connections with their targets.

The increase of AChE-positive cells on the chick pineal, after the embryonic day 12, is far more pronounced than the number of differentiating pinopsin positive cells (Fig. 2.37). Several of these AChE-positive cells end in apoptosis (Fig. 2.45; Fig. 2.46). This is possible, because transcription and translation continue to take place in dying neurons as demonstrated by Martin *et al.*, 1988.

When undergoing either proliferation or apoptosis, cells assume a round shape and show chromatin condensation (King and Cidlowski, 1995). Some apoptotic labeled cells showed a cell rounding morphology, which also can be seen through a close inspection of AChE histochemistry (Fig. 2.44).

Apoptosis has been found to be induced via the stimulation of several different cell surface receptors in association with caspases activation (Hu *et al.*, 1998; Li and Yuan, 1999). AChE has been suggested to be essential for the assembly of the apoptosome, whose function is to activate the caspase-9 (Park *et al.*, 2004). Caspase-9 initiates the activation of the caspases cascade and, therefore, initiates the apoptotic process. However, it was the first time AChE was shown to be associated with naturally occurring apoptosis during development.

2.4.2.1   *Cell apoptosis mechanisms and AChE*

Apoptosis can be triggered by internal signals, in a so called "intrinsic or mitochondrial pathway" or by an "extrinsic pathway" (Fig. 2.49).

The intrinsic pathway is dependent of the formation of the apoptosome, which has been shown to be mediated by AChE (Park *et al.*, 2004). Briefly, the intrinsic pathway comprises the following steps leading to the formation of the apoptosome: a) in a healthy cell, the outer membranes of its mitochondria express the protein Bcl-2 on their surface; b) Bcl-2 binds to a molecule of the protein Apaf-1 (apoptotic protease activating factor-1); c) internal damage to the cell causes Bcl-2 to release Apaf-1 and a related protein, Bax, to penetrate mitochondrial membranes, causing cytochrome c to leak out; d) the released cytochrome c and Apaf-1 bind to molecules of caspase 9. These steps result in a

complex of cytochrome c, Apaf-1, caspase 9 and ATP, which all together form the apoptosome (Becker and Bonni, 2004) in the presence of AChE (Park *et al.*, 2004). Caspase 9 is one of the 11 caspases known in vertebrates. Caspase 9 initiates a cleavage cascade, activating other caspases. The sequential activation of one caspase by another creates an expanding cascade of proteolytic activity, which leads to the digestion of structural proteins in the cytoplasm, the degradation of chromosomal DNA, and the phagocytosis of the cell (Becker and Bonni, 2004). The mechanism of apoptosis via mitochondrial pathway has been also described in *C. elegans* - demonstrating, this cell death pathway has been conserved during evolution (Cryns and Yuan, 1998).

However, apoptosis can also be triggered by external signals of the extrinsic or death receptor pathway, via tumor necrose factor (TNF), not involving the apoptosome complex. It is also dependent on the activation of a caspase cascade (caspase 8 and 10), leading to phagocytosis of the cell (Becker and Bonni, 2004). Apoptosis caused by external signals is usually seen in neurological diseases, while cell death caused by internal signs is often the case in nervous system development, as it was shown here in association with AChE expression. Accordingly, not all apoptotic tissues will present increased AChE expression.

Recalling studies in AChE KO mice retina, photoreceptors degeneration was observed during early post-natal life (Bytyqi *et al.*, 2004). AChE is not expressed by photoreceptive cells in retina, but its expression levels are in association with photoreceptors postnatal development (Hutchins, 1987). The direct association of AChE activity with pineal photoreceptors is shown here to be related to the early death of the photoreceptive cells during pre-hatching periods. In retina, photoreceptor cells are not lost during development; they even accumulate outer-segment discs. In adult rat, they constantly regenerate the membrane discs of the rod outer segments (Goldman, 1982). The fact that photoreceptor cells could not survive in AChE KO mice, indicates a relevance of AChE for their development. The absence of AChE in the photoreceptors, which undergo degeneration, suggests that apoptosis has been generated by the extrinsic pathway in this case. If we consider, that the mechanism of the death receptor pathway is the one acting for the degeneration of the AChE KO mice

retina, it can justify the direct association of AChE with pineal PRCs, which normally die during development.
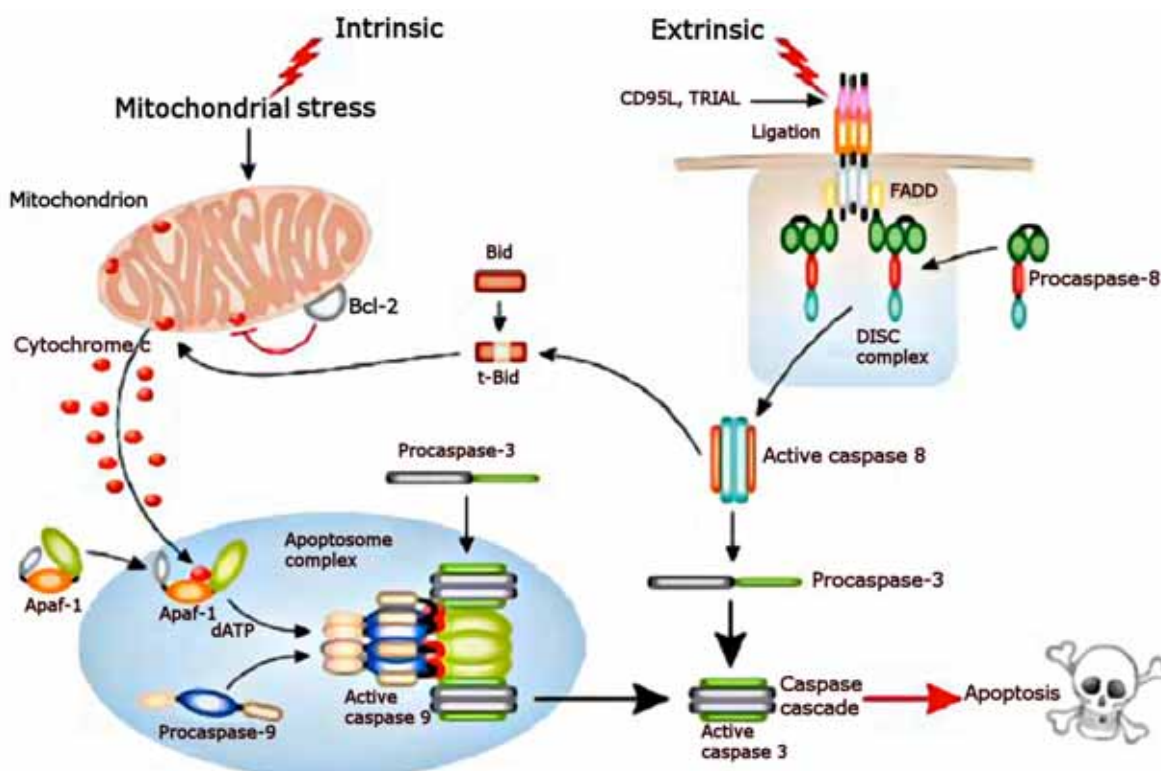
Fig. 2.49: Intrinsic and extrinsic apoptotic pathways (MacFarlane and Williams *et al.*, 2004).

2.4.2.2   *Apoptotic post-mitotic neurons*

Apoptosis and cell proliferation are suggested to be regulated by similar molecular mechanisms. PCNA has a triple function in the life and the death of the cells. It is an essential component of the DNA replication machinery, functioning as the accessory protein for DNA polymerase δ, required for processive chromosomal DNA synthesis, and DNA polymerase ε, required for DNA recombination and DNA damage repair (Celis, 1985). It was already demonstrated that PCNA inhibition prevents cells from entering the S-phase of the cell cycle and eventually leads to cell death (Javier *et al.*, 1997; Mattock, 2001). Cell death after intensive proliferative periods has been observed in several studies of induced apoptosis by neurotoxic stimulus (Feddersen *et al.*, 1992; Copani *et al.*, 1999), and avoided with antisense oligonucleotides to DNA polymerase (Copani *et al.*, 2002).

Intense proliferation activity in the pineal gland is found until E12, whereas apoptotic cells can also be detected (Fig. 2.45). The tendency of apoptosis is to

increase, as it approaches the end of embryogenesis (Fig. 2.46). By E17, interfollicular cells are positive for the proliferation marker PCNA (Fig. 2.31, A), while apoptotic cells are restricted to the follicles (Fig. 2.46, A). By E18, the interfollicular cells do not express PCNA anymore (Fig. 2.31, B) and start to undergo apoptosis (Fig. 2.46; B), causing the decrease and nearly the disappearance of the interfollicular space by the end of pineal development (Fig. 2.15).

During intensive proliferative periods AChE activity is very low and limited to a few follicular cells (Fig. 2.20). After the embryonic day 12, AChE predominates in relation to BChE and increases constantly in activity and number of positive cells towards the end of the chick pineal embryogenesis (Fig. 2.13; Fig. 2.14), and several of these AChE-positive cells become apoptotic (Fig. 2.44; Fig. 2.45; Fig. 2.46). AChE expression has been earlier associated with the decrease of cell proliferation (Soreq *et al.*, 1994a; Robitzki *et al.*, 1998; Grisaru *et al.*, 1999).

AChE correlation to apoptosis has been supported by investigations using cell cultures (Hu *et al.*, 1998; Li and Yuan, 1999; Zhang *et al.*, 2002; Park *et al.*, 2004; Jin *et al.*, 2004). The relation of BChE/AChE activity and apoptosis has been shown by the suppression of BChE in reaggregate retina cell cultures, inducing apoptosis and increasing AChE mRNA expression and enzyme activity (Robitzki *et al.*, 1998). The results presented here, therefore, corroborate the relevance of AChE for the apoptotic process and indicate its involvement with naturally occurring apoptosis.

2.4.2.3   *Melatonin metabolism, cholinesterases, and neurodegenerative processes*

The influence of light on melatonin metabolism, happening in the pineal gland, is accentuated in diseases like Alzheimer. Physiological functions following a circadian rhythm, such as the sleep-wake cycle, are disturbed with aging, and accentuated in Alzheimer's patients (Wu and Swaab, 2005).

An accentuated expression of AChE and BChE has been detected around the amyloid plaques and neurofibrillary tangles in the brains of Alzheimer's patients (Small, 1996). AChE is able to accelerate the amyloid formation and such an effect is sensitive to drugs that block the enzyme, showing AChE inhibitors provide a possibility for treating Alzheimer's disease (Inestrosa *et al.*, 2005).

Therefore, understanding the implications of cholinesterases expression in the pineal gland is also relevant for pathological states involving both cholinesterases and circadian rhythm disturbances.

2.5   Summary

The data presented in this chapter support:

- A role of AChE on pineal epithelium remodeling (follicles development);

- The association of AChE expression with photoreceptors differentiation;

- The organization of follicles with supportive cells is interconnected with PRCs differentiation;

- The existence of at least one PRC morphology type occurring in chick pineal only during the embryonic period;

- A developmentally regulated switch from BChE to AChE expression during pineal embryogenesis related to cell proliferation and differentiation, respectively;

- An inversely proportional co-regulation of AChE and BChE expression;

- The association of AChE expression with apoptosis during development.

CHAPTER 3

3 A malformation of zebrafish (*Danio rerio*) embryogenesis is generated by serotonin administration, and is related to acetylcholinesterase expression

3.1   Overview

The association of cholinesterases with remodeling, differentiation, proliferation, and apoptosis of the chick pineal cells, was demonstrated in the previous chapter. How cholinesterases are involved with most of these processes is still not understood. The possibility that a second activity of ChEs would be participating in developmental events is still open, and will be addressed in this chapter.

Several vertebrates display an aryl-acylamidase (AAA) activity, peculiarly associated with the esterase activity. The functional relevance of AAA associated to cholinesterases is not known. Therefore, the characterization of the AAA activity during ontogenesis of organisms can bring insights into its implication for developmental processes.

The sensitivity of the AAA activity associated to ChEs towards serotonin means that a property of a component of the cholinergic system is making reference to a serotonergic neurotransmitter. The influence of it for AChE or for the serotonin metabolism on the body is not clear. However, a reciprocal influence of the serotonergic system towards cholinergic components has been studied, as both systems influence, in some cases, the same physiological processes.

3.1.1 Zebrafish AChE

Zebrafish (*Brachydanio rerio* or *Danio rerio*) is a promising model organism to study AChE relevance as it does not have the *BCHE* gene, which is supposed to have been lost in zebrafish during evolution, emerging later in birds (McClellan *et al.*, 1998). Zebrafish was shown to have a single AChE gene encoding only T subunits (Bertrand *et al.*, 2001), forming molecular forms mentioned in the chapter 1.

The zebrafish *ACHE* gene presents 62% identity with the mammalian *ACHE*, 64% with the *ACHE* from *Torpedo californica* (Pacific electric ray), and 80% with the *Eletrophorus electricus* (electric fish) *ACHE*.

AChE spatio-temporal expression during zebrafish embryogenesis has been detected, by histochemistry and *in situ* hybridization, in somitic mesodermal cells prior to the onset of somitogenesis (Hanneman, 1992; Bertrand *et al.*,

2001). It starts in presomitic-mesoderm at the sixtieth somite stage (12 h), previously to body movements.

During development of several vertebrates, AChE has been shown to be expressed much earlier than synapses become functional (Layer *et al.*, 1988; Layer 1990). In zebrafish, nicotinic acetylcholine receptors (nAChR) beta3 and alpha2 are known to be transcribed as early as 2 and 5 hours post-fertilization (hpf), respectively (Zirger *et al.*, 2003), suggesting that other components of the cholinergic system could also be present at these early embryonic stages. However, the expression of AChE in zebrafish has not been investigated with more sensitive techniques than *in situ* hybridization or histochemistry.

3.1.2 Esterase activity inhibition or absence during development

As characterized in the previous chapter of this work, AChE and BChE show a spatio-temporal co-relation to developmental processes.

Other studies have attempted to show the relevance of cholinesterases inhibiting them in model organisms. For instance, rats showed behavioral changes, and down regulation of muscarinic receptors in the brain at single oral doses of chlorpyrifos, an esterase activity inhibitor (Moser and Padilla, 1998). Hanneman (1992) also attempted to show the relation of cholinesterases inhibition to malformations of zebrafish embryos, using a broad spectrum inhibitor of serine proteases and related enzymes. He demonstrated that somitogenesis was disrupted in the presence of diisopropylfluorophosphate (DFP). Furthermore, studies in sea urchin, demonstrated the action of chlorpyrifos was essentially restricted to the mid-blastula stage, not affecting cleavage division, and showing a decreased impact on gastrulation (Buznikov *et al.*, 2001).

An impact of the cholinergic system development was shown by a chemically induced recessive mutation in zebrafish AChE gene (Ser226 → Asn226), which abolished the esterase activity of AChE. Impaired motility at the 48 hpf larvae stage, and disruption of the cellular organization of muscle fibers in zebrafish mutants were observed (Behra *et al.*, 2002).

3.1.3 AAA: a side activity of AChE

The vertebrate aryl acylamidase (AAA) activity was first reported in rat brain (Fujimoto, 1974), and later found to be associated with AChE (George and Balasubramanian, 1981). The AChE-associated AAA activity, present in avian and mammals (Boopathy and Layer, 2004; Fujimoto, 1974), is one example of AChE functioning in a noncholinergic manner.

The endogenous substrate for AAA is not known. It splits the artificial substrate *o*-nitroacetanilide (*O*-NAA) into *o*-nitroaniline and acetate. AAA is inhibited by acetylcholine, specific anticholinesterase compounds, tyramine, ethopropazine and serotonin.

The sensitivity of AAA towards serotonin (5-hydroxytryptamine, 5-HT) has drawn attention to this side activity of AChE, implying a direct influence of serotonergic mechanisms on a component of the cholinergic system (and vice versa).

3.1.4 Cholinergic and serotonergic systems

Acetylcholine (ACh) is synthesized from choline and acetyl-CoA through the action of choline acetyltransferase. When an action potential reaches the terminal button of a presynaptic neuron a voltage-gated calcium channel is opened. The influx of calcium (Ca^{2+}) ions stimulates the exocytosis of vesicles containing ACh, which is thereby released into the synaptic cleft. The activation of ACh receptors leads to a large Na^+ influx and a smaller K^+ efflux. The inward Na^+ current depolarizes the postsynaptic membrane and initiates an action potential (Berg *et al.*, 2002). Once released, ACh must be removed rapidly by AChE in order to allow repolarization to take place.

Serotonin (5-hydroxytryptamine, 5-HT) is formed by the hydroxylation and decarboxylation of tryptophan. Virtually all brain tryptophan is converted to serotonin. The greatest concentration of 5-HT (90%) is found in the enterochromaffin cells of the gastrointestinal tract. The remainder 5-HT is found in platelets and on the CNS. Effects of serotonin on the central nervous system are numerous, complex and difficult to systematize. The effects of 5-HT are felt

most prominently in the cardiovascular system, with additional effects in the respiratory system and the intestines (Barnes and Sharp, 1999).

Serotonin (5-HT) does not just function as a neurotransmitter, but also as a hormone, which is primarily used for synthesis of melatonin. Melatonin in turn, regulates physiological processes like diurnal (circadian) and seasonal behavior (Cahill, 2002). The serotoninergic system is known to modulate mood, emotion, sleep and appetite, and thus is implicated in the control of numerous behavioral and physiological functions. Hinman and Szeto (1988) have shown cholinergic influences on sleep-wake patterns in fetal lambs, blocking central cholinergic muscarinic receptors. This is an example of interactions between cholinergic and serotonergic systems leading to a common physiological process.

The first cholinergic neurons in the zebrafish can be detected by Karnovsky-Roots-staining by 13-14 hpf. In contrast, serotonergic neurons first appear around 45 hpf; according to 5-hydroxytryptamine immunoreactivity (Teraoka *et al.*, 2004).

3.1.4.1   *Serotonin receptors*

Seven types of 5-HT specific receptors ($5-HT_1$ to $5-HT_7$) have been described in mammals (Teitler *et al.*, 1994). Within the $5-HT_1$ group, there are five subtypes ($5-HT_{1A}$, $5-HT_{1B}$, $5-HT_{1D}$, $5-HT_{1E}$, and $5-HT_{1F}$). There are three $5-HT_2$ subtypes ($5-HT_{2A}$ to $5-HT_{2C}$), as well as two $5-HT_5$ subtypes ($5-HT_{5a}$ and $5-HT_{5B}$). Most of these receptors are coupled to guanine nucleotide binding proteins (G proteins), inhibiting cAMP formation, as part of their signaling pathway (Meneses, 1998).

Some serotonin receptors are presynaptic and others postsynaptic. The $5-HT_{2A}$ receptors mediate many of the central and peripheral functions of 5-HT. Cardiovascular effects include contraction of blood vessels, vascular permeability, and platelet aggregation. Central nervous system effects include neuronal sensitization to tactile stimuli, anxiety and mediation of hallucinogenic effects (Barnes and Sharp, 1999). 5-HT2 receptors have been characterized in Drosophila and are under investigation in zebrafish (Colas, 1995).

The $5-HT_3$ receptors are present in the gastrointestinal tract and are related to vomiting. Also present in the gastrointestinal tract are $5-HT_4$ receptors where they function in secretion and peristalsis. The $5-HT_6$ and $5-HT_7$ receptors are

distributed throughout the limbic system of the brain, and the 5-HT$_6$ receptors have high affinity for antidepressant drugs.

3.1.4.2 Neurotransmitters during pre-nervous period

The existence of pre-nervous neurotransmitters was investigated in invertebrates (sea urchins and starfish) and vertebrates (amphibian and fish), by Buznikov (1991; 2001). Serotonin and acetylcholine were found during early stages of embryogenesis, and were postulated to be involved with the first cleavage divisions and morphogenetic cell movements during gastrulation and post-gastrulation in sea urchins. 5-HT was shown to block or inhibited cleavage division as an antagonist of acetylcholine, catecholamine and indolylalkylamines (Buznikov, 1991). The endogenous indolealkylamides belong to those factors that determine the length of the lag-period. Exogenic 5-HT (100 µg/ml) retards activation of protein synthesis after fertilization, reliably lengthening the lag-period by 80%. Therefore, immediately before the start of protein synthesis activation, the level of 5-HT like substances decreases (Buznikov, 1971).

3.1.5 Zebrafish embryonic development

With the fertilization of the egg starts the zygote period, and it ends as the first cleavage occurs. According to the zebrafish book (Westerfield, 2000) the embryonic development of zebrafish is comprised by the following periods (Fig. 3.1):

• Cleavage Period (0.7- 2.2 h)

After the first cleavage, the originated cells, denominated then blastomeres, divide at about 15 minute intervals. Until the end of the cleavage period usually six cleavages occur at regular orientations, originating 64 cells. The number of blastomeres can be deduced from their arrangement.

• Blastula Period (2 1/4 - 5 1/4 h)

The beginning of the blastulation occurs with the seventh cleave, at the 128-cell stage, and continues until epiboly begins with the onset of gastrulation. The midblastula transition (MBT) stage is characterized by the cell cycle lengthening (Kane and Kimmel, 1993), as not all of the cycles begin to lengthen synchronously or to the same extent by the tenth cell cycle (512-cell stage).

Throughout MBT the mRNA transcription increases. By the end of the blastula period, epiboly begins (Solnica-Krezel and Driever, 1994). Epiboly appears to depend on functional microtubules (Strähle and Jesuthasan, 1993) and might be under control of early-acting zygotic genes (Kane, 1996). The earliest-expressed genes identified so far code for regionally localized putative transcription factors, and begin expression in the late blastula (e.g. the gene *no tail*, Schulte-Merker *et al.*, 1992; *goosecoid*, Stachel *et al.*, 1993).

• Gastrula Period (5 1/4 - 10 h)

Epiboly continues, and in addition, the morphogenetic cell movements of involution, convergence, and extension occur, producing the primary germ layers and the embryonic axis. By 5.5 h, gastrulation begins with movements of involution by 50% epiboly. Convergence movements promote a local accumulation of cells at one position along the germ ring, the so-called embryonic shield, the future dorsal side of the embryo. Expression of the gene *goosecoid* (gsc) is a reliable marker of where the shield will form, and appears to label the earliest cells to involute at the shield, the axial hypoblast (Stachel *et al.*, 1993). These first cells, expressing *goosecoid*, appear to correspond to precursors of the tetrapod prechordal plate. About an hour and a half after the beginning of gastrulation, the shield extends towards the animal pole. Half way through gastrulation, the axial hypoblast becomes clearly distinct from paraxial hypoblast, which flanks it on the other side. Anterior paraxial hypoblast will generate muscles to move the eyes, jaws, and gills. More posteriorly, much of the paraxial hypoblast is present as the segmental plate that will form somites. By the end of gastrulation, the first signs of a rudiment central nervous system appear with the distinction of the neural plate. The end of gastrula is considered to happen when epiboly is complete, and the tail bud has formed.

• Segmentation Period (10-24 h)

Segmentation is marked by morphogenetic movements. The somites develop, the rudiments of the primary organs become visible, the tail bud becomes more prominent and the embryo elongates. The first cells differentiate morphologically, and the first body movements appear. Furthermore, as the tail extends, the overall body length of the embryo very rapidly increases, reasonably linearly. The somites appear sequentially in the trunk and tail.

Anterior somites develop first and more rapididly than the posterior ones. After the 14th somite (circa 16 h), a new somite will emerge each half an hour. The earliest cells to elongate into muscle fibers appear to derive from a part of the medial somitic epithelium, the "adaxial" region (Thisse *et al.*, 1993) adjacent to the developing notochord, and in the middle, dorsoventrally, of each somite. The neural plate transforms topologically into the neural tube. The medial part of the neural plate (originally from dorsal epiblast in the gastrula) forms ventral structures in the neural tube, and the lateral part of the plate (from lateral and ventral gastrula epiblast) forms dorsal tube. Neurulation and segmentation periods, therefore, overlap in zebrafish. Pigment cells differentiate, the circulatory system forms, and tactile sensitivity appears (touch-response).

• Pharyngula Period (24-48 h)

When the embryos enter the pharyngula stage they already possesse the classic vertebrate architecture. They display a well-developed notochord, and a newly completed set of somites. Five lobes comprise the brain. During the first few hours of the pharyngula period the embryo continues the rapid lengthening that started at 15 h, which decreases as the rapid morphogenetic straightening of the tail ceases. Head-straightening also occurs, making it more compact along the anterior-posterior axis, occasioning the approach of the rudiments of the eye and the ear.

• Hatching Period (48-72 h)

From 48 hpf onwards, the embryo escapes from the chorion. On the second day of development, the interior organs will be formed. After the end of the third day the embryo becomes the denomination of larvae.
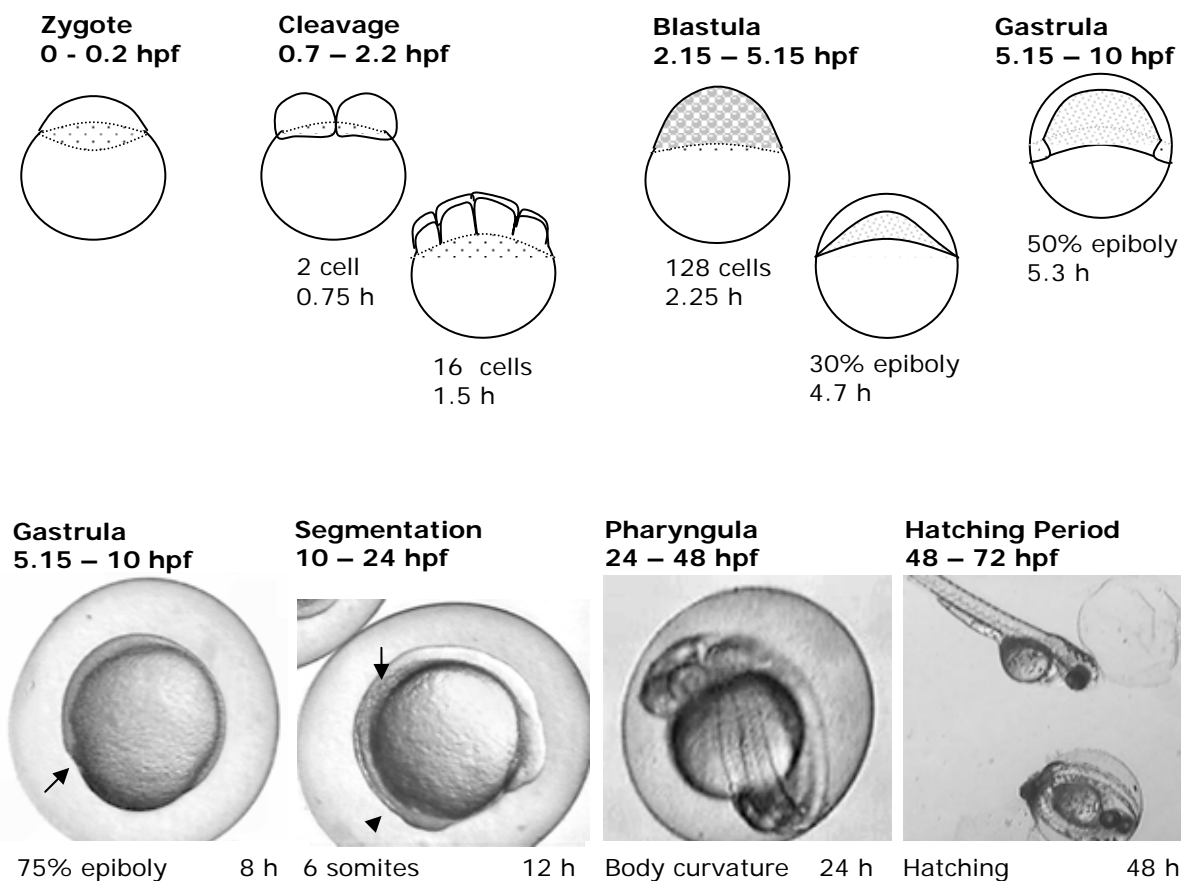
Fig. 3.1: Zebrafish development. Zygote - one cell stage; Cleavage period - the first 6 cleavages; Blastula – 7th cleavage until beginning of epiboly; Gastrula – until the end of epiboly (arrow); Segmentation – formation of the tail (arrow head) and somites (arrow); Pharyngula – primordia of the pharyngeal arches; Hatching period – natural escape from the chorion occurs.

3.1.6 Aims of this work

- To characterize AChE expression during zebrafish embryogenesis by RT-PCR analysis, a more sensitive technique than *in sito* hybridization;

- To investigate the aryl acylamidase (AAA) activity associated to AChE in relation to the esterase activity during zebrafish development;

- To test the sensitivity of zebrafish embryos towards high doses of serotonin, an AAA inhibitor, during embryogenesis.

3.2   *Methodology*

3.2.1 *Zebrafish as a model organism*

The zebrafish (*Brachydanio rerio* or *Danio rerio*) is the ideal model organism to study AChE in the absence of BChE. Besides, its fast and easy reproduction, passing from the egg to the larvae stage in less than three days, it can provide a large amount of embryos for experiments.

The zebrafish is a tropical fish of sweet water belonging to the minnow family (*Cyprinidae*), originally found in some Asian countries. It grows to about five centimeters and lives for around 5 years (Westerfield, 2000).

Care and breeding of zebrafish was conducted according to Westerfield (2000). Zebrafish were grown under day-night cycle with an automatic timer (14 hr light/10 hr dark).

Zebrafish are photoperiodic in their breeding, and produce embryos every morning, shortly after sunrise. Embryos were collected, by siphoning them up from the bottom of the tank, and placed in Petri dishes. Embryonic stage was determined according to Westerfield (2000) under Nomarsky optics, and placed in an incubator at 28.5°C until the desired period for the experiments.

3.2.2 *RT-PCR and subsequent PCR of the AChE cDNA*

The principle of the polymerase chain reaction (PCR) is the repeated copying of a chosen segment of DNA using specific sense and anti-sense primers, usually separated by 200-500 nucleotides on the genome or nucleic acid of interest. With the availability of thermostable DNA polymerases derived from thermophilic bacteria (Taq DNA polymerase) this repetitive copying of the DNA can be done in a single tube by repeatedly heating the DNA to high temperature (94°C) to dissociate the DNA duplex, cooling to allow annealing of the primers to the template (37-60°C, depending on the primers used) and finally heating to the optimum temperature (72°C) for the polymerase to copy the template to produce a new DNA strand. The cycles are repeated 25-35 times (25 cycles theoretically increases the concentration of starting template DNA 107 times) to produce a DNA product which can be directly visualized by ethidium bromide staining on an agarose gel. The size of the DNA product is exactly defined by

the location of the two primers on the genome. The reverse transcription reaction, in contrast, is initiated from a RNA segment to produce a complementary DNA (cDNA). This is possible due a viral enzyme, reverse transcriptase, which transcribes the RNA into DNA, priming at the 3´ poly (A) region of the RNA using Oligo (DT) 15 primers.

Protocol: circa 400 embryos were collected for each embryonic period investigated, and kept at −20°C in RNAlater solution. Total RNA isolation was performed with TRI reagent according to the manufacturer's instructions (Molec. Research Center, Inc.). 1 µg of the RNA was used for reverse transcriptase reaction with the Reverse Transcription System from Promega, according to manufacture instructions.

A fragment of 488 bp of the ACHE gene was amplified by PCR from the cDNA obtained after reverse transcriptase reaction, with forward 5'-gtacacagcaccatgcgagttg-3' and reverse 3'-caagttcttccctggagcag-5' primers (Carl Roth GmbH).

The PCR for AChE consisted of 33 cycles: initial 5 min by 94°C, than 3 cycles by 94 °C for 1 min, 52 °C for 45 sec, and 72 °C for 1 min, followed by 30 cycles by 94 °C for 1 min, 51 °C for 45 sec, and 72 °C for 1 min. Primers and PCR conditions for ß-actin were published elsewhere (Liu *et al.*, 2003). RT-PCR and ACHE PCR reactions components are listed below.

RT-PCR	AChE PCR
1. $MgCl_2$, 25 mM 4 µl	1. First-strand cDNA reaction (diluted 1:5)
2. Reverse Transcription 10X Buffer 2 µl	10–20 µl
3. dNTP Mixture, 10 mM 2 µl	2. dNTP Mixture, 10 mM 1 µl
4. Recombinant RNasin® Ribonuclease Inhibitor 0.5 µl	3. $MgCl_2$, 25 mM 4 µl
5. AMV Reverse Transcriptase (High Conc.) 15 ul	4. Reverse Transcription 10X Buffer 5 µl
6. Oligo(dT)$_{15}$ Primer 0.5 µg	5. upstream primer 50 pmol 0.5 µl
7. Total RNA 1 µg	6. downstream primer 50 pmol 0.5 µl
8. Nuclease-Free Water to a final volume of 20 µl	7. TaqDNA Polymerase(c) 2 units 0.4 µl
	8. Nuclease-Free Water to a final vol.... 50 µl

3.2.3 Esterase and AAA activities measurements

Ten zebrafish developmental stages were investigated. Triton-extracted homogenates were used for activity measurements.

3.2.3.1 Homogenization protocol

Embryos were transferred to cold Ringer's solution with EDTA (which is a pronase inhibitor) and placed on ice. Embryos were washed and centrifuged for 3 min (1000 rpm) for removal of supernatant. After 3x repeating this washing step, cold homogenization buffer (Na-phosphate extraction buffer solution [10 mM Na-phosphate, pH 7.4, 0.5% Triton X-100] with protease inhibitor cocktail (1:200) was added (9 volumes), while stirring the homogenates on ice. Embryos were sonicated 4x 9 sec and again homogenized. The homogenates were passed through a needle (18 gorge) 5x, and let on ice for 1 hour. Homogenates were centrifuged for 45 min at 14.000 rpm at 4°C. Supernatants were aliquoted in eppendorfs and kept at -20°C.

3.2.3.2 Acetylcholinesterase (AChE) activity assay

Principle of the method: the substrate acetylthiocoline is broken into thiocholine and acetate by AChE. The thiocoline reacts with DTNB producing a yellow product. The formation of product is follow in spectrophotometer and the activity is deduced from the linear variance of the optical density in a period of time.

The esterase activity was assayed by the method of Ellman *et al.* (1961) using 3 mM acetylthiocholine (ATCh) in 80 mM sodium phosphate buffer (pH 8.0) containing 0.6 mM DTNB (5,5`- dithio-bis-2-nitro-benzoic acid) and 10 μM eserine, as AChE inhibitor, at 37°C. The increase in absorbance was followed (412 nm) and total enzyme activity was calculated using the KinLab software (Perkin Elmer). Specific enzyme activity was calculated dividing the total activity by the protein concentration in mg/ml. One unit (U) of enzyme hydrolyzes 1 μmol of ATCh per min under this assay conditions.

3.2.3.3 Aryl acylamidase (AAA) activity assay

Principle of the method: o-nitroacetanilide is split by the aryl acylamidase, a side activity of AChE, into o-nitroaniline and acetate (Fig. 3.2). O-nitroaniline is

a visible yellow product allowing the reaction to be measured in spectrophotometer. The amount of o-nitroanelin produced can be deduced from a standard calibration curve of o-nitroanelin versus OD.
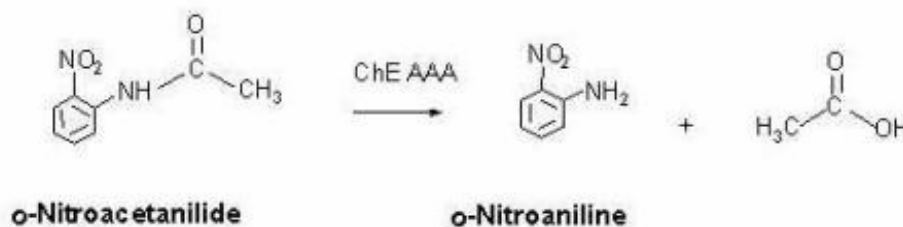
Fig. 3.2: Schema of AChE catalyses of the substrate o-nitroanilide.

The AAA activity of AChE was assayed according to Hoagland and Graf (1971), with modifications. 0.05 - 0.1 ml of sample in a total volume of 0.5 ml was incubated at 37°C for 5 min in 0.2 M of potassium phosphate buffer, pH 8.0, in presence of or absence serotonin (several concentrations) or eserine (10 µM). After the addition of the substrate 0-nitroacetanilide (6.6 mM), the product formation was followed for 15 min at 430 nm in a Perkin-Elmer spectrophotometer. AAA was deduced from calibration curves established with known concentrations of o-nitroaniline. One unit of AAA liberated 1 µmol of o-nitroaniline per min under these conditions.

3.2.3.4 Protein concentration

Protein concentration was estimated by the Bradford method (Bradford, 1976), using known concentrations of BSA as standard. The assay is based on the observation that the absorbance maximum for an acidic solution of Coomassie Brilliant Blue G-250 shifts from 465 nm to 595 nm when binding to protein occurs. Both hydrophobic and ionic interactions stabilize the anionic form of the dye, causing a visible color change.

Procedure: Bradford reagent was prepared with 100 mg Coomassie Brilliant Blue G-250 in 50 ml 95% ethanol, plus 100 ml 85% (w/v) phosphoric acid diluted to 1 liter in distillated water. The solution was filtered through Whatman paper just before use. Standards contained a range of 10 to 40 micrograms BSA in 100 µl volume. 1 ml Bradford reagent was added to 100 µl of diluted samples or BSA standards and incubated for 5 min. Absorbance was measured at 595 nm. The standard curve obtained from the absorbance versus micrograms BSA was used to determine concentrations of samples.

3.2.4 Serotonin (5-HT) experiment

Five embryonic stages were used to test the influence of 5-HT on zebrafish development: cleavage, blastula, gastrula, segmentation and pharymgula. Embryos were treated with 2 to 4 mM 5-HT for 2.5 to 3 h. The effects caused by 5-HT administration were observed in live embryos, and samples were fixed after each experiment by 10 and 14 hpf.

Protocol: 5-HT was diluted in zebrafish culture medium (30 ml), and embryos were placed in 10 cm diameter Petri dishes, with and without serotonin (control), and incubated at 28.5°C. After serotonin treatment, solution was replaced by normal medium 2x and embryos were then removed to a new dish with fresh medium. For each of the embryonic stages investigated, 105 embryos, which were exposed to 5-HT and 45 control non-treated embryos, were collected. Embryos were fixed by 10 and 14 hpf. By embryos fixed by 10 hpf two probes were used (neurogenin-1 and goosecoid), requiring 70 embryos treated with serotonin and 30 non-treated embryos. By 14 hpf fixed embryos one probe was used (myo-D), requiring 35 treated embryos and 15 control embryos. After each experiment and until the last fixation time, records were kept for the number of dead embryos, and the occurrence of embryonic malformations, followed with Normarky optics.

3.2.4.1   Whole mount in situ hybridization (ISH)

In situ hybridization (ISH) was essentially performed as described in "The zebrafish book" (Westerfield, 2000), with immunohistochemical detection using an alkaline phosphatase (AKP) conjugated anti-digoxigenin monoclonal antibody. Hybridization signal was visualized through the substrates of AKP (NBT and BCIP).

Principle of the method: a labeled nucleic acid probe anneals specifically to complementary sequences of target nucleic acids in a fixed specimen. In this work, digoxigenin (DIG) labeled RNA probes were used to hybridize cellular complementary mRNA, followed by detection and visualization of nucleic acid hybrids (Baumgart *et al.*, 2001). This technique can be used to locate DNA sequences on chromosomes, to detect RNA or viral DNA/RNA.

Probes: although three types of probes, DNA, RNA and oligonucleotide probes are generally used in ISH, RNA probes are the best and most sensitive for detecting mRNA transcripts because of the high thermal stability of the RNA-RNA hybrids. The antisense RNA probes with a digoxigenin (DIG) label were prepared according to the DIG-RNA-Labeling Kit (Promega). About 5 to 10 µg of digoxigenin-labeled probe was transcribed from 1 µg of a linearized plasmid. Probes were hydrolyzed to an average length of 150-300 nucleotides following the protocol of Cox *et al.* (1984). After the final precipitation, the hydrolyzed probe was taken up directly in hybridization solution (HYB) and placed first at -80°C for 5 min and then stored at -20°C.

Three digoxigenin labeled anti-sense riboprobes were used: goosecoid (gsc), neurogenin-1 (ngn-1), and myogenic differentiation gene (myo-D). The first two are mesodermal markers, while the latter one is a neuronal marker, as follow:

Goosecoid (Gsc) – early embryos (anterior mesoderm). It is activated at or just after midblastula stage until late gastrulation. In early gastrulation, expression marks the anterior shield and by late gastrulation, expression is restricted to the rostral crescent and medial strip. Levels of gsc then decline and disappear at 12 h post-fertilization.

Neurogenin 1 (Ngn-1) **-** appears to mediate neuronal differentiation (late gastrulation). It is strongly expressed in distinct domains in the neural plate at the 3-somite stage. By 24 hours, it is expressed in specific regions of the developing brain and in the spinal cord.

Myogenic differentiation gene (Myo-D) – can induce myogenic differentiation (posterior mesoderm - gastrula). It encodes a transcription factor of the helix-loop-helix class.

Protocol: embryos were fixed with 4% paraformaldehyde in PBS overnight at 4°C, and washed in PBS (2x 5 min), at RT. For dehydration embryos were transferred to vials with 100% methanol (MeOH), replaced with fresh methanol after 10 min. For permeabilization embryos were kept at -20°C with fresh Methanol for at least 30 min (embryos can be stored that way for months). For rehydration embryos were brought back to RT and immerse 5 min in 75% MeOH/PBS, 50% MeOH/PBS, 5 min in 25% MeOH/PBS, and then 4x 5 min

PBST. For pre-hybridization, embryos were transferred (up to 40) into small eppendorf tubes (0.8ml) in approximately 300 µl of hybridization solution, without probe at 65°C for 1-2 h, to block unspecific binding. For hybridization the probes were chosen according to the embryonic stage. HYB was removed (without letting the embryos touch air) and 50 ul HYB containing DIG labeled RNA probes (0.5 – 2 µg) were added to 450 µl buffer and incubated at 65°C for 5 min before adding to the embryos. Embryos were incubated with the hybridization solution over-night at 65°C. So far as no higher temperatures for hybridization can be used, due tissue damage, the annealing stringency is not high. To avoid hybridization mismatches, the formamid was used to reduce the melting point of DNA double strands. The pH also influences the hybridization and it should be maintained between 5 and 9. To remove unspecific binding probes, a post-hybridization washing with formamid was conducted. Decreasing its concentration, the thermo stability of the hybrids increases. The hybridization incubation was carried out in a high-salt solution to promote base-pairing between probe and target sequences. The critical parameters are the ionic strength of the final wash solution and the temperature at which this wash is done. Embryos were washed 10 min with 75% formamid in 2x SSC at 65°C, 10 min with 60% formamid in 2x SSC at 65°C, 10 min with 25% formamid in 2x SSC at 65°C, 10 min with 2x SSC at 65°C, 10 min with 0.2x SSC at 65°C, 5 min with 0.15x SSC/PBST at RT, 5 min with 0.1x SSC/PBST at RT, 5 min with 0.05x SSC/PBST at RT, and 5 min with PBST at RT. Embryos were blocked for 1 hour at RT with PBST plus blocking reagent (2% serum + 2 mg/ml BSA). Anti-Digoxigenin-AP (coupled with alkaline phosphatase) antibody was added according to manufactures instruction (Boehringer) at a 1:4000 dilution and shacked for 4 hours at RT or overnight at 4°C in PBST plus blocking reagent.

3.2.4.2   *Alkaline phosphatase staining*

Embryos were washed with PBST (2x5 min, 2x15 min, 2x 30 min and 1x 1 h) and 3x 5 min with alkaline phosphatase (AP) buffer, for equilibration (optimum pH for AP). Embryos were then placed in 24 well plates. Colorimetric detection uses the substrates NBT and BCIP to generate purple/brown precipitate directly on the membrane (Fig. 3.3). Per ml AP-buffer, 3.5 µl BCIP [50 mg/ml] and 4.5 µl NBT were added. Embryos were covered with this staining solution, and incubated under dark in a shaker at RT for about 30 min. Under binocular, the

staining intensity was controlled and stopped with PBST washing, as it can take several hours. Embryos were re-fixed in 4% PFA at RT for at least 30 min, washed in PBST and transferred to glycerin.
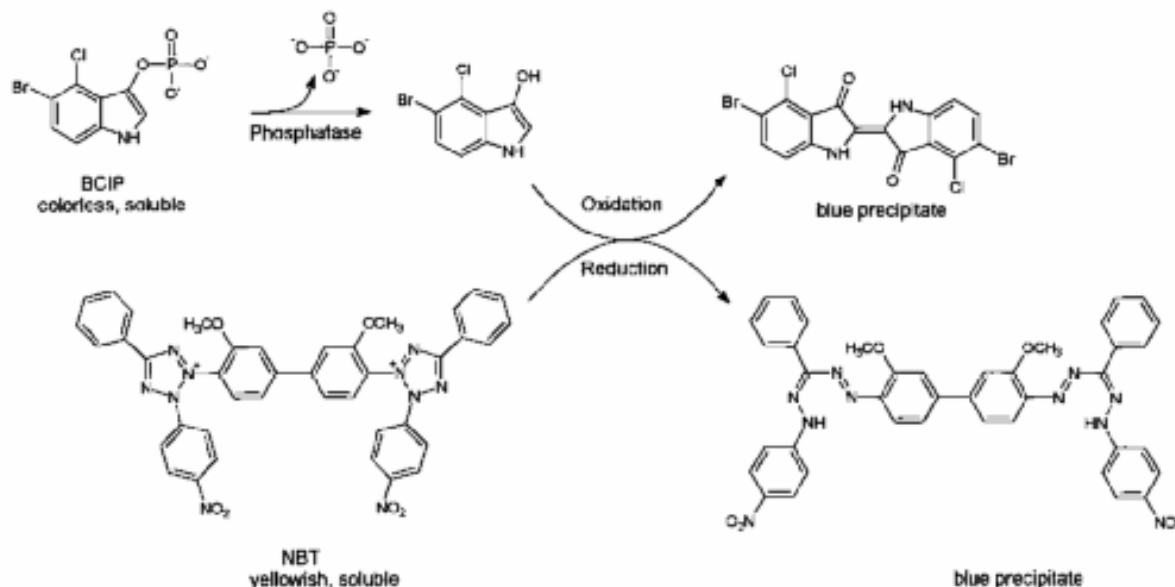
Fig. 3.3: Schema of the NBT/BCIP reaction. When alkaline phosphatase removes the phosphate group of BCIP (5-bromo-4-chloro-3-indolyl-phosphate) the resulting molecules give a blue precipitate (5, 5'-dibromo-4,4'-dichloro-indigo) under oxidazing conditions. During the reaction with BCIP, NBT (nitroblue tetrazolium) is reduced to its colored form to give an enhanced color reaction.

3.2.5 Statistical analyses

Some of the results of this work were statistically compared using t-student´s test and contingency tables, with the objective to show if the observed relationship (e.g., between variables) or a difference (e.g., between means) in a sample occurred by pure chance. The probability (p) value obtained was higher or lower than 0.05, meaning 5% probability that the calculated hypothesis would occur by chance. Probabilities lower than 5% increase the certainty that the observed results did not occurred by change. More technically, the value of the p-value represents a decreasing index of the reliability of a result (Brownlee, 1960). The higher the p-value, the less we can believe that the observed relation between variables in the sample is a reliable indicator of the relation between the respective variables in the population. The p-value represents the probability of error that is involved in accepting the observed result as valid, that is, as "representative of the population."

3.3   Results

3.3.1 AChE mRNA expression during embryonic development of zebrafish

Total RNA was extracted from embryos at 2 to 24 hpf, during five time points comprising five periods of the zebrafish embryonic development (cleavage, blastula, gastrula, segmentation, and the beginning of the pharyngula). The quality of the RNA obtained was similar for all investigated stages (Fig. 3.4, A). RT-PCR was conducted with 1 µg of the purified RNA.

The control gene ß-actin, a gene involved in basic functions needed for the sustenance of the cell, was amplified by PCR from the resulting cDNA obtained with the RT-PCR. Using an aliquot of the same original cDNA, a fragment of the *ACHE* gene was also generated by PCR. The first AChE transcripts were detected in zebrafish embryos at 4 hpf (blastula period), with a respective increase after 8 hpf (Fig. 3.4, B). The control gene ß-actin was already present by 2 hpf, showing similar amounts of amplified product for all of the embryonic periods investigated, assuring the quality of the cDNA used was optimal for all embryonic periods investigated (Fig. 3.4, B).
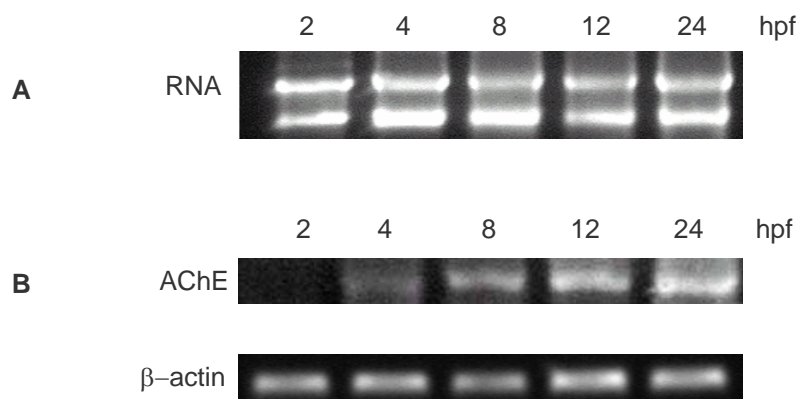
Fig. 3.4: Results of RNA extraction from zebrafish embryos and PCR of a segment of the AChE and ß-actin cDNAs. An RNA aliquot was electrophoresed on agarose gel to access the integrity of total RNA (A). ACHE cDNA (488 bp) amplification was normalized with the control ß-actin (B).

3.3.2 Esterase and aryl acylamidase activities of AChE during zebrafish embryogenesis

Both esterase and aryl acylamidase activities were studied during zebrafish development from 4 to 144 hpf. AAA was compared to the esterase activity in all developmental stages investigated, revealing a particular profile for each one (Fig. 3.5).

Until 12 hpf, negligible esterase activity was detected (Fig. 3.6), increasing significantly after the embryonic period (test t = 2.987; df = 6; p < 0.05). Eserine was very effective towards the esterase activity, as shown with an inhibition curve (Fig. 3.7, A), showing circa 97% inhibition at 10 µM eserine. During zebrafish development, eserine (10 µM) was very effective inhibiting the esterase activity in homogenates from all investigated periods (Fig. 3.7, B).

Early embryogenesis was remarkable for the presence of AAA, which was higher than the esterase activity until 12 hpf (test t = 3.523; df = 4; p < 0.05). On the other hand, after the 24 hpf period, the esterase significantly increased in relation to the AAA activity (test t = 3.980; df = 10; p < 0.01), drastically altering the ratio AAA/esterase activity, from 2.1 at 4 hpf to 0.01 at 144 hpf (Fig. 3.5). The AAA activity displayed circa 80% inhibition at 2 mM towards serotonin (Fig. 3.8). Eserine was not as effective towards AAA as it was for the esterase activity, with circa 50% inhibition of AAA by 10 µM eserine.
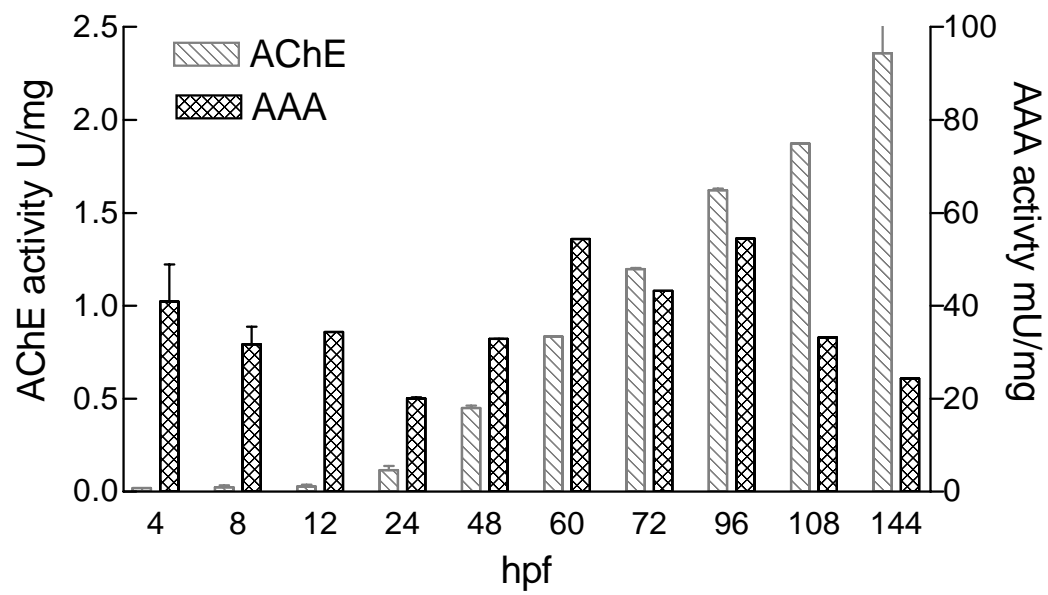
Fig. 3.5: Profiles of the esterase and aryl acylamidase activities from 4 to 144 hpf whole zebrafish embryos and larvae homogenates.
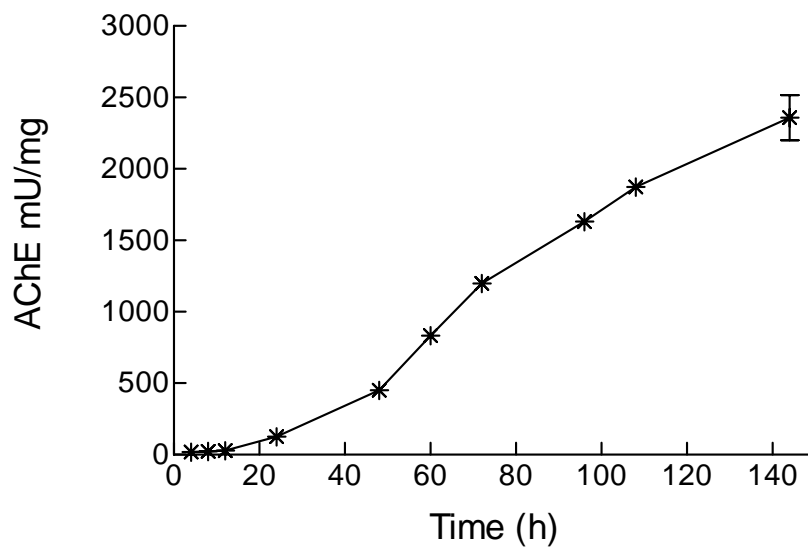
Fig. 3.6: AChE specific esterase activity from 4 to 144 hpf whole zebrafish embryos and larvae homogenates.

A

B
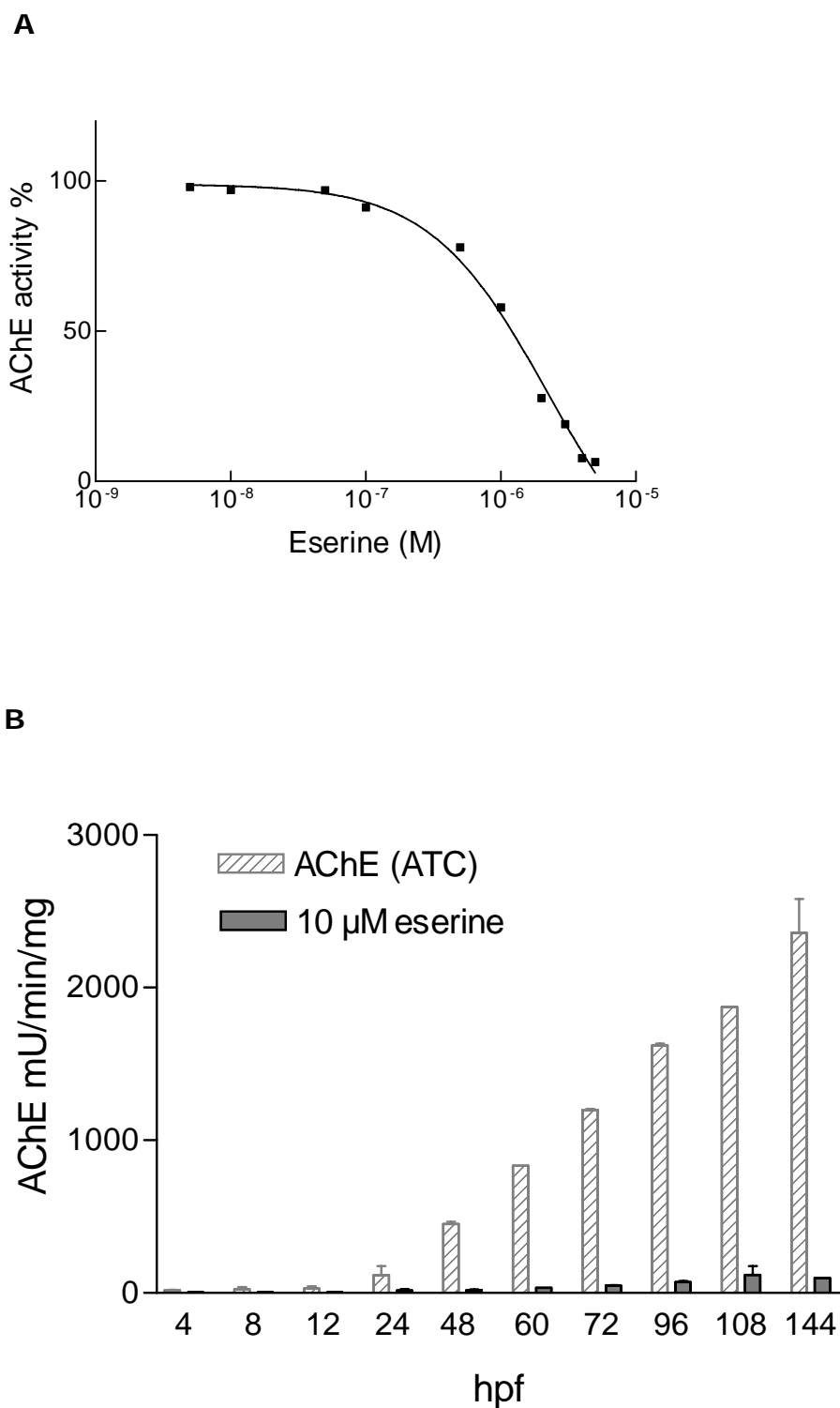
Fig. 3.7: Zebrafish esterase activity inhibited by eserine. (A) AChE inhibition curve towards the compound eserine, using zebrafish larvae (144 hpf) homogenates. (B) Inhibition of the AChE esterase activity towards eserine (10 μM), using homogenates of zebrafish from 10 different developmental stages.
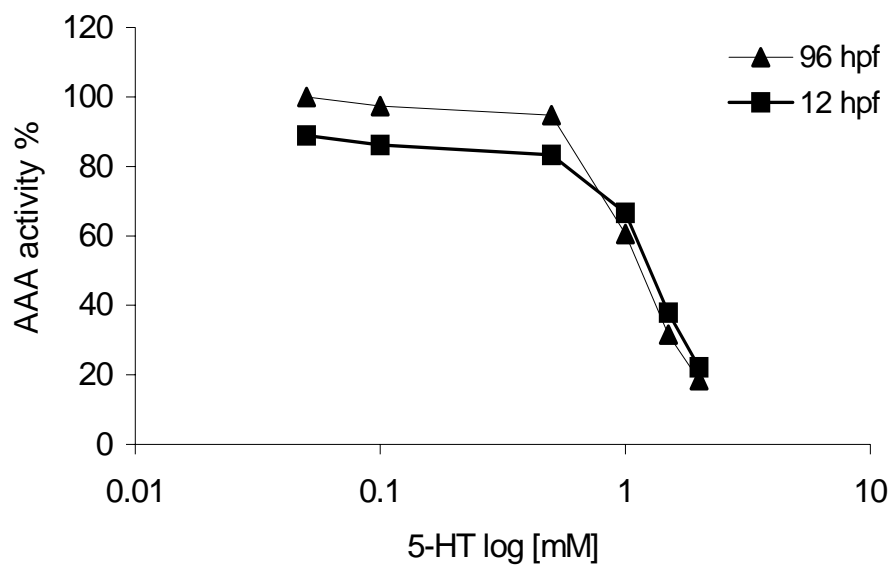
Fig. 3.8: Effect of serotonin (5-HT) at various concentrations on the AAA activity from 96 hpf (▲) and 12 hpf (■) zebrafish homogenates.

3.3.3 The effect of serotonin administration during zebrafish embryonic development

Besides the *in vitro* inhibition of AAA from zebrafish towards serotonin, an *in vivo* experiment was conducted with administration of 2 and 4 mM 5-HT to zebrafish embryos, between 0.3 to 2.5, 2.5 to 5.5, 6 to 9, 10 to 13, and 24 to 27 hpf. Several concentration dependent malformations were observed essentially when embryos received the treatment at 2.5 to 5.5 hpf, the time point when AChE started to be expressed (Fig. 3.4), with no pronounced effects on earlier or later periods of development (Table 3.1).

Developmental stages Period (hpf)	Absolute number of embryos		
	hpf	2 mM 5-HT	4 mM 5-HT
Cleavage (0.7 – 2.2)	0.3 – 2.5	Not affected	8.6% affected
Blastula (2.5 – 5.15)	2.5 – 5.5	**4 %**	**80% affected**
Gastrulation (5.15 – 10)	6 - 9	Not affected	1.9% affected
Segmentation (10 – 24)	10 – 13	Not affected	Not affected
Pharyngula (24 – 48)	24 – 27	Not affected	Not affected

Table 3.1: Occurrence of developmental defects based on investigation of embryos with Nomarsky optics.

Under binocular, the malformations observed were basically restricted to the embryos treated with serotonin during the blastula period. By this period, 4% of the embryos treated with 2 mM 5-HT already presented flattering of the head and malformation of the tail by 14 hpf. With 4 mM serotonin, circa 80% of the embryos presented incomplete epiboly (50 to 75%) by 10 hpf, somitogenesis was affected by 14 hpf, and embryos observed until 24 hpf (20-30%) had severe malformations.

When embryos were treated with 2 mM 5-HT, between 0.3 and 2.5 hpf, no malformations were observed. By 4 mM 5-HT, 8.6% of the embryos presented incomplete epiboly by 10 hpf, and 3.1% flattering of the head by 14 hpf, which evolved to severe malformations by 24 hpf. Serotonin administration during the period 6 to 9 hpf (gastrulation), did not reveal malformations at 2 mM concentration, however, phenotypic alterations were observed in 1.9 % of the

embryos treated with 4 mM 5-HT. The embryos which received serotonin between 10 to 13 hpf (segmentation) and 24 to 27 hpf (pharyngula) did not present malformations when treated with 2 and 4 mM. Therefore, the zebrafish embryos were far more sensitive to serotonin administration during the blastula period, than during other investigated periods.

3.3.3.1 Zebrafish developmental malformations detected by neuronal and mesodermal genes expression after 5-HT administration

A closer investigation of the embryonic malformations, using *in situ* hybridization of mesodermal and neuronal markers, revealed a disruption of the expression pattern of these markers. For embryos treated with 2 mM 5-HT during 2.5 to 5.5 hpf, the expression of the mesodermal marker gsc, by 10 hpf, was decreased and its distribution pattern was slightly disturbed on the pre-chordal plate and anterior mesoderm in relation to controls (Fig. 3.10). By 14 hpf, a delay on somitogenesis, of 1-2 somites, and a decrease in myo-D expression, on the adaxial cells, in 70% of the embryos, was verified (Fig. 3.11, B, D).

The administration of 4 mM 5-HT was conducted between 2.5 to 2.5 hpf and also from 2.25 to 5.25 hpf, resulting in the same effects (Fig. 3.10). The anterior mesoderm, affecting the expression of the marker gsc in 87% of the embryos, and prechordal plate were not well developed in relation to controls (Fig. 3.10). By 14 hpf, myogenic differentiation was more intensively affected with 4 mM than with 2 mM 5-HT. 67% of the embryos showed a delay of the myogenic differentiation, and 33% had no or irregular expression of myo-D on the somites and adaxial cells (Fig. 3.11, F, H). By the expression of the neuronal developmental marker neurogenin-1, it was possible to detect a disruption of the pro-neural cluster cells pattern in 100% of the embryos by 10 hpf (Fig. 3.12, B, D).

Therefore, serotonin administration during blastula period caused concentration dependent malformations in zebrafish embryos. Embryos did not present developmental defects induced by serotonin administration from 6 to 9 (except the 1.9% already mentioned before), and 10 to 13 hpf, as no obvious discrepancy in relation to controls was observed with the mesodermal marker myo-D. 8.6% of the embryos treated between 0.3 and 2.5 hpf presented

phenotypic alterations in relation to controls by 4 mM 5-HT, however, none of the embryos treated with 2 mM serotonin presented morphological problems. Therefore, the only period affected by 2 mM serotonin administration was during blastulation.
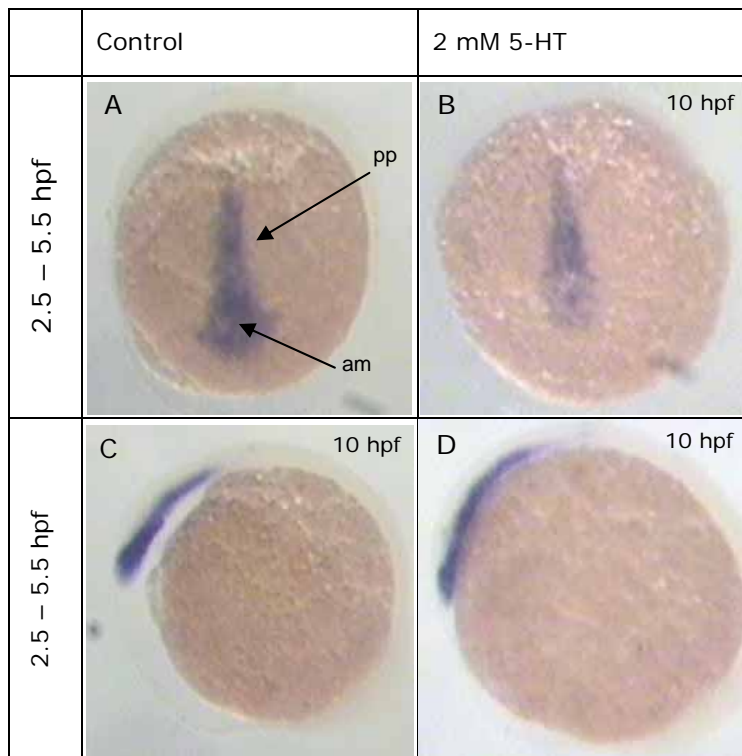
Fig. 3.9: Gsc expression in controls and 5-HT treated embryos fixed by 10 hpf. A,B) Anterior view of control, and 5-HT (2 mM) treated embryos. C,D). Lateral view of control, and 5-HT treated embryos. pp: prechordal platte; am: anterior meso-derm. Magnification, 66x.
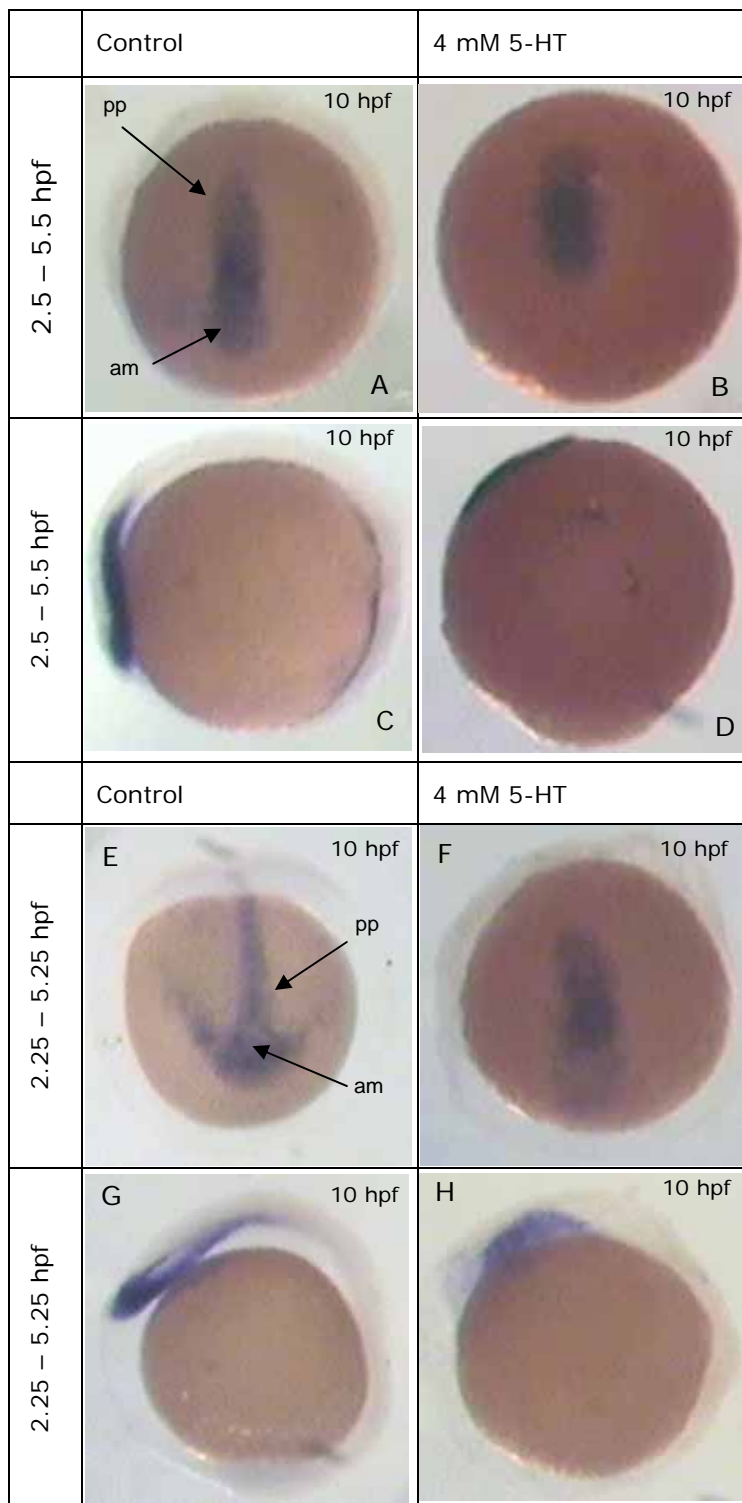
Fig. 3.10: Gsc expression in controls and 5-HT treated embryos fixed by 10 hpf. A,B) Anterior view of control, and 5-HT (4 mM) treated embryos. C,D) Lateral view of control, and 5-HT treated embryos. E,F) Anterior view of control, and 5-HT (4 mM) treated embryos. G,H) Lateral view of control, and 5-HT treated embryos. pp: prechordal platte; am: anterior mesoderm. 66x binocular magnification.
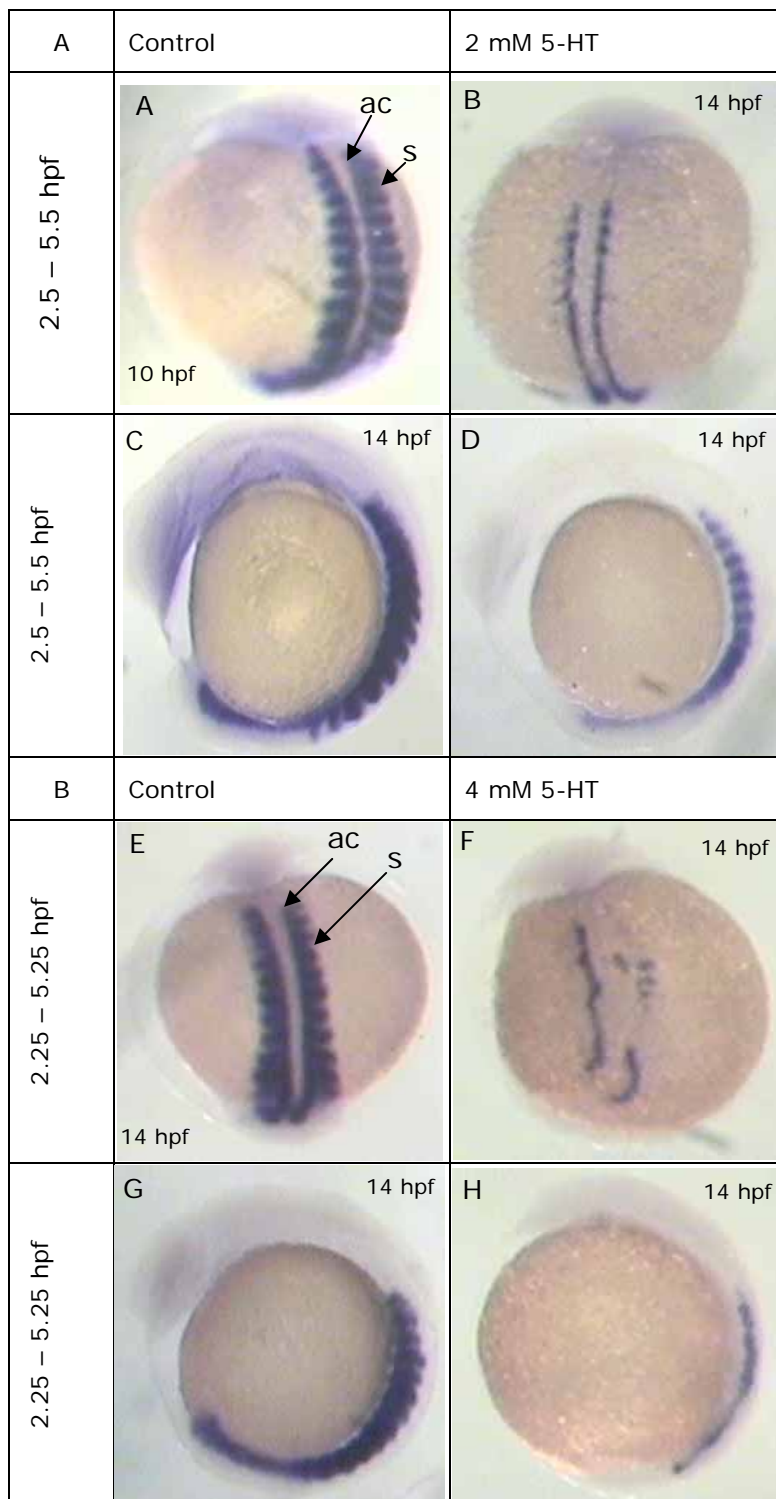
Fig. 3.11: Expression of Myo-D in controls and 5-HT treated embryos fixed by 14 hpf. A,B) Dorsal view of control, and 5-HT (2 mM) treated embryos. C,D) Lateral view of control, and 5-HT (2 mM) treated embryos. E,F) Dorsal view of control, and 5-HT (4 mM) treated embryos. G,H) Lateral view of control, and 5-HT treated embryos. s: somites; ac: adaxial cells. Binocular magnification 66x.
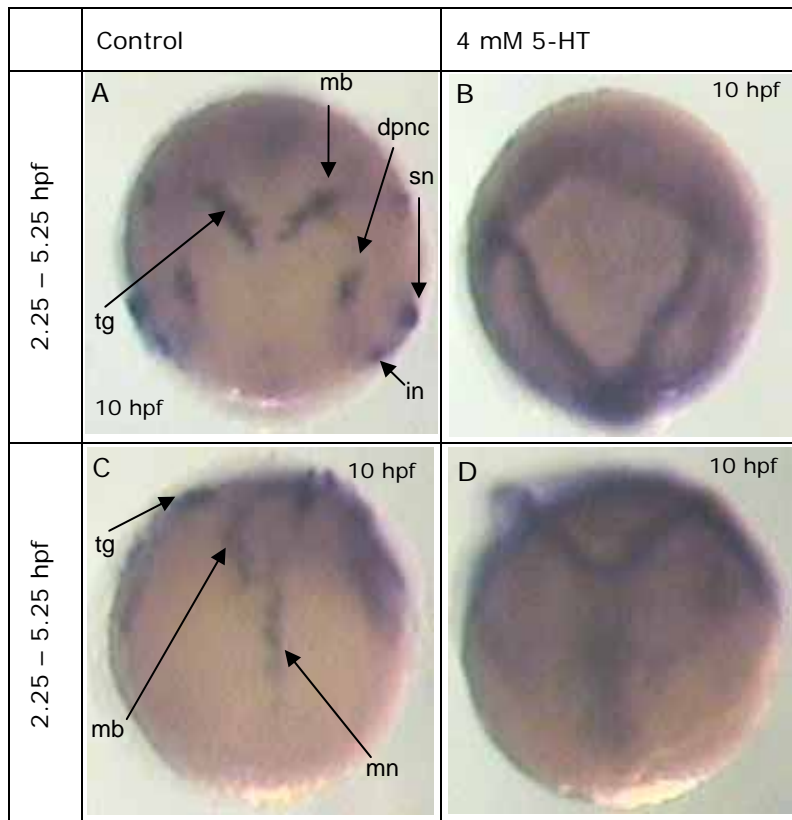
Fig. 3.12: Ngn-1 gene expression in controls and 5-HT treated embryos fixed by 10 hpf. A,B) Dorsal view of control, and 5-HT (4 mM) treated embryos. C,D) Anterior view of control, and 5-HT (4 mM) treated embryos. in: spinal interneurons; mb: mid-brain; mn: spine motor-neurons; sn: spine sensory neurons; dpnc: dorsal proneural cluster; tg: trigeminal ganglion. Magnification of 66x.

3.3.3.2   Zebrafish embryos mortality after 5-HT administration

Increased mortality in relation to controls was only observed when serotonin was administered to embryos during cleavage and blastula periods. During gastrulation, segmentation, and pharyngula, no mortality or no increased mortality in relation to controls was observed for embryos treated with 2 and 4 mM 5-HT. The mortality of embryos, in absolute numbers (Table 3.2:), caused for each of the 5-HT concentrations used, within a period and between the cleavage and blastula periods, was compared by contingency tables to controls.

Developmental stages Period (hpf)	hpf	Absolute number of embryos 5-HT			
		Control	2 mM	Control	4 mM
Cleavage (0.7 – 2.2)	0.3 – 2.5				
Mortality		0	0	0	6
Survival		45	105	45	99
Blastula (2.15 – 5.15)	2.5 – 5.5				
Mortality		0	14	6	63
Survival		45	91	39	42

Table 3.2: Mortality and survival (absolute N) of non-treated and 5-HT treated embryos.

No increased mortality was observed during the cleavage period when embryos were treated with 2 mM 5-HT. When 5-HT concentration was increased to 4 mM, during the same period, no significant increased mortality in relation to controls (X^2 = 2.97, p > 0.10; Table 3.3) was observed. For the blastula period, the mortality rate was significantly higher in 5-HT treated embryos than in controls for both concentrations of serotonin, 2 (X^2 = 6.62, p < 0.010; Table 3.4) and 4 mM (X^2 = 27.62, p < 0.000; Table 3.5). Comparing the mortality of embryos treated with 2 and 4 mM 5-HT, during the blastula period, a 5-HT concentration dependent mortality increase was observed (X^2 = 49.23, p < 0.000; Table 3.6). Comparing the mortality of embryos during cleavage and blastula periods, a significant higher sensitivity of embryos towards both, 2 (X^2 = 15.0, p < 0.000; Table 3.7) and 4 mM (X^2 = 70.12, p < 0.000; Table 3.8) 5-HT was observed during the blastula period. Therefore, these data support that zebrafish embryos display a higher sensitivity towards serotonin administration during blastulation than during other periods, and that this sensitivity was dependent on the serotonin concentration.

0.3 – 2.5 hpf	Absolute number of embryos		
	Control	4 mM 5-HT	Total
Mortality			
Observed	**0**	**6**	**6**
Expected	2	4	
Survival			
Observed	**45**	**99**	**144**
Expected	43	101	
Total	**45**	**105**	**150**
$X^2_{(1)} =$		2.97 (p > 0.10)	

Table 3.3: Contingency table. Mortality, in absolute numbers, of 5-HT embryos treated, during the cleavage period, compared to controls by 4 mM serotonin. X^2 = chi-square; $_{()}$ = degrees of freedom; p = probability.

2.5 − 5.5 hpf	Absolute number of embryos		
	Control	2 mM 5-HT	Total
Mortality			
Observed	**0**	**14**	**14**
Expected	4	10	
Survival			
Observed	**45**	**91**	**136**
Expected	41	95	
Total	**45**	**105**	**150**
$X^2_{(1)}$ =	6.62 (p < 0.010)		

Table 3.4: Contingency table. Mortality, in absolute numbers, of 5-HT embryos treated, during the blastula period, compared to controls by 2 mM serotonin. X^2 = chi-square; ( ) = degrees of freedom; p = probability.

2.5 − 5.5 hpf	Absolute number of embryos		
	Control	4 mM 5-HT	Total
Mortality			
Observed	**6**	**63**	**69**
Expected	21	48	
Survival			
Observed	**39**	**42**	**81**
Expected	24	57	
Total	**45**	**105**	**150**
$X^2_{(1)}$ =	27.62 (p < 0.000)		

Table 3.5: Contingency table. Mortality, in absolute numbers, of 5-HT embryos treated, during the blastula period, compared to controls by 4 mM serotonin. X^2 = chi-square; ( ) = degrees of freedom; p = probability.

	2.5 − 5.5 hpf	2 mM	4 mM	Total
	Absolute number of embryos			
	5-HT			
Mortality				
	Observed	**14**	**63**	**77**
	Expected	38.5	38.5	
Survival				
	Observed	**91**	**42**	**133**
	Expected	66.5	66.5	
Total		**105**	**105**	**210**
$X^2_{(1)} =$		49.23 (p < 0.000)		

Table 3.6: Contingency table. Mortality, in absolute numbers, of embryos treated, during the blastula period, with 2 mM of 5-HT compared to 4 mM serotonin. X^2 = chi-square; $_{( )} =$ degrees of freedom; p = probability.

| Absolute number of embryos | | | |
| | hpf | | |
2 mM 5-HT	**0.3 – 2.5**	**2.5 – 5.5**	**Total**
Mortality			
Observed	**0**	**14**	**14**
Expected	7	7	
Survival			
Observed	**105**	**91**	**196**
Expected	98	98	
Total	**105**	**105**	**210**
$X^2{}_{(1)} =$	15.0 (p < 0.000)		

Table 3.7: Contingency table. Mortality, in absolute numbers, of embryos treated with 2 mM of 5-HT, compared between cleavage and blastula periods. X^2 = chi-square; $()$ = degrees of freedom; p = probability.

| Absolute number of embryos | | | |
| | hpf | | |
4 mM 5-HT	**0.3 – 2.5**	**2.5 – 5.5**	**Total**
Mortality			
Observed	**6**	**63**	**69**
Expected	34.5	34.5	
Survival			
Observed	**99**	**42**	**141**
Expected	70.5	70.5	
Total	**105**	**105**	**210**
$X^2{}_{(1)} =$	70.12 (p < 0.000)		

Table 3.8: Contingency table. Mortality, in absolute numbers, of embryos treated with 4 mM of 5-HT, compared between cleavage and blastula periods. X^2 = chi-square; $()$ = degrees of freedom; p = probability.

3.4   Discussion

AChE is demonstrated here to be transcribed much earlier, 4 hpf, during zebrafish embryogenesis than previously reported, 12 hpf (Bertrand *et al.*, 2001). The relevance of an early AChE expression is not known. Remarkably, there is just a residual esterase activity until 12 hpf, suggesting that AChE might be acting in a non-cholinergic way during this period. The AAA/esterase activities ratio was much higher during the embryonic period (24 hpf) than for the larval stages (48 hpf). In result, the ratio AAA/esterase activities decreased from 2.1, by 4 hpf, to 0.01 by 144 hpf, indicating a relevance of AAA activity in very early zebrafish embryogenesis.

Post-translational modifications of AChE, happening during development, could explain a more pronounced AAA activity during early embryogenesis. A similar profile of AAA activity was previously reported for chicken (Boopathy and Layer, 2004). If it is a general rule for other organisms, it indicates that AAA could play a pivotal role on development, as for adult animals AAA is much less pronounced than the esterase activity itself (Fujimoto, 1974).

This is the first report of AAA activity on fish. The sensitivity of AAA towards serotonin ensures its association with AChE, as the serotonin-sensitive-AAA activity is postulated to be a property of cholinesterases.

3.4.1 The effect of serotonin administration during zebrafish embryonic development and AChE expression

A clear temporal serotonin concentration dependent sensitivity of zebrafish embryos was observed. Anterior mesoderm malformation and disorganization of the prechordal plate cells, marked by the expression of gsc, reflected a malfunction of the gastrulation period caused by serotonin administration. However, this effect was stronger when 5-HT was administered during the blastula period than when embryos were treated with 5-HT during gastrulation.

It was shown here that *ACHE* transcripts appear early after mid-blastula transition starts. Therefore, a relation between AChE expression onset and sensitivity of zebrafish embryos towards serotonin was observed. It is not clear if the developmental malformations observed on zebrafish were originated by AChE down regulation, but it is possible that its expression was retarded by

serotonin. This hypothesis is supported by the work of Buznikov (2001). He has postulated that 5-HT blocks indolylalkylamines, factors that determine the length of the lag-period, retarding the activation of protein synthesis after fertilization in sea urchin.

A temporal related sensitivity of zebrafish embryos towards serotonin is supported by: a) the incidence of a higher mortality among embryos treated with 5-HT during blastulation in relation to earlier and later stages, and b) the 5-HT concentration dependent malformations mostly limited to the blastula period. The connection of the onset of AChE expression with the high sensitivity of the embryos towards serotonin, during the blastula period, also makes reference to another property of AChE, the earlier mentioned AAA activity.

The serotonin-sensitive AAA activity, associated to AChE, suggests a possible influence of the serotonergic system to cholinergic components. It is not possible to show a direct influence of serotonin specifically on the AAA, as it is just a side activity of the AChE protein. However, a disturbed pattern of the expression of the myogenic differentiation gene (myo-D) occurred in areas where AChE is normally expressed in zebrafish. AChE is known to be expressed in paraxial mesodermal segmental plate at 12 h development (6 somites). This expression is probably located in myoblasts, proceeding in a rostro-caudal sequence according to the state of differentiation of the somites. As shown here, mesodermal differentiation showed serotonin concentration dependent malformations when embryos were treated by the time when AChE expression begins.

Furthermore, a disruption of the neural plate cell pattern organization was observed with the marker neurogenin-1 (ngn-1). Ngn-1 is involved in neuronal differentiation at late gastrulation, and had its expression pattern affected in embryos treated with 5-HT during the blastula period. It is known that AChE expression is first detected in small clusters of cells parallel to both sides of the spinal cord of zebrafish embryos (Bertrand *et al.*, 2001). The disruption of the expression of ngn-1 in spine motorneurones of Zebrafish, due to 5-HT treatment, also was observed in areas where AChE would be normally expressed. This spatial correlation of embryonic malformations and potential

sites of AChE expression are additional information suggesting an implication of serotonin administration on the cholinergic system development.

Considering that AChE has been already suggested to be a marker for neuronal differentiation (Layer and Willbold, 1995), its relevance for zebrafish embryogenesis is expected. Also, in sea urchin the action of an esterase inhibitor (chlorpyrifos) was essentially restricted to the mid-blastula stage, not affecting cleavage division and showing a decreased impact on gastrulation (Buznikov *et al.*, 2001).

On the other side, a naturally occurring mutation, resulting in the abolishment of the esterase activity, has been shown to cause only zebrafish impaired motility. This effect was caused by excessive excitation of musculature by acetylcholine, as AChE was not effective on hydrolyzing ACh on the end plates of this zebrafish mutant. However, the AChE protein is present on this zebrafish mutant. Therefore, it could fulfill any structural or side activity, e.g. functionality it might have during zebrafish embryogenesis. Noncholinergic action of AChE, as for example, the proposed roles of AChE on establishing synapses connection and axonal guidance (Layer, 1991), and other morphogenic events, as shown on the previous chapter, are likely to take place during zebrafish embryogenesis. It justifies, therefore, an early expression of AChE during embryogenesis, preceding the gastrulation period.

3.4.1.1   *Serotonin, AChE and AAA*

The primary interest, treating zebrafish embryos with serotonin was due to its inhibitory properties towards AAA. The choice for the serotonin concentrations (2 and 4 mM) used, was based on an inhibition curve of the AAA activity (Fig. 3.8). These concentrations should strongly inhibit the AAA activity. Consistently with this hypothesis, the most affected embryonic period, towards 5-HT administration, coincides with the onset of *ACHE* transcripts and AAA activity. However, once we verified such drastic effects on zebrafish development, it became questionable whether they were just due to AAA inhibition. Beyond that, it is not known how much of the serotonin administered to embryos was absorbed by them. However, the concentrations used were certainly higher than the physiological levels of serotonin.

Nevertheless, serotonin is a well-known neurotransmitter, mitogen, and hormone, which mediates a wide variety of physiological processes. It is not unlikely that 5-HT, which is a multifunctional regulator, acting in signal transduction systems involving c-AMP and calcium ions, influenced AChE during pre-nervous periods of ontogenesis via these second messengers. For instance, AChE expression was reported to be markedly increased during myogenic differentiation of C2C12 cells from myoblasts to myotubes, regulated via c-AMP signaling pathway (Siow, 2002). As serotonin stimulates cAMP (Goy *et al.*, 1984), it could act as a suppressor element for AChE.

The results of this work, therefore, brought new questions to be addressed, like a possible down regulation of AChE by means of serotonin administration during zebrafish early embryogenesis.

3.5   Summary

- AChE is very early expressed in zebrafish development, by 4 hpf.

- The AAA/esterase activities ratio was much higher in zebrafish embryos than in larval stages, suggesting a role for AAA in early embryogenesis.

- The onset of *ACHE* expression correlates with the embryonic period at which the zebrafish embryos were most sensitive to 5-HT, an AAA inhibitor.

- For the first time the AChE-associated AAA activity was investigated during fish development.

CHAPTER 4

4   Aryl acylamidase activity from *in vitro* expressed human BChE wild-type and active site mutant enzymes

4.1   Introduction

The existence of an AAA activity associated to cholinesterases has been the subject of study of a particular group of scientists working on cholinesterases, although, the assumption that AAA is a property of cholinesterases is not undisputed among cholinesterases researchers. Doubtlessly, AAA activity has been co-purified with AChE and BChE (George and Balasubramanian, 1980; 1981; Jayanthi *et al.*, 1992), and proven throughout several biochemical assays to be associated with ChEs. Nevertheless, it is still criticized to be an artifact.

The AChE KO organisms present mutations that abolish the esterase activity. However, the AChE protein is structurally present in these organisms and could display aryl acylamidase (AAA) activity. The existence of a second activity, which can be functional in these mutated cholinesterases, has not been taken into consideration when talking about ChEs relevance for KO organisms. There is, however, no evidence that AAA would be functional in these mutants.

In vitro expressed cholinesterases have also never been demonstrated to display this activity. Therefore, studying *in vitro* over-expressed cholinesterases, and the respective effects of ChEs structural mutations on esterase and AAA activities, would be one step forward to clarify AAA expression and location on cholinesterases.

4.1.1 The origin of the AAA activity

The aryl acylamidase (AAA; EC 3.5.1.13) activity, which hydrolyzes aryl acyl amide bonds, first appeared in bacteria (Engelhardt *et al.*, 1971) and plants (Still and Kuzirian, 1967). In vertebrates, throughout fish (see chapter 3), avian (Weitnauer *et al.*, 1998; Boopathy and Layer, 2004) and mammals (Fujimoto, 1974, 1976), this activity is peculiarly combined with the esterase activity.

Therefore, AAA is an ancient enzyme which was preserved during evolution, and the activity of which became associated to tissues-widespread enzymes like the cholinesterases (ChEs). Considering this selective advantage that AAA encontered, it is unlikely that there is no physiological function for this activity, as for cholinesterases present in non-cholinergic innervated tissues.

4.1.2 The aryl acylamidase activity of cholinesterases

AAA activities associated to ChEs fulfill two notions: a) sensitivity towards serotonin and, b) inhibition by potent esterase inhibitors; differing from the AAA activity non-associated to ChEs, which is not sensitive to these compounds. The sensitivity of AAA ChEs-associated towards serotonin drew attention to a correlation of serotonergic and cholinergic systems. However, little is known about this second activity on ChEs, creating restrictions to approach the subject.

Indeed, it is not known how the aryl acylamidase molecular domain interacts with components binding to the cholinesterases catalytic or peripheral site. However, there is a general belief that both activities are based on the same catalytic triad, once the specific BChE or AChE activity inhibitors also inhibit their associated-AAA activities specifically. On the other side, chemical mutagenesis was conducted to find evidence of a co-relation structure/catalytic efficiency of AAA in comparison to the esterase activity (Majumdar and Balasubramanian, 1984; Boopathy and Balasubramanian, 1985), indicating that these activities might not be sharing the same catalytic site. However, chemical mutagenesis does not allow controlling the position of the mutations, just the type of amino acids, resulting in mutations that can be located anywhere in the protein. The puzzling results produced with this kind of approach could not clarify which amino acids are essential for the functionality of AAA, and if it is reacting differently than the esterase activity due to structural mutations.

Until now, the attempts to elucidate how and why ChEs display the aryl acylamidase activity were not very successful. In particular, it remained unclear, which is the molecular domain responsible for the AAA activity on cholinesterases.

Furthermore, this side activity of ChEs has not often been mentioned in cholinesterases reviews, due to the discredit of its existence or simple not-awareness of it. Reviewing the subject, I studied aryl acylamidase activity from *in vitro* expressed recombinant human BChE.

Provided that several naturally occurring BChE variants display very low esterase activity, though remain as polymorphisms in some populations

(Whittaker-Britten *et al.*, 1989; Alcantara *et al.*, 1995), I hypothesized that AAA might be active on BChE even when the esterase activity is not.

4.1.3 Approach and aims

So far, it is essential to investigate AAA on mutant cholinesterases to understand how this activity is affected in relation to the esterase activity. To simulate this, making use of reverse genetics, human BChE mutants were investigated with respect to their AAA catalytic properties compared with the wild-type enzyme.

For this study, two mutant enzymes were designed: one leading to loss of esterase activity (S198D), and one leading to low esterase activity (E197Q). The effectiveness of the AAA activity associated to BChE mutants was tested towards two substrates; in comparison to the AAA activity from wild-type human BChE.

To understand by which mechanism serotonin is inhibiting the human BChE-associated AAA, wild-type and mutant enzymes were investigated by kinetic studies. Ethopropazin was also used towards AAA to confirm its sensitivity towards such a selective BChE inhibitor, and to verify the response of an active site (S198D) mutant BChE AAA-associated activity.

4.2   Methodology

Chemicals and equipments used are listed in appendices. Biological material with the respective supplier is listed on the tables below:

Enzymes	Supplier/collaborator
Purified recombinant mutant human BChE (E197Q)	Prof. O. Lockridge (Nebraska University)
Purified recombinant wild-type human BChE	
Hind III and Xba I (restriction endonucleases)	New England Biolabs, USA
Cells	
HEK 293 - human embryonic kidney cells	American Type Culture Collection, Manassas, Virginia, USA.

Vectors and bacterial strains	Supplier/collaborator
BChE wild-type cDNA cloned in a pGS plasmid	Prof. O. Lockridge (Nebraska University)
BChE S198D mutant cDNA cloned in a pGS plasmid	
GFP cloned in a LZRSpBMN-z vector plasmid	Prof. G. Thiel (TUD); Prof. G. Nolan (Stanford University)
Bacteria *Escherichia coli* XL1-Blue	Bullock *et al.*, 1987.

Antigen Target	Antibody	Host	Supplier/collaborator
Primary Antibodies			
Human BChE	monoclonal	mouse	Prof. O. Lockridge (Nebraska University)
M2 antibody against Tag-FLAG	monoclonal	mouse	Sigma
Secondary antibodies			
Anti-mouse IGg - Peroxidase	monoclonal	rabbit	Sigma

4.2.1 Expression of recombinant BChE

Two pGS plasmids encoding BChE cDNA for a wild-type enzyme and a silent mutant (S198D) for the esterase activity were propagated in *E. coli* and transfected into human embryonic kidney cells (293HEK) with the liposomal reagent DOTAP. A plasmid containing the reporter gene GFP was co-transfected in 293HEK cells as a control of the efficiency of each transfection. Plasmids containing the wild-type and mutant human BChE cDNAs encoded a rat glutamine synthetase gene for resistance against the methionine sulfoximine, used for selection of positive clones.

4.2.1.1   Propagation of vectors

Protocol: plasmidial DNA was inserted into competent cells (E. coli, strain XL1-Blue MRF) by electroporation. 10 ng of plasmidial DNA were incubated with 100 µl of competent cells on ice. The principle is that by low temperature the plasmids attach to the surface of the bacteria, and with a temperature shock (2 min at 42°C in water bath) the internalization of the plasmidial DNA occurs by bacterial tranformation. After cooling down the transformed bacteria, 1 ml of LB medium was added for bacterial growth at 37°C in a shaker (250 rpm), for the

expression of the penicillin resistance gene. After 1 h incubation, 25 µl of the bacterial solution (1:100) were plated on 85 mm LB agar plates containing ampicillin, and incubated over-night at 37°C. Colonies were placed in new LB medium (2.5 ml) containing penicillin, and incubated for 8 h at 37°C in a shaker. The resulting bacterial culture was diluted 1:500 into new selective LB medium, final volume 100 ml, incubated overnight at 37°C under vigorous shaking (250 rpm). By bacterial transformation, the plasmidial DNA is amplified, and then purified from the resulting bacterial culture.

4.2.1.2   Isolation of plasmidial DNA

After overnight growth, bacterial medium was poured in blue-caps and centrifuged for 15-20 min at 5500 rpm at 4°C. Medium was removed by gentle aspiration, leaving the pellet as dry as possible. Buffers were supplied with the kit for maxipreps plasmidial purification from QIAGEN. After the harvesting step, subsequent lysis with a buffer containing RNAase was conducted. The protocol was based on an alkaline lyses procedure, as DNA is more stable in slightly alkaline conditions, followed by binding of plasmid DNA to QIAGEN anion-exchange resin under appropriate low-salt and pH conditions. RNA, proteins, and low-molecular-weight impurities were removed by a medium-salt wash. Plasmid DNA was eluted in a high-salt buffer and then concentrated and desalted by isopropanol precipitation. After purification, the concentration of plasmidial DNA obtained was measured, and samples were applied to an agarose gel for electrophoresis, to verify the quality of the DNA obtained.

4.2.1.3   Plasmidial DNA quality control

The concentration of plasmidial DNA was measured in spectrophotometer in the UV light spectrum, by 260 nm, in crystal cuvettes. To calculate the concentration of DNA in µg/ml on samples, the OD observed was multiplied by the dilution factor used and by a factor correspondent to a double stranded DNA. The factor for double-stranded DNA was equivalent to 50, as 1.0 OD at 260 nm means a DNA concentration of 50 µg per ml.

To verify if plasmids had the right insert, they were digested with restriction endonucleases (Hind III and Xba I), removing a segment of 885 bp long from the total *BCHE* wild-type and mutant cDNA (1.8 Kb). DNA digestion was conducted using, for 1 µg DNA, ~10 U of each endonuclease with 1 µl restriction

buffer per µl enzyme, in a final volume of 10 µl reaction with DNase free water. The restriction reaction was incubated at 37°C for 1 h. After plasmidial digestion, 5 µl of the reaction were mixed with 0.5 µl 10x loading buffer, and applied in an agarose gel for electrophoresis. A 1% agarose gel (250 mg agarose in 25 ml of 1x TAE buffer, dissolved in microwave oven, plus 1 µg/ml ethidium bromide) was used with the intent to obtain the separation of the plasmidial DNA from the inserted cDNA fragments, in comparison to a DNA molecular weight control marker (0.1 µg/µl). After electrophoresis (~40 min at 80 volts in 1x TAE buffer), the correspondent bands could be visualized placing the gel over a UV light translucid box, as a result of the intercalation of ethidium bromide in the DNA. For data records, pictures with a Polaroid camera were made to capture the results.

4.2.2 HEK293 cells culture

Cells handling was conducted in a sterile as possible environment. To maintain the cultures in a most sterile condition, procedures were carried out under sterile hood (equipped with UV light), and for cells handling, sterile material was used. Cell culture medium and buffers were autoclaved before use, and chemicals administered to cells presented quality standard for molecular biology use.

4.2.2.1   Transfection of HEK cells with liposomal reagent

Principle: Mixing DOTAP liposomal transfection reagent with DNA results in spontaneously formed stable complexes that can be directly added to the culture medium. These complexes adhere to the cell surface, fuse with the cell membrane, and then release the DNA into the cytoplasm.

On the day before the transfection, cells were dissociated with trypsin (500 µl trypsin-EDTA in 50 ml flasks), and the trypsinazion was ended with 5 ml complete medium. Cells were distributed to new plates (35 mm), at a cell density of ~ 2 x 10^5, and incubate with 10% FCS DMEM complete medium for 18-24 h at 37°C in one 5% CO_2 incubator. 2 h before transfection cells received reduced medium (DMEM 2% serum), and should present between 30-70% confluence until transfection takes place. For transfection, DOTAP reagent was vortexed before use, and solution for transfection was prepared as follows (for

35 mm ∅ dishes): 32 µl of DOTAP plus 68 µl DMEM (without antibiotics and serum), pippeting gently to mix. In another Eppendorf cup, the DNA (0.1 µg/µl) was diluted in 50 µl DMEM medium (without antibiotics and serum). The diluted DNA was added to the diluted DOTAP, mixed by gently flicking of the tube or pipetting and incubated for 10 min on ice. The mixture was given to the cell culture plates plus 3 ml reduced DMEM. Cells were incubated for 6 hours with the transfection solution, and medium was replaced for fresh normal growth medium (2% FCS, 2 mM glutamnine plus 20 U streptamicim/20 µg penicillin to a final volume of 500 ml DMEM).

4.2.2.2   *Selection of cells with recombinant DNA*

Stable transfected cells started to be selected 2-3 days after transfection in serum and glutamine free medium containing 25-50 µM of methionine sulfoximine. Surviving cells were trypsinized and expanded in 250 ml flasks, and cell growth was followed by collection in serum free medium (Ultraculture). After six days, there was enough expressed BChE to test. For detection of the proteins, by western blot and activity measurements, concentrated supernatants from cell culture were used. The medium collected was ultrafiltered with membranes to liberate low molecular weight proteins (less than 50 kD weight), concentrating the material of interest.

4.2.3 SDS-PAGE and Western blot

The expression of the wild-type BChE was detected by Western blot using the M2 antibody (5 µg/ml), raised against the tag-FLAG attached to the C-terminus of the protein. A monoclonal antibody specific for human BChE, was also used to detect the wild-type BChE, and could be used to detect the mutant, which did not display a tag-FLAG attached to the protein. Culture medium from mock transfected cells was used as a negative control, and purified BChE as a positive control.

4.2.3.1   *SDS-PAGE (Sodium Dodecyl Sulfate Polyacrylamide Gel Electrophoresis)*

Principle: SDS applies a negative charge to every protein. An electric current is applied across the SDS-PAGE, causing the negatively-charged proteins to migrate across the gel. A tracking dye is added to the protein solution to allow

the experimentor to track the progress of the protein solution through the gel during the electrophoretic run.

Protocol: A non-reducing 7.5% SDS-PAGE (no boiling and no reducing agent) was used. The gel was discontinuous, with a 4% polyacrylamide stacking gel and a 7.5% separation gel (Table 4.1). The function of the stacking gel is to form an ion gradient at the early stage of electrophoresis that causes all of the proteins to focus into a single sharp band. This occurs in a region of the gel that has larger pores, lower concentrated gel, so that the gel matrix does not retard the migration during the focusing or "stacking" event. Proteins subsequently separate by the sieving action in the lower, "resolving" region of the gel. Samples were applied to a SDS-PAGE with the standard buffer system of Laemmli (Laemmli, 1970), and electrophoresis was run in a vertical system (200 V) with running buffer containing SDS. A molecular weight marker was used to control the position of the bands correspondent to proteins.

Reagents	*Stacking gel* (4%)	*Separation gel* (7.5%)
dH_2O	3 ml	4.8 ml
Tris buffer	1.25 ml (0.5 M, pH 6.4)	2.5 ml (1.5 M, pH 8.8)
30% Acrylamide 0.8% bis acrylamide	0.65 ml	2.5 ml
APS 10%	100 µl	100 µl
SDS 10%	50 µl	50 µl
TEMED	5 µl	5 µl
Total Volume	5 ml	5 ml

Table 4.1: Agarose gel components.

4.2.3.2   Western Blot

By the western blot method (Towbin *et al.*, 1979) proteins are blotted from the gel, after electrophoresis, to a membrane. On the membrane immunodetection of specific proteins can be achieved.

Protocol: a membrane (Immobilon-P) was soaked in methanol for 30 min for permeabilization. After electrophoreses the gel was placed in transfer buffer. The membrane was equilibrated in transfer buffer and couple to the gel. Gel and membrane were placed in a western blot apparatus between two layers of blot

paper and submitted to 350 mA for 1 h. *Poison S* was used allowing visualization of the separated proteins.

4.2.3.3   *Immunodetection*

Protocol: after the detection of the proteins transferred to the membrane, a washing step with PBS was followed by a blocking step with 3% nonfat milk in TBS with 0.05% Tween 20 at RT for 1 hour. After blocking, the membrane was washed in TBS with 0.05% Tween 20, twice for 5 minutes each, and incubated with anti-FLAG M2-HRP (against tag-FLAg), or with the antibody against the human BChE, in TBS with 0.05% Tween 20 overnight at 4°C. The membranes were washed in TBS with 0.2% Tween 20, six times for 5 minutes each. Membranes hybridized with the anti-BChE antibody, were again incubated with a second antibody conjugated with horse radish peroxidase (HRP), diluted 1:2000 in TBS 0.2% Tween, 5% milk, overnight at 4°C. This step was omitted for membranes hybridized with the antibody against the tag-FLAG because it was already coupled with HRP. After 6 washing steps, as described above, membranes were treated with a chemiluminescent substrate according to manufactures instruction (Lumiglo, KPL) to detect the proteins of interest. Positive reaction sites were rapidly detected exposing membranes to an X-ray film.

4.2.4 Activity Assays

Culture medium containing recombinant BChE was concentrated, from 150 ml to 5 ml, by ultrafiltration with Amicon PM10 membranes, and assayed for esterase and aryl acylamidase activities (average of three transfections) for the wild-type and S198D mutants with the substrate o-nitroacetanilide, against concentrated cell culture medium from mock transfected cells. The protein concentration was estimated by the Bradford method (see methods-chapter 3).

Purified *in vitro* expressed wild-type and E197Q mutant BChE were assayed with the substrate ONPRA (N-2-nitrophenylpropanamide) presenting the advantage that the assay could be conducted at RT, in contrast with the usual substrate ONACA (o-nitroacetanilide).

The esterase activity assay was conducted for both purified and non-purified enzymes, with the same substrate and conditions. Principle of the activity assays were described in the chapter 3.

4.2.4.1   Ellman assay

The esterase activity was measured by the Ellman method (Ellman *et al.*, 1961) at 412 nm for 4 mM butyrylthiocholine (BTCh) in 80 mM sodium phosphate buffer containing 0.6 mM DTNB, pH 8.0, at 23°C, for 5 min.

4.2.4.2   Recombinant BChE assayed with ONACA

O-nitroacetanilide (ONACA) is the usual substrate used to measure the AAA activity. With this substrate, wild-type and S198D mutant BChE were investigated regarding their AAA activity. For this assay, concentrated medium from cell culture was used. Medium collected from mock transfected cells was used as a negative control.

The AAA activity was measured with a method described by Fujimoto (1976), slightly modified. The assay conditions to measure the AAA activity in cell culture medium were: 6.6 mM of ONACA incubated at 37°C for 1 h in 0.4 M of potassium phosphate buffer, pH 8.0, containing 0.05 ml of probe and 0.05 ml of inhibitor or H_2O in a total volume of 0.5 ml. The extinction was measured for 60-90 min in a continuous assay at 410 nm against ONACA controls processed in the absence of enzyme. Controls with correspondent amounts of probe, from cells transfected with green fluorescence protein, were also assayed as background. AAA was deduced from calibration curves established with known concentrations of *O*-nitroaniline.

4.2.4.3   Recombinant BChE assayed with ONPRA

A second substrate, N-2-nitrophenylpropanamide (ONPRA), was used to measure the activity of the wild-type and E197Q mutant BChE purified enzymes. AAA activity measurements were conducted according to the assay described by Fujimoto (1976), with modifications. The extinction was measured at 430 nm, at 23°C for 30 min against ONPRA controls processed in the absence of enzyme, and with mock transfected cells concentrated medium. In plastic cuvettes: 1.35 ml of 0.06 M Tris HCl buffer (pH 8.0), 0.05 ml of dH_2O or inhibitor, 0.1 ml of buffer containing BChE and 0.05 ml of substrate were added

to the final volume of 1.5 ml. The substrate ONPRA and inhibitor 5-HT were used to final concentrations ranging from 0.4 to 5 mM and 25 to 330 µM, respectively, assayed in at least duplicates. Fixed amounts of enzymes were used to measure aryl acylamidase activity, 3 esterase units (U) for the E197Q and 5 U for the wild-type BChE. AAA activity was deduced from calibration curves established with known concentrations of o-nitroaniline (2-nitrobenzenamine), a product generated by AAA catalysis of ONPRA, as it was for o-nitroacetanilide. Protein concentration was determined by the Bradford method (see methodology of chapter 3).

4.2.5 Substrate Kinetics

The enzyme substrate dissociation constants were calculated according to the Michaelis-Menten kinetics, following the equation below:

$$V = V_m * S / (K_m + S)$$

V is the velocity, V_m is the maximum velocity for the ES (enzyme/substrate) complex (µM/mg protein), K_m is the concentration of substrate at which half of the maximal velocity of the enzyme was achieved, and S is substrate concentration in mM.

By double-reciprocal plot (Lineweaver-Burk plot) V_{max} and Km ($V_{max}/2$) can be also determined. On the y axis, velocities ($1/V_0$) are plotted versus substrate concentrations ($1/S$) on the x axis. The slope is determined by K_m/V_{max}, the intercept of the vertical axis by the $1/V_{max}$, and the intercept of the horizontal axis is -1/Km.

K_{cat} is the catalytic constant or "turnover number". The k_{cat}/K_m (catalytic efficiency) describes the conversion of free E and free S into E + P. The rate at low [S] is directly proportional to the rate of enzyme-substrate encounter. The kinetic parameters (k_{cat} and K_m) were determined employing 6 different substrate concentrations (bracketing the K_m values) and the data were fitted to Michaelis–Menten equation.

4.2.5.1   Inhibition Kinetics

Dissociation constants (Ki) for the enzyme-inhibitor complexes were calculated from the effect of substrate concentration on the apparent dissociation constants by applying non-linear regression to fit the model to experimental data. Data used for calculations were: inhibitor concentrations [I], the initial velocities V_0, and the substrate concentrations [S] for each reaction. Essentially, the following models were tested:

Pure competitive inhibition: $V = V_m*S/ (K_s*(1 + I/K_i) + S)$

Partial competitive inhibition: $V = V_m*S/ (K_s*(1 + I/K_i)/ (1 + I/ (a*K_i)) + S)$

Non-competitive inhibition: $V = V_m*S/ ((K_s + K_s * I/K_i) + (S + S*I/K_i))$

Uncompetitive inhibition: $V = V_m*S/ (K_s + S * (1 + I/K_i))$

Linear mixed type: $V = V_m*S/ ((K_s + K_s*I/K_i) + (S + S*I/(a*K_i)))$

Hiperbolic mixed type: $V = V_m*S/ ((a*K_s*(I/K_i)/ (b*I + a*K_i) + S*(I + a* K_i)/ (b*I + a*K_i))$

The K_s was obtained by the ratio of the rate of breakdown of the E-S complex divided by its rate of formation. Ks is defined by the equilibrium formed between the enzyme (E) and substrate (S) and the E-S complex. The K_i is the dissociation constant for inhibitor binding (in the same concentration units as the inhibitors), and I is the inhibitor concentration in μM. Experimental results were analyzed by non-linear regression using the Systat software, the lower the standard deviation obtained, the better the data were considered to fit a model. The Lineweaver-Burk plot was used to visualize the effect of inhibitors, and therefore, to distinguish the type of inhibition.

Determining the appropriate plot to calculate the inhibition constant Ki: if the Lineweaver-Burk plots of several inhibitor concentrations intersect on the vertical axis, a competitive inhibitor is being used and the Km type of plot is the appropriate for that. Competitive inhibitors have the effect to increase the Km of the reaction and therefore to reduce the affinity of the enzyme for its substrate. If the Lineweaver-Burk plots of several inhibitor concentrations intersect on the base line, a non-competitive inhibitor is the case, and the

$1/V_{max}$ type of plot is the right one. Non-competitive inhibitors do not affect the combination of the substrate with the enzyme, but it does affect the velocity. If the Lineweaver-Burk plots of several inhibitor concentrations are parallel, the type of inhibition is uncompetitive and the $1/K_m$ type of plot is used. Uncompetitive inhibitors have the effect of decreasing the K_m and the velocity of the reaction to the same extent. If the Lineweaver-Burk plots of several inhibitor concentrations intersect above or below the $1/[S]$ axis, a mixed inhibitor is the case and $1/K_m$ type of plot is used. Mixed inhibitors have the affect of decreasing the velocity of the reaction and either increasing or decreasing the K_m.

For instance, for non-competitive inhibition the y intercept is determined by the equation below, which result will vary with the concentration of inhibitor:

Y intercept = $1/V_{max}$ {1 + [I]/Ki}

4.3 *Results*

4.3.1.1 *Detection of the in vitro expressed enzymes: wild-type and S198D BChE*

After plasmid recovery and purification, digestion of specific restriction sites within the BChE cDNA inserted segment was performed to confirm that plasmids contained the right insert (Fig. 4.1).

Several transfection methodologies were tested to achieve the desired transfection efficiency. The liposomal reagent was considered efficient with HEK293 cells, according to the results obtained with the reporter gene GFP (Fig. 4.2).

The *in vitro* expressed wild-type and mutant S198D BChE were detected by immunoaffinity in western blot, by using concentrated cell culture supernatants. Two antibodies were used to confirm the expression of BChE, one for the tag-FLAG attached to the C-terminus of the protein, and one monoclonal antibody specific for human BChE (Fig. 4.3).
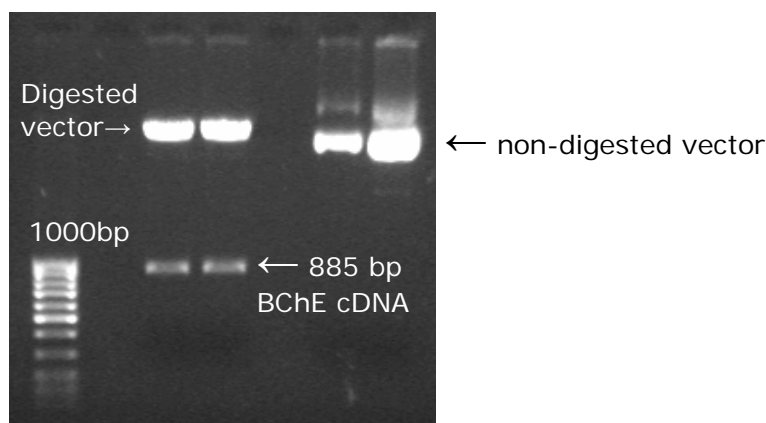
Fig. 4.1: Digestion of the recombinant DNA after plasmid amplification. Bands correspondent to digested DNA from plasmid and BChE cDNA insert (a), and non-digested vector (b) were visualized in 1% agarose gel, after electrophoresis.
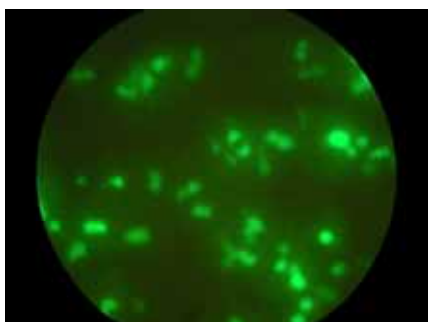
Fig. 4.2: Experiment control for the transfection efficiency with liposomal reagent. Green fluorescent protein expressed by the reporter gene GFP, encoded by plasmids transfected into HEK293 cells.
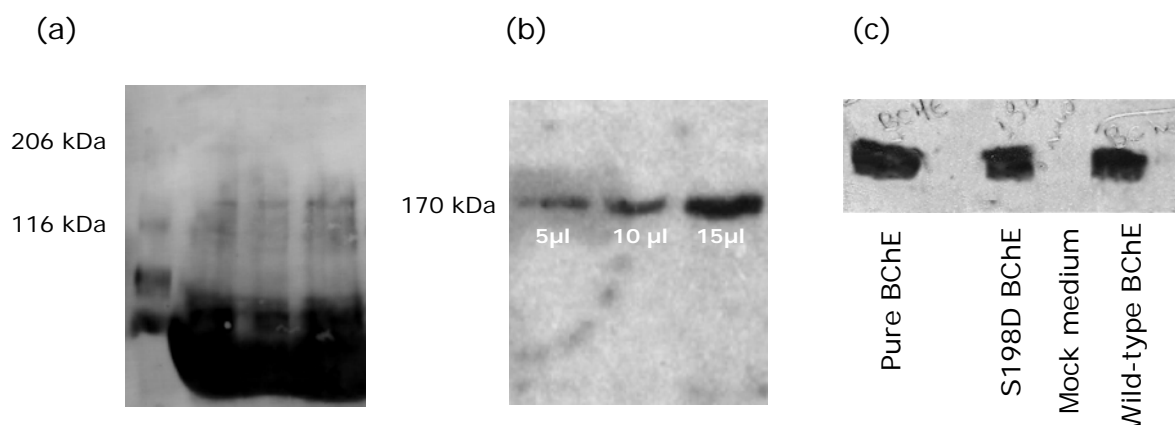
Fig. 4.3: Western blot results. (a) SDS-PAGE (7.5%) stained with *Ponceau S.* (b) Immunostaining with a specific antibody for the tag-FLAG (M2) attached to the C-terminus of the wild-type BChE, revealed by chemiluminescence and exposure to X-ray film, with increasing concentrations of sample. (c) Immunostaining with an antibody against human BChE, with positive (purified BChE) and negative controls (mock transfected cells concentrated medium), and S198D mutant and wild-type BChE.

4.3.2 AAA activity on the active site mutant (S198D) and wild-type BChE

The recombinant human S198D *BCHE* cDNA encodes a BChE variant with an amino acid substitution at the active site, position 198 (Ser198 → Asp198).

The AAA activity assay, for the mutant (S198D) and wild-type BChE, was conducted with the substrate o-nitroacetanilide. Concentrated supernatants, from recombinant BChE transfected cells culture, were used as samples against controls. Supernatant from mock transfected cells were used as a background control. The presence of the recombinant BChE in cell culture supernatants was in parallel confirmed by western blot analysis (Fig. 4.3).

The BChE mutant S198D displayed 34.6% of the specific AAA activity of the wild-type enzyme (Fig. 4.4), and did not show significant esterase activity in comparison to controls. The ratio of AAA/esterase activity on BChE for the wild-type enzyme was 0.69, according to the values of specific activity in U/mg, as given on the table below:

AAA specific activity U/h/mg	Esterase specific activity U/min/mg
Wild-type BChE = 2.08	Wild-type BChE = 3.03
S198D BChE = 0.72	S198D BChE = no activity

The legitimacy of an AAA activity expressed by the recombinant human wild-type BChE, from cell culture supernatants, was confirmed by serotonin inhibition (Fig. 4.5). 1 mM serotonin inhibited 79% of the total AAA activity in agreement with earlier reports; viz. amniotic fluid AAA activity from BChE and AChE are inhibited to 80% (Jayanthi *et al.*, 1992). On the other side, the AAA activity of the mutant S198D BChE was very poorly inhibited by serotonin.

The AAA activities of the *in vitro* expressed wild-type and mutant (S198D) BChE were also tested towards ethopropazine, a potent reversible inhibitor of BChE. Concentrations of 1 and 10 µM inhibited about 62% and 89%, respectively, of the wild-type BChE AAA-associated activity, while only about 7% and 13% of the S198D activity, respectively (Fig. 4.6; Fig. 4.7).
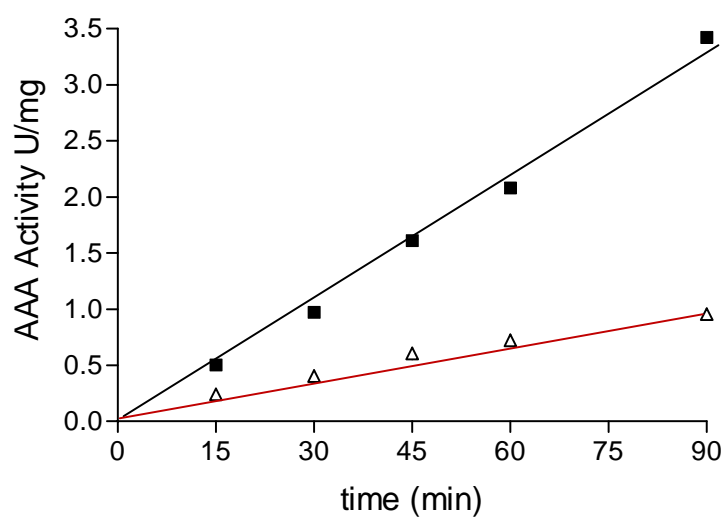
Fig. 4.4: Aryl acylamidase activity of the in vitro expressed human (■) wild-type BChE and (Δ) mutant S198D BChE, with the substrate ONACA.
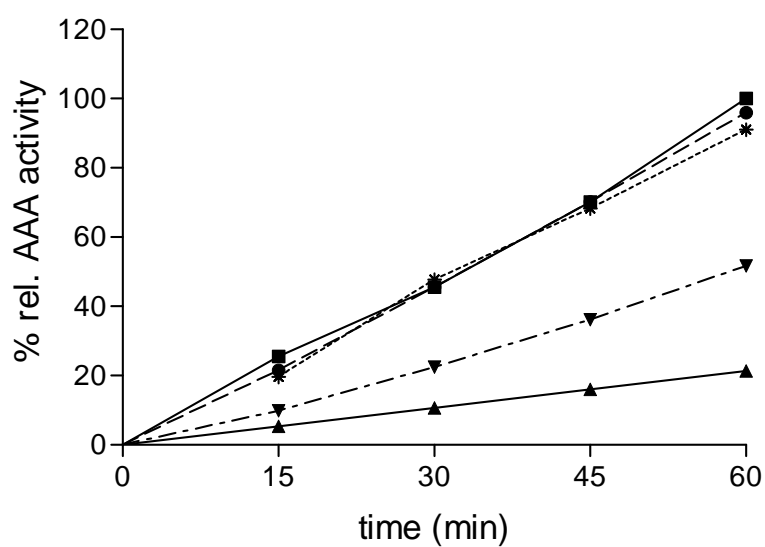
Fig. 4.5: Aryl acylamidase activity of the in vitro expressed wild-type BChE, from cell culture concentrated supernatants, with the substrate ONACA in the presence and absence of serotonin. (■) No inhibitor, (●) 1 x 10^{-6} M, (*) 1 x 10^{-5} M, (▼) 1 x 10^{-4} M and, (▲) 1 x 10^{-3} M of serotonin.
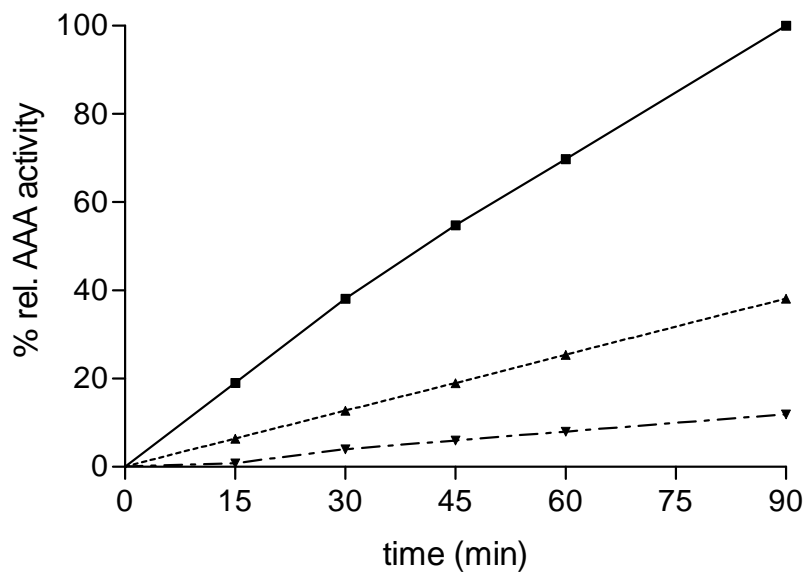
Fig. 4.6: Aryl acylamidase activity of in vitro expressed human butyrylcholinesterase, from cell culture concentrated supernatants, with the substrate ONACA in the presence and absence of ethopropazine. (■) No inhibitor, (▲) 1 x 10^{-6} M and, (▼) 1 x 10^{-5} M ethopropazine.
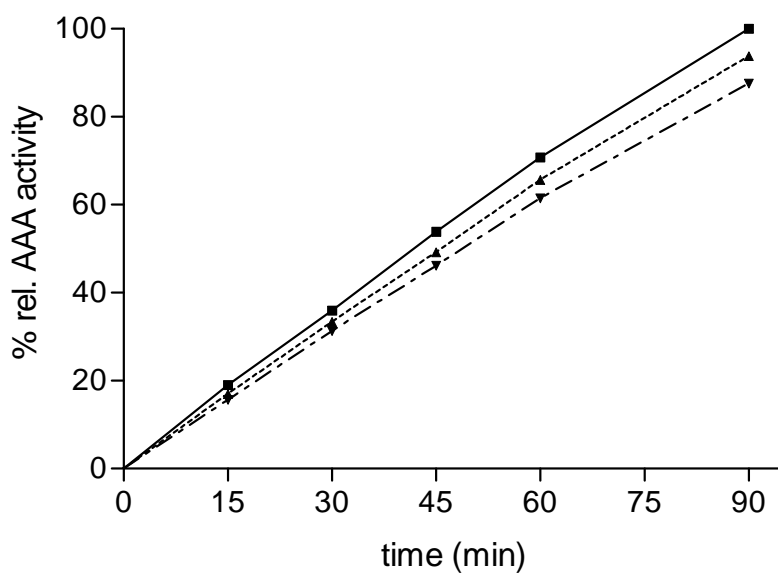
Fig. 4.7: Aryl acylamidase activity on the in vitro expressed mutant (S198D) butyrylcholinesterase, from cell culture concentrated supernatants, with the substrate ONACA in the presence and absence of ethopropazine. (■) No inhibitor, (▲) 1 x 10^{-6} M and, (▼) 1 x 10^{-5} M ethopropazine.

4.3.3 Kinetic studies with ONPRA and serotonin on purified wild-type and E197Q BChE

The aryl acylamidase activity was also investigated in recombinant human wild-type and mutant BChE purified enzymes. In this case, however, a different recombinant mutant BChE was investigated (E197Q). This mutant *BCHE* cDNA, encoding for a BChE variant with a single nucleotide substitution (G → C), displays a replacement of the active site glutamic acid (E) by a glutamine (Q) residue, at the position 197 (Glu197 → Gln197). This amino acid substitution did not abolish completely the esterase activity of BChE, which presented almost 15% of the total wild-type BChE specific activity under standard assay conditions, with the substrate butyrylthiocholine.

To investigate wild-type and mutant (E197Q) BChE-associated AAA activities, substrate and inhibitor affinities, purified recombinant BChEs were used. Besides, a new substrate for AAA (ONPRA) was tested aiming a faster activity assay.

Under normal assay condition, six substrate concentrations were tested. The mutant E197Q showed a lower affinity than the wild-type BChE for ONPRA, according to Km values. The substrate concentration needed to achieve the half maximum velocity was about three fold higher for the E197Q BChE (Km = 12.7 ± 1.49 mM), than for the wild-type BChE (Km = 4.4 ± 0.29 mM).

By definition, the binding of a non-competitive inhibitor occurs in a peripheral site of the enzyme and not on the active site. Therefore, substrate and inhibitor do not compete for the access to the same site. However, inhibitors binding on peripheral sites alter the molecular conformation of the enzyme, preventing the substrate to bind to the active site. Consequently, Vmax is altered, as demonstrated for AAA activity when using serotonin as inhibitor. By Lineweaver-Burk plots a decrease in Vmax, and no alteration in Km, were observed for both E197Q mutant and wild-type BChE-associated AAA activities (Fig. 4.8; Fig. 4.9), fitting a non-competitive inhibition mechanism. However, E197Q (K_i = 308 ± 10.67 μM) displayed much lower affinity to serotonin than the wild-type BChE (K_i = 63 ± 2.58 μM), presenting a higher deviation for the non-competitive model of inhibition.

4.3.3.1   Catalytic efficiency of the E197Q and wild-type BChE-associated AAA activities with the ONPRA substrate

The natural affinity and catalytic power of BChE-associated AAA activity were affected by the replacement of glutamic acid 197 by glutamine. The K_{cat}/K_m constant was about 10-fold lower for the AAA BChE-associated E197Q mutant (0.78) compared to the wild-type enzyme (7.8).
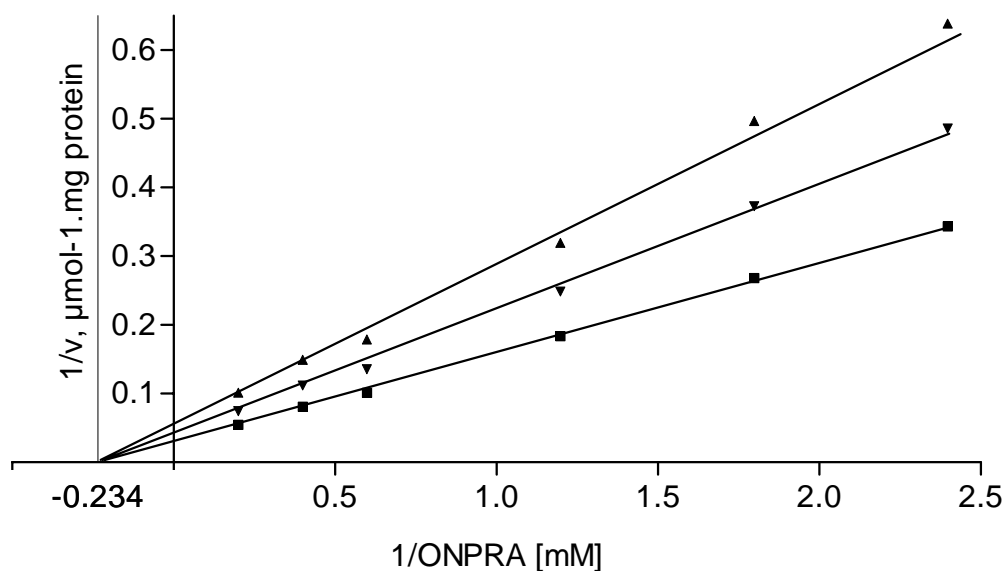
Fig. 4.8: Lineweaver-Burk plot of the aryl acylamidase activity of the purified wild-type BChE in the absence and presence of serotonin, with several concentrations of the substrate ONPRA. (■) No inhibitor, (▼) 2.5 x 10^{-5} M, and (▲) 5 x 10^{-5} M serotonin.
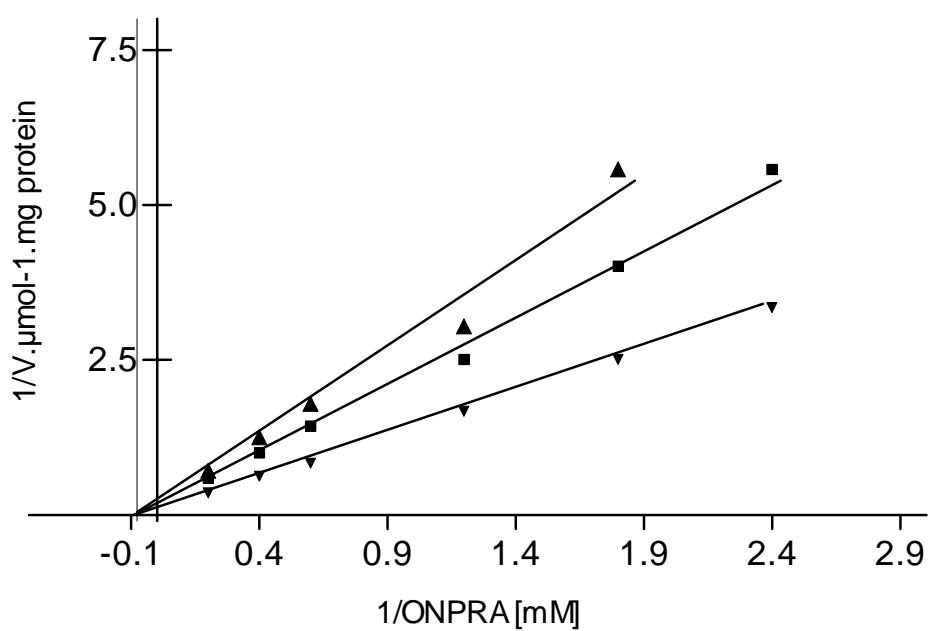
Fig. 4.9: Lineweaver-Burk plot of the aryl acylamidase activity of the purified mutant E197Q BChE in the absence and presence of serotonin, with several concentrations of the substrate ONPRA. ($\blacktriangledown$) No inhibitor, ($\blacksquare$) 1.8×10^{-4} M, and ($\blacktriangle$) 3.3×10^{-4} M.

4.4 Discussion

In this study, it was shown that human recombinant wild-type and a mutant (S198D) BChE, over-expressed in a cell culture system, showed AAA activity (Fig. 4.4). Moreover, purified recombinant wild-type BChE and a second mutant type (E197Q), also showed AAA activities, which were inhibited by serotonin, confirming the existence of this side activity on BChE (Fig. 4.8; Fig. 4.9).

4.4.1 AAA activity on the active site S198D BChE mutant

The amino acid serine (S), present on the active site catalytic triad of cholinesterases, is the main amino acid responsible for the esterase activity (Shafferman *et al.*, 1992; Ordentlich *et al.*, 1993). As expected, its replacement by aspartic acid (D) abolished the esterase activity. Like serine, aspartic acid often occurs in active sites. However, in contrast to serine, which is a small residue displaying intermediate hydrophobicity, aspartic acid is an intermediately large, hydrophilic residue, implying molecular conformational changes when one is replaced by the other. However, catalysis was still possible for the BChE S198D associated aryl acylamidase activity (Fig. 4.4); indicating that esterase and AAA activities have distinct active sites.

The AAA activity of the mutant BChE S198D decreased circa 65% in relation to the wild-type enzyme, and could not be efficiently inhibited by a specific BChE inhibitor (ethopropazin), which was effective towards the wild-type enzyme (Fig. 4.6). Ethopropazin inhibits the esterase activity of the usual human BChE in a competitive way (Simeon-Rudolf *et al.*, 2001). It is not clear how the AAA molecular domain is interacting with this compound, but its binding affinity is affected on the BChE S198D active site mutant. This is not surprising, once the mutation in the BChE active site might be critical for the binding of this inhibitor, leading to loss of affinity due to polarity and conformational changes that interfere with EI interaction.

4.4.2 New substrates for the aryl acylamidase activity

New substrates have been developed with the intent to allow a faster AAA activity assay. With the usual o-nitroacetanilide substrate, the AAA catalytic reaction is slow and dependent on a temperature condition of 37°C.

The binding affinity of the purified human wild-type BChE-associated AAA activity for the N-2-nitrophenylpropanamide substrate was 3.4 fold higher (K_m = 4.4 mM), than for the o-nitroacetanilide (K_m = 14 mM; Darvesh, 2003) substrate, meaning that the AAA assay became more effective with N-2-nitrophenylpropanamide.

The catalytic power and affinity of the AAA activity of the BChE E197Q mutant was weakened by 10-fold compared to the wild-type BChE. Similarly, the catalytic affinity (K_{cat}/K_m) of the esterase activity of BChE, with the substrate butyrylthiocholine, also decreased about 10-fold for the E197Q mutant (Millard *et al.*, 1998). In this sense, the kinetic behaviors of aryl acylamidase and esterase activities were affected similarly for the E197Q mutant. Therefore, AAA and esterase activities, of the BChE active site mutant E197Q, had similar response regarding their substrate affinities.

4.4.2.1   Serotonin inhibition mechanism

Serotonin here was demonstrated to act as a non-competitive inhibitor of the human recombinant wild-type BChE-associated AAA activity. For the BChE E197Q AAA activity, the non-competitive inhibition mechanism model is also accepted. However, it is on the limit of acceptance to fit this non-competitive model of inhibition towards serotonin.

AAA affinity for serotonin was greatly affected in the E197Q active site BChE mutant, which showed a ~4.8 fold higher Ki than for the wild-type BChE (Fig. 4.8; Fig. 4.9). Therefore, the esterase active site modification E197Q affected serotonin binding. Nevertheless, the binding site for serotonin on BChE is not known. However, if one considers that the BChE active site replacement, of a negatively charged amino acid (E) by a polar residue (Q), changes the esterasic site affinity for positively charged compounds, the decrease in affinity of the mutant BChE for serotonin (a positively charged compound) could be justified. Furthermore, the S198D BChE mutant AAA associated activity lost its sensitivity towards serotonin, implying that the substitution of the amino acid serine (S) for the aspartic acid (D), in the esterasic active site, drastically affected serotonin binding.

These data ultimately reveal an interesting relation of serotonin and cholinesterases: a) serotonin inhibits BChE-associated AAA activity in a non competitive manner, and b) the affinity of serotonin towards BChE active site mutants is affected. It is not known if serotonin inhibits the esterase activity through a competitive mechanism. However, it is known that ChEs are slightly inhibited by this compound (Gilboa-Garber *et al.*, 1978). The fact that serotonin inhibits AAA in a non-competitive manner, indicates that it is binding to a site in the periphery of the AAA active site. On the other hand, a reduced affinity of BChE active site mutants for serotonin shows that the esterasic catalytic triad is essential for serotonin binding. In fact, the behavior of some inhibitors towards esterase and AAA activities was previously reported to be ambiguous. Competitive inhibitors of the esterase activity, like eserine and neostigmine, behave non-competitively towards the AAA activity (Oommen and Balasubramanian, 1978). Second, cholinesterases substrates (acetylcholine and butyrylcholine), act as non-competitive inhibitors of the AAA activity (Oommen and Balasubramanian, 1978). Therefore, these substrates and inhibitors bind to a site in the periphery of the AAA active site. It indicates that the esterasic active site, where these compounds are binding to, might be functioning as a peripheral site for the AAA activity.

It is not clear if a high concentration of serotonin could provoke direct inhibition, or a down regulation of cholinesterases *in vivo*. However, as shown here, it binds to cholinesterases in enzymatic assays. It implies that serotonin could act as an inhibitor or as a substrate of cholinesterases *in vivo*. If cholinesterases are involved with serotonin metabolism, physiological levels of this compound could influence their expression, and vice versa, as a feedback mechanism. For instance, the administration of cholinesterases inhibitors has been reported to increase serotonin levels in mice and rat (Mehta *et al.*, 2005; Aldridg *et al.*, 2005). Of course the mechanism behind the relation of ChEs inhibition versus serotonin increase is not clear. However, it is not an isolated case, as the occurrence of cholinesterases and serotonin is also inversely proportional in the AD brain (Small, 1996; Wu and Swaab, 2005).

4.5   Summary

- AAA activity is present in recombinant BChE; it is decreased, but not abolished, in BChE active site mutants (S198D; E197Q);

- Esterase and AAA activities can have their catalytic powers identically decreased due to a specific amino acid alteration (E197Q), indicating that both activities are a property of the same protein;

- The esterase and AAA activities were not affected in the same way by a mutation of the BChE esterasic active site (S198D), indicating they have distinct active sites;

- Serotonin acts as a non-competitive inhibitor of the AAA activity of a purified human wild-type BChE, demonstrating that it is directly interacting with cholinesterases;

- The affinity of BChE E197Q mutant for serotonin was affected, indicating that the glutamic acid (E) at the position 197 of the BChE active site is relevant for serotonin binding;

- Serotonin inhibition was not effective towards the AAA activity of the BChE S198D mutant. This indicates that the amino acid serotonin (S), of the esterasic catalytic triad, is essential for serotonin binding.

CHAPTER 5

5   Final considerations

5.1 General findings

Novel functions of cholinesterases have been supported by this work. AChE and BChE have been shown to present a developmentally regulated spatio-temporal expression pattern during chick (*Gallus gallus*) pineal embryogenesis in chapter 2. The involvement of AChE expression with pineal remodeling and photoreceptor cell differentiation, and a high activity of it in apoptotic cells were shown during embryogenesis of the chick. BChE activity was intense in proliferative stages and was down-regulated in less proliferative periods of the pineal development, in corroboration with earlier findings of its involvement with proliferation (Layer, 1987; Robitzki *et al.*, 2000).

In chapter 3, the relevance of AChE for the development of another model organism, the zebrafish (*Danio rerio*), was investigated with focus on a serotonin related non-cholinolytic activity of cholinesterases. It was demonstrated that the AChE mRNA starts to be transcribed shortly after the genomic transcription activity begins in this organism, although, initially no cholinergic activity is present. The presence of a non-cholinolytic side activity of AChE, the aryl acylamidase, was detectable as early as the first AChE transcripts, indicating a relevance of it for early zebrafish development. During *in vivo* experiments, a strong malfunction of zebrafish embryogenesis, as a result of serotonin administration (a neurotransmitter and AAA inhibitor) was observed by the period when the genomic activity of ACHE should be activated. Therefore, serotonin administration disrupted early developmental events, in association with the AChE expression onset.

Regarding the interaction of serotonin with cholinesterases molecules, *in vitro* experiments revealed a non-competitive mechanism of inhibition of human aryl acylamidase, associated to wild-type and mutants BChEs over-expressed in cell culture (chapter 4). Besides, the esterase and AAA catalytic powers were not affected in the same way in an esterasic active site recombinant mutant enzyme (S198D), but could identically respond to another active site specific mutation (E197Q). Therefore, both activities are indeed located on the BChE molecule, presenting not identical catalytic sites.

5.2   Concluding remarks

This was a broad study on novel functions of cholinesterases, through the achievements of this work new research directions were opened, delivering interesting findings for promising future investigations.

5.2.1 The chick pineal gland embryogenesis and the spatio-temporal expression of ChEs

Investigating the onset of photoreceptors differentiation during embryogenesis of the chick pineal gland, a new photoreceptor (PRC) morphology was detected, which was not described in the post-hatching pineal gland. The characterization of this PRC morphology remains to be done by electron microscopy. The aim is to identify whether it has associated lamellar complexes, which are lost after embryogenesis, or if it is a unique PRC type appearing only during the chick pineal embryogenesis period.

A second interesting point to be investigated is the pineal basal lamina rupture, which appears with the formation of the mammilliform projections during pineal expansion. It is already known that cells migrate through the basal lamina to form new vesicles, but it is not known if the rosettes of cells (AChE-positive) on the apices of the mammilliform projections are leading to ruptures of the basal lamina. AChE was found here to guide the surrounding proliferating cells on the mammilliform projections, and is possibly leading to the rupture of the basal lamina. This question can be also answered by investigating this material by electron microscopy.

The expression of ACHE in pineal photoreceptors and not in retina PRCs is intriguing. A relation of AChE expression to photoreceptors cells undergoing apoptosis in the pineal organ has been shown in this work. AChE has been earlier shown to be relevant for the development of retina photoreceptors, which degenerated during development of AChE KO mice (Bytyqi *et al.*, 2004). Photoreceptors cannot well develop in the absence of AChE, but were demonstrated to need its expression to initiate the apoptotic process by the intrinsic pathway (Park *et al.*, 2004). The contradiction of these premises can be explained by the fact that apoptosis can be activated by two different pathways, which can be dependent or not on AChE expression. Therefore, PRCs death can

occurr with the involvement of AChE or without it, in accordance with the type of apoptotic process. In retina, PRCs normally do not die in postnatal periods, but their death can be induced, e.g. by the absence of AChE in KO mice. It would be interesting to verify if the death of these PRCs is happening by an extrinsic pathway, which does not involve AChE expression. For this purpose, the levels of factors involved in the extrinsic death pathway, e.g. TNF, can be investigated in the retina of AChE KO animals. Other approaches like si-RNA, to silence AChE expression, can also be used as a tool to characterize its relation to the apoptotic process in retina and pineal organ.

In this study, the involvement of AChE with pineal remodeling was demonstrated. Essentially, the repetition of this study using the pineal organ of an AChE KO organism can support my findings. AChE KO mice are available and could be used for this purpose.

Nevertheless, the presence of cholinesterases on the mature pineal gland raises the question whether there would be a physiological functionality for these proteins in this tissue. Daily alterations of serotonin concentration, controlling the circadian rhythm, have been correlated with AChE activity fluctuations (Quay *et al.*, 1971; Schiebeler, 1974; Mohan, 1974; Wood, 1979; Lewandowski, 1986; Pan, 1991). Therefore, AChE expression is suggested to be dependent of serotonin physiological levels. However, this point has never been investigated in detail, making use of molecular approaches. Meanwhile, the possibility remains that AChE expression is under circadian rhythm control.

5.2.2 AChE-AAA expression in zebrafish and embryogenesis malfunction under serotonin administration

The aryl acylamidase and esterase activities show different profiles during zebrafish development, indicating that AChE is suffering post-translational modifications occurring during the transition from the embryonic to the larval period. The existence of post-translational modifications can be verified by mass spectrometry, more specifically, by the Quadrupole-time-of-flight (Q-TOF) tandem mass spectrometry. This is a relatively new approach with a high performance analysis, which requires powerful instruments and proper training. It was not possible to conduct such analysis during this work; however, it can

be conducted at any time using zebrafish homogenates to investigate this matter.

Regarding the sensitivity of zebrafish embryos towards serotonin, embryonic malformations were found to be related to the onset of AChE expression during the blastula period. A direct influence of serotonin down regulating AChE expression is hypothesized to happen by this period, resulting in future developmental malformations. The expression of developmental markers (myo-D, gsc, and ngn-1) was affected in areas where AChE is also normally active. Therefore, AChE expression in these areas will be investigated by *in situ* hybridization to establish whether its expression has also been affected. A delay on AChE expression under serotonin administration can also be investigated by quantitative RT-PCR, to reveal its effect on the *ACHE* transcription activity.

Moreover other zebrafish developmental markers can be used to follow the embryogenesis disruption pattern under serotonin administration.

5.2.3 AAA activity active site on BChE

The aryl acylamidase activity is suggested to be a property of cholinesterases. Therefore, its existence can be just approached by its activity, limiting the methodologies to show its relevance.

Developmental biology can bring interesting insights about the relevance of AAA, as investigated with zebrafish. However, to understand how this activity is working in relation to the esterase activity, and where it is located on cholinesterases molecules, an essentially biochemical strategy has to be drawn, designing meaningful mutant enzymes to obtain sound results with molecular modeling of kinetics studies. In the present study, only two human BCHE mutant enzymes were investigated in relation to their AAA activity. However, several other mutants can be investigated to really underline which amino acids comprise the AAA catalytic site.

5.3   Further work

Two new lines of research, which opened within this work, will be closer investigated:

During the investigations of chick pineal PRC cells differentiation, one PRC morphology was identified as characteristic of embryonic pineals, as it was not reported to occur in the mature pineal organ. Further characterization of this PRC morphology will be conducted by electron microscopy, bringing the ultimate answer whether it is a PRC type present only at embryonic periods. In parallel, also by electron microscopy, the pineal basal lamina limits will be investigated with the intent to verify if its rupture is caused by the AChE-positive cells migration during pineal expansion.

Regarding the zebrafish embryonic malformations resulting from serotonin administration, a complementary study will address its connection with the onset of AChE transcripts. Furthermore, *in situ* hybridization studies, to localize AChE expression, will be conducted in embryos affected by serotonin administration. Moreover, other zebrafish developmental markers will be used, to better characterize the zebrafish development disruption pattern under serotonin administration.

Furthermore, other possibilities of further research, based on the work here reported, are still open, as already mentioned in concluding remarks.

6   Summary

The non-specificity of cholinesterases to cholinergic innervated tissues, their early onset during embryogenesis of many organisms, and their non-cholinolytic aryl acylamidase activity, indicate that these enzymes are involved with physiological processes other than the termination of nervous impulse. In this study, cholinesterases expression and function were investigated during the development of two model organisms, chicken (*Gallus gallus*) and zebrafish (*Danio rerio*), with the focus on non-cholinolytic and non-catalytic events. In chicken, the pineal organ was investigated taking into consideration: a) its similarity to the eye, as earlier studies suggested a relevance of cholinesterases to retina embryogenesis, b) its relevance on controlling physiological functions following a circadian rhythm, and c) its disfunction in pathological states, which also present altered cholinesterases expression, like Alzheimer's disease. Indeed, in this study, a remarkable developmentally regulated switch from butyrylcholinesterase (BChE) to acetylcholinesterase (AChE) expression during pineal embryogenesis was found, in association with cell proliferation and differentiation, respectively. Even more, AChE-positive cells were shown to guide the pineal epithelium remodeling (leading to follicles development), indicating it plays a pivotal role in pineal embryogenesis. Besides, the appearance of follicular supportive cells correlated with this remodeling onset, followed by photoreceptor cells differentiation, indicating that these events are interconnected. Furthermore, AChE was demonstrated to be active in cells undergoing apoptosis during pineal embryogenesis, corroborating earlier *in vitro* studies indicating its involvement with the apoptotic process. However, the mechanism of action of cholinesterases in most of these developmental events is not clear, in particular whether the function could be structural or non-cholinolytic. Using zebrafish as a second model organism, a non-cholinolytic activity of AChE was investigated, from the time its transcription begins until larval development of this organism. This study revealed a particular profile of the AChE-associated aryl acylamidase activity (AAA) during development of zebrafish. AAA was particularly more pronounced than the esterase activity during zebrafish embryogenesis, indicating a relevance of this activity during early development. This non-cholinolytic activity was further investigated in

human recombinant BChE wild-type and mutant proteins to address its catalytic power in enzymes with low cholinergic functionality. The results of this study indicate that the esterase and AAA activities are displayed by separate catalytic sites on cholinesterases. Altogether, these three studies on novel functions of cholinesterases address aspects of these enzymes also in relation to serotonin, as follow: a) cholinesterases are implicated in the development of the pineal gland, an organ controlling serotonin metabolism; b) a temporal high sensitivity of zebrafish embryos towards serotonin administration correlated with AChE expression onset during their blastula period, and c) serotonin directly interacts with cholinesterases, demonstrated through a non-competitive inhibition of the AAA activity on purified recombinant human BChE.

This PhD work, therefore, presents strong evidence of the AChE involvement with morphogenesis, with further implications of its expression for pineal cells differentiation and apoptosis. It also writes further history on the little investigated side activity of cholinesterases, the aryl acylamidase, and supports a link between cholinergic and serotonergic systems.

7 References

Alber, R.; Sporns, O.; Weikert, T.; Willbold, E.; Layer, P.G. (1994) Cholinesterases and peanut agglutinin binding related to cell proliferation and axonal growth in embryonic chick limbs. *Anat Embryol* (Berl), **190**, 429-38.

Alcantara, V.M.; De Lourenco, M.A.; Salzano, F.M.; Petzl-Erler, M.L.; Coimbra, C.E. Jr.; Santos, R.V. and Chautard-Freire-Maia, E.A. (1995) Butyrylcholinesterase polymorphisms (BCHE and CHE2 loci) in Brazilian Indian and admixed populations. *Hum Biol*, **67**, 717-26.

Aldridge, J.E.; Meyer, A.; Seidler, F.J. and Slotkin, T.A. (2005) Alterations in central nervous system serotonergic and dopaminergic synaptic activity in adulthood after prenatal or neonatal chlorpyrifos exposure. *Environ Health Perspect*, **113**, 1027-31.

Aloyo, V.J. and Walker, R.F. (1987) Noradrenergic stimulation of serotonin release from rat pineal glands *in vitro*. *J Endocrinol*, **114**, 3-9.

Alt, J.; Heymann, E. and Krisch, K. (1975) Characterization of an inducible amidase from Pseudomonas acidovorans. *Eur J Biochem*, **53**, 357-69.

Alvarez, A.; Bronfman, F.; Perez, C.A.; Vicente, M.; Garrido, J. and Inestrosa, N.C. (1995) Acetylcholinesterase, a senile plaque component, affects the fibrillogenesis of amyloid-beta-peptides. *Neurosci Lett*, **201**, 49-52.

Alvarez, A.; Alarcon, R.; Opazo, C.; Campos, E.O.; Munoz, F.J.; Calderon, F.H.; Dajas, F.; Gentry, M.K.; Doctor, B.P.; De Mello, F.G. and Inestrosa, N.C. (1998) Stable complexes involving acetylcholinesterase and amyloid-beta peptide change the biochemical properties of the enzyme and increase the neurotoxicity of Alzheimer's fibrils. *J Neurosci*, **18**, 3213-23.

Araki, M.; Fukada, Y.; Shichida, Y.; Yoshizawa, T. and Tokunaga, F. (1992) Differentiation of both rod and cone types of photoreceptors in the in vivo and in vitro developing pineal glands of the quail. *Brain Res Dev Brain Res*, **65**, 85-92.

Arendt, D.; Tessmar-Raible, K.; Snyman, H.; Dorresteijn, A.W. and Wittbrodt, J. (2004) Ciliary photoreceptors with a vertebrate-type opsin in an invertebrate brain. *Science*, **306**, 869-71.

Arpagaus, M.; Kott, M.; Vatsis, K.P.; Bartels, C.F.; La Du, B.N. and Lockridge, O. (1990) Structure of the gene for human butyrylcholinesterase. Evidence for a single copy. *Biochemistry*, **29**, 124-31.

Auld, V.J.; Fetter, R.D.; Broadie, K. and Goodman, C.S. (1995) Gliotactin, a novel transmembrane protein on peripheral glia, is required to form the blood-nerve barrier in Drosophila. *Cell*, **81**, 757-67.

Avidan, A.Y. (2005) Sleep in the geriatric patient population. *Semin Neurol*, **25**, 52-63.

Axelrod, J. and Daly, J. (1965) Pituitary gland: enzymic formation of methanol from S-adenosylmethionine. *Science*, **150**, 892-3.

Balasubramanian, A.S. and Bhanumathy, C.D. Noncholinergic functions of cholinesterases. (1993) *FASEB J*, **7**, 1354.

Barak, D.; Kronman, C.; Ordentlich, A.; Ariel, N.; Bromberg, A.; Marcus, D.; Lazar, A.; Velan, B. and Shafferman, A. (1994) Acetylcholinesterase peripheral anionic site degeneracy conferred by amino acid arrays sharing a common core. *J Biol Chem*, **269**, 6296-305.

Barnes, N.M. and Sharp, T. (1999) A review of central 5-HT receptors and their function. *Neuropharmacology*, **38**, 1083-152.

Bartels, C.F.; Jensen, F.S.; Lockridge, O.; van der Spek, A.F.; Rubinstein, H.M.; Lubrano, T. and La Du, B.N. (1992) DNA mutation associated with the human butyrylcholinesterase K-variant and its linkage to the atypical variant mutation and other polymorphic sites. *Am J Hum Genet*, **50**, 1086-103.

Barthalay, Y.; Hipeau-Jacquotte, R.; de la Escalera, S.; Jimenez, F. and Piovant, M. (1990) Drosophila neurotactin mediates heterophilic cell adhesion. *EMBO J*, **9**, 3603-9.

Baumgart, E.; Schad, A. and Grabenbauer M. (2001) *In situ* hybridization: general principles and application of digoxigenin-labeled cRNA for the detection of mRNAs. *In*: *Immunocytochemistry and In Situ Hybridization in the Biomedical Sciences.* Ed. Beesley JE., Boston, Birkhauser. p. 108-137.

Bechmann, I. and Nitsch, R. (2000) Involvement of non-neuronal cells in entorhinal-hippocampal reorganization following lesions. *Ann N Y Acad Sci,* **911**, 192-206.

Behra, M.; Cousin, X.; Bertrand, C.; Vonesch, J.L.; Biellmann, D.; Chatonnet, A. and Strahle, U. (2002) *Nat Neurosci*, **5**, 111-118.

Becker, E.B. and Bonni, A. (2004) Cell cycle regulation of neuronal apoptosis in development and disease. *Prog Neurobiol*, **72**, 1-25.

Berg J.M.; Tymoczko, J.L. and Stryer, L. (2002) *Biochemistry.* 5. ed, Freeman and Worth Publishing Group, Bedford.

Berman, H.A.; Yguerabide, J. and Taylor, P. (1980) Fluorescence energy transfer on acetylcholinesterase: spatial relationship between peripheral site and active center. *Biochemistry*, **19**, 2226-35.

Bernard, M.; Klein, D.C. and Zatz, M. (1997) Chick pineal clock regulates serotonin N-acetyltransferase mRNA rhythm in culture. *Proc Natl Acad Sci*, **94**, 304-9.

Bertrand, C.; Chatonnet, A.; Takke, C.; Yan, Y.L.; Postlethwait, J.; Toutant, J.P. and Cousin, X. (2001) Zebrafish acetylcholinesterase is encoded by a single gene localized on linkage group 7, Gene structure and polymorphism; molecular forms and expression pattern during development. *J Biol Chem*, **276**, 464-474.

Bigbee, J.W.; Sharma, K.V.; Gupta, J.J. and Dupree, J.L. (1999) Morphogenic role for acetylcholinesterase in axonal outgrowth during neural development. *Environ Health Perspect*, **107** Suppl 1:81-7.

Binkley S. (1983) Rhythms in ocular and pineal N-acetyltransferase: a portrait of an enzyme clock. *Comp Biochem Physiol A*, **75**, 123-9.

Bischoff, M.B. (1969) Photoreceptoral and secretory structures in the avian pineal organ. *J Ultrastruct Res*, **28**, 16-26.

Blackshaw, S. and Snyder, S.H. (1999) Encephalopsin: a novel mammalian extraretinal opsin discretely localized in the brain. *J Neurosci*, **19**, 3681-90.

Boopathy, R. and Balasubramanian, A.S. (1985) Chemical modification of the bifunctional human serum pseudocholinesterase. Effect on the pseudocholinesterase and aryl acylamidase activities. *Eur J Biochem,* **151**, 351-60.

Boopathy, R. and Layer, P.G. (2004) Aryl acylamidase activity on acetylcholinesterase is high during early chicken brain development. *Protein J*, **23**, 325-333.

Boya, J. and Zamorano, L. (1975) Ultrastructural study of the pineal gland of the chicken (Gallus gallus). *Acta Anat Basel*, **92**, 202-26.

Boya, J. and. Calvo, J.L. (1993) Immunohistochemical study of the pineal astrocytes in the postnatal development of the cat and dog pineal gland. *J Pineal Res*, **15**, 13-20.

Bradford, M. M. (1976) A rapid and sensitive method for the quantitation of microgram quantities of protein utilizing the principle of protein-dye binding. *Anal Biochem*, **72**, 248.

Brimijoin, S.; Mintz, K.P. and Alley, M.C. (1983) Production and characterization of separate monoclonal antibodies to human acetylcholinesterase and butyrylcholinesterase. *Mol Pharmacol*, **24**, 513-20.

Brimijoin, S. and Koenigsberger, C. (1999) *Environ Health Perspect,* **107** Suppl 1, 59-64.

Brownlee, K.A. (1960) *Statistical Theory and Methodology in Science and Engineering.* John Wiley and Sons, Inc., New York, p. 236.

Bullock, S.; Csillag, A. and Rose, S.P. (1987) Synaptic vesicle proteins and acetylcholine levels in chick forebrain nuclei are altered by passive avoidance training. *J Neurochem*, **49**, 812-20.

Buznikov, G.A.; Manukhin, B.N. and Podmarev, V.I. (1971) Effect of serotonin on activation of protein synthesis in sea urchin ovicells following fertilization. *Dokl Akad Nauk SSSR*, **200**, 1254-6.

Buznikov, G.A. (1991) The biogenic monoamines as regulators of early (pre-nervous) embryogenesis: new data. *Adv Exp Med Biol*, **296**, 33-48.

Buznikov, G.A.; Lambert, H.W. and Lauder, J.M. (2001) Serotonin and serotonin-like substances as regulators of early embryogenesis and morphogenesis. *Cell Tissue Res*, **305**, 177-86.

Bytyqi, A.H.; Lockridge, O.; Duysen, E.; Wang, Y.; Wolfrum, U. and Layer, P.G. (2004) Impaired formation of the inner retina in an AChE knockout mouse results in degeneration of all photoreceptors. *Eur J Neurosci*, **20**, 2953-62.

Cahill, G.M. (1996) Circadian regulation of melatonin production in cultured zebrafish pineal and retina. *Brain Res*, **708**, 177-81.

Cahill, G.M. (2002) Clock mechanisms in zebrafish. *Cell Tissue Res*, **309**, 27-34.

Calvo, J, Boya J. (1978) Embryonic development of the pineal gland of the chicken (Gallus gallus). *Acta Anat Basel,* **101**, 289-303.

Calvo, J. and Boya, J. (1981) Ultrastructural study of the embryonic development in the rat pineal gland. *Anat Rec*, **199**, 543-53.

Calvo, J.L.; Boya, J.; Borregón, A. and García-Mauriño, J.E. (1988) Presence of glial cells in the rat pineal gland: a light and electron microscopic immunohistochemical study. *Anatomical Record*, **220**, 4*24-28.*

Cameron, J. (1903) On the origin of the epiphysis cerebri as a bilateral structure in the chick. *Proc Roy Soc Edinburg*, **25**, 160-7.

Campbell, E. and Gibson, M.A. (1970) A histological and histochemical study of the development of the pineal gland in the chick, Gallus domesticus. *Can J Zool*, **48**, 1321-8.

Casarosa, S.; Andreazzoli, M.; Simeone, A. and Barsacchi, G. (1997) Xrx1, a novel Xenopus homeobox gene expressed during eye and pineal gland development. *Mech Dev*, **61**, 187-98.

Cassone, V.M. and Menaker, M. (1984) Is the avian circadian system a neuroendocrine loop? *J Exp Zool*, **232**, 539-49.

Celis, J.E. and Celis, A. (1985) Cell cycle-dependent variations in the distribution of the nuclear protein cyclin proliferating cell nuclear antigen in cultured cells: subdivision of S phase. *Proc Natl Acad Sci U S A*, **82**, 3262-6.

Cepko, C.L. (1996) The patterning and onset of opsin expression in vertebrate retinae. *Curr Opin Neurobiol*, **6**, 542-6.

Chatonnet, A. and Lockridge, O. (1989) Comparison of butyrylcholinesterase and acetylcholinesterase. *Biochem J*, **260**, 625-34.

Chaurasia, S.S.; Rollag, M.D.; Jiang, G.; Hayes, W.P.; Haque, R.; Natesan, A.; Zatz, M.; Tosini, G.; Liu, C.; Korf, H.W.; Iuvone, P.M. and Provencio, I. (2005) Molecular cloning, localization and circadian expression of chicken melanopsin (Opn4): differential regulation of expression in pineal and retinal cell types. *J Neurochem*, **92**, 158-70.

Checler, F.; Grassi, J. and Vincent, J.P. (1994) Cholinesterases display genuine arylacylamidase activity but are totally devoid of intrinsic peptidase activities. *J Neurochem*, **62**, 756-63.

Chen, C.M. and Cepko, C.L. (2002) The chicken RaxL gene plays a role in the initiation of photoreceptor differentiation. *Development*, **129**, 5363-75.

Chu, M.I.; Fontaine, P.; Kutty, K.M.; Murphy, D. and Redheendran, R. (1978) Cholinesterase in serum and low density lipoprotein of hyperlipidemic patients. *Clin Chim Acta*, **85**, 55-9.

Clarke, P.G. and Cowan, W.M. (1975) Ectopic neurons and aberrant connections during neural development. *Proc Nat Acad Sci U S A*, **72**, 4455-8.

Clarke, P.G. and Cowan, W.M. (1976) The development of the isthmo-optic tract in the chick, with special reference to the occurrence and correction of developmental errors in the location and connections of isthmo-optic neurons. *J Comp Neurol*, **167**, 143-64.

Colas, J.F.; Launay, J.M.; Kellermann, O.; Rosay, P. and Maroteaux, L. (1995) Drosophila 5-HT2 serotonin receptor: coexpression with fushi-tarazu during segmentation. *Proc Natl Acad Sci U S A*, **92**, 5441-5.

Coleman, B.A. and Taylor, P. (1996) Regulation of acetylcholinesterase expression during neuronal differentiation. *J Biol Chem*, **271**, 4410-6.

Cook, L.J.; Ho, L.W.; Wang, L.; Terrenoire, E.; Brayne, C.; Evans, J.G.; Xuereb, J.; Cairns, N.J.; Turic, D.; Hollingworth, P.; Moore, P.J.; Jehu, L.; Archer, N.; Walter, S.; Foy, C.; Edmondson, A.; Powell, J.; Lovestone, S.; Williams, J. and Rubinsztein, D.C. (2005) Candidate gene association studies of genes involved in neuronal cholinergic transmission in Alzheimer's disease suggests choline acetyltransferase as a candidate deserving further study. *Am J Med Genet B Neuropsychiatr Genet*, **132**, 5-8.

Copani, A.; Condorelli, F.; Caruso, A.; Vancheri, C.; Sala, A.; Giuffrida-Stella, A.M.; Canonico, P.L.; Nicoletti, F. and Sortino, M.A. (1999) Mitotic signaling by beta-amyloid causes neuronal death. *FASEB J,* **13**, 2225-34. Erratum in: (2000) *FASEB J*, **14**, 220.

Copani, A.; Sortino, M.A.; Caricasole, A.; Chiechio, S.; Chisari, M.; Battaglia, G.; Giuffrida-Stella, A.M.; Vancheri, C. and Nicoletti, F. (2002) Erratic expression of DNA polymerases by beta-amyloid causes neuronal death. *FASEB J*, **16**, 2006-8.

Costagli, C. and Galli, A. (1998) Inhibition of cholinesterase-associated aryl acylamidase activity by anticholinesterase agents: focus on drugs potentially effective in Alzheimer's disease. *Biochem Pharmacol*, **55**, 1733-7.

Cousin, X.; Hotelier, T.; Lievin, P.; Toutant, J.P. and Chatonnet, A. (1996) A cholinesterase genes server (ESTHER): a database of cholinesterase-related sequences for multiple alignments, phylogenetic relationships, mutations and structural data retrieval. *Nucleic Acids Res*, **24**, 132-6.

Cousin, X.; Hotelier, T.; Giles, K.; Lievin, P.; Toutant, J. and Chatonnet, A. (1997) The α/β fold family of proteins database and the cholinesterase gene server ESTHER. *Nucleic Acids Res*, **25**, 143-6.

Cox, K.H.; De Leon, D.V.; Angerer, L.M.; Angerer, R.C. (1984) Detection of mRNas in sea urchin embryos by *in situ* hybridization using asymmetric RNA probes. *Dev Biol*, **101**, 485-502.

Coyle, J.T.; Price, D.L.; DeLong, M.R. (1983) Alzheimer's disease: a disorder of cortical cholinergic innervation. *Science*, **219**, 1184-90.

Cryns, V. L. and Yuan, J. (1998) Proteases to die for. *Genes Dev*, **12**, 1551-1570.

Curtis, A.S. and Seehar, G.M. (1978) The control of cell division by tension or diffusion. *Nature*, **274**, 52-3.

Dale, H. H. (1914) The action of certain esters and ethers of choline, and their relation to muscarine. J. Pharmacol. *Exptl Therap*, **6**, 147-190.

Darvesh, S.; Walsh, R. and Martin, E. (2003) Enantiomer effects of huperzine A on the aryl acylamidase activity of human cholinesterases. *Cell Mol Neurobiol*, **23**, 93-100.

Davies, R.O.; Marton, A.V. and Kalow, W. (1960) The action of normal and atypical cholinesterase of human serum upon a series of esters of choline. *Can J Biochem Physiol*, **38**, 545-51.

Davis, K.L. and Yamamura, H.I. (1978) Related Cholinergic underactivity in human memory disorders. *Life Sci*, **23**, 1729-33.

De Ferrari, G. V., Mallender, W. D., Inestrosa, N. C., and Rosenberry, T. L. (2001) Thioflavin T is a fluorescent probe of the acetylcholinesterase peripheral site that reveals conformational interactions between the peripheral and acylation sites. *J Biol Chem*, **276**, 23282–23287.

Deguchi, T. (1981) Rhodopsin-like photosensitivity of isolated chicken pineal gland. *Nature*, **290**, 706-7.

Drews U. (1975) Cholinesterase in embryonic development. *Prog Histochem Cytochem*, **7**, 1-53.

Ellman, G.L.; Courtney, K.D., Andres, V. and Featherstone, R.M. (1961) A new and rapid colorimetric determination of acetylcholinesterase activity. *Biochem Pharmacol*, **7**, 88.

Engelhardt, G.; Wallnofer, P.R. and Plapp, R. (1971) Degradation of linuron and some other herbicides and fungicides by a linuron-inducible enzyme obtained from Bacillus sphaericus. *Appl Microbiol*, **22**, 284-8.

Feddersen, R.M.; Ehlenfeldt, R.; Yunis, W.S., Clark, H.B. and Orr, H.T. (1992) Disrupted cerebellar cortical development and progressive degeneration of Purkinje cells in SV40 T antigen transgenic mice. *Neuron*, **9**, 955-66.

Feng, G.; Krejci, E.; Molgo, J.; Cunningham, J.M.; Massoulie, J. and Sanes, J.R. (1999) Genetic analysis of collagen Q: roles in acetylcholinesterase and butyrylcholinesterase assembly and in synaptic structure and function. *J Cell Biol*, **144**, 1349-60.

Fontoura-da-Silva, S.E. and Chautard-Freire-Maia, E.A. (1996) Butyrylcholinesterase variants (BCHE and CHE2 Loci) associated with erythrocyte acetylcholinesterase inhibition in farmers exposed to pesticides. *Hum Hered*, **46**, 142-7.

Froede, H.C. and Wilson, I.B. (1970) On the subunit structure of acetylcholinesterase. *Isr J Med Sci*, **6**, 179-84.

Fujieda, H.; Sato, T.; Shi, J. and Wake, K. (1997) Remodeling of pineal epithelium in the fetal rat as delineated by immunohistochemistry of laminin and cadherin. *Cell Tissue Res*, **287**, 263-74.

Fujimoto D. (1974) Serotonin-sensitive aryl acylamidase in rat brain. *Biochem Biophys Res Commun*, **61**, 72-4.

Fujimoto D. (1976) Serotonin-sensitive aryl acylamidase activity of acetylcholinesterase. *FEBS Lett*, **72**, 121-3.

Fukada, Y. and Okano, T. (2002) Circadian clock system in the pineal gland. *Mol Neurobiol*, **25**, 19-30.

Gaughan, G.; Park, H.; Priddle, J.; Craig, I. and Craig, S. (1991) Refinement of the localization of human butyrylcholinesterase to chromosome 3q26.1-q26.2 using a PCR-derived probe. *Genomics*, **11**, 455-8.

Gennari, K.; Brunner, J. and Brodbeck U. (1987) Tetrameric detergent-soluble acetylcholinesterase from human caudate nucleus: subunit composition and number of active sites. *J Neurochem*, **49**, 12-8.

George, S.T. and Balasubramanian A.S. (1980) The identity of the serotonin-sensitive aryl acylamidase with acetylcholinesterase from human erythrocytes, sheep basal ganglia and electric eel. *Eur J Biochem*, **111**, 511-24.

George, S.T. and Balasubramanian, A.S. (1981) The aryl acylamidases and their relationship to cholinesterases in human serum, erythrocyte and liver. *Eur J Biochem*, **121**, 177.

Getman, D.K.; Eubanks, J.H.; Camp, S.; Evans, G.A. and Taylor, P. (1992) The human gene encoding acetylcholinesterase is located on the long arm of chromosome 7. *Am J Hum Genet*, **51**, 170-7.

Geula, C.; Mesulam, M.M. (1989) Cortical cholinergic fibers in aging and Alzheimer's disease: a morphometric study. *Neuroscience*, **33**, 469-81.

Gilboa-Garber, N.; Katz-Bergman, Y. and Pinsky A. (1978) Comparative study of the sensitivity of acetylcholinesterases and cholinesterases from animal and bacterial sources to inhibition by serotonin and its derivatives. *Experientia*, **34**, 992-3.

Gnatt, A.; Prody, C.A., Zamir, R.; Lieman-Hurwitz, J.; Zakut, H. and Soreq, H. (1990) Expression of alternatively terminated unusual human butyrylcholinesterase messenger RNA transcripts, mapping to chromosome 3q26-ter, in nervous system tumors. *Cancer Res*, **50**, 1983-7.

Goldman, A.I. (1982) The sensitivity of rat rod outer segment disc shedding to light. *Invest Ophthalmol Vis Sci*, **22**, 695-700.

Gomez-Ramos, P.; Bouras, C. and Moran, M.A. (1994) Ultrastructural localization of butyrylcholinesterase on neurofibrillary degeneration sites in the brains of aged and Alzheimer's disease patients. *Brain Res*, **640**, 17-24.

Grauso, M.; Culetto, E.; Combes, D.; Fedon, Y.; Toutant, J.P. and Arpagaus, M. (1998) Existence of four acetylcholinesterase genes in the nematodes Caenorhabditis elegans and Caenorhabditis briggsae. *FEBS Lett*, **424**, 279-84.

Graybiel, A.M. and Ragsdale, C.W. (1982) Pseudocholinesterase staining in the primary visual pathway of the macaque monkey. *Nature*, **299**, 439-442.

Greenberg, C.P.; Primo-Parmo, S.L.; Pantuck, E.J. and La Du, B.N. (1995) Prolonged response to succinylcholine: a new variant of plasma cholinesterase that is identified as normal by traditional phenotyping methods. *Anesth Analg*, **81**, 419-21.

Grisaru, D.; Sternfeld, M.; Eldor, A.; Glick, D. and Soreq, H. (1999) Structural roles of acetylcholinesterase variants in biology and pathology. *Eur J Biochem*, **264**, 672-86.

Goy, M.F.; Schwarz, T.L. and Kravitz, J.E. (1984) Serotonin-induced protein phosphorylation in a lobster neuromuscular preparation. *J Neurosc*, **4**, 611-626.

Gwinner, E. and Brandstatter, R. (2001) Complex bird clocks. *Philos Trans R Soc Lond B Biol Sci*, **356**, 1801-10.

Hada, T.; Muratani, K.; Ohue, T.; Imanishi, H.; Moriwaki, Y.; Itoh, M.; Amuro, Y. and Higashino, K. (1992) A variant serum cholinesterase and a confirmed point mutation at Gly-365 to Arg found in a patient with liver cirrhosis. *Intern Med*, **31**, 357-62.

Hall, J.C. Alahiotis SN, Strumpf DA, White K. (1980) Behavioral and biochemical defects in temperature-sensitive acetylcholinesterase mutants of Drosophila melanogaster. *Genetics*, **96**, 939-65.

Hall, P.A.; Levison, D.A.; Woods, A.L.; Yu, C.C.; Kellock, D.B.; Watkins, J.A.; Barnes, D.M.; Gillett, C.E.; Camplejohn, R; Dover, R.; *et al.* (1990) Proliferating cell nuclear antigen (PCNA) immunolocalization in paraffin sections: an index of cell proliferation with evidence of deregulated expression in some neoplasms. *J Pathol*, **62**, 285.

References

Hall, Z.W. (1973) Multiple forms of acetylcholinesterase and their distribution in endplate and non-endplate regions of rat diaphragm muscle. *J Neurobiol*, **4**, 343-61.

Hamm, H.E. and Menaker, M. (1980) Retinal rhythms in chicks: circadian variation in melantonin and serotonin N-acetyltransferase activity. *Proc Natl Acad Sci U S A*, **77**, 4998-5002.

Hamburger, V. and Hamilton, H. L. (1951) A series of normal stages in the development of the chickembryos. *J Morphol*, **88**, 49-22.

Hanneman, E.H. (1992) Diisopropylfluorophosphate inhibits acetylcholinesterase activity and disrupts somitogenesis in the zebrafish. *J Exp Zool*, **263**, 41-53.

Harel, M.; Sussman, J.L.; Krejci, E.; Bon, S.; Chanal, P.; Massoulie, J. and Silman, I. (1992) Conversion of acetylcholinesterase to butyrylcholinesterase: modeling and mutagenesis. *Proc Natl Acad Sci U S A*, **89**, 10827-31.

Hatten, M.E. (1990) Riding the glial monorail: a common mechanism for glial-guided neuronal migration in different regions of the developing mammalian brain. *Trends Neurosci*, **13**, 179-84.

Henderson, Z. and Greenfield, S.A. (1984) Ultrastructural localization of acetylcholinesterase in substantia nigra: a comparison between rat and guinea pig. *J Comp Neurol*, **230**, 278-86.

Hidaka, K.; Iuchi, I.; Yamasaki, T.; Ohhara, M.; Shoda, T.; Primo-Parmo, S. and Ladu, B.N. (1992) Identification of two different genetic mutation associated with silent phenotypes for human serum cholinesterase in Japanese. *Rinsho Byori*, **40**, 535-40.

Hill, C. (1900) Two epiphyses in a four day chick. Bull. Northwestern Uni. Med. School Chicago, **2**, 238-241.

Hinman, D.J. and Szeto, H.H. (1988) Cholinergic influences on sleep-wake patterns and breathing movements in the fetus. *J Pharmacol Exp Ther*, **247**, 372-8.

Hirunagi, K.; Ebihara, S; Okano, T.; Takanaka, Y. and Fukada, Y. (1997) Immunoelectron-microscopic investigation of the subcellular localization of pinopsin in the pineal organ of the chicken. *Cell Tissue Res*, **289**, 235-41.

Hoagland, R.E. and Graf, G. (1971) Nitroacetanilides as chromogenic substrates for assaying de-acetylating activity: the isolation and partial purification of aryl acylamidases from erepsin and tulip. *Enzymologia*, **41**: 313.

Hsiung, K.P.; Kuan, S.S. and Guilbault, G.G. (1975) An inducible amidase from Pseudomonas striata. *Biochem Biophys Res Commun*, **66**, 1225-30.

Hu Y, Ding L, Spencer DM, Nunez G. (1998) WD-40 repeat region regulates Apaf-1 self-association and procaspase-9 activation. *J Biol Chem*, **273**, 33489-94.

Hutchins, J.B. (1987) Acetylcholine as a neurotransmitter in the vertebrate retina. *Exp Eye Res*, **45**, 1-38.

Ichtchenko, K.; Hata, Y.; Nguyen, T.; Ullrich, B.; Missler, M.; Moomaw, C. and Sudhof, T.C. (1995) Neuroligin 1: a splice site-specific ligand for beta-neurexins. *Cell*, **81**, 435-43.

Inestrosa, N.C.; Roberts, W.L.; Marshall, T.L. and Rosenberry, T.L. (1987) Acetylcholinesterase from bovine caudate nucleus is attached to membranes by a novel subunit distinct from those of acetylcholinesterases in other tissues. J Biol Chem, **262**, 4441-4.

Ingber, D.E.; Dike, L.; Hansen, L.; Karp, S.; Liley, H.; Maniotis, A.; McNamee, H.; Mooney, D.; Plopper, G.; Sims, J. *et al.* (1994) Cellular tensegrity: exploring how mechanical changes in the cytoskeleton regulate cell growth, migration, and tissue pattern during morphogenesis. *Int Rev Cytol*, **150**, 173-224.

Iuvone, P.M.; Brown, A.D.; Haque, R; Weller, J.; Zawilska, J.B.; Chaurasia, S.S.; Ma, M. and Klein, D.C. (2002) Retinal melatonin production: role of proteasomal proteolysis in circadian and photic control of arylalkylamine N-acetyltransferase. *Invest Ophthalmol Vis Sci*, **43**, 564-72.

Javier, A.F.; Bata-Csorgo, Z.; Ellis, C.N.; Kang, S.; Voorhes, J.J. and Cooper, K.D. (1997) Rapamycin (Sirolimus) Inhibits Proliferating Cell Nuclear Antigen Expression and Blocks Cell cycle in the G1 Phase in Human Keratinocyte *Stem Cells. J Clin Invest*, **99**, 2094–2099.

Jayanthi, L.D. and Balasubramanian, A.S. (1992) Isolation of a tripeptide (Ala-Gly-Ser) exhibiting weak acetylthiocholine hydrolyzing activity from a high-salt soluble form of monkey diaphragm acetylcholinesterase. Neurochem Res, **17,** 351-9.

Jensen, F.S.; Bartels, C.F.; La Du, B.N. (1992) Structural basis of the butyrylcholinesterase H-variant segregating in two Danish families. *Pharmacogenetics*, **2**, 234-40.

Jin, Q.H.; He, H.Y.; Shi, Y.F.; Lu, H. and Zhang, X.J. (2004) Overexpression of acetylcholinesterase inhibited cell proliferation and promoted apoptosis in NRK cells. *Acta Pharmacol Sin*, **25**, 1013-21.

Jones, S.A.; Dickie, B.G.; Klegeris, A. and Greenfield, S.A. (1994) The subthalamo-nigral pathway regulates movement and concomitant acetylcholinesterase release from the substantia nigra. *J Neural Transm Gen Sect*, **98**, 23-37.

Kane, D.A. and Kimmel, C.B. (1993) The zebrafish midblastula transition. *Development*, **119**, 447-56.

Kane, D.A.; Hammerschmidt, M.; Mullins, M.C.; Maischein, H.M.; Brand, M.; van Eeden, F.J.; Furutani-Seiki, M.; Granato, M.; Haffter, P., Heisenberg, C.P.; Jiang, Y.J.; Kelsh. R.N.; Odenthal, J.; Warga, R.M. and Nusslein-Volhard, C. (1996) The zebrafish epiboly mutants. *Development*, **123**, 47-55.

Karnovsky, M.J. and Roots, L. (1964) A direct-coloring thiocholine method for cholinesterases. *J Histochem Cytochem*, **12**, 219-21.

Keilhauer, G.; Meier, D.H.; Kuhlman; n-Krieg, S.; Nieke, J. and Schachner, M. (1985) Astrocytes support incomplete differentiation of an oligodendrocyte precursor cell. *EMBO J*, **4**, 2499-504.

King, K.L. and Cidlowski, J.A. (1995) Cell cycle and apoptosis: common pathways to life and death. *J Cell Biochem*, **58**, 175-80.

Klein, D.C. (2004) The Aschoff/Pittendrigh lecture: Theory of the origin of the pineal gland – a tale of conflict and resolution. *J Biol Rhythms*, **19**, 264-279.

Koenigsberger, C.; Chiappa, S. and Brimijoin, S. (1997) Neurite differentiation is modulated in neuroblastoma cells engineered for altered acetylcholinesterase expression. *J Neurochem*, **69**, 1389-97.

Korf, H.W. (1994) The pineal organ as a component of the biological clock. Phylogenetic and ontogenetic considerations. *Ann N Y Acad Sci*, **719**, 13-42.

Kostovic, I. and Goldman-Rakic, P.S. (1983) Transient cholinesterase staining in the mediodorsal nucleus of the thalamus and its connections in the developing human and monkey brain. *J Comp Neurol*, **219**, 431-447.

Kutty, K.M. (1980) Biological function of cholinesterase. *Clin Biochem*, **13**, 239-43.

Laemmli, U.K. (1970) Cleavage of structural proteins during the assembly of the head of bacteriophage T4. Nature, **227**, 680-5.

LaMotta, R.V.; Woronick, C.L. (1971) Molecular heterogeneity of human serum cholinesterase. *Clin Chem*, **17**, 135-44.

Lapidot-Lifson, Y.; Patinkin, D.; Prody, C.A.; Ehrlich, G.; Seidman, S.; Ben-Aziz, R.; Benseler, F.; Eckstein, F.; Zakut, H. and Soreq, H. (1992) Cloning and antisense oligodeoxynucleotide inhibition of a human homolog of cdc2 required in hematopoiesis. *Proc Natl Acad Sci U S A*, **89**, 579-83.

Layer, P.G. (1983) Comparative localization of acetylcholinesterase and pseudocholinesterase during morphogenesis of the chicken brain. *Proc Natl Acad Sci U S A*, **80**, 6413-7.

Layer, P.G. and Sporns, O. (1987) Spatiotemporal relationship of embryonic cholinesterases with cell proliferation in chicken brain and eye. *Proc Natl Acad Sci U S A*, **84**, 284-288.

Layer, P.G.; Alber, R. and Rathjen, F.G. (1988) Sequential activation of butyrylcholinesterase in rostral half somites and acetylcholinesterase in motoneurones and myotomes preceding growth of motor axons. *Development*, **102**, 387-96.

Layer, P.G. (1990) Cholinesterases preceding major tracts in vertebrate neurogenesis. *BioEssays*, **12**, 415-420.

Layer, P.G. and Alber, R. (1990) Patterning of chick brain vesicles as revealed by peanut agglutinin and cholinesterases. *Development*, **109**, 613-24.

Layer, P.G. (1991) Cholinesterases during development of the avian nervous system. *Cell Mol Neurobiol*, **11**, 7-33.

Layer, P.G. and Kaulich, S. (1991) Cranial nerve growth in birds is preceded by cholinesterase expression during neural crest cell migration and the formation of an HNK-1 scaffold. *Cell Tissue Res*, **265**, 393-407.

Layer, P.G.; Weikert, T. and Alber, R. (1993) Cholinesterases regulate neurite growth of chick nerve cells *in vitro* by means of a non-enzymatic mechanism. *Cell Tissue Res*, **273**, 219-26.

Layer, P.G. and Willbold, E. (1994) Cholinesterases in avian neurogenesis. *Intl Rev Cytol*, **151**,139-181.

Layer, P.G. and Willbold, E. (1995) Novel functions of cholinesterases in development, physiology and disease. *Prog Histochem Cytochem*, **29**, 1-94.

Layer, P.G.; Rothermel, A.; Hering, H.; Wolf, B.; deGrip, W.J.; Hicks, D. and Willbold, E. (1997a) Pigmented epithelium sustains cell proliferation and decreases expression of opsins and acetylcholinesterase in reaggregated chicken retinospheroids. *Eur J Neurosci*, **9**, 1795-803.

Layer, P.G.; Berger, J. and Kinkl, N. (1997b) Cholinesterases precede "ON-OFF" channel dichotomy in the embryonic chick retina before onset of synaptogenesis. *Cell Tissue Res*, **288**, 407-16.

Lewandowski, M.H. (1986) Seasonal variations in the circadian activity of acetylcholinesterase (AChE, EC 3.1.1.7) in the brain stem reticular formation of the mouse in constant darkness. *Folia Biol Krakow*, **34**, 187-98.

Lev-Lehman, E.; Deutsch, V.; Eldor, A. and Soreq, H. (1997) Immature human megakaryocytes produce nuclear-associated acetylcholinesterase. *Blood*, **89**, 3644-53.

Lawrence, S.H. and Melnick, P.J. (1961) Enzymatic activity related to human serum beta-lipoprotein: histochemical, immunoelectrophoretic and quantitative studies. *Proc Soc Exp Biol Med*, **107**, 998-1001.

Li, B.; Stribley, J.A.; Ticu, A.; Xie, W.; Schopfer, L.M.; Hammond, P.; Brimijoin, S.; Hinrichs, S.H. and Lockridge, O. (2000) Abundant tissue butyrylcholinesterase and its possible function in the acetylcholinesterase knockout mouse. *J Neurochem*, **75**, 1320-31.

Li, H. and Yuan, J. (1999) Deciphering the pathways of life and death. *Curr Opin Cell Biol*, **11**, 261-6.

Liu, R.; Denovan-Wright, E.M. and Wright, J.M. (2003). Structure, mRNA expression and linkage mapping of the brain-type fatty acid-binding protein gene (FABP7) from zebrafish (Danio rerio). *Eur J Biochem*, **270**, 715-725.

Loewi, O. and Navratil, E. (1926) Über humorale Übertragbarkeit der Herznervenwirkung. *Pflügers Arch*, **214**, 689-696.

Lopez-Muñoz, F.; Boya, J.; Calvo, J.L. and F. (1992) Marin Immunohistochemical localization of glial fibrillary acidic protein (GFAP) in rat pineal stalk astrocytes. *Histol Histopathol*, *7, 643-646.*

MacFarlane, M. and Williams, A.C. (2004) Apoptosis and disease: a life or death decision. *EMBO Rep*, **5**, 674-8.

Maekawa, M.; Sudo, K.; Kanno, T.; Kotani, K.; Dey, D.C.; Ishikawa, J.; Izumi, M. and Etoh, K. (1995) Genetic basis of the silent phenotype of serum butyrylcholinesterase in three compound heterozygotes. *Clin Chim Acta*, **235**, 41-57.

Maekawa, M.; Sudo, K.; Dey, D.C.; Ishikawa, J.; Izumi, M.; Kotani, K. and Kanno, T. (1997) Genetic mutations of butyrylcholine esterase identified from phenotypic abnormalities in Japan. *Clin Chem*, **43**, 924-9.

Majumdar, R. and Balasubramanian, A.S. (1982) Essential and non-essential phosphatidylinositol residues in acetylcholinesterase and arylacylamidase of sheep basal ganglia. *FEBS Lett*, **146**, 335-8.

Majumdar, R.; George, S.T. and Balasubramanian, A.S. (1982) Serotonin-sensitive aryl acylamidase activity of platelet acetylcholinesterase. *Biochem Pharmacol*, **31**, 2319-25.

Majumdar, R. and Balasubramanian, A.S. (1984) Chemical modification of acetylcholinesterase from eel and basal ganglia: effect on the acetylcholinesterase and aryl acylamidase activities. *Biochemistry*, **23**, 4088-93.

Marieb, E.N. (2001). *Human anatomy and physiology* (5th ed.). San Francisco: Benjamin Cummings.

Martin, D.P.; Schmidt, R.E.; DiStefano, P.S.; Lowry, O.H.; Carter, J.G. and Johnson, Jr. E.M. (1988) Inhibitors of protein synthesis and RNA synthesis prevent neuronal death caused by nerve growth factor deprivation. *J Cell Biol*, **106**, 829-844.

Masson, P. (1979) Multiple molecular forms of human plasma butyrylcholinesterase. I. Apparent molecular parameters and broad pattern of the quaternary structure. *Biochim Biophys Acta*, **578**, 493-504.

Masson, P.; Froment, M.T.; Bartels, C.F. and Lockridge, O. (1996) Asp7O in the peripheral anionic site of human butyrylcholinesterase. *Eur J Biochem*, **235**, 36-48.

Masson, P.; Legrand, P.; Bartels, C.F.; Froment, M.T.; Schopfer, L.M. and Lockridge, O. (1997) Biochemistry **36**, 2266–2277.

Massoulie, J. and Bon, S. (1982) The molecular forms of cholinesterase and acetylcholinesterase in vertebrates. *Annu Rev Neurosci*, **5**, 57-106.

Massoulie, J.; Sussman, J.; Bon, S. and Silman I. (1993a) Structure and functions of acetylcholinesterase and butyrylcholinesterase. *Prog Brain Res*, **98**, 139-46.

Massoulié, J.; Pezzementi, L.; Bon, S.; Krejci, E. and Vallette, F-M. (1993b) Molecular and cellular biology of cholinesterases. *Prog Neurobiol*, **41**, 31-91.

Massoulie, J.; Anselmet, A.; Bon, S.; Krejci, E.; Legay, C.; Morel, N. and Simon, S. (1998) Acetylcholinesterase: C-terminal domains, molecular forms and functional localization. *J Physiol Paris J*, **92**, 183-90.

Massoulié, J. (2002) The Origin of the Molecular Diversity and Functional Anchoring of Cholinesterases Neurosignals, **11**, 130-143.

Mattock, H.; Lane, D.P. and Warbrick, E. (2001) Inhibition of cell proliferation by the PCNA-binding region of p21 expressed as a GFP miniprotein. *Exp Cell Res*, **265**, 234-41.

McClellan, J.S.; Coblentz, W.B.; Sapp, M.; Rulewicz, G.; Gaines, D.I.; Hawkins, A.; Ozment, C.; Bearden, A.; Merritt, S.; Cunningham, J.; Palmer, E.; Contractor, A. and Pezzementi, L. (1998) cDNA cloning, in vitro expression, and biochemical characterization of cholinesterase 1 and cholinesterase 2 from amphioxus--comparison with cholinesterase 1 and cholinesterase 2 produced in vivo. *Eur J Biochem*, **258**, 419-29.

McGuire, M.C.; Nogueira, C.P.; Bartels, C.F.; Lightstone, H.; Hajra, A.; Van der Spek, A.F.; Lockridge, O. and La Du, B.N. (1989) Identification of the structural mutation responsible for the dibucaine-resistant (atypical) variant form of human serum cholinesterase. *Proc Natl Acad Sci U S A*, **86**, 953-7.

McTiernan, C.; Adkins, S.; Chatonnet, A., Vaughan, T.A.; Bartels, C.F.; Kott, M.; Rosenberry, T.L.; La Du, B.N. and Lockridge, O. (1987) Brain cDNA clone for human cholinesterase. *Proc Natl Acad Sci U S A*, **84**, 16682-6.

Meakin, R. (1973) The third eye. *Univ of California Press*.

Mehta, H.; Haobam, R.; Usha, R. and Mohanakumar, K.P. (2005) Evidence for the involvement of central serotonergic mechanisms in cholinergic tremor induced by tacrine in Balb/c mice. *Behav Brain Res*, **163**, 227-36.

Meneses, A. (1998) Physiological, pathophysiological and therapeutic roles of 5-HT systems in learning and memory. *Rev Neurosci*, **9**, 275-89.

Meneses, A. (2004) Effects of the 5-HT7 receptor antagonists SB-269970 and DR 4004 in autoshaping Pavlovian/instrumental learning task. *Behav Brain Res*, **155**, 275-82.

Miki, A. and Mizoguti, H. (1982) Acetylcholinesterase activity in the myotome of the early chick embryo. *Cell Tissue Res*, **227**, 23-40.

Millard, C.B.; Lockridge, O. and Broomfield, C.A. (1998) Organophosphorus acid anhydride hydrolase activity in human butyrylcholinesterase: synergy results in a somanase. *Biochemistry*, **37**, 237-47.

Minic, J.; Chatonnet, A.; Krejci, E. and Molgo, J. (2003) Butyrylcholinesterase and acetylcholinesterase activity and quantal transmitter release at normal and acetylcholinesterase knockout mouse neuromuscular junctions. *Br J Pharmacol*, **138**, 177-87.

Mishima, K.; Tozawa, T.; Satoh, K.; Matsumoto, Y.; Hishikawa, Y. and Okawa, M. (1999) Melatonin secretion rhythm disorders in patients with senile dementia of Alzheimer's type with disturbed sleep-waking. *Biol Psychiatry*, **45**, 417-21.

Mohan, C. and Radha, E. (1974) Circadian rhythm in acetylcholinesterase activity during aging of the central nervous system. *Life Sci*, **15**, 231-7.

Moser, V.C. and Padilla, S. (1998) Age- and gender-related differences in the time course of behavioral and biochemical effects produced by oral chlorpyrifos in rats. *Toxicol Appl Pharmacol*, **149**, 107-109.

Muensch, H.; Goedde, H.W. and Yoshida, A. (1976) Human-serum cholinesterase subunits and number of active sites of the major component. *Eur J Biochem*, **70**, 217-23.

Muratani, K.; Hada, T.; Yamamoto, Y.; Kaneko, T.; Shigeto, Y.; Ohue, T.; Furuyama, J. and Higashino, K. (1991) Inactivation of the cholinesterase gene by Alu insertion: possible mechanism for human gene transposition. *Proc Natl Acad Sci U S A*, **88**, 11315-9.

Nachon, F.; Ehret-Sabatier, L.; Loew, D.; Colas, C.; van Dorsselaer, A. and Goeldner, M. (1998) Trp82 and Tyr332 are involved in two quaternary ammonium binding domains of human butyrylcholinesterase as revealed by photoaffinity labeling with [3H]DDF. *Biochemistry*, **37**, 10507–10513.

Nakahara, K.; Murakami, N.; Nasu, T.; Kuroda, H. and Murakami T. (1997) Individual pineal cells in chick possess photoreceptive, circadian clock and melatonin-synthesizing capacities *in vitro*. *Brain Res*, **774**, 242-5.

Nicolet, Y.; Lockridge, O.; Masson, P.; Fontecilla-Camps, J.C. and Nachon, F. (2003) Crystal Structure of Human Butyrylcholinesterase and of Its Complexes with Substrate and Products. *J Biol Chem*, **278**, 41141-7.

Nogueira, C.P.; Bartels, C.F.; McGuire, M.C.; Adkins, S.; Lubrano, T.; Rubinstein, H.M.; Lightstone, H.; Van der Spek, A.F.; Lockridge, O. and La Du, B.N. (1992) Identification of two different point mutations associated with the fluoride-resistant phenotype for human butyrylcholinesterase. *Am J Hum Genet*, **51**, 821-8.

Ohshima, K. and Matsuo, S. (1988) Cytodifferentiation of the chick pineal gland, with special reference to the photosensory and secretory elements. *J Pineal Res*, **5**, 397-410.

Okano, T.; Yoshizawa, T. and Fukada, Y. (1994) Pinopsin is a chicken pineal photoreceptive molecule. *Nature*, **372**, 94-7.

Okano, T.; Takanaka, Y.; Nakamura, A.; Hirunagi, K.; Adachi, A.; Ebihara, S. and Fukada, Y. (1997) Immunocytochemical identification of pinopsin in pineal glands of chicken and pigeon. *Brain Res Mol Brain Res*, **50**, 190-6.

Okano, T. and Fukada, Y. (2000) Photoreceptors in pineal gland and brain: cloning, localization, and overexpression. *Methods Enzymol*, **316**, 278-91.

Okano, T. and Fukada, Y. (2001) Photoreception and circadian clock system of the chicken pineal gland. *Microsc Res Tech*, **53**, 72-80.

Oksche, A. and Vaupel-von Harnack, M. (1965) On the structure of the rudimentary sense cell of the pineal body of the chicken. *Naturwissenschaften*, **52**, 662-3.

Omura, Y. (1977) Ultrastructural study of embryonic and post-hatching development in the pineal organ of the chicken (brown leghorn, gallus demosticus). *Cell Tissue Res*, **183**, 255-71.

Oommen, A. and Balasubramanian, A.S. (1977) The inhibition of brain aryl acylamidase by 5-hydroxytryptamine and acetylcholine. *Biochem Pharmacol*, **26**, 2163-7.

Oommen, A. and Balasubramanian, A.S. (1978) Aryl acylamidase of monkey brain and liver: response to inhibitors and relationship to acetylcholinesterase. *Biochem Pharmacol*, **27**, 891-5.

Oommen, A. and Balasubramanian, A.S. (1979) The association of the serotonin-sensitive aryl acylamidase with acetylcholinesterase in the monkey brain. *Eur J Biochem*, **94**, 135-43.

Oommen, A.; George, S.T. and Balasubramanian, A.S. (1980) Phenacetin-N-deacetylase and its non-identity with the serotonin sensitive aryl acylamidase of brain. *Life Sci*, **26**, 2129-36.

Oppenheim, R.W. (1991) Cell death during development of the nervous system. *Annu Rev Neurosci*, **14**, 453-501.

Ordentlich, A.; Barak, D.; Kronman, C.; Flashner, Y.; Leitner, M.; Segall, Y.; Ariel, N.; Cohen, S.; Velan, B. and Shafferman, A. (1993) Dissection of the human acetylcholinesterase active center determinants of substrate specificity. Identification of residues constituting the anionic site, the hydrophobic site, and the acyl pocket. *Biol Chem*, **268**, 17083-95.

Pan, S.Y. (1991) Circadian changes of acetylcholine, choline acetyltransferase, acetylcholinesterase and muscarinic receptors in mouse brain. *Zhongguo Yao Li Xue Bao*, **12**, 148-51.

Park, S.E.; Kim, N.D. and Yoo, Y.H. (2004) Acetylcholinesterase plays a pivotal role in apoptosome formation. *Cancer Res*, **64**, 2652-5. Erratum in: (2004) *Cancer Res*, **64**, 9230.

Patinkin, D.; Seidman, S.; Eckstein, F.; Benseler, F.; Zakut, H. and Soreq, H. (1990) Manipulations of cholinesterase gene expression modulate murine megakaryocytopoiesis *in vitro*. *Mol Cell Biol*, **10**, 6046-50.

Perrier, A.L.; Massoulie, J. and Krejci, E. (2002) PRiMA: the membrane anchor of acetylcholinesterase in the brain. *Neuron*, **33**, 275-85.

Perry, E.K.; Perry, R.H.; Blessed, G. and Tomlinson, B.E. (1978) Changes in brain cholinesterases in senile dementia of Alzheimer type. *Neuropathol Appl Neurobiol*, **4**, 273-7.

Pfrieger, F.W. (2002) Role of glia in synapse development. *Curr Opin Neurobiol*, **12**, 486-90.

Primo-Parmo, S.L.; Bartels, C.F.; Wiersema, B.; van der Spek, A.F.; Innis, J.W.; La Du, B.N. (1996) Characterization of 12 silent alleles of the human butyrylcholinesterase (BCHE) gene. *Am J Hum Genet*, **58**, 52-64.

Prody, C.A.; Zevin-Sonkin, D.; Gnatt, A.; Goldberg, O. and Soreq H. (1987) Isolation and characterization of full-length cDNA clones coding for cholinesterase from fetal human tissues. *Proc Natl Acad Sci U S A*, **84**, 3555-9.

Quay, W.B.; Bennett, E.L.; Morimoto, H. and Hebert, M. (1971) Evidence for the absence of 24-hour rhythms in cholinesterase activities of brain regions. *Comp Gen Pharmacol*, **2**, 402-10.

Quay, W.B. (1974) Pineal canaliculi: demonstration, twenty-four-hour rhythmicity and experimental modification. *Am J Anat*, **139**, 81-93.

Quinn, D.M. (1987) Acetylcholinesterase - enzyme structure, reaction dynamics, and virtual transition-states. *Chem Rev*, **87**, 955–979.

Rachinsky, T.L.; Camp, S.; Li, Y.; Ekstrom, T.J.; Newton, M. and Taylor, P. (1990) Molecular cloning of mouse acetylcholinesterase: tissue distribution of alternatively spliced mRNA species. *Neuron*, **5**, 317-327.

Radic, Z.; Pickering, N.A.; Vellom, D.C.; Camp, S. and Taylor, P. (1993) Three distinct domains in the cholinesterase molecule confer selectivity for acetyl- and butyrylcholinesterase inhibitors. *Biochemistry*, **32**, 12074-84.

Rausch, J.L.; Janowsky, D.S.; Risch, S.C. and Huey, L.Y. (1985) Physostigmine effects on serotonin uptake in human blood platelets. *Eur J Pharmacol*, **109**, 91-6.

Raygani, A.V.; Zahrai, M.; Soltanzadeh, A.; Doosti, M.; Javadi, E. and Pourmotabbed, T. (2004) Analysis of association between butyrylcholinesterase K variant and apolipoprotein E genotypes in Alzheimer's disease. *Neurosci Lett*, **371**, 142-6.

Redecker, P. (1998) Developmental pattern of cell type-specific calretinin immunoreactivity in the postnatal gerbil pineal gland. *Brain Res Dev Brain Res*, **105**, 43-50.

Rees, T.M.; Brimijoin, S. (2003) The role of acetylcholinesterase in the pathogenesis of Alzheimer's disease. *Drugs Today Barc*, **39**, 75-83.

Robitzki, A.; Mack, A.; Chatonnet, A. and Layer, P.G. (1997) Transfection of reaggregating embryonic chicken retinal cells with an antisense 5'-DNA butyrylcholinesterase expression vector inhibits proliferation and alters morphogenesis. *J Neurochem*, **69**, 823-33.

Robitzki, A.; Mack, A.; Hoppe, U.; Chatonnet, A. and Layer, P.G. (1998) Butyrylcholinesterase antisense transfection increases apoptosis in differentiating retinal reaggregates of the chick embryo. *J Neurochem*, **71,** 413-20.

Romanoff, A.L. (1939). *From the Egg to the Chick.* Cornell Rural School Leaflet, V 1, p. 57-63.

Rotundo, R.L.; Thomas, K.; Porter-Jordan, K.; Benson, R.J.; Fernandez-Valle, C. and Fine, R.E. (1989) Intracellular transport, sorting, and turnover of acetylcholinesterase. Evidence for an endoglycosidase H-sensitive form in Golgi apparatus, sarcoplasmic reticulum, and clathrin-coated vesicles and its rapid degradation by a non-lysosomal mechanism. *J Biol Chem*, **264**, 3146-52.

Ryhanen, R.J.; Jauhianen, M.S.; Laitinen, M.V. and Puhakainen, E.V. (1982) The relationships between human serum pseudocholinesterase, lipoproteins, and apolipoproteins (APOHDL). *Biochem Med*, **28**, 241-5.

Sato, T. and Wake, K. (1983) Innervation of the avian pineal organ. A comparative study. *Cell Tissue Res*, **233**, 237-64.

Sato, T. and Wake, K. (1984) Regressive post-hatching development of acetylcholinesterase-positive neurons in the pineal organs of Coturnix coturnix japonica and Gallus gallus. *Cell Tissue Res*, **237**, 269-75.

Sato, T.; Ebisawa, S. and Wake, K. (1988) Neuronal degeneration in the pineal ganglion during the post-hatching development of the domestic fowl. *Cell Tissue Res*, **254**, 25-30.

Sato, T. (2001) Sensory and endocrine characteristics of the avian pineal organ. *Microsc Res Tech*, **53**, 2-11.

Schachner, M.; Sommer, I. and Lagenaur, C. (1984) Expression of glial antigens C1 and M1 in the peripheral nervous system during development and regeneration. *Brain Res*, **316**, 165-78.

Schiebeler, H. and von Mayersbach, H. (1974) Circadian variations of acetylcholine esterase (E.C.3.1.1.7) in rat brains. *Int J Chronobiol*, **2**, 281-9.

Schulte-Merker, S.; Ho, R.K.; Herrmann, B.G. and Nusslein-Volhard, C. (1992) The protein product of the zebrafish homologue of the mouse T gene is expressed in nuclei of the germ ring and the notochord of the early embryo. *Development*, **116**, 1021-32.

Schumacher, M.; Camp, S.; Maulet, Y.; Newton, M.; McPhee-Quigley, K.; Taylor, S.S.; Friedmann, T. and Taylor, P. (1986) Primary structure of Torpedo californica acetylcholinesterase deduced from cDNA sequence. *Nature*, **319**, 409-409.

Schwarz, M.; Glick, D.; Loewenstein, Y. and Soreq, H. (1995) Engineering of human cholinesterases explains and predicts diverse consequences of administration of various drugs and poisons. *Pharmacol Ther*, **67**, 283-322.

Shafferman, A.; Kronman, C.; Flashner, Y.; Leitner, M.; Grosfeld, H.; Ordentlich, A.; Gozes, Y.; Cohen, S.; Ariel, N.; Barak, D.; *et al*. (1992) Mutagenesis of human acetylcholinesterase. Identification of residues involved in catalytic activity and in polypeptide folding. *J Biol Chem*, **267**, 17640-8.

Silver, A. (1974) *The Biology of Cholinesterases*. Amsterdam: Elsevier-North Holland, p. 67-98.

Simeon-Rudolf, V.; Goran, I.; Tuglin, A. and Reiner, E. (2001) Inhibition of Human Blood Acetylcholinesterase and Butyrylcholinesterase by Ethopropazine. *Croatia Chemica Acta*, **74**, 173-182.

Simon, S. and Massoulie, J. (1997) Cloning and expression of acetylcholinesterase from Electrophorus. Splicing pattern of the 3' exons in vivo and in transfected mammalian cells. *J Biol Chem*, **272**, 33045-55.

Simon, S.; Krejci, E. and Massoulie, J. (1998) A four-to-one association between peptide motifs: four C-terminal domains from cholinesterase assemble with one proline-rich attachment domain (PRAD) in the secretory pathway. *EMBO J*, **17**, 6178-87.

Simpson, N.E. (1966) Factors influencing cholinesterase activity in a Brazilian population. *Am J Hum Genet*, **18**, 243-52.

Siow, N.L.; Choi, R.C., Cheng, A.W.; Wan, D.C.; Zhu, S.Q. and Tsim, K.W. (2002) A cyclic AMP-dependent pathway regulates the expression of acetylcholinesterase during myogenic differentiation of C2C12 cells. *J Biol Chem*, **277**, 36129-36136.

Small, D.H. (1995) A function for butyrylcholinesterase? *J Neurochem*, **64**, 466-7.

Smith, J.; Fauquet, M.; Ziller, C. and Le Douarin, N.M. (1979) Acetylcholine synthesis by mesencephalic neural crest cells in the process of migration in vivo. *Nature*, **282**, 853-5.

Solnica-Krezel, L. and Driever, W. (1994) Microtubule arrays of the zebrafish yolk cell: organization and function during epiboly. *Development*, **120**, 2443-55.

Soreq, H. and Prody, C.A. (1989) Sequence similarities between human acetylcholinesterase and related proteins: putative implications for therapy of anticholinesterase intoxication. *Prog Clin Biol Res*, **289**, 347-59.

Soreq, H.; Ben Aziz, R.; Prody, C.A.; Seidman, S.; Gnatt, A.; Neville, L.; Lieman-Hurwitz, J.; Lev-Lehman, E.; Ginsberg, D. and Lapidot-Lifson, Y. (1990) Molecular cloning and construction of the coding region for human acetylcholinesterase reveals a G + C-rich attenuating structure. *Proc Natl Acad Sci U S A*, **87**, 9688-9692.

Soreq, H.; Lapidot-Lifson, Y. and Zakut, H. (1991) A role for cholinesterases in tumorigenesis? *Cancer Cells*, **3**, 511-6.

Soreq H, Ehrlich G, Lapidot-Lifson Y, Gnatt A, Neville L, Ben-Aziz R, Seidman S, Ginzberg D, Zakut H. (1992) Amplification and mutagenesis of the acetylcholinesterase and butyrylcholinesterase genes in primary human tumors. *In: Gene Amplification in Mammalian Cells*, Kellem RF ed, New York: Marcel Dekker, p. 417-428.

Soreq, H.; Patinkin, D.; Lev-Lehman, E.; Grifman, M.; Ginzberg, D.; Eckstein, F. and Zakut, H. (1994a) Antisensense oligonucleotide inhibition of acetylcholinesterase gene expression induces progenitor cell expansion and suppresses hematopoietic apoptosis ex vivo. *Proc Natl Acad Sci U S A*, **91**, 7907-7911.

Soreq, H.; Ehrlich, G.; Schwarz, M.; Loewenstein, Y.; Glick, D. and Zakut, H. (1994b) Mutations and impaired expression in the ACHE and BCHE genes: neurological implications. *Biomed Pharmacother*, **48**, 253-9.

Soreq, H.; Malinger, G. and Zakut, H. (1987) Expression of cholinesterase genes in human oocytes revealed by in-situ hybridization. *Hum Reprod*, **2**, 689-93.

Spiroff, B.E.N. (1958) Embryonic and post-hatching development of the pineal body of the domestic fowl. *Amer J Anat*, **103**, 375-401.

Stachel, S.E.; Grunwald, D.J. and Myers, P.Z. (1993) Lithium perturbation and goosecoid expression identify a dorsal specification pathway in the pregastrula zebrafish. *Development*, **117**, 1261-74.

Stedman, E.; Stedman, E. and Easson, L.H. (1932) Choline-esterase. An enzyme present in the blood-serum of the horse. *Biochem J*, **26**, 2056-2066.

Still, C.C. and Kuzirian, O. (1967) Enzyme detoxication of 3',4'-dichloropropionanilide in rice and barnyard grass, a factor in herbicide selectivity. *Nature*, **216**, 799-800.

Strahle, U. and Jesuthasan, S. (1993) Ultraviolet irradiation impairs epiboly in zebrafish embryos: evidence for a microtubule-dependent mechanism of epiboly. *Development*, **119**, 909-19.

Sudo, K.; Maekawa, M.; Akizuki, S.; Magara, T.; Ogasawara, H. and Tanaka, T. (1997) Human butyrylcholinesterase L330I mutation belongs to a fluoride-resistant gene, by expression in human fetal kidney cells. *Biochem Biophys Res Commun*, **240**, 372-5.

Sussman, J.L.; Harel, M.; Frolow, F.; Oefner, C.; Goldman, A.; Toker, L. and Silman, I. (1991) Atomic structure of acetylcholinesterase from Torpedo californica: a prototypic acetylcholine-binding protein. *Science*, **253**, 872-9.

Szegletes, T.; Mallender, W.D.; Thomas, P.J. and Rosenberry, T.L. (1999) Substrate binding to the peripheral site of acetylcholinesterase initiates enzymatic catalysis. Substrate inhibition arises as a secondary effect. *Biochemistry*, **38**, 122–133.

Takahashi, J.S.; Hamm, H. and Menaker, M. (1980) Circadian rhythms of melatonin release from individual superfused chicken pineal glands *in vitro*. *Proc Natl Acad Sci U S A*, **77**, 2319-22.

Takahashi, J.S.; Murakami, N.; Nikaido, S.S.; Pratt, B.L. and Robertson, L.M. (1989) The avian pineal, a vertebrate model system of the circadian oscillator: cellular regulation of circadian rhythms by light, second messengers, and macromolecular synthesis. *Recent Prog Horm Res*, **45**, 279-348; discussion 348-52.

Taylor, P. and Radic, Z. (1994) The cholinesterases: from genes to proteins. *Annu Rev Pharmacol Toxicol*, **34**, 281-320.

Teitler, M. and Herrick-Davis, K. (1994) Multiple serotonin receptor subtypes: molecular cloning and functional expression. *Crit Rev Neurobiol*, **8**, 175-88.

Teraoka, H.; Russell, C.; Regan, J.; Chandrasekhar, A.; Concha, M.L.; Yokoyama, R.; Higashi, K.; Take-Uchi, M.; Dong, W.; Hiraga, T.; Holder, N. and Wilson, S.W. (2004) Hedgehog and Fgf signaling pathways regulate the development of tphR-expressing serotonergic raphe neurons in zebrafish embryos. Hedgehog and Fgf signaling pathways regulate the development of tphR-expressing serotonergic raphe neurons in zebrafish embryos. *J Neurobiol*, **60**, 275-88.

Thisse, C.; Thisse, B.; Schilling, T.F. and Postlethwait, J.H. (1993) Structure of the zebrafish snail1 gene and its expression in wild-type, spadetail and no tail mutant embryos. *Development*, **119**, 1203-15.

Towbin, H.; Staehelin, T. and Gordon, J. (1979) Electrophoretic transfer of proteins from polyacrylamide gels to nitrocellulose sheets: procedure and some applications. *Proc Natl Acad Sci U S A*, **76**, 4350-4.

Tsim, K.W.; Randall, W.R. and Barnard, E.A. (1988) Monoclonal antibodies specific for the different subunits of asymmetric acetylcholinesterase from chick muscle. *J Neurochem*, **51**, 95-104.

Tsim, K.W.; Choi, R.C.; Dong, T.T. and Wan, D.C. (1997) A globular, not asymmetric, form of acetylcholinesterase is expressed in chick motor neurons: down-regulation toward maturity and after denervation. *J Neurochem*, **68**, 479-87.

Tsujita, T. and Okuda, H. (1983) Carboxylesterases in rat and human sera and their relationship of serum aryl acylamidases and cholinesterases. *Eur J Biochem*, **133**, 215-220.

Underwood, H.; Steele, C.T. and Zivkovic, B. (2001) Circadian organization and the role of the pineal in birds. *Microsc Res Tech*, **53**, 48-62.

Wake, K.; Ueck, M. and Oksche, A. (1974) Acetylcholinesterase-containing nerve cells in the pineal complex and subcommissural area of the frogs, Rana ridibunda and Rana esculenta. *Cell Tissue Res*, **154**, 423-42.

Wang, K.; Bekar, L.K.; Furber, K. and Walz, W. (2004) Vimentin-expressing proximal reactive astrocytes correlate with migration rather than proliferation following focal brain injury. *Brain Res*, **1024**, 193-202.

Weitnauer, E.; Robitzki, A. and Layer, P.G. (1998) Aryl acylamidase activity exhibited by butyrylcholinesterase is higher in chick than in horse, but much lower than in fetal calf serum. *Neurosci Lett*, **254**, 153-6.

Westerfield, M. (2000) *The zebrafish book*. 4th ed. Univ of Oregon Press, Eugene, U S A.

Whittaker, M. and Britten, J.J. (1989) Segregation of the E1j gene for plasma cholinesterase in family studies. *Hum Hered*, **39**, 1-6.

Wilson, I.B.; Bergmann, F. and Nachmansohn, D. (1950) Acetylcholinesterase X. Mechanism of the catalysis of acylation reactions. *J Biol Chem*, **186**, 781-790.

Whitehouse, P.J.; Price, D.L.; Clark, A.W.; Coyle, J.T. and DeLong, M.R. (1981) Alzheimer disease: evidence for selective loss of cholinergic neurons in the nucleus basalis. *Ann Neurol*, **10**, 122-6.

Whittaker, M. and Britten, J.J. (1980) Inhibition of the plasma cholinesterase variants by pancuronium bromide and some of its analogues. *Clin Chim Acta*, **108**, 89-94.

Wood, N. and Rose, S.P. (1979) Changes in acetylcholinesterase with light exposure, time of day, and motor activity in the rat. *Behav Neural Biol*, **25**, 79-89.

Wu, Y.H. and Swaab, D.F. (2005) The human pineal gland and melatonin in aging and Alzheimer's disease. *J Pineal Res*, **38**, 145-52.

Xie, W.; Wilder, P.J.; Stribley, J.; Chatonnet, A.; Rizzino, A.; Taylor, P.; Hinrichs, S.H. and Lockridge, O. (1999) Knockout of one acetylcholinesterase allele in the mouse. *Chem Biol Interact*, **119-120**, 289-99.

Yamao, M.; Araki, M.; Okano, T.; Fukada, Y. and Oishi, T. (1999) Differentiation of pinopsin-immunoreactive cells in the developing quail pineal organ: an in-vivo and in-vitro immunohistochemical study. *Cell Tissue Res*, **296**, 667-71.

Yu, H.S.; Hernandez, V.; Haywood, M. and Wong, C.G. (1993) Melatonin inhibits the proliferation of retinal pigment epithelial (RPE) cells *in vitro*. *In vitro Cell Dev Biol Anim*, **29A**, 415-8.

Zimmerman, N.H. and Menaker, M. (1979) The pineal gland: a pacemaker within the circadian system of the house sparrow. *Proc Natl Acad Sci U S A*, **76**, 999-1003.

Zirger, J.M.; Beattie, C.E.; McKay, D.B. and Boyd, R.T. (2003) Cloning and expression of zebrafish neuronal nicotinic acetylcholine receptors. *Gene Expr Patterns*, **3**, 747-54.

Zhang, X.J.; Yang, L.; Zhao, Q.; Caen, J.P.; He, H.Y.; Jin, Q.H.; Guo, L.H.; Alemany, M., Zhang, L.Y. and Shi, Y.F. (2002) Induction of acetylcholinesterase expression during apoptosis in various cell types. *Cell Death Differ*, **9**, 790-800.

Zweig, M., Snyder, S.H. and Axelrod, J. (1966) Evidence for a nonretinal pathway of light to the pineal gland of newborn rats. *Proc Natl Acad Sci U S A*, **56**, 515-20.

8   Appendices

8.1   Preparation of solutions

Solutions used in experiments described in the chapter 2	
4% Formaldehyde	10 ml 37% Formalin 90 ml 1 x PBS 100 ml
30 mM cupper sulphate (M = 250 g/mol)	0.41 g/250 ml dH$_2$O
0.1 M Sodium citrate (M = 294 g/mol)	7.35 g/250 ml dH$_2$O
PBS (Phosphate buffered saline)	dH$_2$O 140 mM NaCl 3 mM KCl 13.7 mM Na2HPO4 1.5 mM KH2PO4 pH 7.1 Autoclave
PBST	1x PBS 0.1% Tween 20
25% Sucrose	2.5g Sucrose Add dH$_2$O to a final volume of 10 ml.
0.1 M Tris-maleic-buffer pH 6.0 (1 L)	12.2 g Tris (M = 121.14 g/mol) 11.6 g Maleic acid (M = 116.1 g/mol) dH$_2$O to a final volume of 900 ml Adjust to pH 6.0 with 2.5 M NaOH Add dH$_2$O to a final volume of 1 L.
Additional solutions used in experiments described in the chapter 3	
Alkaline phosphatase staining buffer	100 mM Tris-HCl, pH 9.5 50 mM MgCl2 100 mM NaCl 0.2% Tween-20 0.2% Triton X 60 mg/50 ml Levamisol

BCIP	50 mg/ml in 100% DMF (Dimethylformamid)
Culture medium for zebrafish (10x)	28 ml 5 M NaCl 5.4 ml 1 M KCl 250 µl 1 M Na2HPO4 440 µl 1 M KH2PO4 13 ml CaCl2 10 ml 1 M MgSO4 10 ml 1 M Hepes adjust pH 7.0 with 1 M NaOH dH2O to 1 L solution Dilute 1:10 plus 0.1% Methylenblue (2 mg/ml) in a final volume of 500 ml.
Esterase assay buffers:	0.1 M Potassium phosphat, pH 8.0 a) 1 M K_2HPO_4 b) 1 M KH_2PO_4 Use 93.4 ml 1M K_2HPO_4 buffer for final volume of 950 ml with dH2O. Add the amount necessary of KH_2PO_4 buffer to achieve pH 8.0. Add dH_2O to a final volume of 1 L.
Fish water	30 L dH2O 1.2 g see salt plus $NaHCO_3$ to achieve pH 6.5 – 7.5
Hybridization buffer	50% formamide 5xSSC 50 µg/ml heparin 500 mg/ml torula (yeast) RNA* 0.1% Tween-20 Final volume of 50 ml with distillate water plus 92µl 1M Citric acid.
Homogenization buffer	Na-phosphate extraction buffer [10 mM Na-phosphate, pH 7.4, 0.5% Triton X-100] with protease inhibitor cocktail (1:200 before use- 2.5 µl/5 ml buffer).

KpI buffer for AAA assay	1 M Potassium phosphat, pH 8.0
	a) 1 M $K_2 HPO_4$
	b) 1 M $KH_2 PO_4$
	Mix both solutions, adding the amount necessary of KH_2PO_4 buffer to achieve pH 8.0. Final volume of 1 L with dH2O.
Na HCO3 buffer for DTNB dilution	100 mg $NaHCO_3$ /100 ml 0.1 M Potassium phosphate, pH 8.0 (= 0.1%).
NBT	75 mg/ml in 70% DMF
Ringer's Solution	116 mM NaCl
	2.9 mM KCl
	5 mM HEPES, pH 7.2
	1 mM EDTA
20x SSC	3 M NaCl
	0.3 M sodium citrate
	pH 7.0 (with 1M HCl)
	Autoclave the solution.
Additional solutions used in experiments described in the chapter 4	
DMEM reduced medium	2% FCS
	1% Glutamine
	0.1% Penicillin/Streptomycin
DMEM complete medium	Gibco plus
	10% FCS
	1% Glutamine
	0.1% Penicillin/Streptomycin
LB agar	LB agar 32 g
	Final volume 1 L dH_2O
	Autoclave and after cooling (50 °C) add antibiotics if desired. For plates, 40 – 100 ml solution gives 85 -150 mm plates. Flame plate to avoid air bubbles. Store at 4°C.

LB medium	LB 20 g 1 L dH$_2$O Autoclave and store at RT
10x loading buffer	57% glycerol 100 mM Tris pH 8.0, 10 mM EDTA·Na$_2$ 2H$_2$O, ~ 0.001% bromophenol blue
Ponceau-S staining solution	5% HCl, 0.2% Ponceau-S
Running buffer	15 g Tris-base 72 g Glycin 0.1% SDS Final volume 2 L DH$_2$O
50x TAE:	2 M Tris 50 mM EDTA·Na$_2$. 2H$_2$O 4% HCl, pH 8.5
TE buffer	10 mM Tris 1 mM EDTA·Na$_2$ 2H$_2$O, pH 8.0.
Transfer buffer	3 g Tris 14.4 g glycine Add dH$_2$O to a final volume of 1 L.

8.2   Materials

8.2.1 Drugs/chemicals

Aceton	Merck, Darmstadt
Agarose	Peqlab, Erlangen
Alkaline phophatase	Roche, Mannheim
Ampicilline, sodium salt	Sigma, Deisenhofen
APS	Roth, Karlsruhe
ATC	Serva, Heidelberg
ATP	Sigma, Deisenhofen
BCIP	Roche, Manheim
Brilliant Blue G-250	Merck, Darmstadt
Bromophenol blue	Merck, Darmstadt
BrdU	Roche, Mannheim
BSA	Sigma, Deisenhofen
BTC	Fluka, Buchs
BW 284C51	Sigma, Deisenhofen
$CaCl_2$	Merck, Darmstadt
Citric acid	Merck, Darmstadt
Cuper sulphate	Merck, Darmstadt
DAB	Sigma, Deisenhofen
DAPI	Boehringer, Mannheim
DEPC	Sigma, Deisenhofen
Dianisidine	Fulka, Bucsh
Diethanolamine	Sigma, Deisenhofen
DMF	Merck, Darmstadt
DMSO	Sigma, Deisenhofen
DNase	Roche, Manheim
DNA standard	Roth, Karlsruhe
DTNB(5,5'-Dithio-bis-2-nitro-benzoacid)	Serva, Heidelberg
EDTA·	Merck, Darmstadt
Eserine	Sigma, Deisenhofen
Ethanol	Roth, Karlsruhe
Ethidium bromide	Roth, Karlsruhe
Ethopropazin (10-(2-diethylaminopropyl)phenothiazine hydrochloride	Sigma, Deisenhofen
Eukobrom Tetenal developer	Hirrlinger, Stuttgart
Film developer T Max 400 Kodak	Hirrlinger, Stuttgart
Formaline 37%	Merck, Darmstadt
Formamide	Sigma, Deisenhofen
Gelatin	Sigma, Deisenhofen
Glucose	Merck, Darmstadt

Glutamin	Serva, Heidelberg
Glycin	Merck, Darmstadt
Glycerol	Merck, Darmstadt
H_2O_2	Merck, Darmstadt
HCl (Chloridric acid)	Merck, Darmstadt
Heparin	Sigma, Deisenhofen
HEPES, sodium salt	Merck, Darmstadt
5-hydroxitryptamine	Sigma, Deisenhofen
Iso-OMPA	Sigma, Deisenhofen
Isopropanol	Merck, Darmstadt
Kaisers Glyceringelatin	Merck, Darmstadt
KCl (Potassium chloride)	Merck, Darmstadt
K2HPO4 (di-Potassium hydrogen phosphate)	Merck, Darmstadt
KH2PO4 (Potassium di-hydrogen phosphate)	Merck, Darmstadt
Levamisol	Sigma, Deisenhofen
Maleic acid	Merck, Darmstadt
Methanol	Merck, Darmstadt
Methylenblue	Merck, Darmstadt
MgCl2 (Magnesium chloride)	Merck, Darmstadt
MgSO4 (Magnesium sulphate)	Merck, Darmstadt
Milk powder	Roth, Karlsruhe
Na3Citrat (Sodium citrate)	Merck, Darmstadt
$NaCH_3COO$ (Sodium acetate)	Merck, Darmstadt
NaCl (Sodium chloride)	Merck, Darmstadt
NaHCO3 (Sodium hydrogen carbonate)	Merck, Darmstadt
Na_2HPO_4 (di-Sodium hydrogen phosphate)	Merck, Darmstadt
NaOH (Sodium hydroxid)	Merck, Darmstadt
NBT	Boehringer, Mannheim
o-Nitroacetanilid	Merck, Darmstadt
o-Nitroanilin	Merck, Darmstadt
ONPRA	Prof. Darvesh (Dalhousie University)
PBS	Gibco, Eggenstein
Phenol	VWR, Darmstadt
Phosphoric acid	Merck, Darmstadt
Ponceau S	Sigma, Taufkirchen
Protease inhibitor cocktail	Sigma, Taufkirchen
RNA*later* solution	Sigma, Taufkirchen
SDS	Merck, Darmstadt
Sucrose	Merck, Darmstadt
TEMED	Roth, Karlsruhe
Tissue freezing medium	Miles Scientific, USA
Torula (yeast) RNA	Sigma, Deisenhofen
Tris	Sigma, Deisenhofen

Tri-reagent	Molec. Research Center, USA
Tri-sodium citrate·2H$_2$O	VWR, Darmstadt
Triton X-100	Sigma, Deisenhofen
Tryptone-peptone	Difco, UK
Trypsin/EDTA	Gibco, Eggenstein
Tween-20	Roth, Karlsuhe
Vectorschield mounting medium	Vector Lab, USA

8.2.2 Kits

Avidin-Biotin Vectastain Elite ABC kit PK-6102	Vector lab, USA
BrdU Labeling and Detection Kit I – N° 1 296 736	Roche, Mannheim
DAB Vectastain peroxidase substrate kit, SK-4100	Vector lab, USA
DOTAP liposomal transfection reagent	Roche, Mannheim
In Situ Cell Death Detecion Kit – N° 2 156 795	Roche, Mannheim
LuniGLO Chemiluminescent substrate – N° 546102	KPL, UK
Plasmid Maxi Kit	Qiagen, Hilden
Reverse trascriptase reaction kit	Promega, Manheim
TUNEL assay for apoptosis – N° 1767305	Roche, Mannheim
Vip substrate kit for peroxidase activity, SK - 4600	Vector lab, USA

8.2.3 Enzymes and supplements

Alcalin phosphatase (2000 U/mg)	Boehringer, Manheim
Hexanucleotide mix	Roth, Karlsruhe
Nuclease free water	Promega, Mannheim
Restriction endonucleases	New England Biolabs, USA
Restriction endonucleases buffers	New England Biolabs, USA
RQ1 Rnase-free DNase	Promega, Manheim
Taq DNA polymerase	Roche, Mannheim

8.2.4 Cell culture medium and supplements

DMEM powder	Gibco, Eggenstein
FCS	Gibco, Eggenstein
F12 Nutrient mixture	Gibco, Eggenstein
Horse serum (normal)	Vector Lab, USA
L-Glutamine	Seromed, Berlin
L- Methionine sulfoximine	Sigma, Taufkirchen
Penicillin/Streptamycin	Gibco, Eggenstein

Ultraculture serum free medium- BioWhittaker	Cambrex, USA

8.2.5 Consume material

Blotting paper	Whatman, Maidstone, UK
Filter - paper	Schleider & Schül, Dasel
Crystal cuvettes	BrandTech Scientific, USA
Falcon tubes (14 ml)	Greiner, Frickenhausen
Films	Röntgen films, Sigma, Deisenhofen Polaroid Films, Amersham
Flascks - cell culture (50 and 250 ml)	Greiner, Frickenhausen
Glass coverslips	Menzel-Gläser, Braunschweig
Glass slides	Menzel-Gläser, Braunschweig
Membrane Immobilon-P	Millipor, Eschborn
Molecular weight markers	Roth, Karlsuhe
Nitrocellulose membranes	Whatman Biometra, Göttingen
Parafilm	Neolab, Heidelberg
Pasteur pipettes	Volac, UK
Petry-disches (3.5 and 10 cm ⌀)	Greiner, Frickenhausen
Plates – 24 well	Greiner, Frickenhausen
Pipettes (1 ml, 5 ml, 10 ml, 25 ml)	VWR, Darmstadt
Pipette tips	AHN Biotechnologie, Nordhausen
Plastic cuvettes	BrandTech Scientific, USA
Reaction tubes (0.5, 1 and 2 ml)	AHN Biotechnologie, Nordhausen
Ultrafiltration membrane - PM10	Amicon/Millipor, Eschborn

8.3   Equipments

Autoclave	Webeco, Bad Schwartau
Axiophot microscope equiped with Nomarski and fluorescent light supply	Carl Zeiss, Jena
Binocular Stemi SV 11	Carl Zeiss, Jena
Cammera Olympus IMT-2 SC 35	Olympus, Hamburg
Cell culture hood	Heraeus, Hanau
Centrifuges J2-21	Beckman, USA
Centrifuges model 1, OR	Biorad, München
CO2-incubator	Heraeus, Hanau
Confocal – TCS laser scanning spectral microscope, equipped with argon-cripton-laser	Leica, Bensheim
Cryostat H 11500 OM	Microm, Walldorf
Digital camara (coupled to bonocular)	EHD KamPro 04
Electrophoresis chamber	Peq-lab, Erlangen
Electrophoresis chamber	Bio-Rad, München
Electrophoresis power supply	Bio-Rad, Consort E321, München, Biometra Powerpack P25
Freezers	Queue Systems, USA
Heat block	Janke & Kunkel, Staufen
Incubators, for *E. coli* culture	Heraeus, Hanau
Incubator, for HEK cells culture	Nuaire, Sarstedt
Incubator, for zebrafish culture	Memmert, Schwabach
Incubator-shaker	New Brunswick Scientific, USA
Magnetic stirring plates	Itec, Staufen
Microwave oven	Bosch, Stuttgart
pH meter	WTW (Wissenschaftlich Technische Werkstätten), Weilheim
Pipettes	Eppendorf, Hamburg
Scales	Sartorius, Göttingen
Shakers	GFL, Burgwedel
Sonicator	Bandelin Electronic, Berlin
Spectrophotometer - Lambda 2	Perkin Elmer, Langen
Sterilization oven	Memmert, Schwabach
Thermocycler	Biometra, Göttingen
Ultracentrifuge	Beckman, Krefeld
UV transilumination	AGS, Heidelberg
Vacuum concentrator, Speedvac	Bachofer, Reutlingen
Vortex	Heidolph, GFL, Burgwedel
Waterbaths	Memmert, Schwabach

Personal Data: Born on September 20th, 1975
Brazilian, single

Education:

2005   Ph.D, Natural Sciences, Darmstadt University of Technology
Department of Developmental Biology & Neurogenetics

2001   M.Sc. (*magna cum laude*), Genetics,
Federal University of Parana, Brazil

1999   B.Sc., Biology
Federal University of Parana, Brazil

Teaching Activities:

Experimental instructions in site-directed-mutagenesis and enzyme kinetics,
Lecture: Cholinesterases - organophosphates inhibition mechanism.
      July 2003, Darmstadt University of Technology

Laboratory instructions for *in situ* hybridization (zebrafish embryos) and histochemistry
Lecture: AChE expression during zebrafish and chicken pineal development.
      July 2004, Darmstadt University of Technology

Lecture: Liver and pancreas – stem cells
Seminar: Remodeling of the chick pineal gland and spatio-temporal implication for ChEs
      expression. July 2005, Darmstadt University of Technology

List of Publications:

Allebrandt, K.V.; Andermann, P. & Layer, P.G. A zebrafish (*Danio rerio*) embryogenesis
malformation is generated by serotonin administration, and is related to
acetylcholinesterase expression onset (in preparation).

Allebrandt, K.V.; Okano, T. & Layer, P.G. Remodeling of the chick pineal gland and
spatio-temporal implication for cholinesterases expression (in preparation).

Allebrandt, K.V. & Layer P.G. (2005) Cholinesterases during development of the avian
pineal gland. *J Neroforum* 1 (Suppl. - 30th Göttingen Neurobiology Conference).

Allebrandt, K.V.; Rajesh, V. & Layer, P.G. Expression of Acetylcholinesterase (AChE) and
Aryl acylamidase (AAA) during zebrafish embryogenesis. *Chem Bio Interactions*
(*in press*).

Souza, L.R.; Fadel-Picheth, C.; Allebrandt, K.V.; Furtado, L. & Chautard-Freire-Maia,
E.A. (2005) Possible influence of the *BCHE* locus of butyrylcholinesterase on
stature and body mass index. *Am J Physic Anthrop* 126(3):329-34.

Allebrandt, .K.V.; Souza, R.L.; & Chautard-Freire-Maia, E.A. (2002) Variability of the
paraoxonase gene (*PON1*) in Euro- and Afro-Brazilians. *Toxicol Appl Pharmacol*
180(3):151-6.

Book Chapter:

Allebrandt, K.V. & Strapasson, F. (1999) Pesticide misuse and its implications *In:* The
production of the teaching knowledge on the education of science. Ed. IBPEX,
Curitiba, Brazil. P. 136-59.

Posters:

Allebrandt, K.V.; Okano, T. & Layer, P.G. Cholinesterases during development of the avian pineal gland. Sixth Meeting of the German Neuroscience Society. Göttingen, Germany. February, 2005.

Allebrandt, K.V.; Rajesh, V.; Andermann, P. & Layer, P.G. Expression of acetylcholinesterase (AChE) and aryl acylamidase (AAA) during zebrafish embryogenesis. VIII International Meeting on Cholinesterases. Perugia, Italy. October, 2004.

Allebrandt, K.V. & Layer, P.G. Aryl Acylamidase Activity of *In vitro* Expressed Human Butyrylcholinesterase. VII International Meeting on Cholinesterases. Pucon, Chile. October, 2002.

Oral Presentations:

Allebrandt, K.V. & Layer, P.G. Aryl acylamidase and cholinesterases: evolutionary, molecular and developmental aspects. Summer Academy Deutsch Forschungsgemeichaft. Riezlern, Austria. September, 2004.

Allebrandt, K.V. & Layer, P.G. Insights on the aryl acylamidase activity. Summer Academy Deutsch Forschungsgemeichaft. Riezlern, Austria. September, 2003.

Allebrandt, K.V. & Layer, P.G. Aryl acylamidase activity on human butyrylcholinesterase. Summer Academy Deutsch Forschungsgemeichaft. Riezlern, Austria. September, 2002.

Allebrandt, K.V. & Chautard-Freire-Maia, Variability of the paraoxonase gene (*PON1*) in Euro- and Afro-Brazilians. Master thesis defense at the Federal University of Parana, Brazil, 2001.

Allebrandt, K.V. & Chautard-Freire-Maia, E. Human butyrylcholinesterase variability and its implication for pesticides poisoning. Annals of the 7th EVINCI. Federal University of Parana, Brazil, 1999.

Allebrandt, K.V. & Strapasson, F. The pesticide use and its implications. 3rd Latino-American and Caribbean Symposia of the Education in Science of the International Council of Associations for Science Education - 3rd ICASE, Curitiba, Brazil, 1999.

Allebrandt, K.V., Souza, R.L., Cazarote, H.B. & Chautard-Freire-Maia, E. BCHE UF1 and *BCHE* UF2 phenotype frequencies in blood donors from CTBA. Annals of the 6th EVINCI. Federal University of Parana, Brazil, 1998.

Graduate Student Committees:

2004   2nd Student representative member of the Biology Graduate College Council, Darmstadt University of Technology, Germany.

1999   Student representative member of the Genetics Graduate College Council, Federal University of Parana, Brazil.

Languages:

English, Portuguese, German and Spanish

Eidesstattliche Erklärung

Hiermit erkläre ich an Eides statt, daß ich die vorliegende Dissertation selbständig und nur unter Verwendung der angegebenen Hilfsmittel angefertigt habe.

Karla Viviani Allebrandt

Darmstadt, den 20.09.2005